

TL
242
.M22
1985



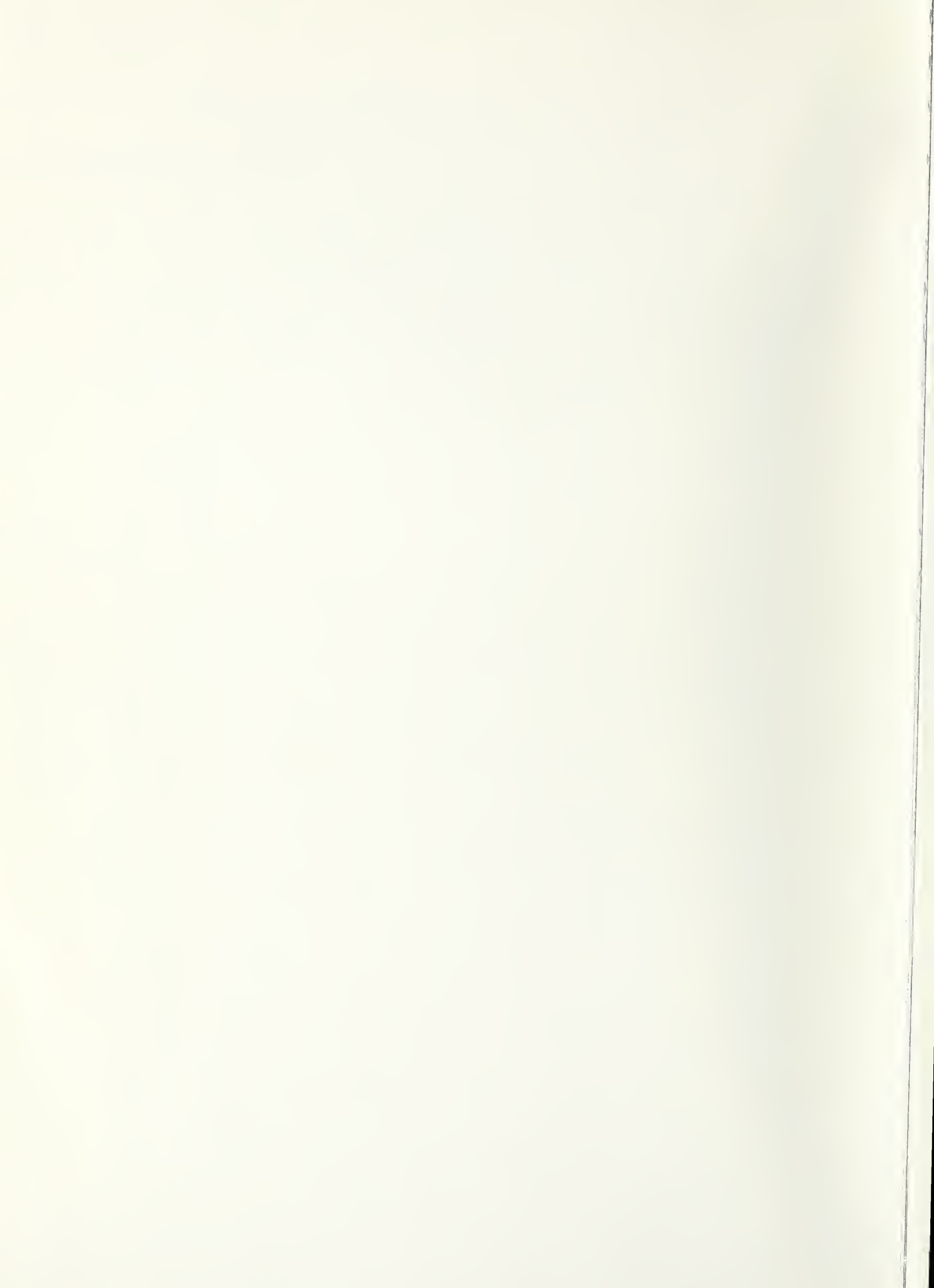
U.S. Department
of Transportation
**National Highway
Traffic Safety
Administration**

DOT HS 806 749

APRIL 1985

FINAL REPORT

CRASHWORTHINESS, AGGRESSIVENESS AND
CRASH TEST PROCEDURES



1. Report No. DOT HS 806 749	2. Government Accession No.	3. Recipient's Catalog No.	
4. Title and Subtitle Crashworthiness, Aggressiveness and Crash Test Procedures		5. Report Date APRIL 1985	6. Performing Organization Code NRD-22
		8. Performing Organization Report No. SRL-20	
7. Author(s) MacLaughlin, T.F. and Saul, R.A.		10. Work Unit No. (TRAIS)	
9. Performing Organization Name and Address National Highway Traffic Safety Administration Vehicle Research and Test Center P.O. Box 37 East Liberty, Ohio 43319		11. Contract or Grant No.	
		13. Type of Report and Period Covered FINAL	
12. Sponsoring Agency Name and Address National Highway Traffic Safety Administration 400 7th Street, S.W. Washington, D.C. 20590		14. Sponsoring Agency Code	
		15. Supplementary Notes Final Report for Project SRL-20, "Vehicle Aggressiveness and Compatibility"	
16. Abstract Several aspects of the Agency's Frontal and Side Impact programs were addressed. Barrier crash test data were analyzed to determine front structural characteristics associated with good crash survival potential. Car/car crash tests were performed which demonstrated significant aggressiveness differences among large cars, and enabled characteristics associated with aggressive behavior to be identified. The standard fixed rigid barrier was evaluated as a crashworthiness-measuring device, and three different barriers were evaluated for their ability to measure frontal structural aggressiveness. Finally, the importance of striking vehicle front structural stiffness distribution on struck vehicle occupant injury severity in side collisions was considered, and crash data were analyzed which showed differences in front stiffness distribution between two mid-size automobiles.			
17. Key Words Crashworthiness Aggressiveness Crash Barriers Frontal Impact Side Impact Occupant Protection		18. Distribution Statement DOCUMENT IS AVAILABLE TO THE U.S. PUBLIC THROUGH THE NATIONAL TECHNICAL INFORMATION SERVICE, SPRINGFIELD, VIRGINIA 22161	
19. Security Classif. (of this report) Unclassified	20. Security Classif. (of this page) Unclassified	21. No. of Pages	22. Price

JUN 19 1985
 LIBRARY

72
242
11122
198

METRIC CONVERSION FACTORS

Approximate Conversions to Metric Measures

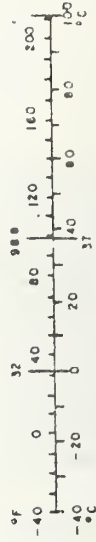
Symbol	What You Know	Multiply by	To Find	Symbol
LENGTH				
in	inches	2.5	centimeters	cm
ft	feet	30	centimeters	cm
yd	yards	0.9	meters	m
mi	miles	1.6	kilometers	km
AREA				
m ²	square inches	6.5	square centimeters	cm ²
ft ²	square feet	0.09	square meters	m ²
yd ²	square yards	0.8	square meters	m ²
mi ²	square miles	2.6	square kilometers	km ²
	acres	0.4	hectares	ha
MASS (weight)				
oz	ounces	28	grams	g
lb	pounds	0.45	kilograms	kg
	short tons (2000 lb)	0.9	tonnes	t
VOLUME				
teaspoon	teaspoons	5	milliliters	ml
Tablespoon	tablespoons	15	milliliters	ml
fl oz	fluid ounces	30	milliliters	ml
c	cup	0.24	liters	l
pt	pint	0.47	liters	l
qt	quart	0.95	liters	l
gal	gallon	3.8	liters	l
l	liter	0.03	cubic meters	m ³
cu ft	cubic feet	0.76	cubic meters	m ³

TEMPERATURE (exact)

°F	Fahrenheit temperature	subtracting 32)	°C	Celsius temperature
----	------------------------	-----------------	----	---------------------

Approximate Conversions from Metric Measures

Symbol	What You Know	Multiply by	To Find	Symbol
LENGTH				
mm	millimeters	0.04	inches	in
cm	centimeters	0.4	inches	in
m	meters	3.3	feet	ft
m	meters	1.1	yards	yd
km	kilometers	0.6	miles	mi
AREA				
cm ²	square centimeters	0.16	square inches	in ²
m ²	square meters	1.2	square feet	ft ²
km ²	square kilometers	0.4	square miles	mi ²
ha	hectares (10,000 m ²)	2.5	acres	ac
MASS (weight)				
g	grams	0.036	ounces	oz
kg	kilograms	2.2	pounds	lb
t	tonnes (1000 kg)	1.1	short tons	sh
VOLUME				
ml	milliliters	0.03	fluid ounces	fl oz
l	liters	2.1	pints	pt
l	liters	1.06	quarts	qt
l	liters	0.26	gallons	gal
m ³	cubic meters	36	cubic feet	ft ³
m ³	cubic meters	1.3	cubic yards	yd ³
TEMPERATURE (exact)				
°C	Celsius temperature	multiply by 1.8 (then add 32)	°F	Fahrenheit temperature



* 1 in = 2.54 (exact). For other exact conversions and more detailed tables, see NBS Mon. Publ. 288, Units of Weights and Measures, Price \$2.25. SO Catalog No. C13-10-288

TABLE OF CONTENTS

<u>Section</u>	<u>Page</u>
Technical Report Documentation Page	i
Metric Conversion Factors	ii
List of Figures	v
List of Tables	xi
Acknowledgements	xiii
Technical Summary	xv
1.0 Introduction	1
2.0 Frontal Protection -- Vehicle Structural Characteristics	2
2.1 Characteristics of Crashsurvivable Vehicles	2
2.1.1 Introduction	2
2.1.2 Data Processing	2
2.1.3 Measurement of Occupant Protection	3
2.1.4 Results	7
2.1.4.1 Dummy Measurements	8
2.1.4.2 Restraint Survival Distance Calculations	20
2.1.4.3 ABAG Model Simulations	29
2.1.5 Conclusions	42
2.1.5.1 General Observations	42
2.1.5.2 Reasons for Enhanced Crashsurvivability	42
2.1.5.3 Selection of Vehicles for Future Modification	43
2.2 Characteristics of Non-Aggressive Vehicles	43
2.2.1 Introduction	43
2.2.2 Experimental Approach	44
2.2.3 Vehicle Selection	44
2.2.4 Car/Car Crash Test Results	59
2.2.4.1 Full Frontal Collisions	59
2.2.4.2 Offset Frontal Collisions	66
2.2.5 Conclusions	71
2.3 Comparison of Crashsurvivable and Non-Aggressive Characteristics	75

TABLE OF CONTENTS

(Continued)

<u>Section</u>	<u>Page</u>
3.0 Frontal Protection -- Test Procedure Development	75
3.1 Ability of Fixed Rigid Barrier for Measuring Crashworthiness	75
3.1.1 Introduction	75
3.1.2 Measurement of Occupant Protection	76
3.1.3 Crash Test Data	77
3.1.4 Equivalent Impact Velocity Assumptions	78
3.1.5 Results	79
3.1.5.1 Honda Series	79
3.1.5.2 Rabbit Series	84
3.1.5.3 Horizon Series	89
3.1.6 Conclusions	93
3.2 Barriers for Measuring Aggressiveness	98
3.2.1 Introduction	98
3.2.2 Test Results	101
3.2.2.1 Repeatability	101
3.2.2.2 Fixed Rigid Barrier (FRB)	105
3.2.2.3 Fixed Load Cell Barrier (FLCB)	105
3.2.2.4 Moving Deformable Barrier (MDB)	116
3.2.2.5 Summary of Results	122
3.2.3 Conclusions and Recommendations	122
4.0 Side Protection -- Vehicle Structural Characteristics	123
4.1 Introduction	123
4.2 Crash Test Data	123
4.3 Analysis Results	125
4.4 Conclusions and Recommendations	131
REFERENCES	136
APPENDIX A -- Difficulties in Obtaining Static Crush Values	138
APPENDIX B -- Summary of Occupant/Airbag Modeling Improvements	140

LIST OF FIGURES

<u>Figure</u>		<u>Page</u>
1	Velocity-Time Responses of Vehicle and Occupant	6
2	Head Injury Criterion Values Determined From Dummy Measurements -- Driver	10
3	Head Injury Criterion Values Determined From Dummy Measurements -- Passenger	11
4	Maximum Chest Accelerations Determined From Dummy Measurements -- Driver	12
5	Maximum Chest Accelerations Determined From Dummy Measurements -- Passenger	13
6	Minicompact Vehicle Responses (Dummy Measurement Criteria)	16
7	Subcompact Vehicle Responses (Dummy Measurement Criteria)	17
8	Intermediate Vehicle Responses (Dummy Measurement Criteria)	18
9	Standard Vehicle Responses (Dummy Measurement Criteria)	19
10	Required Internal Distance Calculations	22
11	Minicompact Vehicle Responses (RID Criterion)	24
12	Subcompact and Light Intermediate Vehicle (<3000 lbs) Responses (RID Criterion)	25
13	Heavy Intermediate Vehicle (>3000 lbs) Responses (RID Criterion)	26
14	Standard Vehicle Responses (RID Criterion)	27
15	Maximum Chest Accelerations Determined From ABAG Model -- 5th Percentile Female Driver	31
16	Maximum Chest Accelerations Determined From ABAG Model -- 50th Percentile Male Driver	32
17	Maximum Chest Accelerations Determined From ABAG Model -- 95th Percentile Male Driver	33

LIST OF FIGURES
(Continued)

<u>Figure</u>		<u>Page</u>
18	Maximum Chest Accelerations Determined From ABAG Model -- 5th Percentile Female Passenger	34
19	Maximum Chest Accelerations Determined From ABAG Model -- 50th Percentile Male Passenger	35
20	Maximum Chest Accelerations Determined From ABAG Model -- 95th Percentile Male Passenger	36
21	Minicompact and Subcompact Vehicle Responses (ABAG Modeling Criterion)	38
22	Intermediate Vehicle Responses (ABAG Modeling Criterion)	39
23	Standard Vehicle Responses (ABAG Modeling Criterion)	40
24	Crush Comparison From 35 mph Fixed Rigid Barrier Impact	47
25	Compartment Responses of 1980 AMC Concord and 1979 Olds Cutlass Supreme in 35 mph Fixed Rigid Barrier Impact	48
26	Occupant Compartment Responses -- 35 mph Fixed Rigid Barrier Impacts	50
27	Dummy Peak Chest Acceleration Measurement Comparison -- 35 mph Fixed Rigid Barrier Impacts	53
28	Dummy Measurement HIC Comparison -- 35 mph Fixed Rigid Barrier Impacts	54
29	Restraint Survival Distances -- 35 mph Fixed Rigid Barrier Impacts	56
30	ABAG Computer Simulation Comparison for 50th Percentile Male -- 35 mph Fixed Rigid Barrier Impacts	58
31	Rabbit Occupant Compartment Responses -- Full Frontal Car/Car Collisions	61
32	Rabbit Shoulder Belt and Steering Column Behavior -- Concord Collision	63

LIST OF FIGURES
(Continued)

<u>Figure</u>		<u>Page</u>
33	Rabbit Shoulder Belt and Steering Column Behavior -- Marquis Collision	64
34	Rabbit Shoulder Belt and Steering Column Behavior -- Cutlass Collision	65
35	Left Compartment Responses in Rabbits -- Offset Frontal Car/Car Collisions	69
36	Right Compartment Responses in Rabbits -- Offset Frontal Car/Car Collisions	70
37	Honda Occupant Compartment Responses	80
38	Honda Steering Column Behavior -- Car/Car Collision	82
39	Honda Steering Column Behavior -- FRB Collision	83
40	Rabbit Occupant Compartment Responses	86
41	Rabbit Shoulder Belt and Steering Column Behavior -- FRB Collision	88
42	Horizon Occupant Compartment Responses	91
43	Horizon Shoulder Belt and Steering Column Behavior -- Citation Collision	94
44	Horizon Shoulder Belt and Steering Column Behavior -- Mustang Collision	95
45	Horizon Shoulder Belt and Steering Column Behavior -- FRB Collision	96
46	Fixed Load Cell Barrier	99
47	Moving Deformable Barrier	100
48	Occupant Compartment Responses of Concords -- FRB and FLCB Collisions	103
49	Occupant Compartment Responses of Marquis -- FRB and FLCB Collisions	104

LIST OF FIGURES
(Continued)

<u>Figure</u>		<u>Page</u>
50	Occupant Compartment Responses of Concord and Marquis -- FRB Collisions	106
51	Occupant Compartment Responses of Concord and Marquis -- FLCB Collisions	107
52	Total Force -- Concord and Marquis Collisions with FLCB	109
53	Load Cell Groups and Vehicle Profile Heights	110
54	FLCB Group I Forces -- Concord and Marquis Collisions	111
55	FLCB Group II Forces -- Concord and Marquis Collisions	111
56	FLCB Group III Forces -- Concord and Marquis Collisions	112
57	FLCB Group IV Forces -- Concord and Marquis Collisions	112
58	FLCB Group V Forces -- Concord and Marquis Collisions	113
59	FLCB Group VI Forces -- Concord and Marquis Collisions	113
60	Magnitude and Centroid of Impulse on Load Cell Barrier From Collisions With AMC Concord and Mercury Marquis	115
61	Occupant Compartment Responses of Concord and Marquis -- MDB Collisions	117
62	MDB Responses -- Collisions with Concord and Marquis	118
63	Crush of Moving Deformable Barrier from Collisions with AMC Concord and Mercury Marquis	119
64	Citation and Fairmont Total FLCB Force -- Full Frontal	126

LIST OF FIGURES
(Continued)

<u>Figure</u>		<u>Page</u>
65	Cutlass and Impala Total FLCB Force -- Full Frontal	126
66	Citation and Fairmont Total FLCB Force -- 30° Frontal	127
67	Cutlass and Impala Total FLCB Force -- 30° Frontal	127
68	Car/MLCB Load Cell Interface and Load Cell Grouping -- 30° Frontal Impacts	128
69	MLCB Group 3 and 4 Forces -- Citation and Fairmont 30° Frontal	129
70	MLCB Group 5 and 6 Forces -- Citation and Fairmont 30° Frontal	129
71	MLCB Group 1 and 2 Forces -- Citation and Fairmont 30° Frontal	130
72	MLCB Group 3 Forces -- Citation and Fairmont 30° Frontal	130
73	MLCB Group 4 Forces -- Citation and Fairmont 30° Frontal	132
74	MLCB Group 5 Forces -- Citation and Fairmont 30° Frontal	132
75	MLCB Group 6 Forces -- Citation and Fairmont 30° Frontal	133
76	MLCB Group 1 Forces -- Citation and Fairmont 30° Frontal	133
77	MLCB Group 2 Forces -- Citation and Fairmont 30° Frontal	134
78	MLCB Group 3 and 4 Forces -- Cutlass and Impala 30° Frontal	134
79	MLCB Group 5 and 6 Forces -- Cutlass and Impala 30° Frontal	135
80	MLCB Group 1 and 2 Forces -- Cutlass and Impala 30° Frontal	135

LIST OF TABLES

<u>Table</u>		<u>Page</u>
1	Comparison of Contractor and VRTC Dynamic Crush Data	4
2	Weight Categories	7
3	Crash Test Parameter and Dummy Measurement Summary	9
4	Identification of "Best" and "Worst" Vehicles in Terms of Measured Occupant Protection	14
5	Dynamic Crush Values of Vehicles Determined to be "Best" and "Worst" by Dummy Measurements	14
6	Calculation Summary for Minimum Required Internal Distance (RID)	21
7	Dynamic Crush Values of Vehicles Determined to be "Best" and "Worst" by RID Calculations	23
8	ABAG Model Simulation Summary	30
9	Identification of "Best" and "Worst" Vehicles as Determined from ABAG Simulation Results	37
10	Dynamic Crush Values of Vehicles Determined to be "Best" and "Worst" by ABAG Measurements	37
11	Large Vehicle FRB Crash Test Summary	46
12	Large Car Specifications for Testing of Potential Aggressiveness Test Devices	45
13	Crash Test and Dummy Measurement Summary from 35 mph Barrier Impacts	52
14	Restraint Survival Distance Calculation Summary from 35 mph Barrier Impacts	55
15	ABAG Computer Simulation Summary from 35 mph Barrier Impacts	57
16	Small, Crashworthy Car Specifications for the Crash Test Matrix	51
17	Vehicle Data and Test Condition Summary -- Car/Car Collisions	60

LIST OF TABLES
(Continued)

<u>Table</u>		<u>Page</u>
18	Rabbit Dummy Measurements -- Full Frontal Crash Tests	62
19	Restraint Survival Distance Calculations -- Full Frontal Crash Tests	67
20	ABAG Simulation Results -- Rabbit Occupants -- Cutlass/Rabbit, marquis/Rabbit and Concord/Rabbit Full Frontal Crash Tests	68
21	Rabbit Dummy Measurements -- Offset Frontal Crash Tests	72
22	Restraint Survival Distance Calculations -- Offset Frontal Crash Tests	73
23	ABAG Simulation Results -- Rabbit Occupants -- Cutlass/Rabbit, marquis/Rabbit and Concord/Rabbit Offset Frontal Crash Tests	74
24	Groups of Vehicle Crash Tests Analyzed	77
25	Test and Equivalent Impact Velocities	79
26	RSD Calculations -- Honda Series	81
27	ABAG Simulations -- Honda Series	85
28	Dummy Measurements -- Rabbit Series	87
29	RSD Calculations -- Rabbit Series	89
30	ABAG Simulations -- Rabbit Series	90
31	Dummy Measurements -- Horizon Series	92
32	RSD Calculations -- Horizon Series	93
33	ABAG Simulations -- Horizon Series	97
34	Vehicle Data and Crash Test Summary -- Car/Barrier Collisions	102
35	Energy Dissipation Estimates -- Barrier Collisions	121
36	MLCB Car Crash Test Data Summary	124

ACKNOWLEDGEMENTS

The discussion and conclusions in this report represent the opinions of the authors and not necessarily those of the NHTSA. The United States Government does not endorse products or manufacturers. Trade or manufacturer's names appear herein solely because they are essential to the object of the report. This document is disseminated under the sponsorship of the Department of Transportation in the interest of information exchange. The United States Government assumes no liability for the contents or use thereof.

There are many individuals who participated in this program. The authors would like to acknowledge the valuable contributions of Susan Enouen and Paul Chou, Ohio State University Master's Degree candidates, who performed some of the research; and Mary Lou Gonterman, Gerda England and Claude Melton, who processed most of the data contained herein. The authors are also grateful to Susan Weiser for her efficient preparation of this report.



TECHNICAL SUMMARY

CONTRACTOR	CONTRACT NUMBER
REPORT TITLE	REPORT DATE
Crashworthiness, Aggressiveness and Crash Test Procedures	April 1985
REPORT AUTHOR(S)	
MacLaughlin, T.F. and Saul, R.A.	

This research addressed several aspects of the Agency's Frontal and Side Impact Protection programs. Front structural characteristics of passenger cars having superior crash survival potential for airbag-restrained occupants were identified, along with characteristics which make large cars relatively non-aggressive to smaller cars in frontal collisions. The standard fixed rigid barrier was evaluated as a crashworthiness-measuring device, and three different barriers were evaluated for their ability to measure frontal structural aggressiveness. Finally, the distribution of front structural stiffness of several vehicles was studied. A recommendation was made to explore the effect differences in striking vehicle stiffness distribution might have on struck vehicle occupant injury severity in side collisions.

Characteristics of Crashsurvivable Vehicles -- Frontal Collisions

To identify characteristics associated with crashsurvivability, an analysis of 29 frontal barrier crash tests, conducted at 35 mph under the New Car Assessment Program, was performed. Three methods of determining occupant protection were used: dummy measurements, Restraint Survival Distance (RSD) calculations, and occupant/airbag simulations (using the ABAG model). The latter two methods give indication of "potential" crashworthiness (protection provided by the vehicle structure, given the presence of a nearly ideal restraint system).

A consistent trend of increased potential occupant survivability with increasing vehicle weight was seen (32% increase in protection from 1700 to 4800 pounds). Furthermore, potential occupant protection was found to be highly dependent upon the structural response of the vehicle. In general, vehicles showing potential for superior protection experienced large dynamic crush values, and had occupant compartment responses characterized by long pulse durations, low accelerations early in the crash event, and late peak accelerations.

Characteristics of Non-Aggressive Vehicles -- Frontal Collisions

Three fullsize passenger cars and one crashworthy subcompact car (VW Rabbit) were selected for car/car crash testing. One of the fullsize cars (AMC Concord) was hypothesized to be structurally aggressive, and two (Oldsmobile Cutlass and Mercury Marquis), structurally non-aggressive, on the basis of fixed rigid barrier test results. Each large car was crashed full-frontally into the Rabbit, and two of the three large cars were crashed into the Rabbit in a half-offset frontal mode. Crash test results were analyzed to test the initial hypothesis regarding relative aggressiveness of the

(Continue on additional pages)

"PREPARED FOR THE DEPARTMENT OF TRANSPORTATION, NATIONAL HIGHWAY TRAFFIC SAFETY ADMINISTRATION UNDER CONTRACT NO.: _____ . THE OPINIONS, FINDINGS, AND CONCLUSIONS EXPRESSED IN THIS PUBLICATION ARE THOSE OF THE AUTHORS AND NOT NECESSARILY THOSE OF THE NATIONAL HIGHWAY TRAFFIC SAFETY ADMINISTRATION."

large cars, and to determine vehicle characteristics associated with structural aggressiveness. Dummy measurements, RSD calculations and ABAG simulations were used in the analysis.

The Concord was found to be significantly more aggressive than the Marquis or Cutlass in the full frontal collision with the Rabbit. The Concord was also more aggressive than the Cutlass in the offset collision mode, although the aggressiveness difference was considerably less than in the full frontal tests. The greater front structural stiffness of the Concord was suspected to be the primary cause of the aggressiveness difference.

The aggressiveness difference hypothesized from the fixed rigid barrier tests was confirmed in the car/car tests, providing evidence of a relationship between structural response parameters in a barrier collision and aggressiveness exhibited in a frontal car/car collision. In the barrier tests, the aggressive Concord experienced a small crush value, and had an occupant compartment response characterized by a short pulse duration with acceleration rising rapidly to an early peak value. In contrast, the less aggressive Cutlass and Marquis had large crush values (approximately 45% greater than the Concord), and responses with long pulse durations (about 30% longer), low accelerations early in the crash event, and late peak accelerations (about 65% later).

From the results of the analysis of the New Car Assessment tests, previously described, it appears that the characteristics of crashsurvivable and non-aggressive vehicles are the same. In fixed rigid barrier crash testing, both exhibit large crush values and long-duration occupant compartment responses, with low accelerations early in the event and late (but not necessarily low) peak values.

Crashworthiness Measurement -- Fixed Rigid Barrier

Responses in three different subject vehicles resulting from fixed rigid barrier collisions were compared with responses measured in the same subject vehicles when struck full frontally by other (larger) vehicles. The objective was to determine how well the occupant responses in full frontal car/car collisions can be expected to be simulated in fixed rigid barrier collisions. The level of occupant protection was determined (or inferred) from occupant compartment responses, dummy measurements, steering column behavior, RSD calculations and ABAG simulations.

It was found that most of these responses and indicators of occupant protection agreed closely between the fixed rigid barrier and car/car collisions, if the impact velocities were chosen such that the energy dissipated by the subject vehicle was the same in both the barrier test and the car/car tests. It was concluded, therefore, that the fixed rigid barrier is an accurate crashworthiness-measuring device for high speed full frontal car/car collisions, if test velocities are chosen on the basis of equivalent energy dissipation.

Aggressiveness Measurement

In a previous section, it was determined that a significant aggressiveness difference existed between the AMC Concord (aggressive) and the Mercury Marquis (non-aggressive). These two cars were crashed into three different barriers to determine which measurements from the three barrier tests best correlated with the degree of aggressiveness of the large cars, and thereby provided the best measure of aggressiveness.

The three barriers were the fixed rigid barrier (FRB), fixed load cell barrier (FLCB), and moving deformable barrier (MDB). The FLCB consisted of a load cell barrier unit which contained 36 independent loading surfaces, each of which transmitted force through a single load cell. The unit was attached to a standard FRB. It did not deform under load, providing essentially identical loading to a vehicle as did the FRB, but allowed load distribution over the vehicle's front surface to be measured with a high degree of resolution.

The MDB, developed primarily for side impact testing, contained a crushable front portion constructed of aluminum honeycomb. It was designed to provide crush characteristics similar to a typical domestic automobile.

Differences in responses of the two cars (acceleration pulse shape and duration, and maximum crush) were somewhat greater in the FRB and FLCB tests than in the MDB tests. Barrier load cell data from the FLCB collisions revealed substantial differences in load distribution and time-phasing between the two cars. The Concord's stiffness was more centrally concentrated and forces peaked much earlier. Energy levels in the MDB collisions were probably too high. Bottoming of the honeycomb occurred over a large area of the barrier face in the Concord collision and it appeared that the Marquis nearly caused bottoming. Thus, maximum barrier crush values were nearly the same in the two tests. Evidence of the Concord's more centrally located stiffness and the Marquis' more uniform stiffness distribution was seen, confirming results of the FLCB tests.

The three barriers were approximately equal in their ability to discriminate structural aggressiveness differences between the Concord and the Marquis. The FRB and the FLCB produced a somewhat greater response difference between the two cars than did the MDB. Both the FLCB and the MDB demonstrated their potential for measuring stiffness distribution over the front area of the vehicles. However, it could not be determined how significant the observed stiffness distribution differences were with respect to aggressiveness.

It is recommended that, in further car/MDB testing, vehicle impact velocities be reduced from what they were in the Concord and Marquis MDB collisions. This will prevent bottoming of the barrier's honeycomb face and will reduce the amount of energy being dissipated by the car to a more reasonable value.

In this study, test results from only two vehicles (Concord and Marquis) were evaluated to indicate how structural aggressiveness might best be measured. It is recognized that additional testing with later model year vehicles will be necessary to firmly establish a reliable aggressiveness-measuring test methodology. It is important that these tests include enough frontal offset collisions to enable determination of the significance of frontal stiffness distribution on aggressiveness. If not significant, the importance of measuring stiffness distribution would be greatly diminished, and use of the simple FRB test for measuring aggressiveness may be sufficient.

Front Stiffness Distribution -- Side Collision

It has been postulated that occupant injury severity in car-to-car side collisions may be a function of the frontal stiffness distribution of the striking car. Several car/load cell barrier crash tests were analyzed in order to determine how much difference exists in the frontal stiffness distributions of similar weight cars.

Significant differences were found in the frontal force distributions between the Citation and the Fairmont in 30° frontal collisions. The Citation was much stiffer than the Fairmont on the left front corner, and was softer in the center, due primarily to stiffness differences at the bumper level.

It is recommended that frontal stiffness distribution differences among vehicles be further explored, and that the effects of these differences on side impact struck car occupant injury severity be investigated. This could be done by component testing, sled testing, and/or crash testing with either car/car or MDB/car impacts.

1.0 INTRODUCTION

This report presents the results of Project SRL-20, "Vehicle Aggressiveness and Compatibility," conducted at the Vehicle Research and Test Center (VRTC) of the National Highway Traffic Safety Administration. The major emphasis of this research related to two tasks of the Agency's Frontal Crash Protection program. These two tasks were determination of vehicle structural characteristics and test procedure development.

Results of the following activities contribute to the accomplishment of the vehicle structural characteristics task. First, the characteristics of passenger cars having superior crashsurvival potential were identified, through detailed analysis of 35 mph barrier crash test data used in conjunction with simple occupant models. Second, the characteristics of large passenger cars which make them relatively non-aggressive to smaller cars in frontal collisions were identified. Finally, characteristics responsible for good crashsurvivability and low aggressiveness were compared.

Two studies were conducted which contributed to the accomplishment of the test procedure development task. First, an evaluation was performed of how well the standard fixed rigid barrier measures the crashworthiness of small cars involved in car/car collisions. And secondly, three different crash barriers were evaluated for their ability to measure frontal structural aggressiveness.

All of the work addressing frontal crashworthiness and aggressiveness involved restrained front seat occupants.

A secondary emphasis of Project SRL-20 had application to the vehicle structural characteristics task of the Agency's Side Protection program. A study was made of how the front structural stiffnesses of vehicles were distributed over the vehicles' frontal areas. Recommendations were made on determining the effect of stiffness distribution differences among striking vehicles on occupant survivability in struck vehicles.

2.0 FRONTAL PROTECTION -- VEHICLE STRUCTURAL CHARACTERISTICS

2.1 Characteristics of Crashsurvivable Vehicles

2.1.1 Introduction:

An analysis of 35 mph frontal barrier crash tests, conducted under the Agency's New Car Assessment Program, was performed for the following purposes:

- 1) To determine the degree and variability of frontal crashsurvivability of cars in all weight classes using Restraint Survival Distance (RSD) calculations and occupant/airbag simulations (using the ABAG model) to supplement dummy measurements.
- 2) To find general reasons for enhanced crashworthiness exhibited by some of the vehicles by looking at such factors as the shape of the vehicle acceleration-time pulse.
- 3) To provide general recommendations regarding the selection of vehicles to be modified as future demonstration vehicles.

This analysis was not conducted to determine rating information or crashworthiness comparisons among vehicles; therefore, the names of the vehicles have been omitted, and they have been identified only by a letter or number designation.

2.1.2 Data Processing

The data analyzed in this study were obtained from digital magnetic computer tapes and reports of New Car Assessment and Standards Enforcement Indicant Tests conducted by three contractors. The vehicles included in the study are primarily 1979 model cars. The data obtained from the crash tests included occupant responses and vehicle accelerations.

The longitudinal compartment acceleration data were obtained from accelerometers located below the front seat, below the rear seat, or at the vehicle center of gravity. All compartment acceleration data were digitally processed at the

VRTC through a phaseless, low pass Butterworth filter with a 40 Hz cutoff frequency and -40dB attenuation at a stop band frequency of 127 Hz. The 40 Hz filter was chosen as the lowest frequency which eliminated extraneous high frequencies while preserving the fundamental crash pulse features (such as pulse duration and dynamic crush). Higher frequency components of the compartment responses were not judged to contribute to the occupant response. Unfortunately, however, the analog filtering of the data at the contractor sites was not uniform (although conforming to SAE J211 recommended filtering practice) for all crash tests, resulting in errors for the indicated time zero for some tests. For each of those tests, the acceleration pulse was shifted prior to digital filtering to allow the initial rise in acceleration to correspond to time zero. The acceleration pulse was then examined to insure that the velocity change for the test was within reason.

Summarized in Table 1 are the dynamic crush differences between the contractor and VRTC which resulted from the detailed compartment pulse examination described above. Static crush values were not used in this analysis due to uncertainties which were encountered in extracting these values from the test reports (see Appendix A).

2.1.3 Measurement of Occupant Protection

Three methods were used in this study for determining occupant protection: dummy measurements, Restraint Survival Distance (RSD) calculations and advanced restraint system modeling with the ABAG computer model. Dummy responses provide a measure of "actual" crashworthiness, while the other two methods give a good indication of "potential" crashworthiness (i.e., occupant protection that theoretically would be provided by the vehicle if it contained a more nearly ideal restraint system).

The use of dummy measurements is the most direct method of determining occupant crash survival. Occupant injury severity indicators derived from dummy measurements are dependent upon the crash pulse (crash severity), compartment integrity, and performance of the occupant restraint and containment system. They are, however, subject to some degree of variation due to variables such as placement of the surrogate within the restraint system, positioning of the seat, etc. And, because they are dependent upon the restraint system, dummy measurements do not allow determination of the potential for occupant protection that would exist in a particular vehicle structure if a different restraint system were installed in the vehicle.

TABLE 1
Comparison of Contractor and VRTC Dynamic Crush Data

CLASS	VEHICLE		VRTC CHANNEL SELECTED	TEST CONTRACTOR	DYNAMIC CRUSH -- IN.	
	YEAR	SYMBOL			VRTC	CONTRACTOR
Mini-Compact	1979	A	Front	Calspan	25.7	24.5
	1979	B	Rear	Dynamic Science	31.5	32.5
	1979	C	Rear	Calspan	29.5	28.1
	1979	D	Rear	Dynamic Science	28.7	31.0
Sub-Compact	1979	E	Rear	Dynamic Science	28.6	32.4
	1979	F	Rear	Calspan	28.8	27.3
	1979	G	Rear	Calspan	31.0	28.5
	1979	H	Rear	Dynamic Science	37.3	34.8
	1979	I	Front	Dynamic Science	35.8	35.6
Intermediate	1979	J	Rear	Dynamic Science	26.7	31.0
	1979	K	Front	Calspan	30.7	29.7
	1980	L	Front	Calspan	31.6	30.6
	1979	M	Front	Calspan	29.7	30.0
	1979	N	Front	MSE	30.3	31.1
	1980	O	Rear	Calspan	23.8	22.8
	1979	P	Rear	Calspan	31.5	30.7
	1979	Q	Rear	Dynamic Science	34.8	38.0
	1979	R	Rear	Dynamic Science	35.1	41.2
Standard	1979	S	Rear	Calspan	31.5	38.8
	1979	T	Front	Calspan	31.0	31.2
	1979	U	Rear	Dynamic Science	27.9	32.7
	1979	V	Front	Dynamic Science	38.4	38.3
	1979	W	Front	Calspan	35.7	34.2
	1979	X	Rear	Calspan	33.6	33.0
	1979	Y	Rear	Dynamic Science	32.8	37.4
	1979	Z	Front	Dynamic Science	32.7	34.4
	1979	2	Rear	Dynamic Science	33.5	37.9
	1979	3	Front	Dynamic Science	39.2	39.9
	1979	4	Rear	Dynamic Science	41.1	39.4

Restraint Survival Distance (RSD) is a useful indicator of the potential for occupant crash survival. The RSD is the occupant stroking distance remaining after the crash, and is defined as

$$RSD = AID - (D_p - D_c), \quad [1]$$

where:

AID is the Available Internal Distance (i.e., the distance between occupant and interior vehicle surfaces); and

D_p and D_c are the distances represented by the areas under the dashed and solid curves, respectively, in the interval between t_0 and t^* , of Figure 1. t^* is the time beyond which the vehicle velocity exceeds the maximum human tolerance velocity and ridedown occurs.

The quantity $D_p - D_c$ can be thought of as the minimum amount of internal distance required to safely bring the occupant's velocity down to the vehicle's velocity. Defined as the Required Internal Distance (RID), it is represented by the shaded area in Figure 1. Beyond t^* , it is assumed that the occupant can safely ride down the vehicle for the remainder of the crash. It is clear from equation [1] that minimizing the RID (i.e., the quantity $D_p - D_c$) serves to maximize the RSD (and also the crashworthiness). If the computed RSD is a positive number, it indicates that the available internal distance exceeded the required internal distance. If negative, it indicates that the available distance was not sufficient to adequately protect the occupant. The derivation of RSD is contained in Reference 1.

The parameters needed to define the occupant's velocity-time response (the dashed line of Figure 1) are restraint system deployment time, maximum tolerable acceleration rate and maximum tolerable acceleration level. For this study, the values used were 30 milliseconds, 3000 g's/second and 60 g's, respectively.

The ABAG computer model provides prediction of the degree of occupant crash survival that would result from equipping the vehicle with an airbag restraint system. The model is a one-dimensional program which simulates the cushioning of an occupant's torso with an airbag that is being simultaneously inflated and vented. The program utilizes the vehicle crash pulse to produce occupant acceleration, velocity, and displacement time histories. Unfortunately, the model does not account for compartment integrity and, therefore, occupant injury which might result from intrusion.

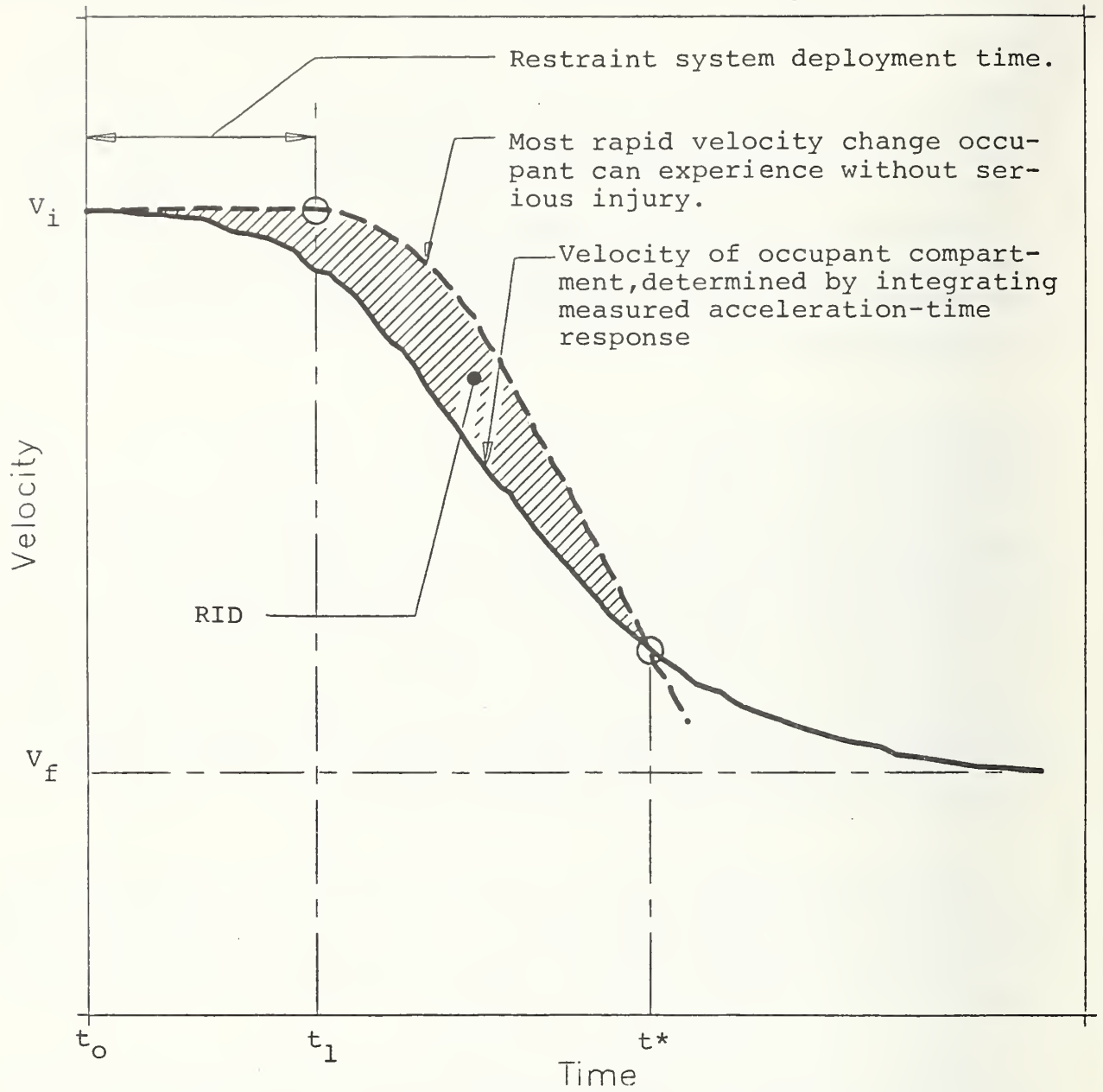


FIGURE 1. Velocity-Time Responses of Vehicle and Occupant.

The approach in this study was to utilize the ABAG program to differentiate between different crash pulses (i.e., different vehicles) by simulating "standard" driver and passenger air cushion restraint systems. No effort was made to optimize the ABAG parameters for each individual vehicle.

Prior to selecting the ABAG model for this analysis, an extensive evaluation was made of two different occupant models: ABAG and HSRI-3D. The objective was to define a revised set of input parameters for each of these models which would allow the prediction of occupant survivability in many different vehicles. It was generally concluded that, using revised input parameter values derived from 35 mph barrier crash test data, both the ABAG and HSRI-3D models provided reasonably accurate simulations of driver and passenger responses. Although the models are about equal in their simulation capability, the ABAG model was felt to be more suitable for use in comparing overall crash survivability levels in different vehicles, because of its simplicity, ease of use and better documentation; and the HSRI-3D model was felt to have greater potential for use in detailed modeling in a particular vehicle for design purposes, because of the more detailed input parameter requirements. A summary of the model evaluation study appears in Appendix B. The complete study is contained in Reference 2.

An advantage of the RSD calculation and the ABAG simulation is that they allow determination and comparison of the potential for occupant protection provided by different vehicle structures, all containing the same "idealized" restraint system.

2.1.4 Results

The analysis results are presented and discussed according to the vehicle weight category. The vehicles were categorized by curb weights as shown in Table 2.

TABLE 2
Weight Categories

NUMBER	CLASSIFICATION	WEIGHT
1	Mini-Compact	Below 2,150 pounds
2	Sub-Compact	2,150 to 2,650 pounds
3	Intermediate	2,651 to 3,350 pounds
4	Standard	Above 3,350 pounds

2.1.4.1 Dummy Measurements

The crash test parameters and dummy measurements are summarized in Table 3. Driver and passenger HIC measurements and peak chest accelerations are presented in Figures 2-5. Each vehicle is represented by a symbol (letter or number) which corresponds to that in Table 3. A least squares line was fit to the data in each figure. Three observations were immediately apparent:

- 1) There was a very large amount of variability among vehicles, especially in HIC.
- 2) There was a slight trend of improved occupant protection in the larger vehicles.
- 3) There were a large number of vehicles in which occupant injury criteria were exceeded. (In fact, the least squares lines for HIC for both occupants are higher than 1000 over most of the weight range.)

An attempt was made to identify the "best" and the "worst" vehicles in terms of occupant head and chest protection, and to determine whether or not good and poor occupant protection could be correlated with any occupant compartment response characteristics. In each of Figures 2-5, the five vehicles whose injury measures were the furthest distances above the least squares line were singled out. Similarly, the five vehicles whose injury measures were the furthest distances below the least squares line were identified. Then those vehicles appearing more than once among the "best five" (or the "worst five") were listed. The result of this exercise is shown in Table 4. Although somewhat arbitrary, this scheme identified two distinctly different groups of vehicles in terms of measured occupant protection.

The crash responses of these ten vehicles were then examined, in hopes of identifying features which appeared to correlate with good or poor protection.

Table 5 shows average dynamic crush values for the two groups of vehicles, along with the overall average for all vehicles. It is seen that the "best five" vehicles had a slightly greater average crush than did the "worst five" vehicles, even

TABLE 3
Crash Test Parameter and Dummy Measurement Summary

VEHICLE			Curb Wt. (lbs)	Test Wt. (lbs)	Crash Vel. (mph)	Dynamic Crush (in)	DRIVER				PASSENGER				
Class	Year	Symbol					Head Acc. (g)	HIC	Chest Acc. (g)	Femur Loads	Head Acc. (g)	HIC	Chest Acc. (g)	Femur Loads	
Mini-Compact	1979	A	1690	2180	34.8	25.7	116.0	2029.6	92.6	1080/838	142.0	2093.3	46.0	1520/1460	
	1979	B	1830	2313	35.3	31.5	127.1	1270.2	72.1	893/435	207.0	1919.4	66.3	686/561	
	1979	C	1860	2600	34.8	29.5	90.0	1023.9	67.0	1170/630	47.0	428.8	33.0	937/1460	
	1979	D	1960	2425	35.1	28.7	122.4	1358.0	68.9	-1536	183.7	1745.0	59.4	781/2183	
Sub-Compact	1979	E	2206	2661	34.9	28.6	91.9	652.7	51.6	974/708	69.9	780.4	38.2	580/657	
	1979	F	2240	2720	34.8	28.8	118.0	871.4	47.0	1280/1600	88.0	858.6	45.0	990/1400	
	1979	G	2510	3025	34.8	31.0	94.0	848.8	61.0	2920/435	158.0	1862.0	59.0	400/520	
	1979	H	2515	2943	34.7	37.3	122.0	818.6	41.1	221/946	73.0	567.1	33.1	781/376	
	1979	I	2629	3067	35.0	35.8	NA	NA	NA	1322/NA	131.3	770.2	44.3	676/397	
	1979	J	2707	2998	35.1	26.7	58.8	723.3	64.2	463/1343	247.4	1877.5	51.4	741/571	
Intermediate	1979	K	2730	3240	35.1	30.7	103.0	1107.6	42.0	580/400	87.0	1032.6	41.0	600/325	
	1980	L	2750	3260	35.0	31.6	79.0	845.0	48.0	560/760	64.0	623.0	34.5	1040/350	
	1979	M	2820	3300	35.4	29.7	102.0	939.4	54.0	825/1155	94.0	1583.2	85.0	1245/600	
	1979	N	2890	3374	35.0	30.3	79.0	1782.0	52.0	320/900	168.0	1889.0	61.0	700/320	
	1980	O	3130	3700	34.7	23.8	94.0	1077.8	61.0	1300/910	79.0	1457.2	39.0	375/337	
	1979	P	3260	3820	35.0	31.5	74.0	724.2	40.0	1000/1000	200.0	1677.2	40.0	1200/570	
	1979	Q	3298	3799	34.8	34.8	71.1	694.6	41.5	1130/2082	50.3	500.5	39.7	567/562	
	Standard	1979	R	3390	3908	35.2	35.1	74.2	964.5	42.2	582/472	74.4	1297.0	46.8	503/717
		1979	S	3490	3950	34.6	31.5	110.0	1441.6	61.0	1750/350	99.0	1278.6	56.0	390/570
		1979	T	3600	4160	35.0	31.0	235.0	2402.4	45.0	740/300	102.0	1070.8	39.0	420/440
1979		U	3659	4179	35.2	27.9	240.7	1277.0	61.8	580/804	123.2	1254.0	51.1	670/391	
1979		V	3695	4224	35.4	38.4	158.2	1204.4	60.8	368/802	90.0	868.2	42.4	378/---	
1979		W	3790	4370	35.4	35.7	143.0	1452.4	38.0	750/180	93.0	616.0	34.0	510/360	
1979		X	3880	4440	35.3	33.6	58.0	645.5	39.0	250/725	58.0	730.7	44.0	360/170	
1979		Y	3935	4457	35.0	32.8	133.6	1908.5	66.7	832/531	102.2	NA	50.3	647/588	
1979		Z	3941	4440	35.3	32.7	104.4	541.0	42.2	943/892	60.4	782.1	39.0	137/---	
1979		2	4187	4709	35.0	33.5	113.3	909.8	59.4	774/534	165.1	1734.2	53.5	370/439	
1979	3	4283	4815	34.9	39.2	150.0	1088.0	61.4	1062/2775	134.0	781.0	40.2	584/429		
1979	4	4846	5362	35.0	41.1	138.7	520.5	44.6	335/393	117.8	919.0	52.5	577/981		

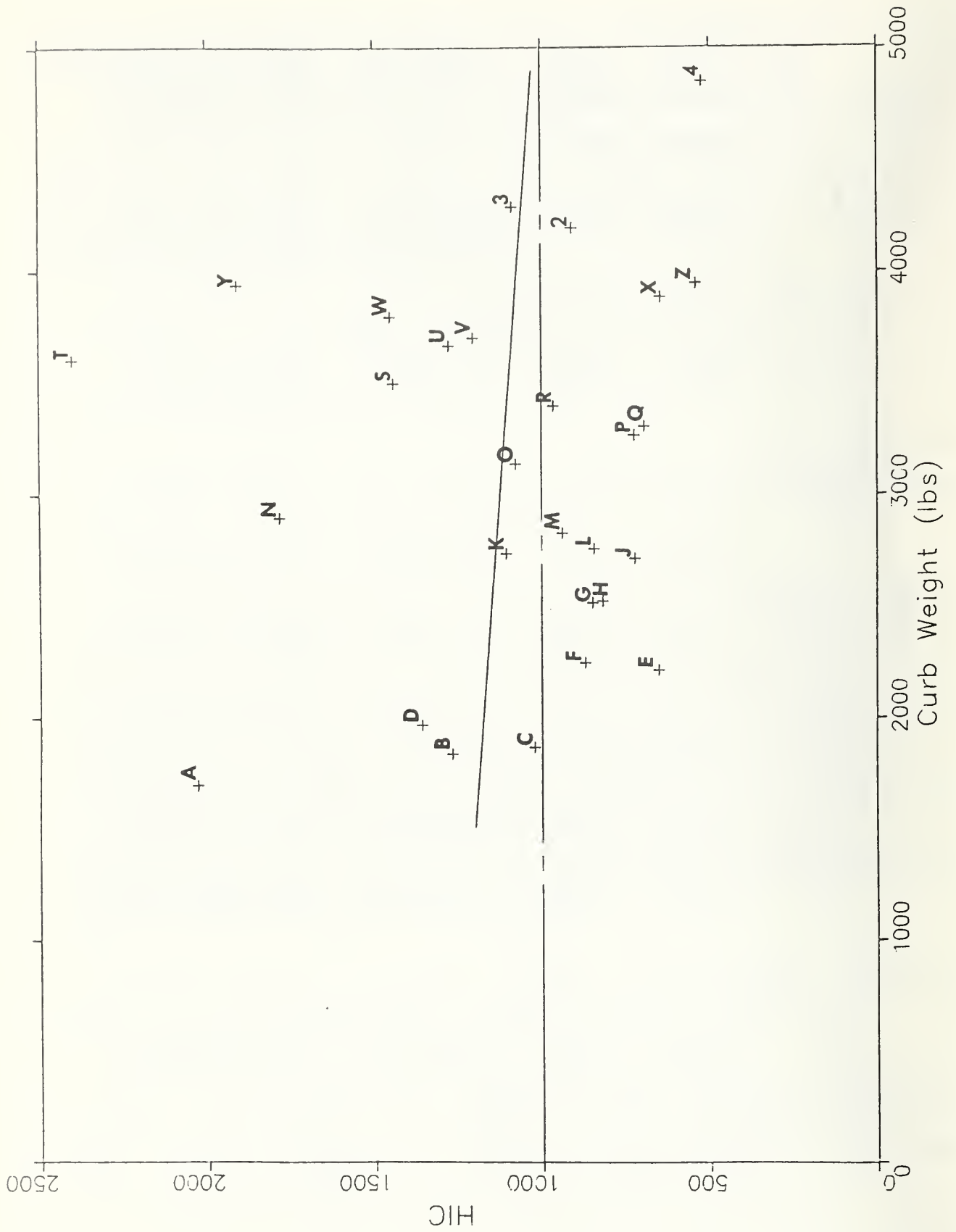


FIGURE 2. Head Injury Criterion Values Determined From Dummy Measurements -- Driver

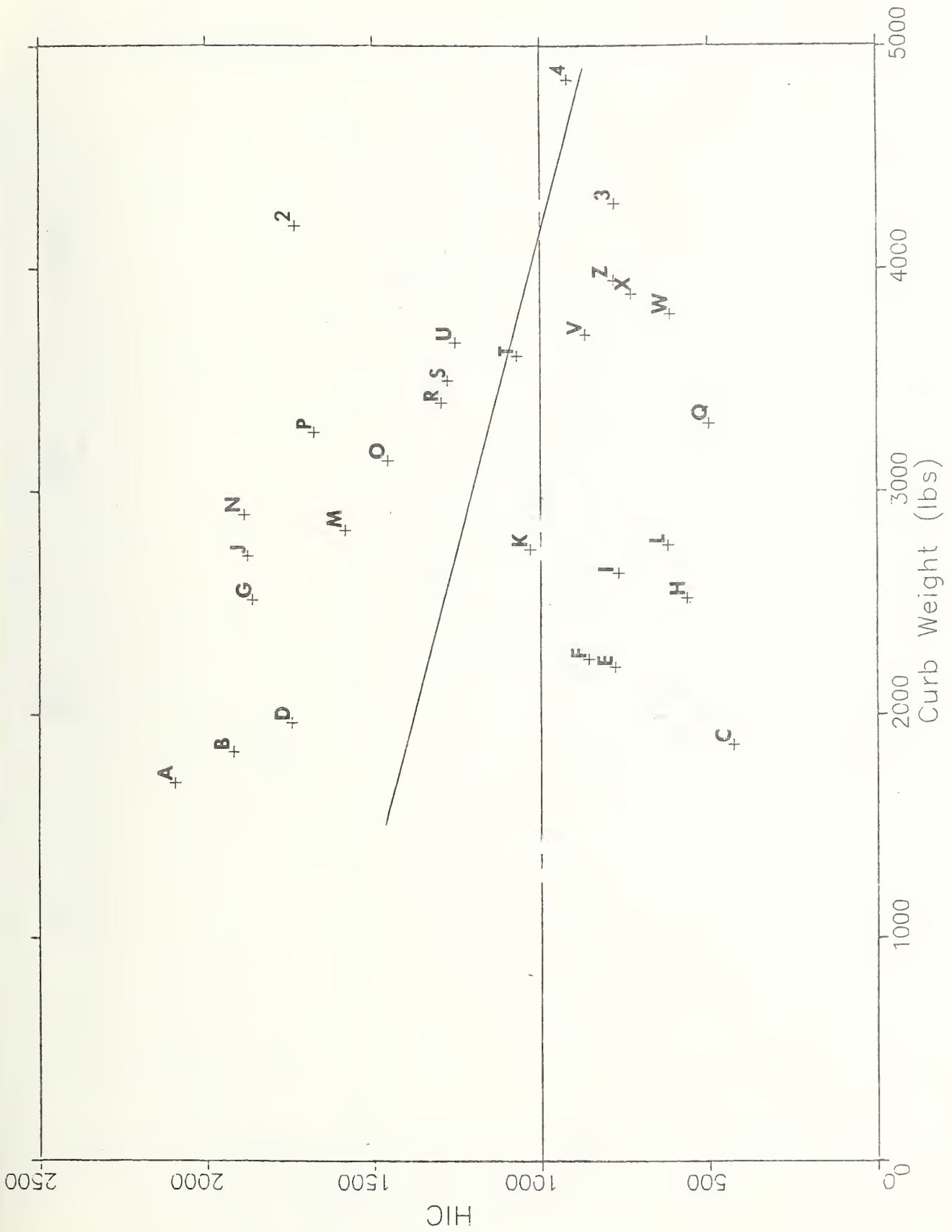
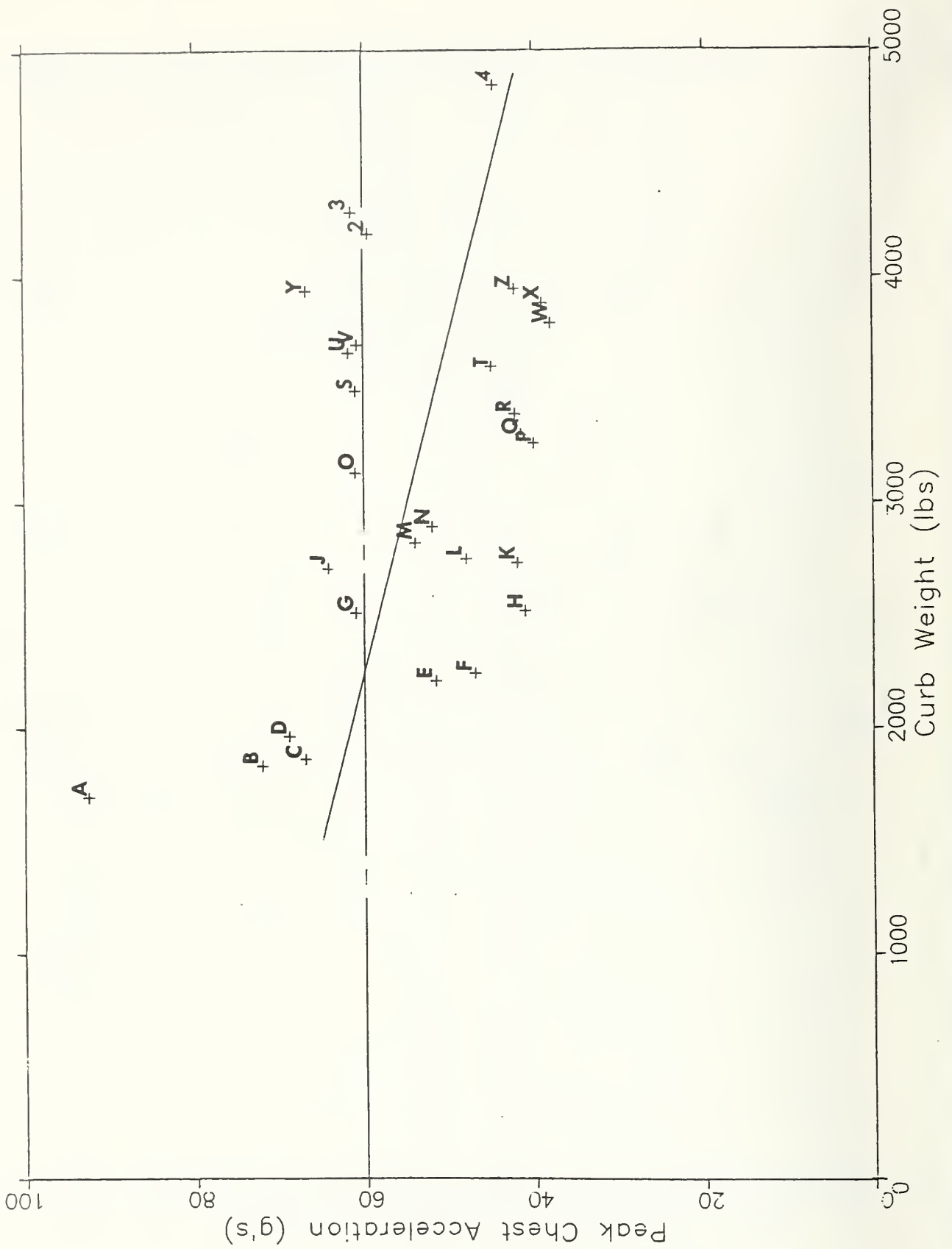


FIGURE 3. Head Injury Criterion Values Determined From Dummy Measurements -- Passenger



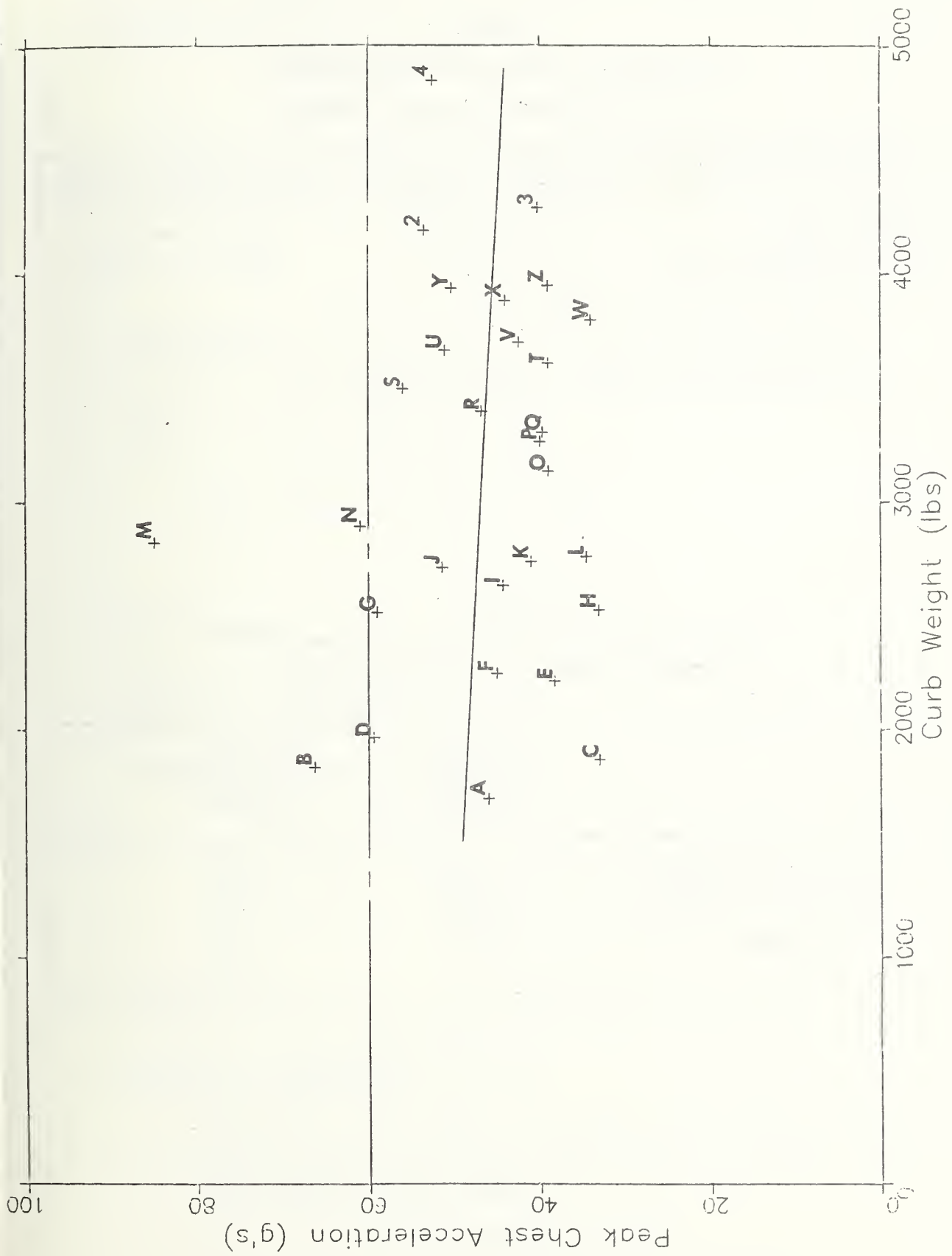


FIGURE 5. Maximum Chest Accelerations Determined From Dummy Measurements -- Passenger

TABLE 4
 Identification of "Best" and "Worst" Vehicles
 in Terms of Measured Occupant Protection

DUMMY MEASUREMENT	"BEST FIVE" VEHICLES	"WORST FIVE" VEHICLES
Driver HIC	E J X Z 4	A N T W Y
Passenger HIC	C E H L Q	A G J N 2
Driver Peak Chest Accel.	F H K P W	A U Y 2 3
Passenger Peak Chest Accel.	C E H L W	B D G M N
<p style="text-align: center;">Vehicles appearing more than once among the "Best Five": C E H L W</p> <p style="text-align: center;">Vehicles appearing more than once among the "Worst Five": A G N Y 2</p>		

TABLE 5
 Dynamic Crush Values of Vehicles Determined to be
 "Best" and "Worst" by Dummy Measurements

	Average Curb Weight (pounds)	Average Dynamic Crush (inches)
"Best Five" Vehicles	2624	32.54
"Worst Five" Vehicles	3042	30.66
All Vehicles	3094	32.02

though they averaged a lighter weight. This would indicate, not unexpectedly, that a softer front structure (resulting in greater crush) is correlated with enhanced occupant protection in a 35 mph barrier collision.

Occupant compartment acceleration- and velocity-time responses for the 10 vehicles are shown in Figures 6-9. Each figure contains the responses of the two or three vehicles within a given weight category. It turned out that each category contained both "good" and "poor" vehicles. Observations were made within each weight category, as follows:

Mini-Compact:

Vehicle A -- "poor" occupant protection.

Vehicle C -- "good" occupant protection.

Vehicle responses were similar in shape, but Vehicle C had a slightly lower peak acceleration, a longer pulse duration, and considerably greater dynamic crush.

Sub-Compact:

Vehicle E -- "good" occupant protection.

Vehicle G -- "poor" occupant protection.

Vehicle H -- "good" occupant protection.

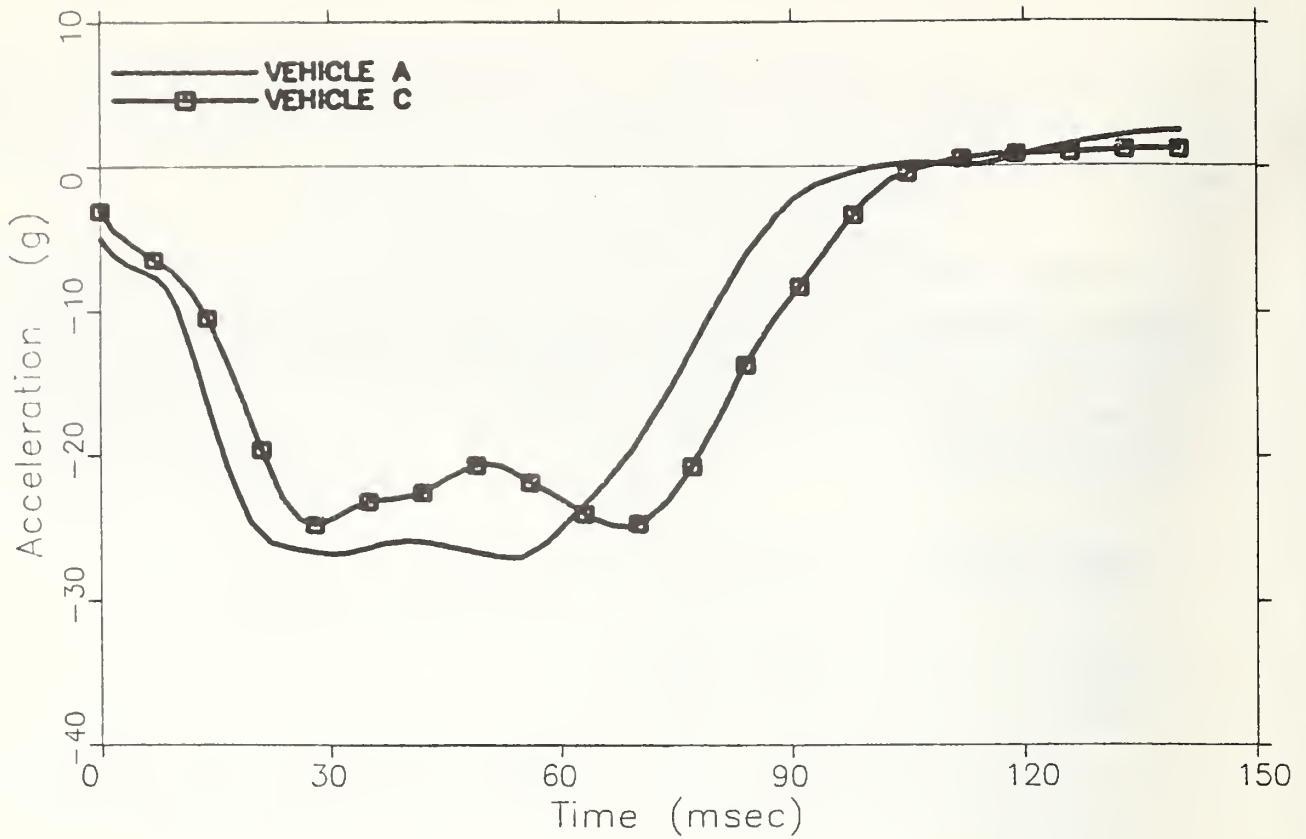
Acceleration responses were quite different in shape. Vehicle G had a considerably higher peak acceleration than the other two cars, and it occurred earlier. Vehicle E had the shortest pulse duration, the smallest dynamic crush, and the smoothest acceleration and velocity response shape.

Intermediate:

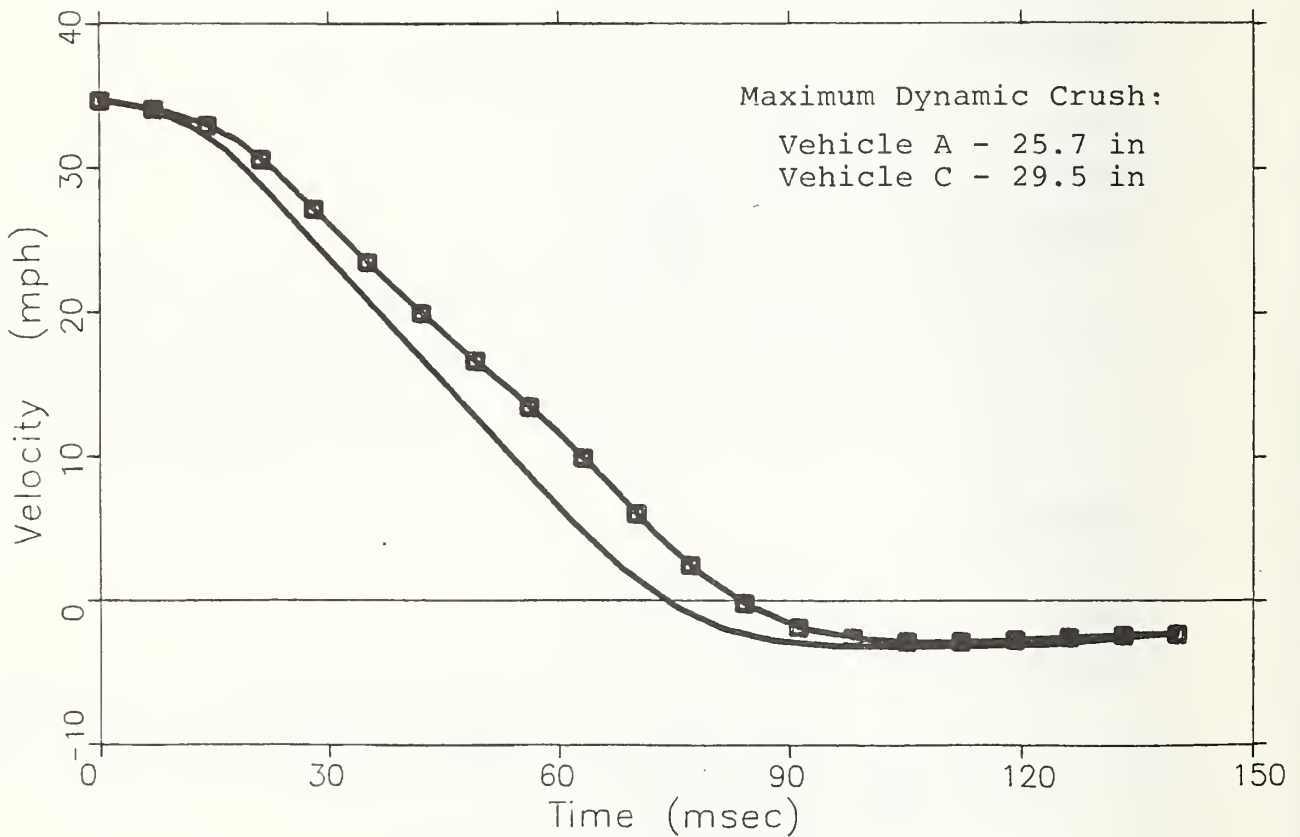
Vehicle L -- "good" occupant protection.

Vehicle N -- "poor" occupant protection.

Acceleration pulse shapes and durations were similar, with the notable exception of the very high peak acceleration for Vehicle N. Vehicle L had slightly greater dynamic crush.

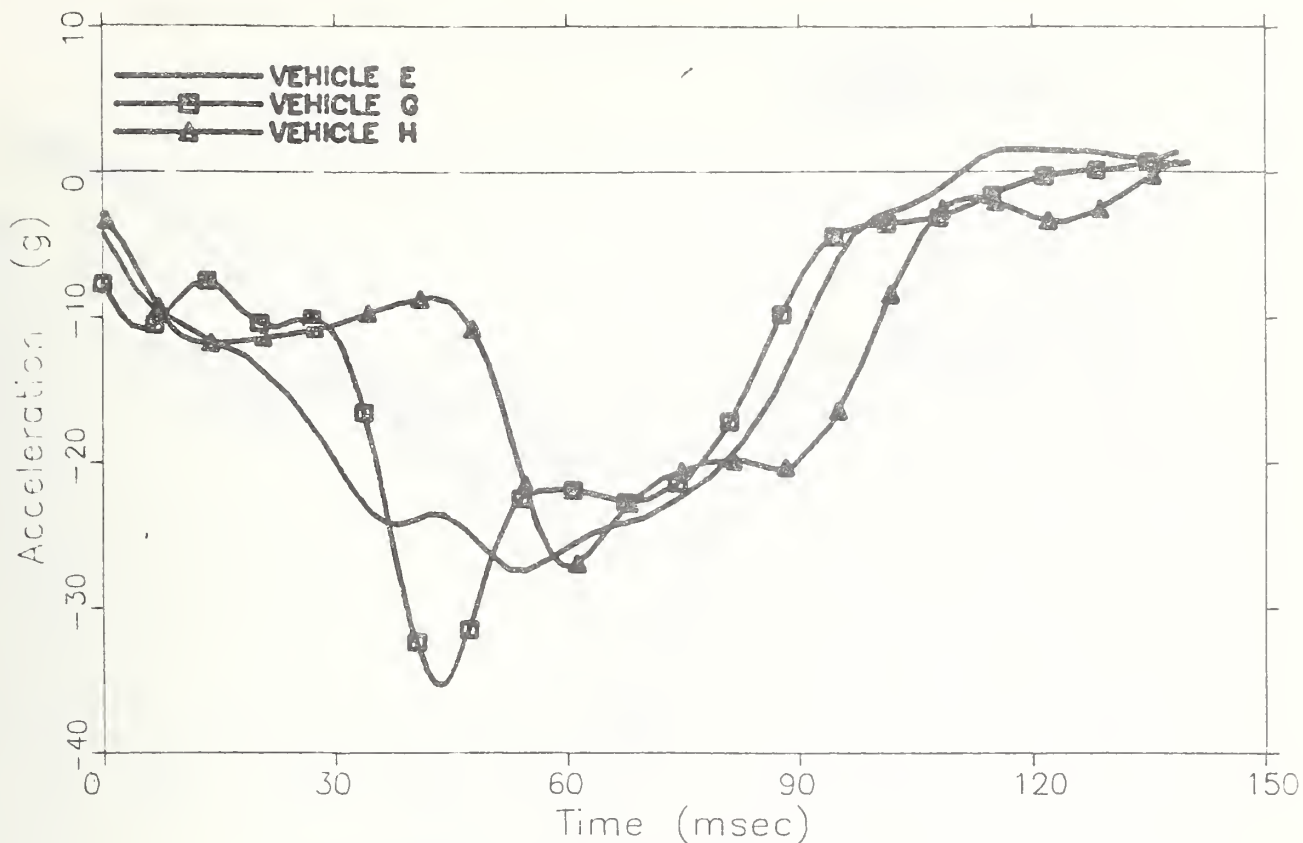


a) Acceleration Response

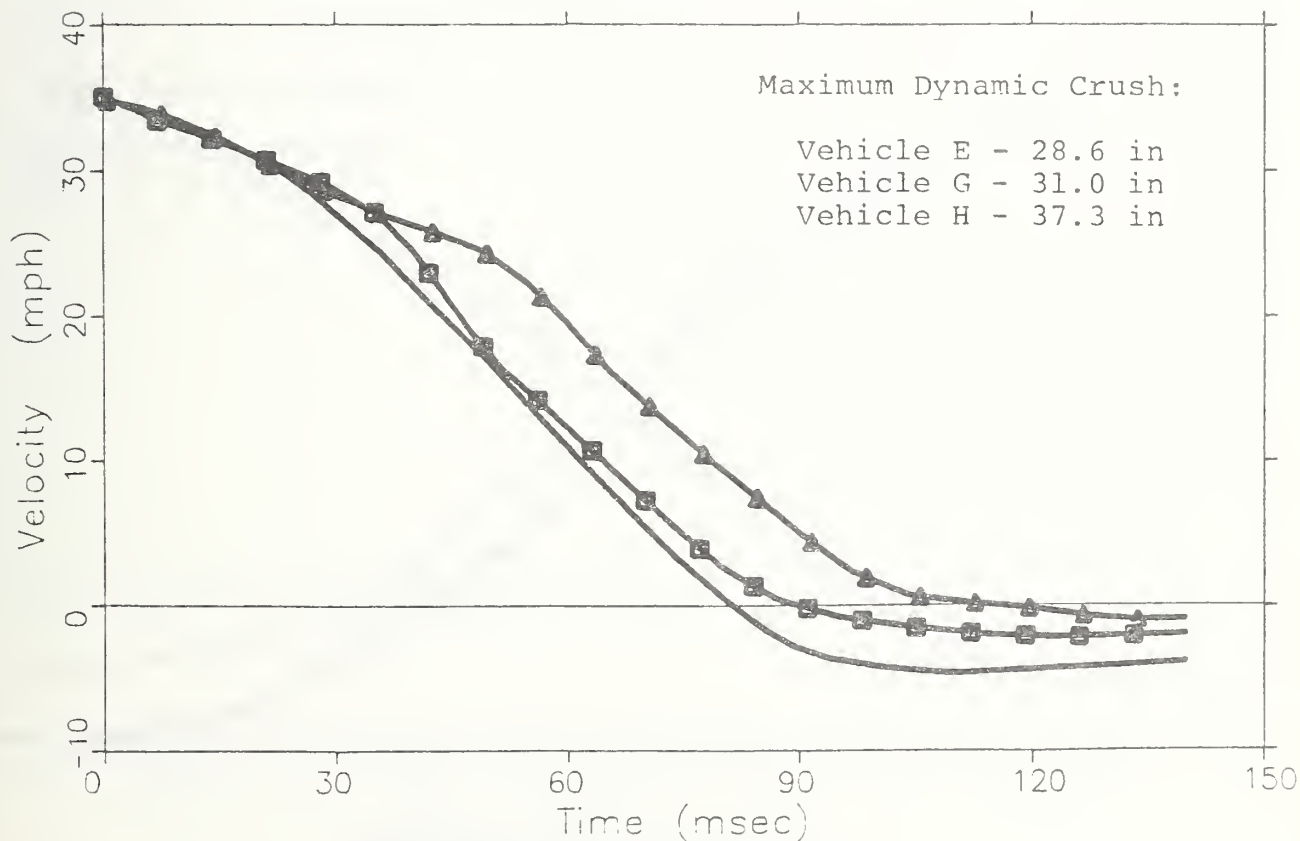


b) Velocity Response

FIGURE 6. Minicompact Vehicle Responses (Dummy Measurement Criteria)

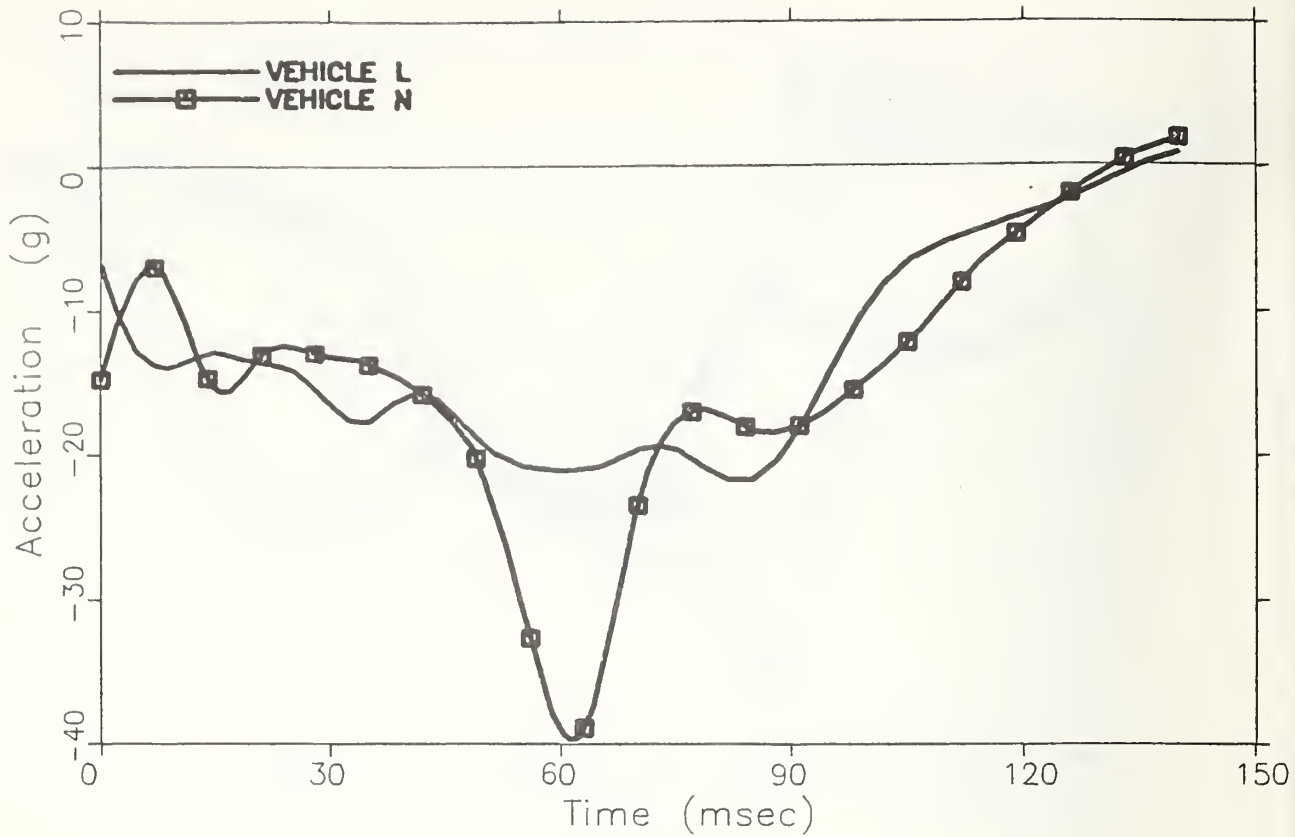


a) Acceleration Response

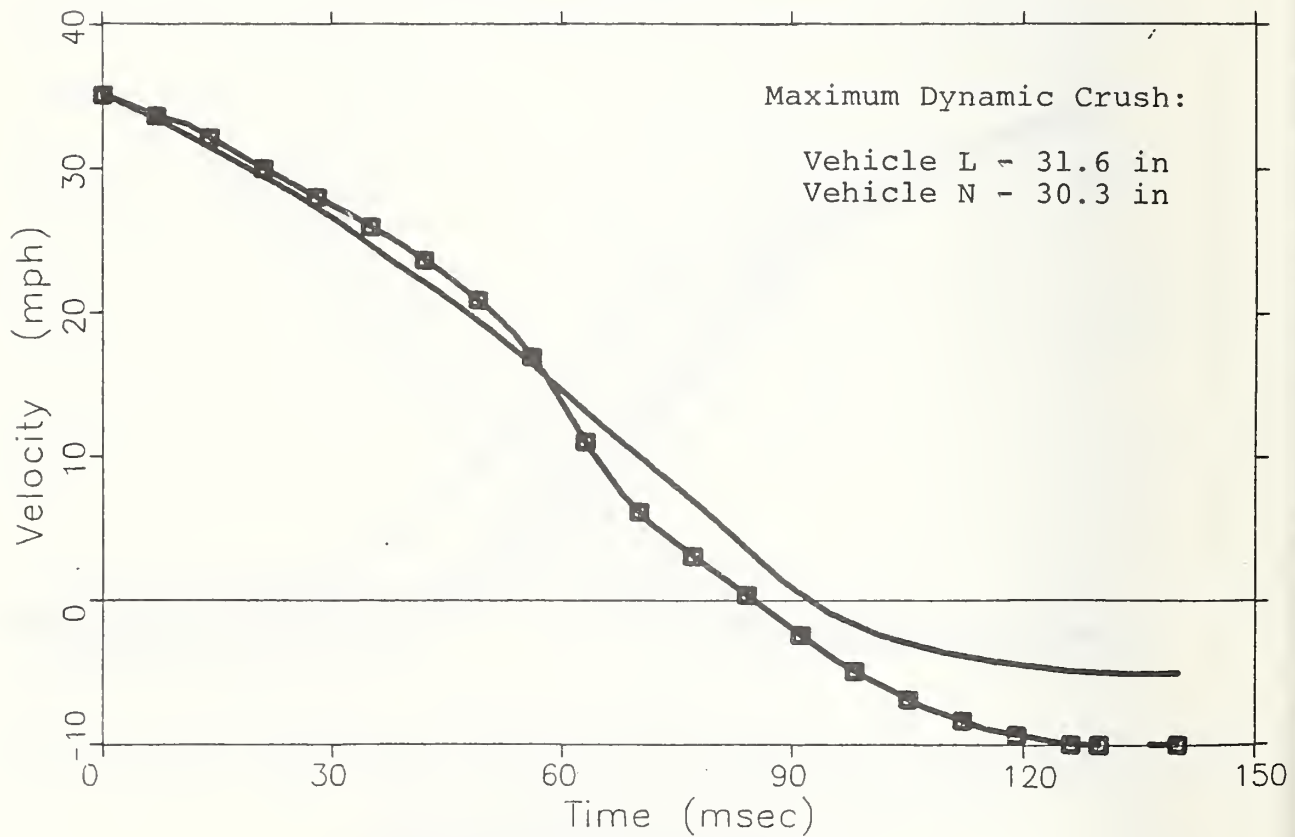


b) Velocity Response

FIGURE 7. Subcompact Vehicle Responses
(Dummy Measurement Criteria)

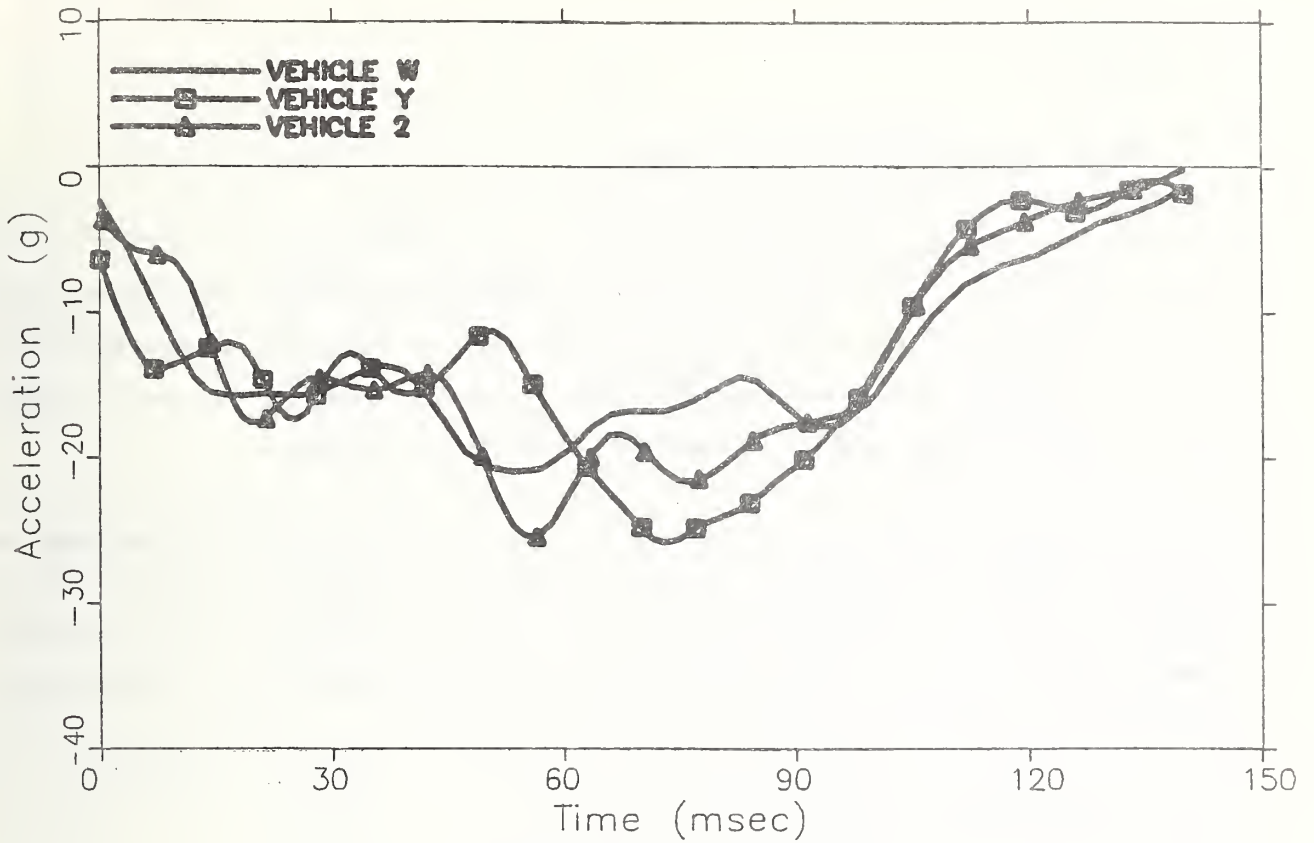


a) Acceleration Response

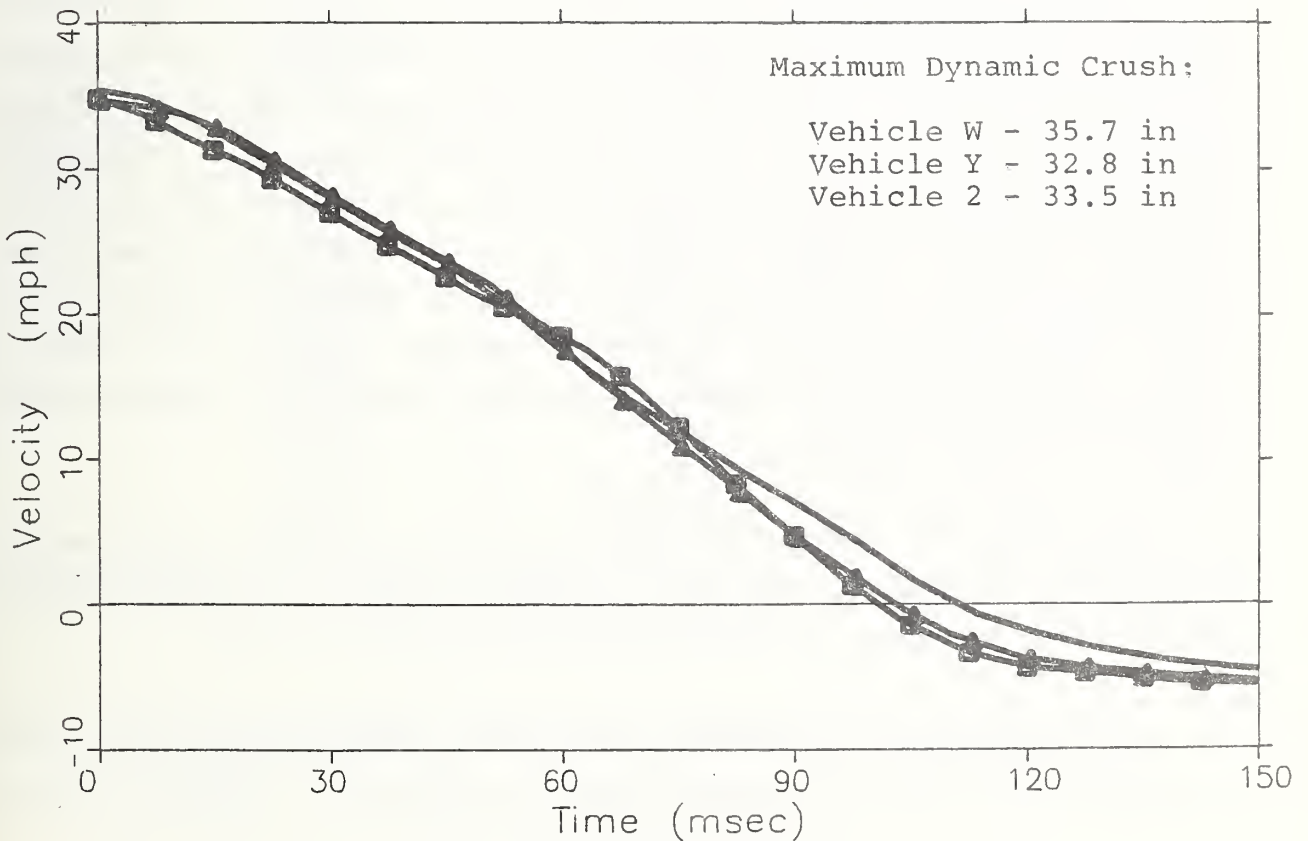


b) Velocity Response

FIGURE 8. Intermediate Vehicle Responses (Dummy Measurement Criteria)



a) Acceleration Response



b) Velocity Response

FIGURE 9. Standard Vehicle Responses (Dummy Measurement Criteria)

Standard:

Vehicle W -- "good" occupant protection.

Vehicle Y -- "poor" occupant protection.

Vehicle 2 -- "poor" occupant protection.

Vehicle W had a somewhat smoother acceleration pulse, with a lower peak value, than the other cars. The velocity-time responses were similar, but Vehicle W had a less rapid change in velocity after 75 ms, and a slightly longer pulse duration, resulting in greater dynamic crush.

In summary, vehicles offering "good" occupant protection generally had longer and smoother acceleration responses with lower peak acceleration and greater dynamic crush values than did vehicles offering "poor" occupant protection. The only exception was Vehicle E, a "good" vehicle, which had a shorter pulse duration and smaller dynamic crush than the "poor" vehicles in its weight category.

2.1.4.2 Restraint Survival Distance Calculations

A problem was encountered in the data analysis which prevented the calculation of the RSD. It was found that there was no uniform way to determine a value for the AID from the test reports. Calspan Corporation provided two measurements which were suitable for AID: CD (dummy chest to dash) and HW (dummy head to windshield). According to the figure provided in their reports, HW was measured from the dummy's forehead. Dynamic Science, Inc. (DSI), presented a table listing two suitable measurements: chest to instrument panel and nose to windshield. Unfortunately, the chest to instrument panel measurement was not recorded in all of the DSI reports; and DSI's nose to windshield measurement was obviously different from Calspan's forehead to windshield measurement.

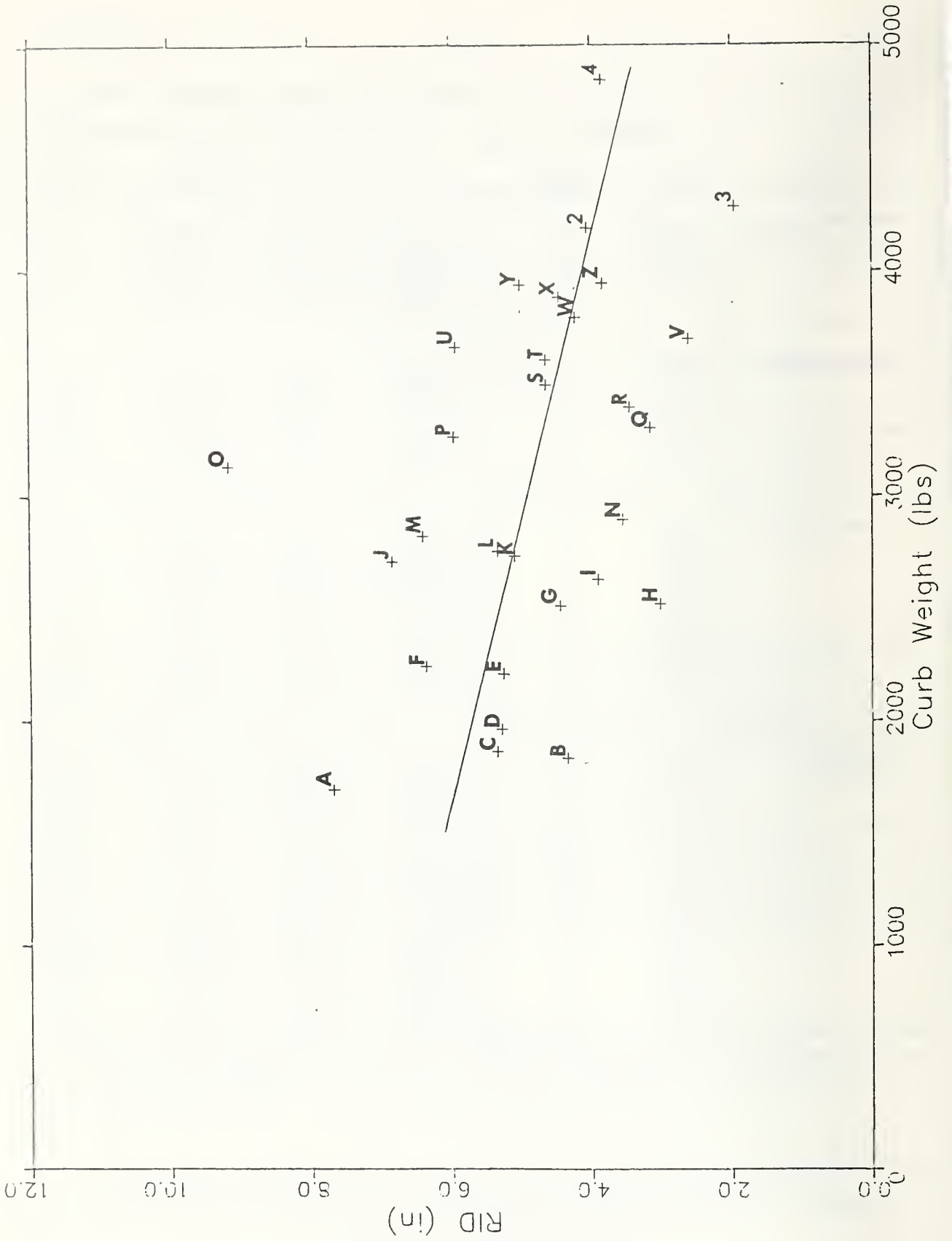
Consequently, only the RID (which is the second term of equation 1) is presented in this analysis. The calculation summary is presented in Table 6, and RID is plotted in Figure 10 for each vehicle. A least squares line has been fit to the data.

It was expected that the variability of RID among vehicles would be much less than that observed for the dummy measurements, since experimental variability inherent in

TABLE 6

Calculation Summary for Minimum Required Internal Distance (RID)

VEHICLE			T* (Sec)	DC (in.)	DP (in.)	RID (in.)
CLASS	YEAR	SYMBOL				
Mini-Compact	1979	A	0.0625	24.35	32.03	7.68
	1979	B	0.0539	26.52	30.87	4.35
	1979	C	0.0564	25.68	31.03	5.35
	1979	D	0.0567	26.21	31.50	5.29
Sub-Compact	1979	E	0.0573	26.08	31.34	5.26
	1979	F	0.0596	25.30	31.66	6.36
	1979	G	0.0552	26.30	30.75	4.45
	1979	H	0.0473	24.87	27.90	3.03
	1979	I	0.0486	24.77	28.68	3.91
Intermediate	1979	J	0.0601	25.22	32.06	6.84
	1979	K	0.0586	26.70	31.80	5.10
	1980	L	0.0536	25.14	30.48	5.34
	1979	M	0.0577	25.53	31.93	6.40
	1979	N	0.0518	25.33	28.89	3.56
	1980	O	0.0641	22.86	32.03	9.17
	1979	P	0.0530	24.34	30.30	5.96
	1979	Q	0.0483	25.22	28.39	3.17
Standard	1979	R	0.0492	25.75	29.21	3.46
	1979	S	0.0545	25.72	30.37	4.65
	1979	T	0.0555	26.37	31.02	4.65
	1979	U	0.0576	25.77	31.70	5.93
	1979	V	0.0465	25.48	28.10	2.62
	1979	W	0.0521	26.15	30.38	4.23
	1979	X	0.0518	25.72	30.18	4.46
	1979	Y	0.0515	24.70	29.71	5.01
	1979	Z	0.0528	26.69	30.53	3.84
	1979	2	0.0503	25.23	29.29	4.06
	1979	3	0.0447	24.90	26.86	1.96
	1979	4	0.0490	25.11	28.95	3.84



obtaining dummy data, and variability due to different belt restraint systems and different occupant compartment geometry among the vehicles are not factors in the determination of RID. However, it is seen that a large amount of variability does exist in RID, indicating that the potential occupant protection capability is very sensitive to the structural response of the vehicle. Also, a definite trend of improved protection capability with increasing vehicle weight can be observed.

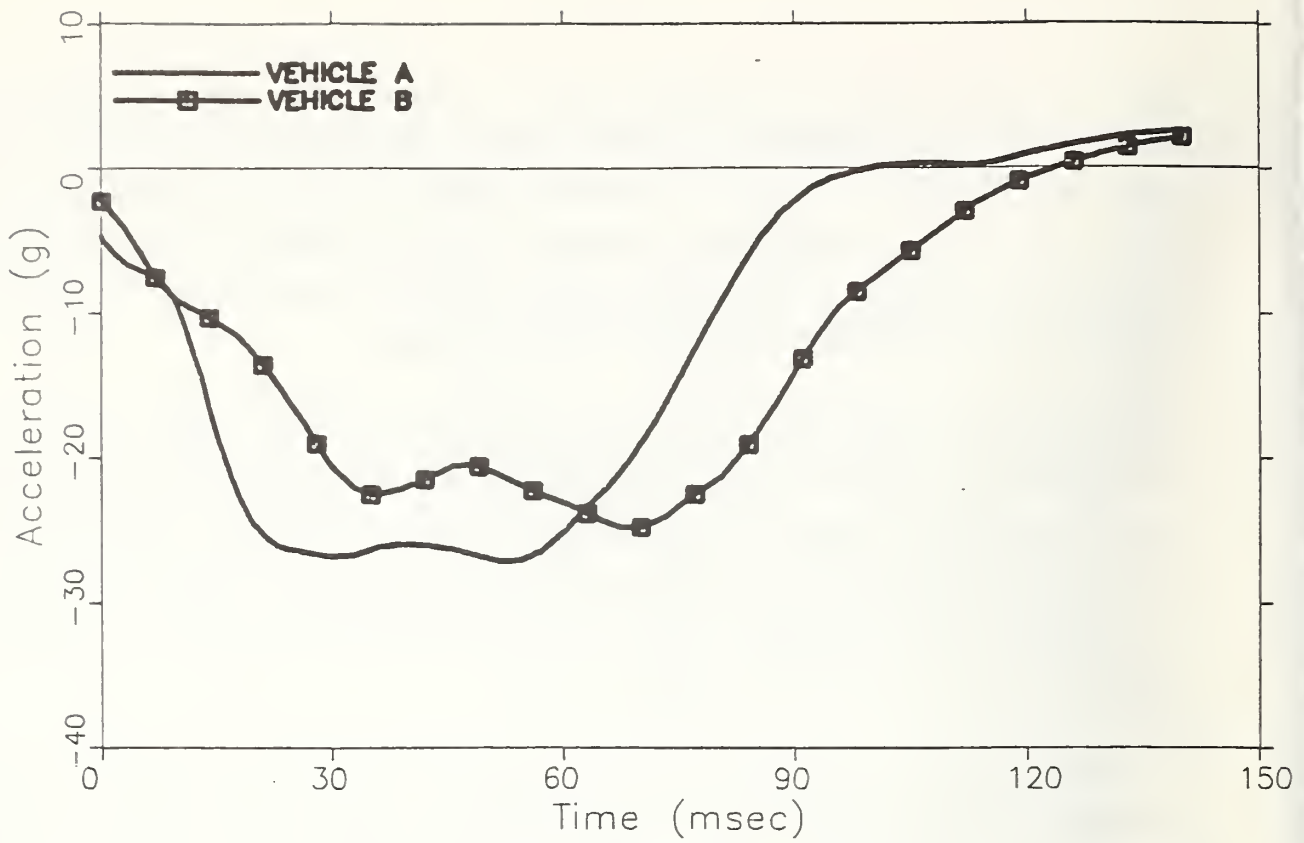
As was done with the dummy data, the "best five" and "worst five" vehicles were identified (those vehicles whose RID calculations were furthest from the least squares line). The "best five" vehicles were B, H, Q, V and Z; the "worst five" were A, J, M, O and U. It is interesting that only one vehicle (H) appears in the "best five" based on both criteria (dummy measurements and RID calculation); and only one vehicle (A) appears in the "worst five" based on both criteria.

Table 7 shows average dynamic crush values for the two groups of vehicles, compared with the average for all vehicles. The "best five" vehicles average significantly greater crush values than the "worst five", a similar (but more pronounced) trend as was observed in Table 5 for the dummy measurement criteria.

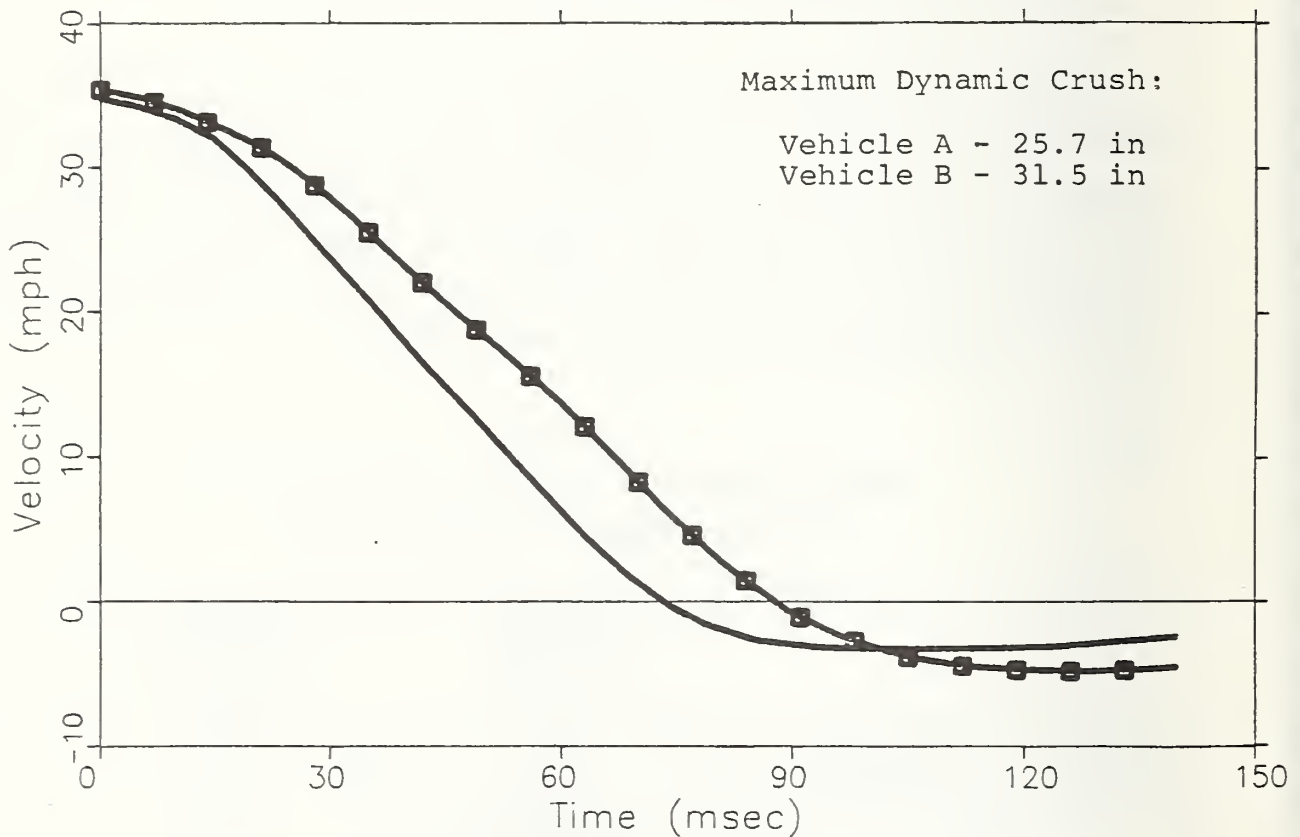
Occupant compartment responses (filtered at 40 hz) for the ten vehicles are shown in Figures 11-14. Of the ten, there was only one vehicle (H) in the Sub-Compact weight category, and four (J, M, O and Q) were in the Intermediate category. Therefore, for ease of comparison, the Sub-Compact vehicle was plotted with the two lightest Intermediates (Figure 12), and the two heaviest Intermediates were plotted together in Figure 13. Observations within these groups are as follows:

TABLE 7
Dynamic Crush Values of Vehicles Determined to be
"Best" and "Worst" by RID Calculations

	Average Curb Weight (pounds)	Average Dynamic Crush (inches)
"Best Five" Vehicles	3124	36.24
"Worst Five" Vehicles	2801	26.76
All Vehicles	3094	32.02

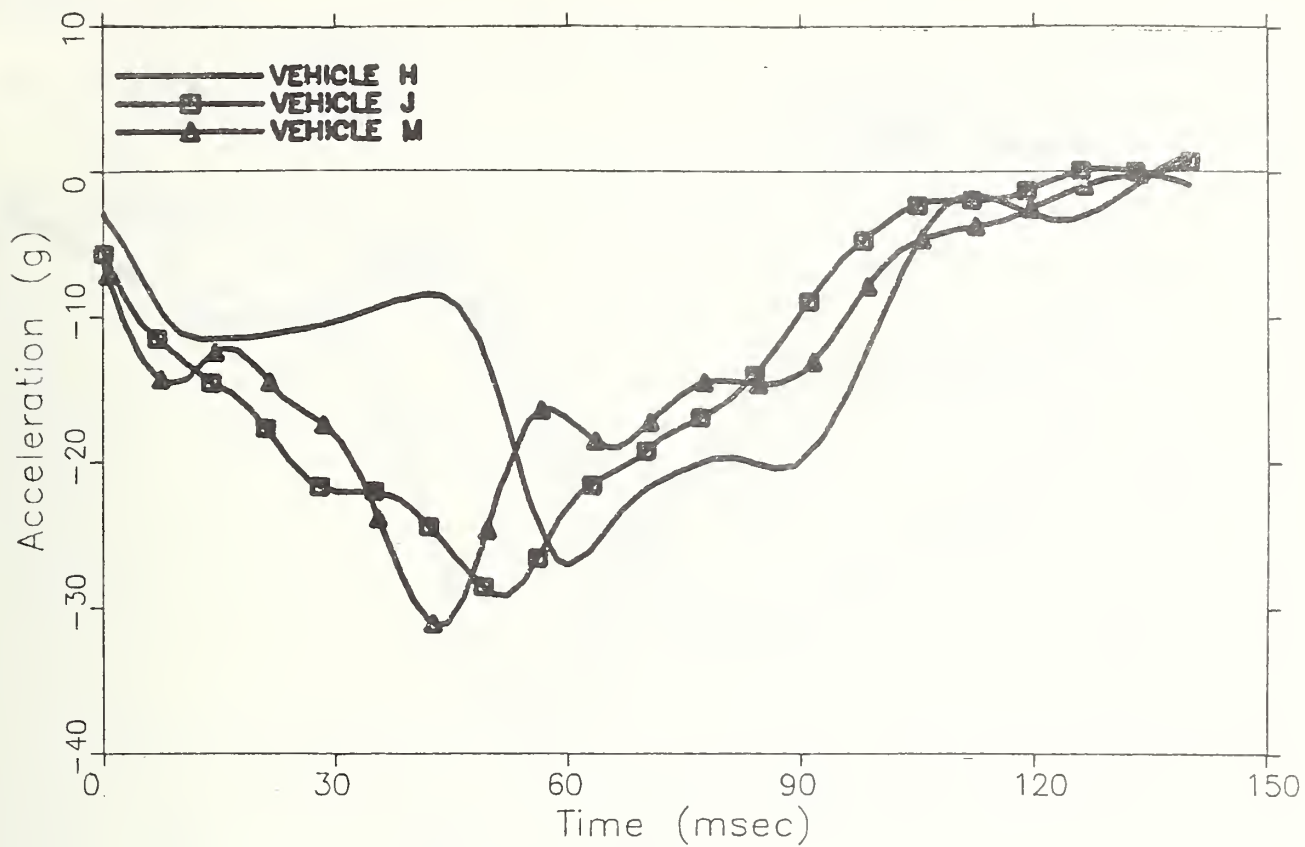


a) Acceleration Response

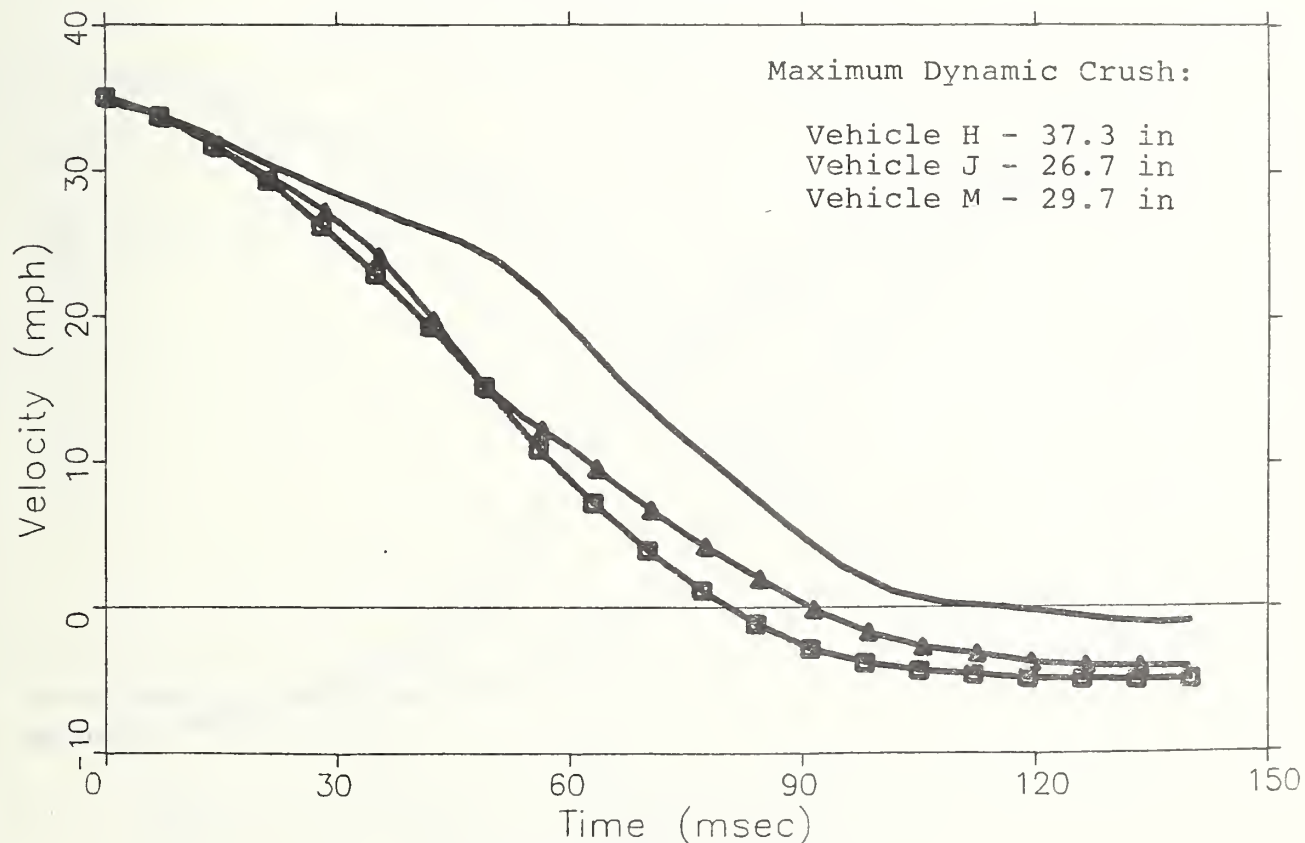


b) Velocity Response

FIGURE 11. Minicompact Vehicle Responses (RID Criterion)

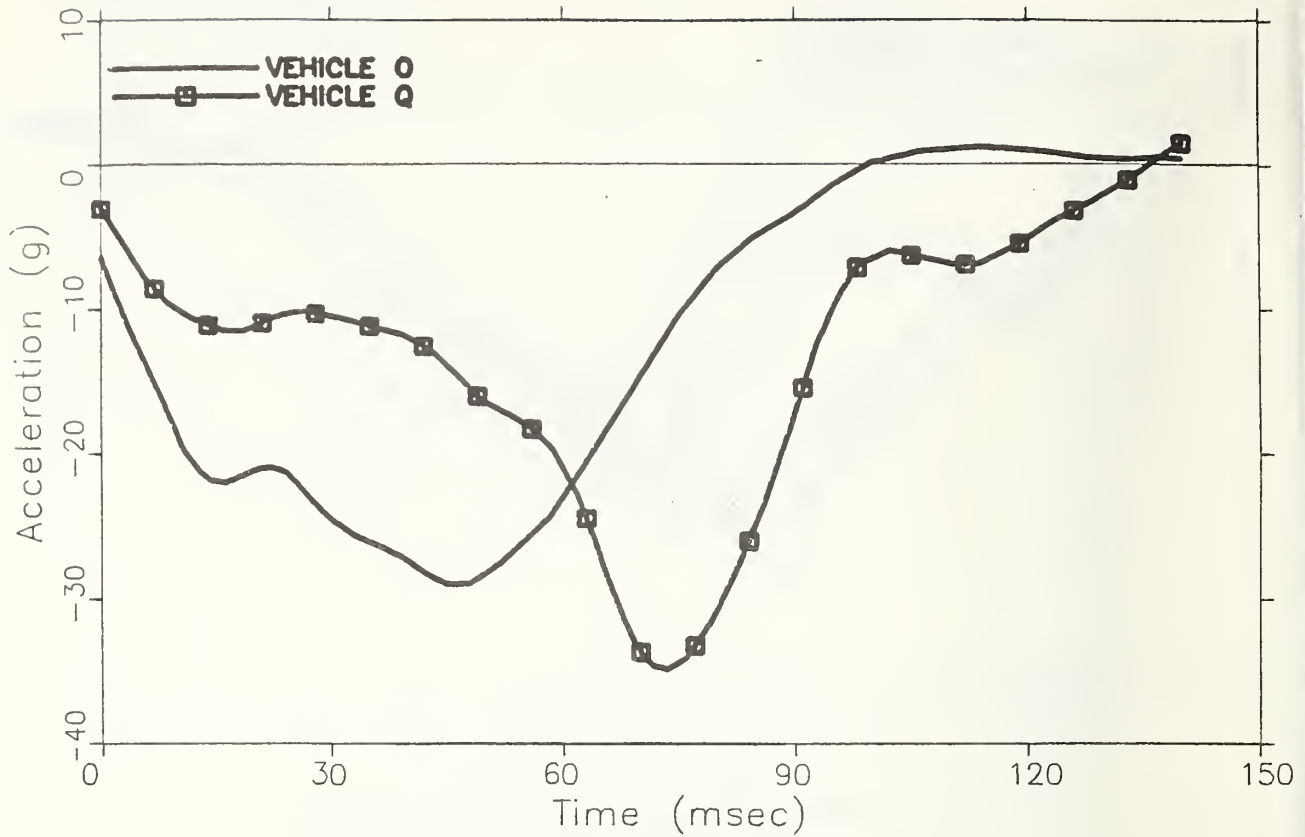


a) Acceleration Response

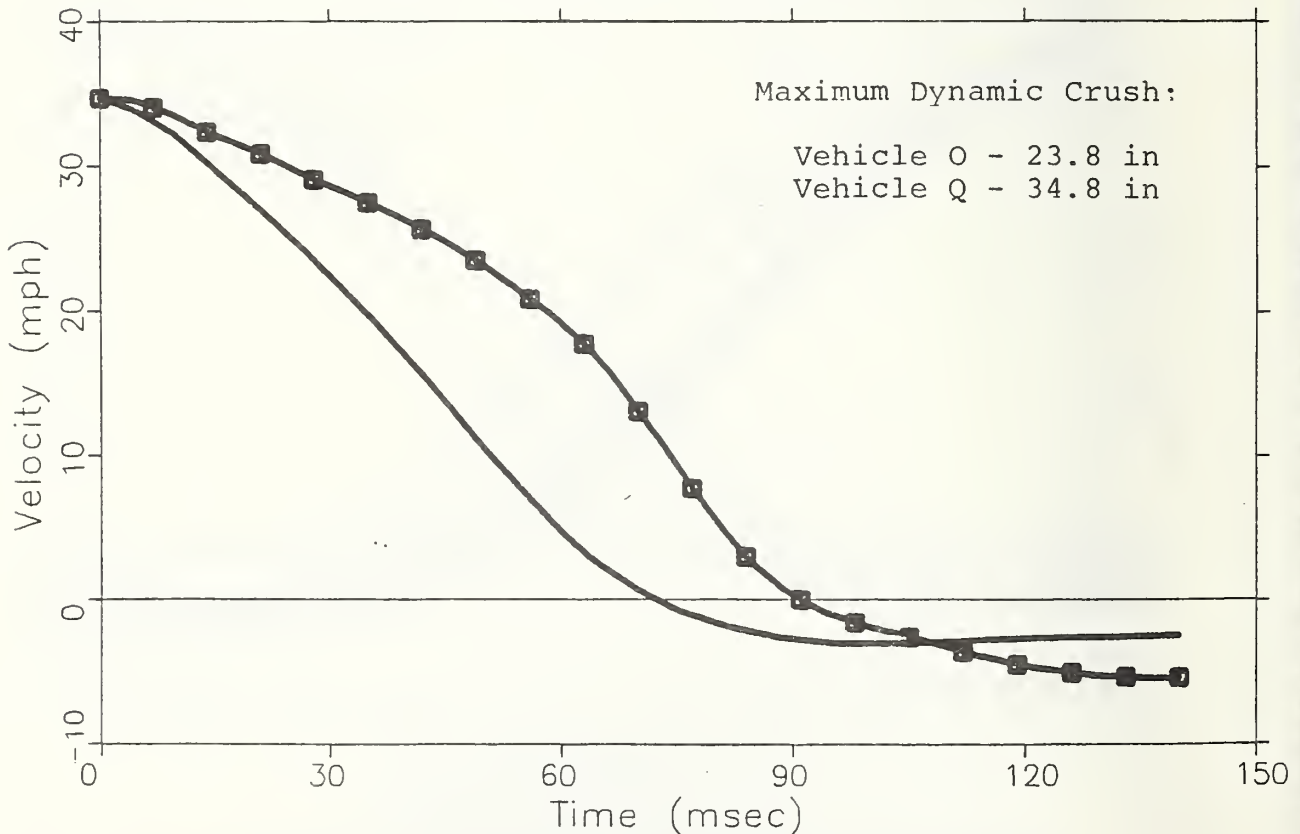


b) Velocity Response

FIGURE 12. Subcompact and Light Intermediate Vehicle (<3000 lbs) Responses (RID Criterion)

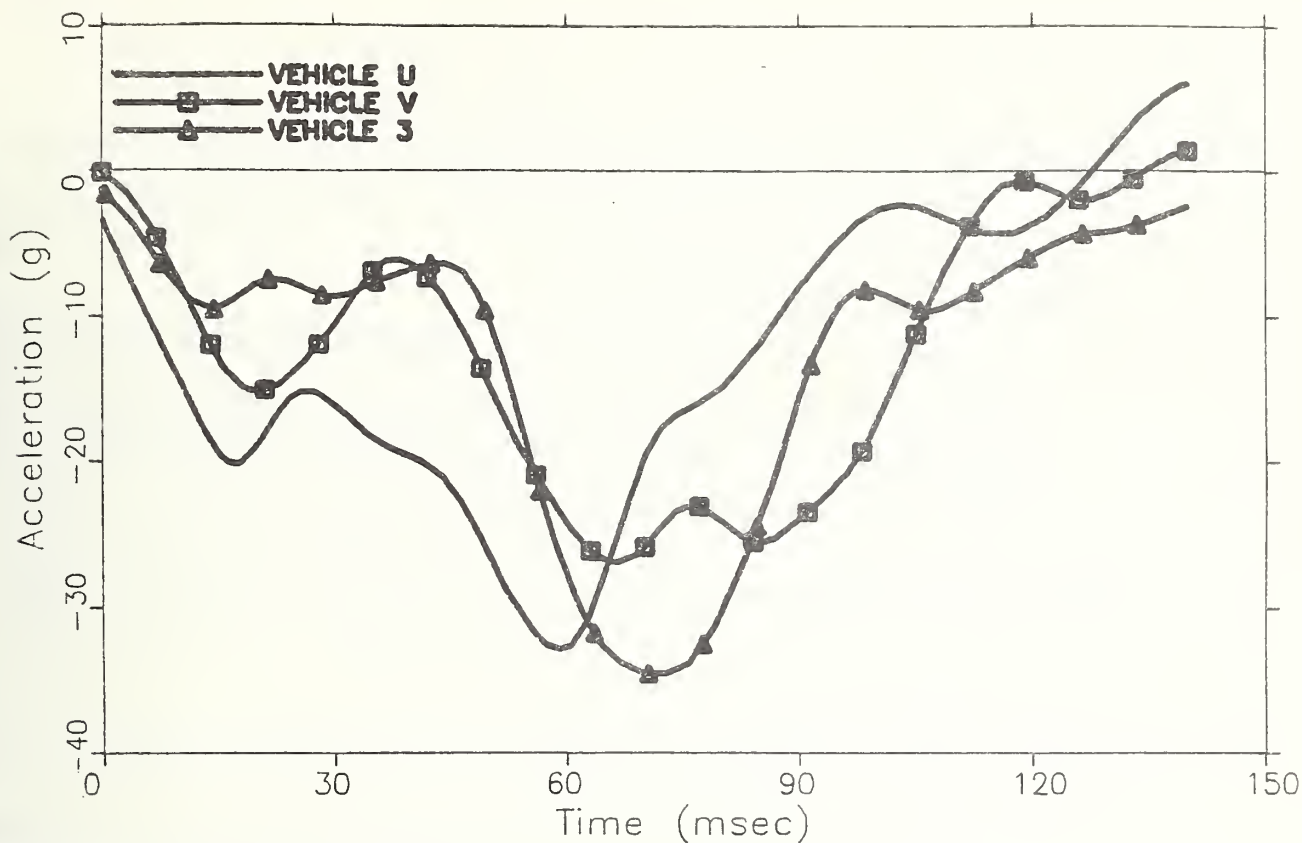


a) Acceleration Response

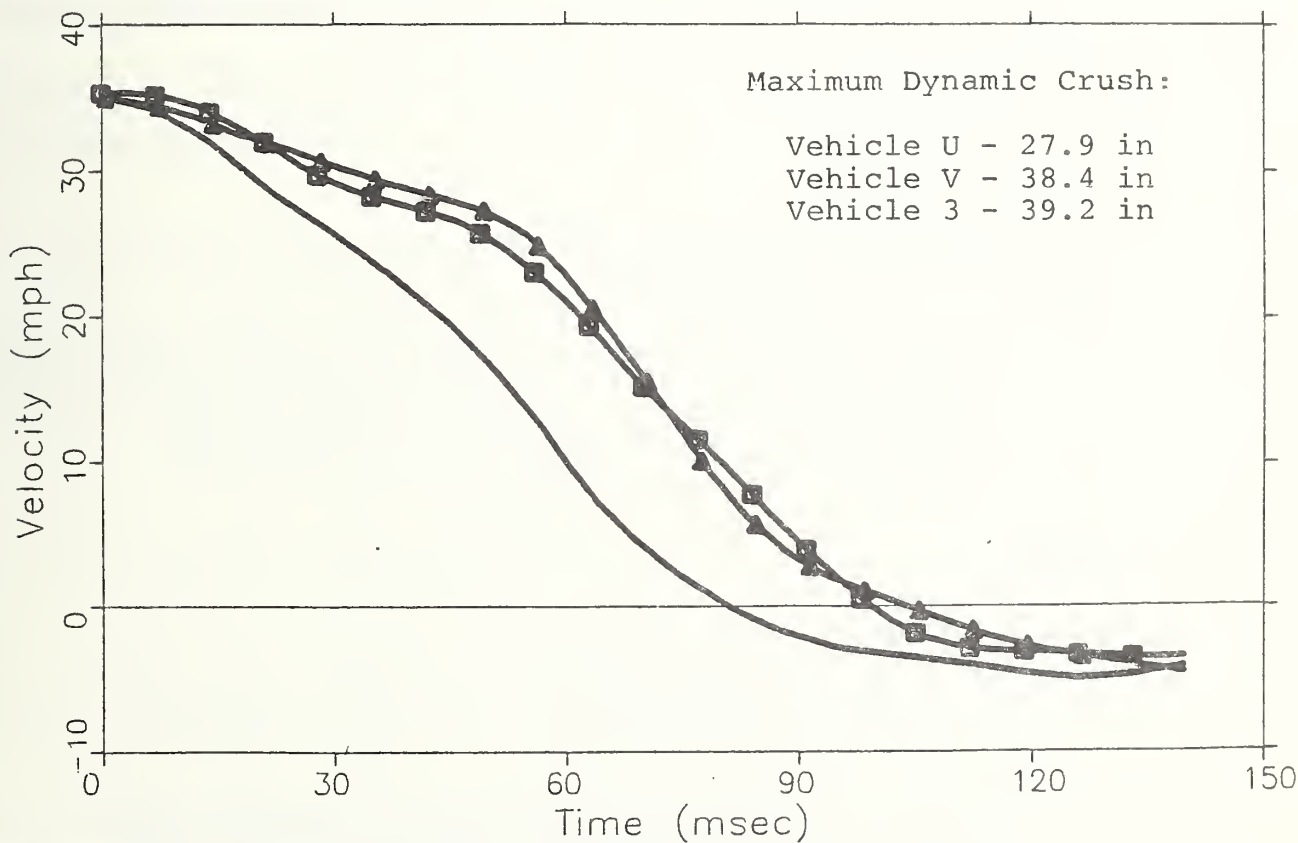


b) Velocity Response

FIGURE 13. Heavy Intermediate Vehicle (>3000 lbs) Responses (RID Criterion)



a) Acceleration Response



b) Velocity Response

FIGURE 14. Standard Vehicle Responses (RID Criterion)

Mini-Compact:

Vehicle A -- "poor" occupant protection.

Vehicle B -- "good" occupant protection.

Acceleration pulse shapes were similar, but Vehicle B had a slightly lower peak acceleration, a longer pulse duration and much greater dynamic crush. (Note the similarity of this comparison with that of Vehicles A and C, for the dummy measurement criterion.)

Sub-Compact and Light Intermediate:

Vehicle H -- "good" occupant protection.

Vehicle J -- "poor" occupant protection.

Vehicle M -- "poor" occupant protection.

Acceleration pulse shapes were similar for Vehicles J and M. For Vehicle H, however, the shape was noticeably different, with a very low acceleration early in the event and a later peak. Also, the dynamic crush of Vehicle H was much greater.

Heavy Intermediate:

Vehicle O -- "poor" occupant protection.

Vehicle Q -- "good" occupant protection.

Differences are very pronounced. Vehicle O developed high accelerations very early in the event, and had a very short pulse duration. Vehicle Q had a very late peak acceleration and much greater dynamic crush.

Standard:

Vehicle U -- "poor" occupant protection.

Vehicle V -- "good" occupant protection.

Vehicle 3 -- "good" occupant protection.

Responses were similar for Vehicles V and 3, both of which had low accelerations early in the event and late peaks. In contrast, Vehicle U exhibited a higher acceleration early in the event, a much shorter pulse duration and much less dynamic crush.

In summary, vehicles offering "good" occupant protection had long pulse durations, large dynamic crushes, and acceleration pulse shapes characterized by low values early in the event and late peaks (which often were higher than those for vehicles offering "poor" protection).

2.1.4.3 ABAG Model Simulations

ABAG computer model simulations were run for 5th percentile female, 50th percentile male and 95th percentile male drivers and passengers. Maximum chest accelerations and steering column displacements are reported in Table 8. Figures 15-20 contain maximum chest accelerations plotted against vehicle curb weights, along with least squares lines. The following observations were made:

- 1) Although a large amount of variability among vehicles was apparent, it was somewhat less than that seen for dummy measurements and RID.
- 2) Peak chest acceleration was fairly insensitive to occupant size, with the exception of the 5th percentile female passenger.
- 3) A definite trend of improved occupant protection potential with increasing vehicle weight was observed.

Using the same procedure as was done with the dummy data and RID calculations, the "best five" and "worst five" vehicles were identified from each of the six occupant plots (Figures 15-20). Those vehicles appearing among the "best five" or "worst five" at least four times were listed, as shown in Table 9. Of the four vehicles identified as "best", two (H and Q) were among the "best five" based on the RID calculation criterion, and one (H) was among the "best" according to all three criteria. All four of the "worst" vehicles were among the "worst five" based on the RID calculation criterion, and one (A) was identified in the "worst" category by all three criteria.

In Table 10, it is seen that the "best four" vehicles averaged significantly greater dynamic crush than the "worst four", as was the case for the RID criterion.

Occupant compartment responses (filtered at 40 hz) for the eight vehicles appear in Figures 21-23. There was only one vehicle (A) in the Mini-Compact weight category,

TABLE 8
ABAG Model Simulation Summary

CLASS	VEHICLE		DRIVER PEAK ACC. (g's)				COLUMN DISPLACEMENT (in.)				PASSENGER PEAK ACCELERATION (G's)		
	YEAR	SYMBOL	5% F		50% M		95% M		5%F	50%M	95%M		
			Acc.	Disp.	Acc.	Disp.	Acc.	Disp.					
Mini Compact	1979	A	57.9	2.31	57.3	3.70	57.1	4.93	70.9	57.5	59.9		
	1979	B	42.2	1.68	45.5	2.93	47.1	4.08	59.6	44.8	43.1		
	1979	C	46.5	1.87	48.1	3.11	48.9	4.25	62.8	48.2	46.9		
	1979	D	47.5	1.91	51.4	3.30	52.9	4.55	64.1	49.2	50.1		
Sub-Compact	1979	E	46.8	1.85	49.4	3.20	51.5	4.43	64.0	49.9	48.9		
	1979	F	52.2	2.12	50.3	3.24	48.7	4.18	69.8	53.7	53.2		
	1979	G	44.7	1.78	46.9	3.04	48.6	4.19	64.9	47.0	46.1		
	1979	H	26.6	1.06	32.1	2.07	35.7	3.04	39.3	39.7	33.9		
	1979	I	32.7	1.31	39.8	2.55	43.6	3.74	48.8	42.0	36.7		
	1979	J	51.4	2.03	51.1	3.33	52.0	4.46	69.2	54.1	53.1		
Intermediate	1979	K	46.5	1.87	48.6	3.11	49.1	4.17	64.5	49.8	49.8		
	1980	L	38.5	1.53	37.7	2.44	38.4	3.31	58.4	44.9	39.3		
	1979	M	48.9	1.94	47.2	3.05	47.1	4.02	67.0	52.1	48.5		
	1979	N	39.0	1.55	45.2	2.94	48.8	4.16	58.6	46.5	46.6		
	1980	O	59.9	2.39	58.3	3.76	57.6	4.95	75.0	63.9	63.9		
	1979	P	40.0	1.61	36.4	2.35	36.6	3.15	60.5	44.4	38.1		
	1979	Q	29.7	1.21	40.4	2.62	44.2	3.82	41.0	40.1	35.4		
	1979	R	32.2	1.28	37.3	2.39	41.1	3.52	44.2	41.1	34.7		
	1979	S	36.2	1.53	40.5	2.59	42.4	3.62	57.4	44.2	39.7		
	1979	T	42.7	1.71	46.2	2.99	47.7	4.11	64.2	46.8	46.3		
Standard	1979	U	46.1	1.84	49.8	3.23	51.1	4.41	65.2	51.4	49.9		
	1979	V	28.2	1.13	36.4	2.36	40.7	3.48	37.6	40.4	36.1		
	1979	W	36.3	1.46	36.1	2.31	36.7	3.16	52.2	43.3	36.8		
	1979	X	34.4	1.38	36.4	2.34	39.8	3.44	51.3	43.2	36.0		
	1979	Y	35.8	1.42	31.9	2.06	34.4	2.95	50.7	43.6	35.1		
	1979	Z	40.4	1.61	45.3	2.92	46.8	4.05	55.5	43.4	41.1		
	1979	2	36.1	1.43	37.9	2.45	39.3	3.40	51.5	42.1	37.4		
	1979	3	37.5	1.50	43.8	2.83	45.8	3.98	39.0	40.0	36.5		
	1979	4	29.1	1.16	31.4	2.02	34.5	2.95	44.2	40.3	34.9		

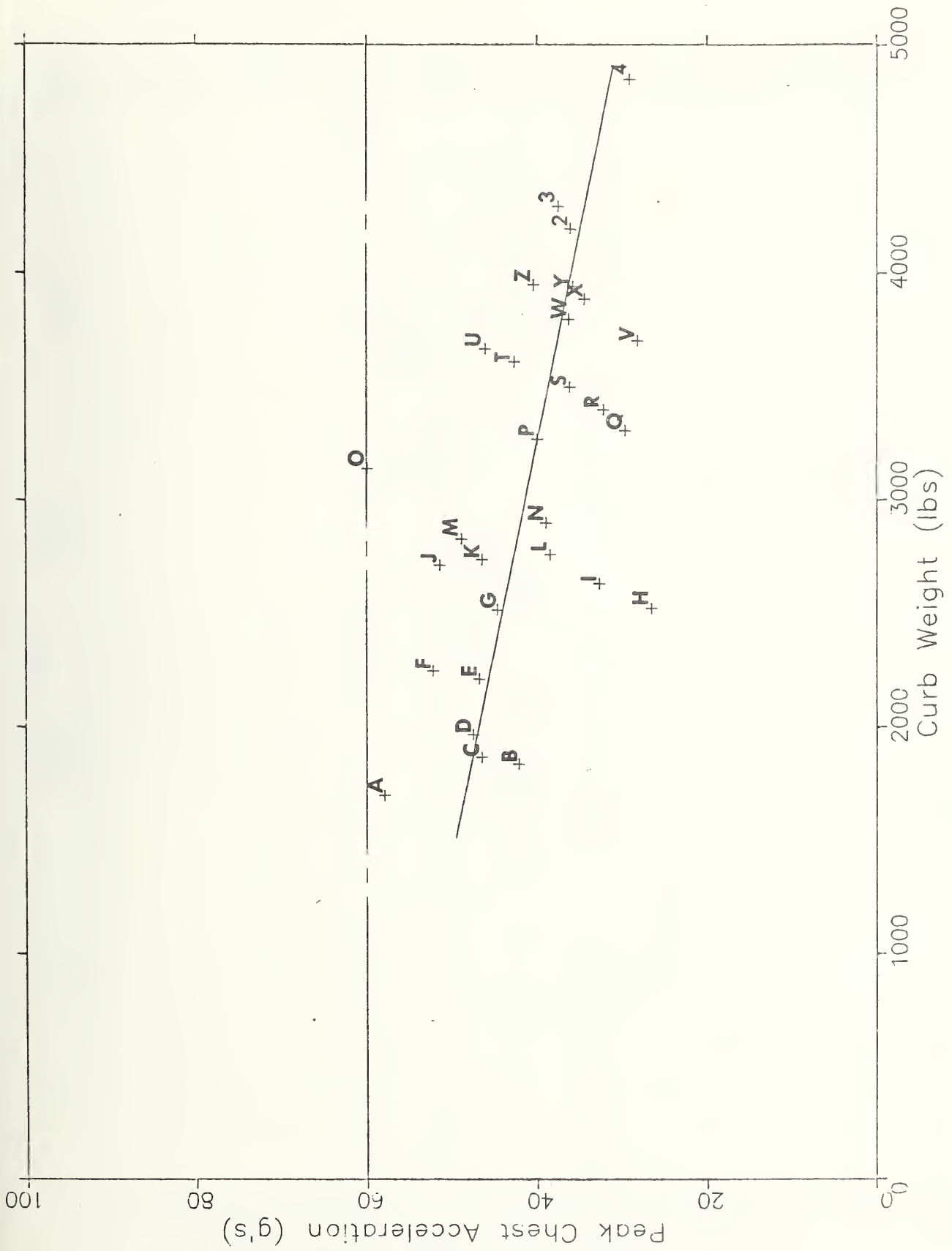


FIGURE 15. Maximum Chest Accelerations Determined From ABAG Model -- 5th Percentile Female Driver

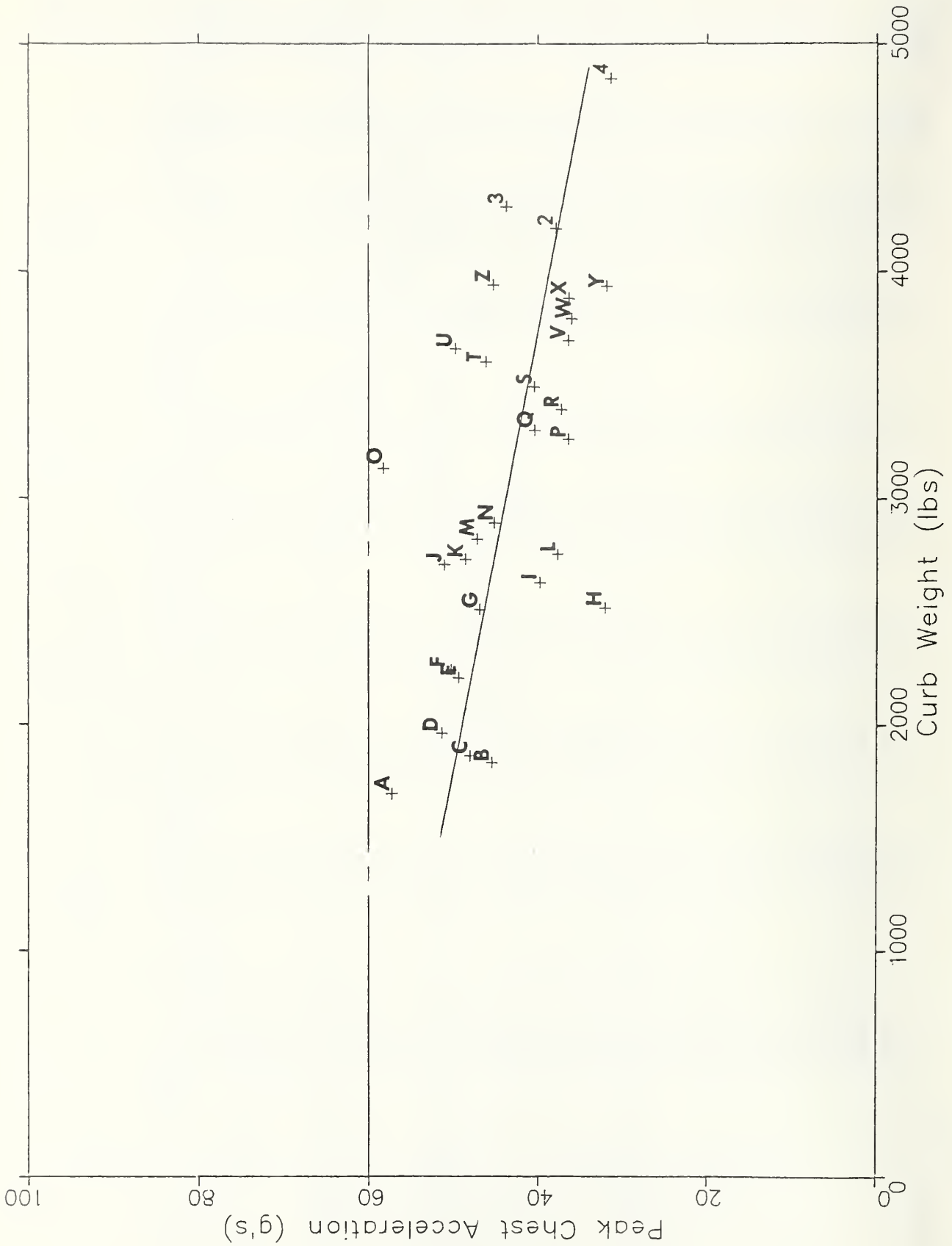


FIGURE 16. Maximum Chest Accelerations Determined From ABAG Model -- 50th Percentile Male Driver

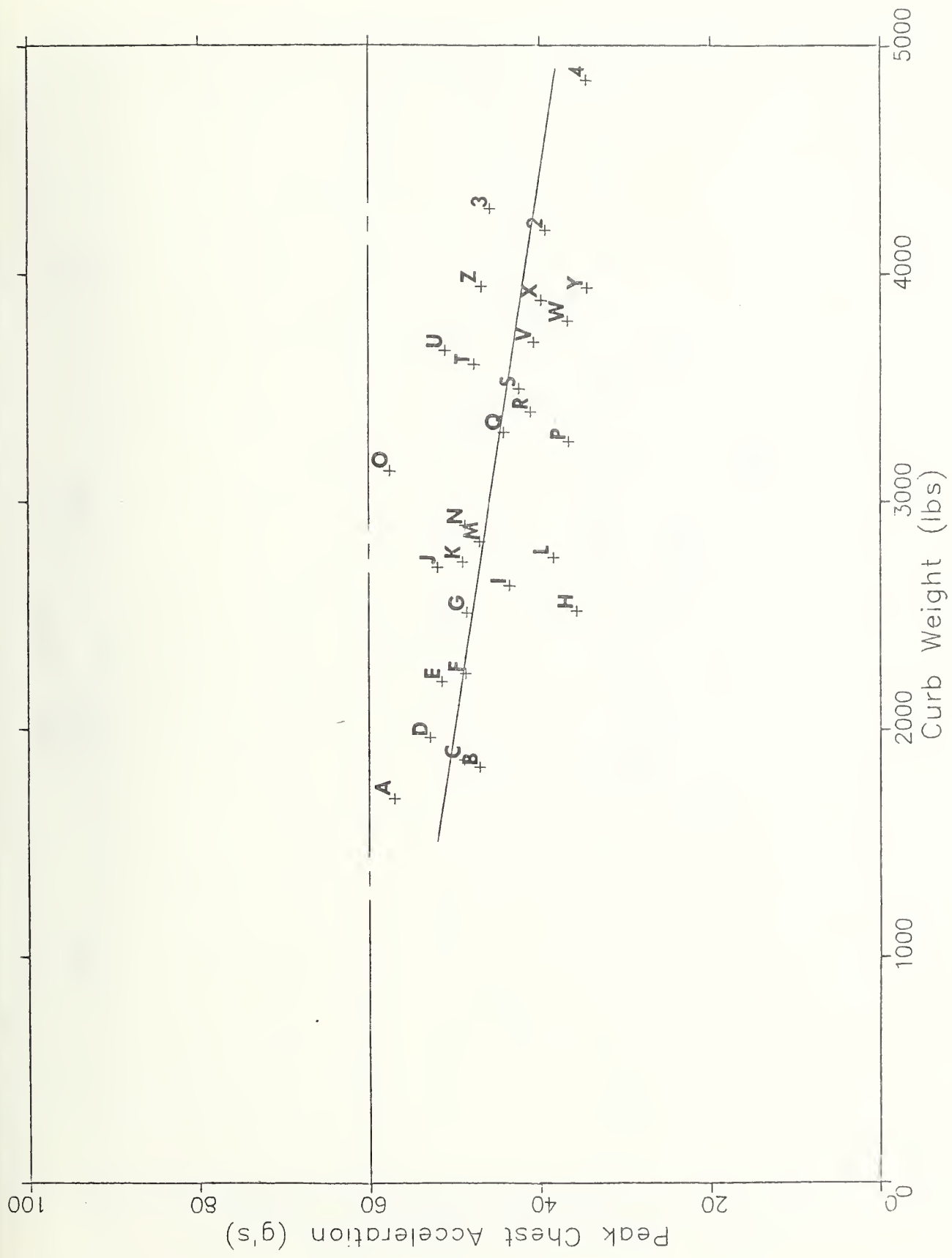


FIGURE 17. Maximum Chest Accelerations Determined From ABAG Model -- 95th Percentile Male Driver

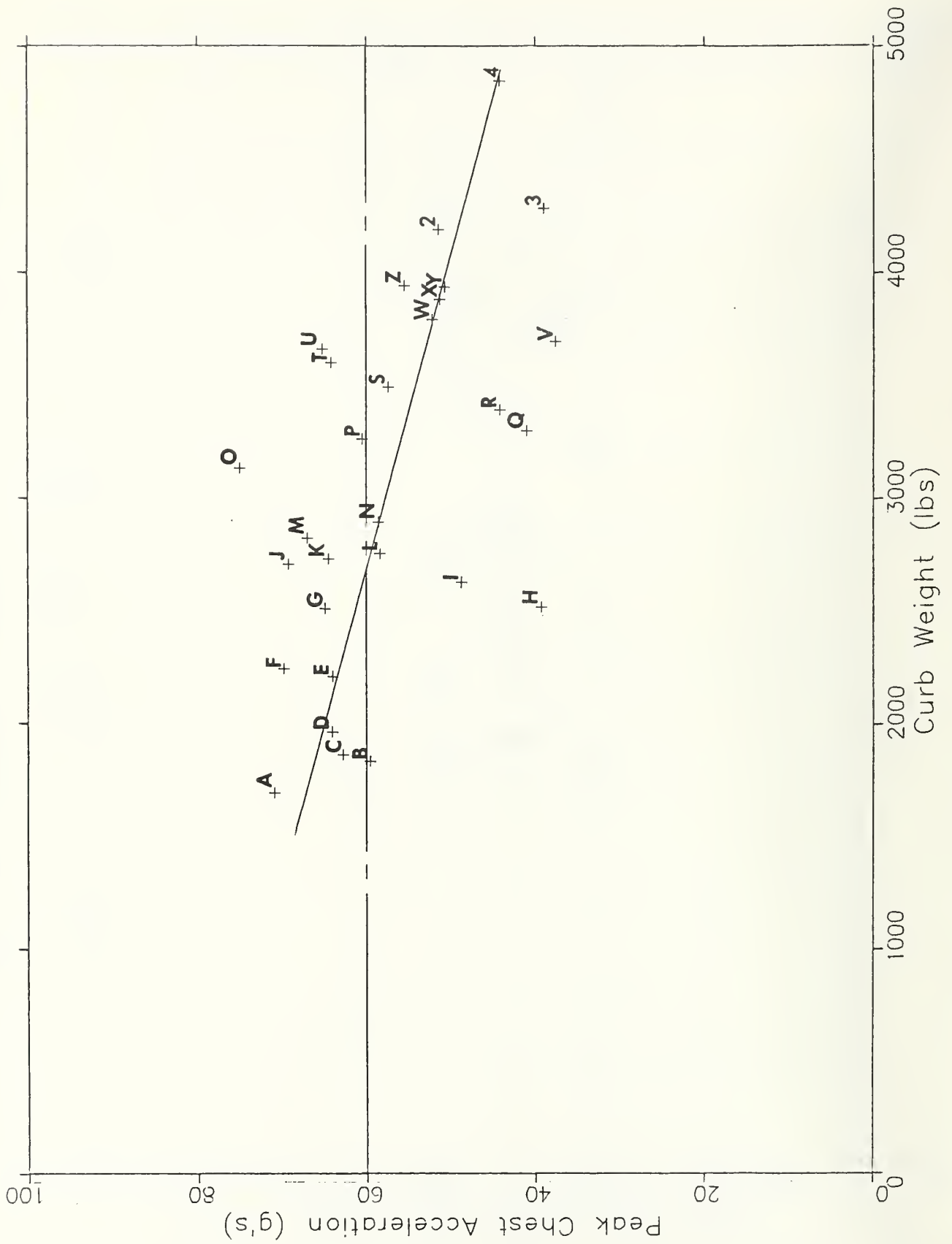


FIGURE 18. Maximum Chest Accelerations Determined From ABAG Model -- 5th Percentile Female Passenger

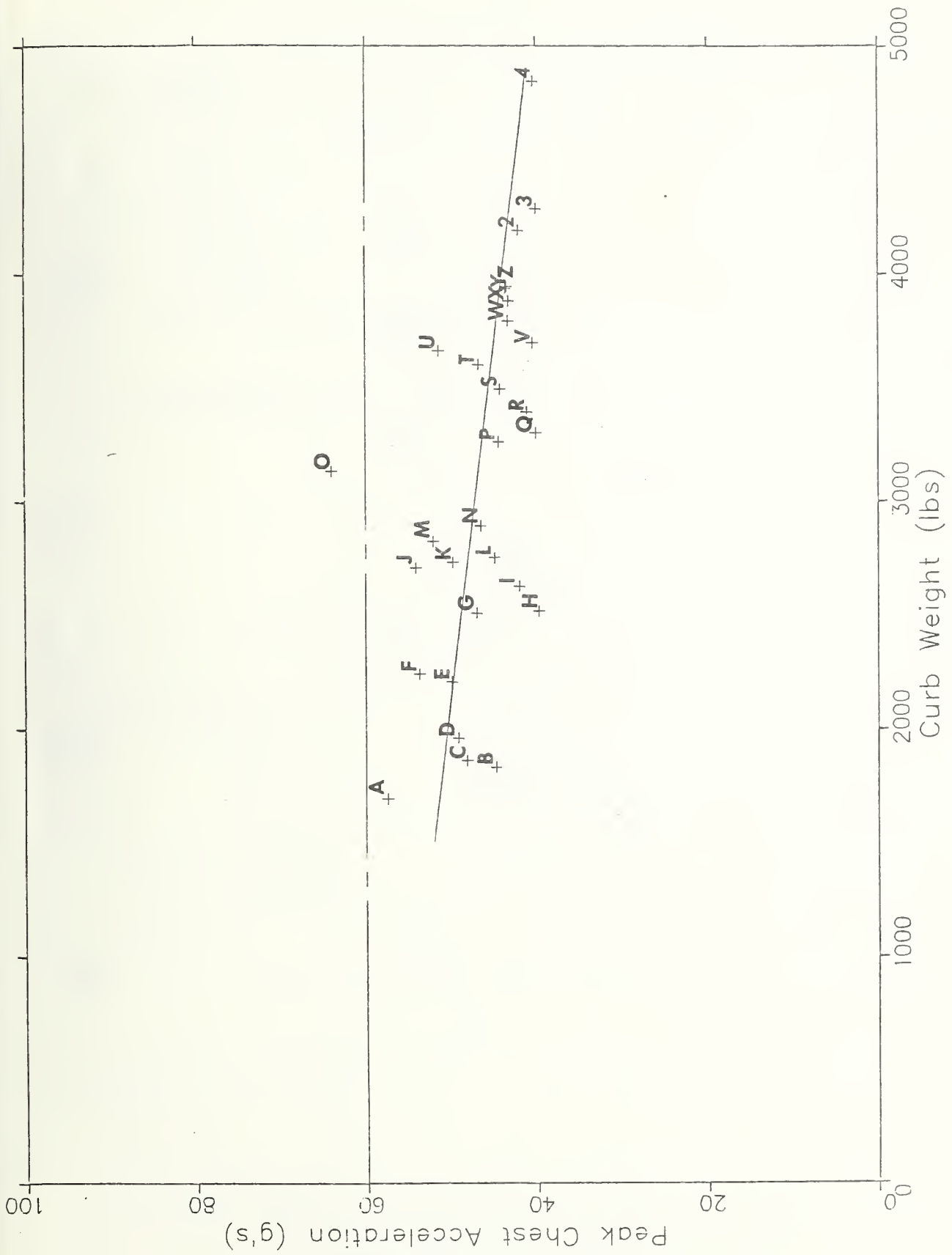


FIGURE 19. Maximum Chest Accelerations Determined From ABAG Model -- 50th Percentile Male Passenger

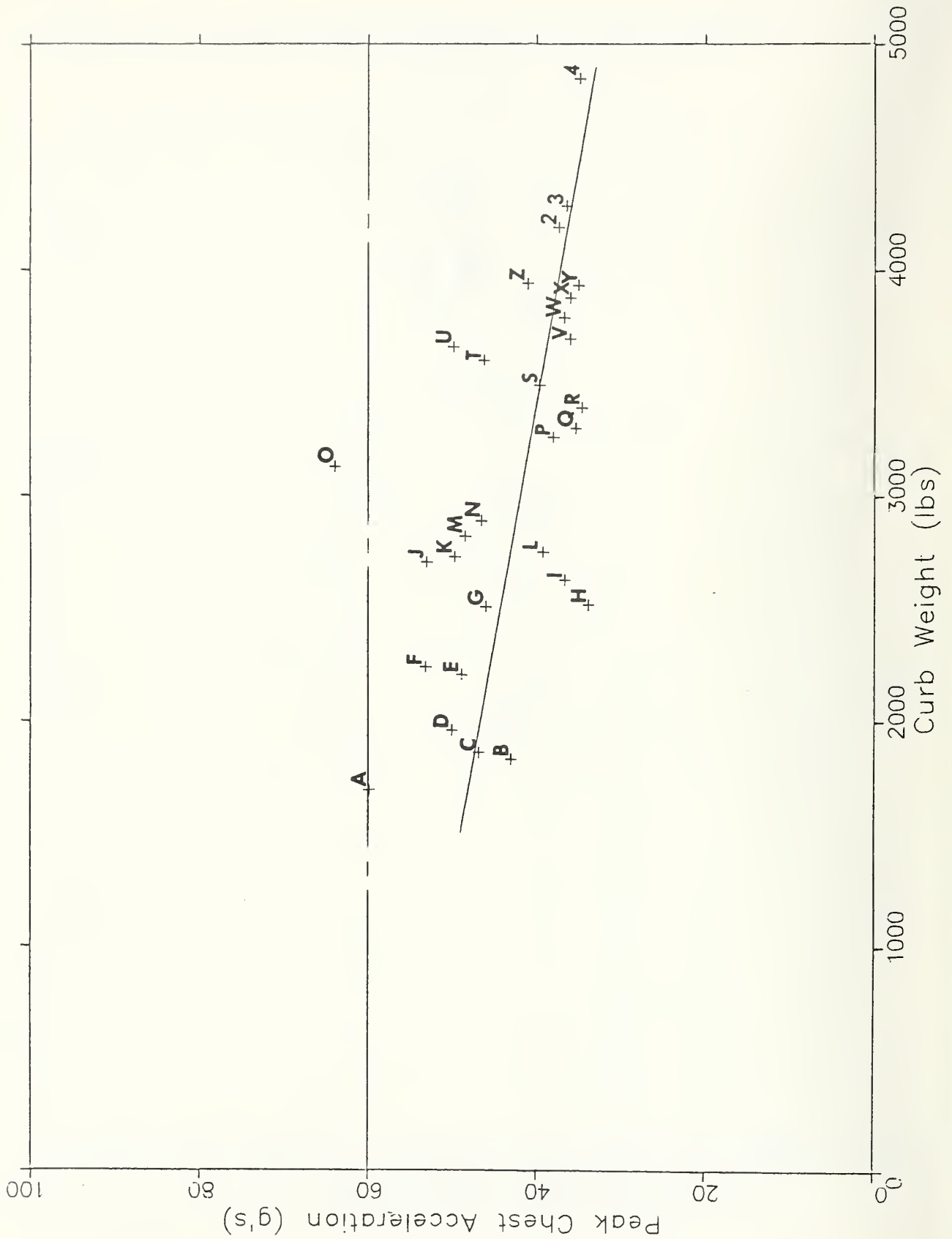


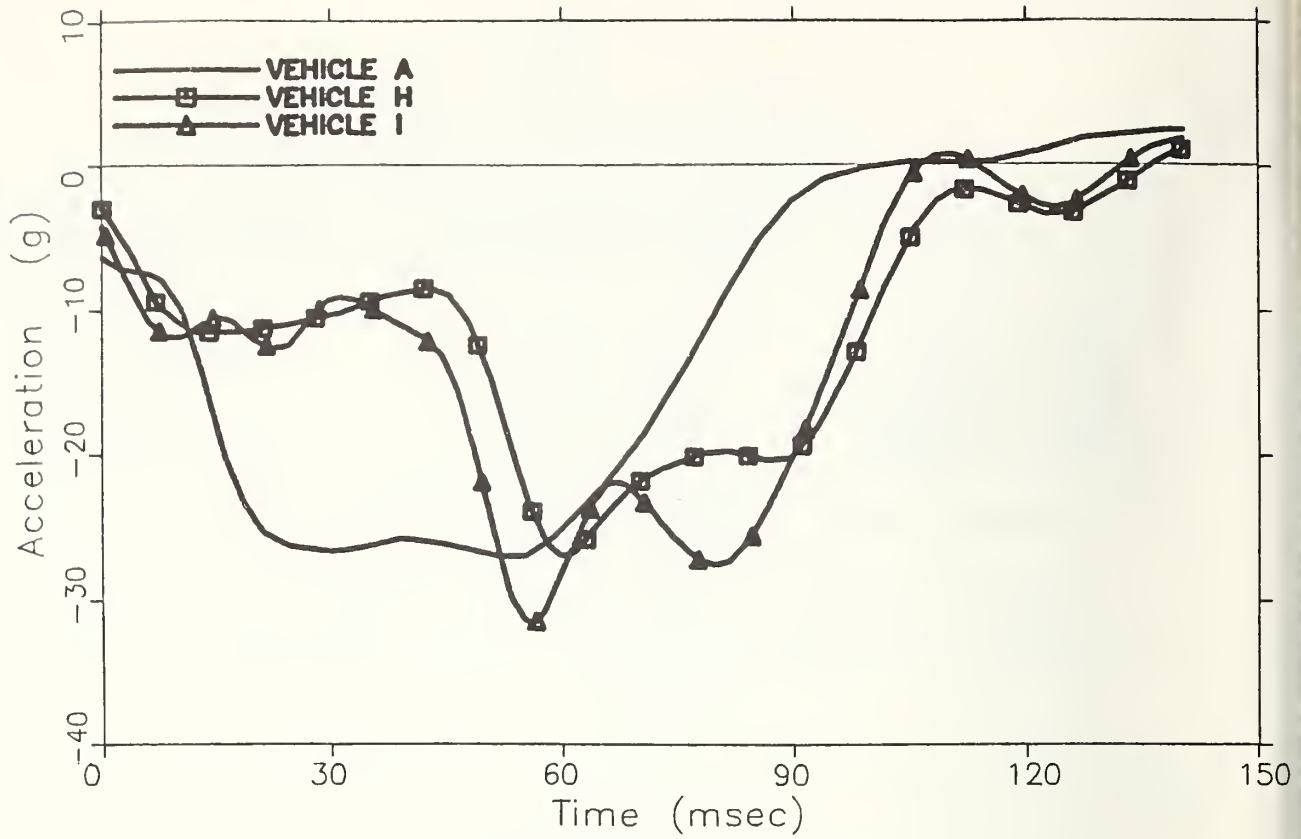
FIGURE 20. Maximum Chest Accelerations Determined From ABAG Model -- 95th Percentile Male Passenger

TABLE 9
 Identification of "Best" and "Worst" Vehicles
 as Determined from ABAG Simulation Results

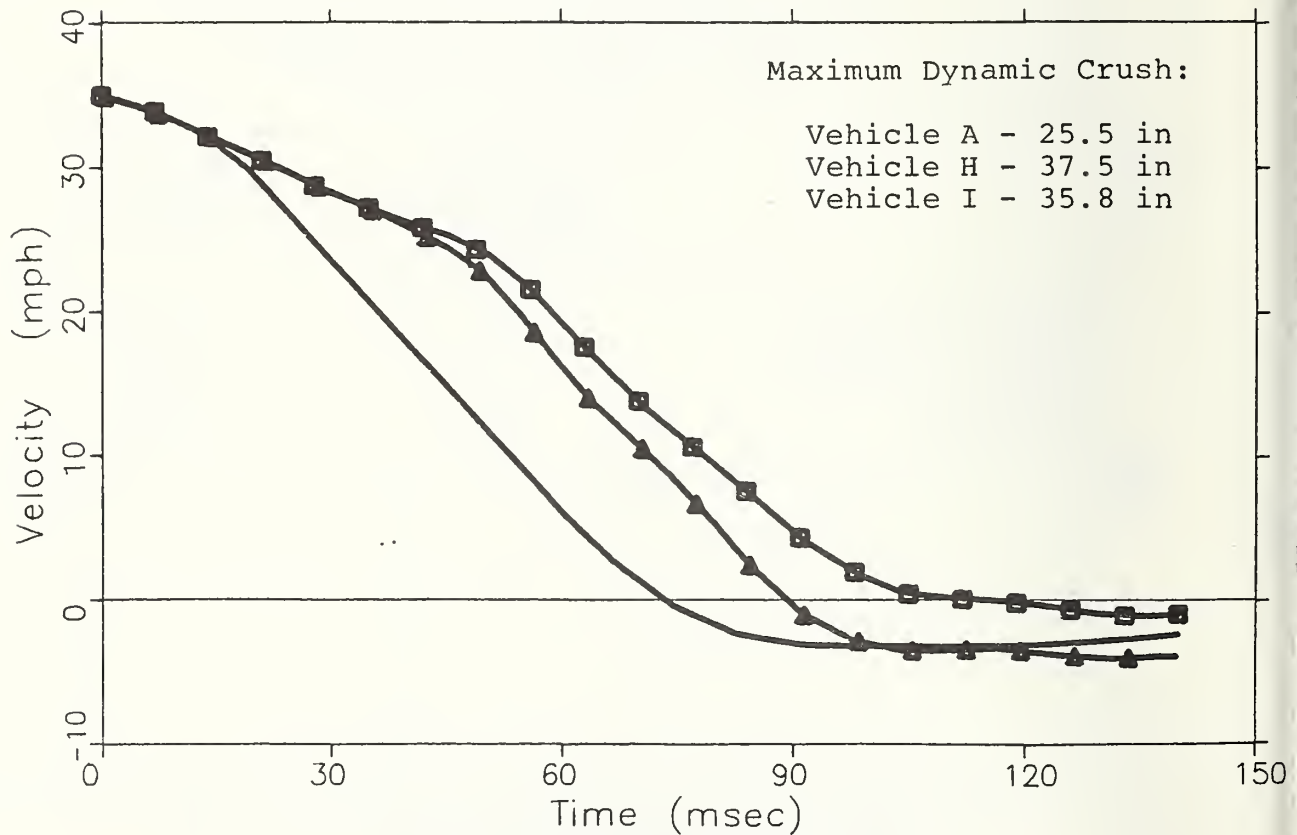
OCCUPANT	"BEST FIVE" VEHICLES	"WORST FIVE" VEHICLES
5th % F Driver	H I Q R V	A F J O U
50th % M Driver	H I L P Y	A O U Z 3
95th % M Driver	H L P W Y	A O U Z 3
5th % F Passenger	H I Q R V	J M O T U
50th % M Passenger	B H I Q R	A J M O U
95th % M Passenger	B H I Q R	A J O T U
<p style="text-align: center;">Vehicles appearing at least four times among the "Best Five": H I Q R</p> <p style="text-align: center;">Vehicles appearing at least four times among the "Worst Five": A J O U</p>		

TABLE 10
 Dynamic Crush Values of Vehicles Determined to be
 "Best" and "Worst" by ABAG Simulations

	Average Curb Weight (pounds)	Average Dynamic Crush (inches)
"Best Four" Vehicles	2958	35.60
"Worst Four" Vehicles	2797	25.98
All Vehicles	3094	32.02

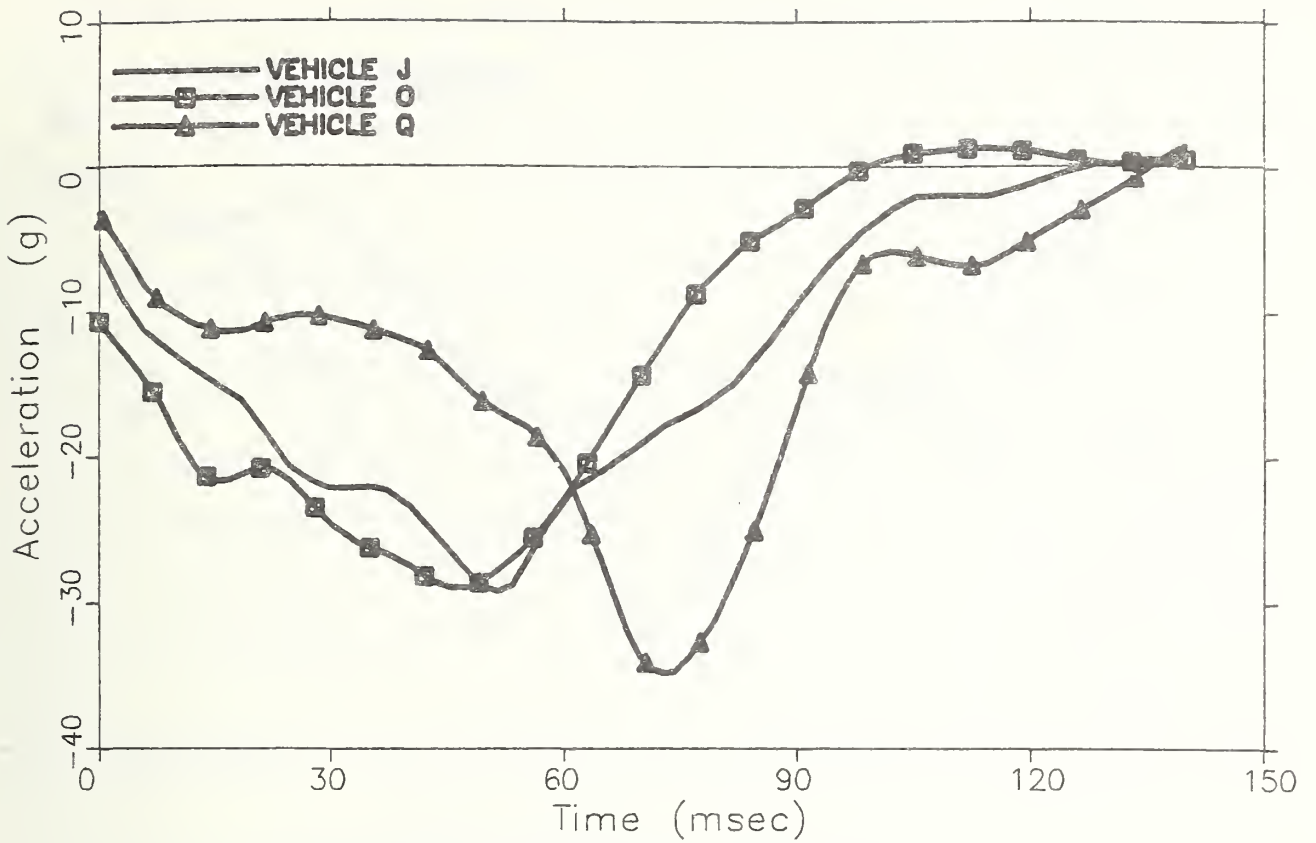


a) Acceleration Response

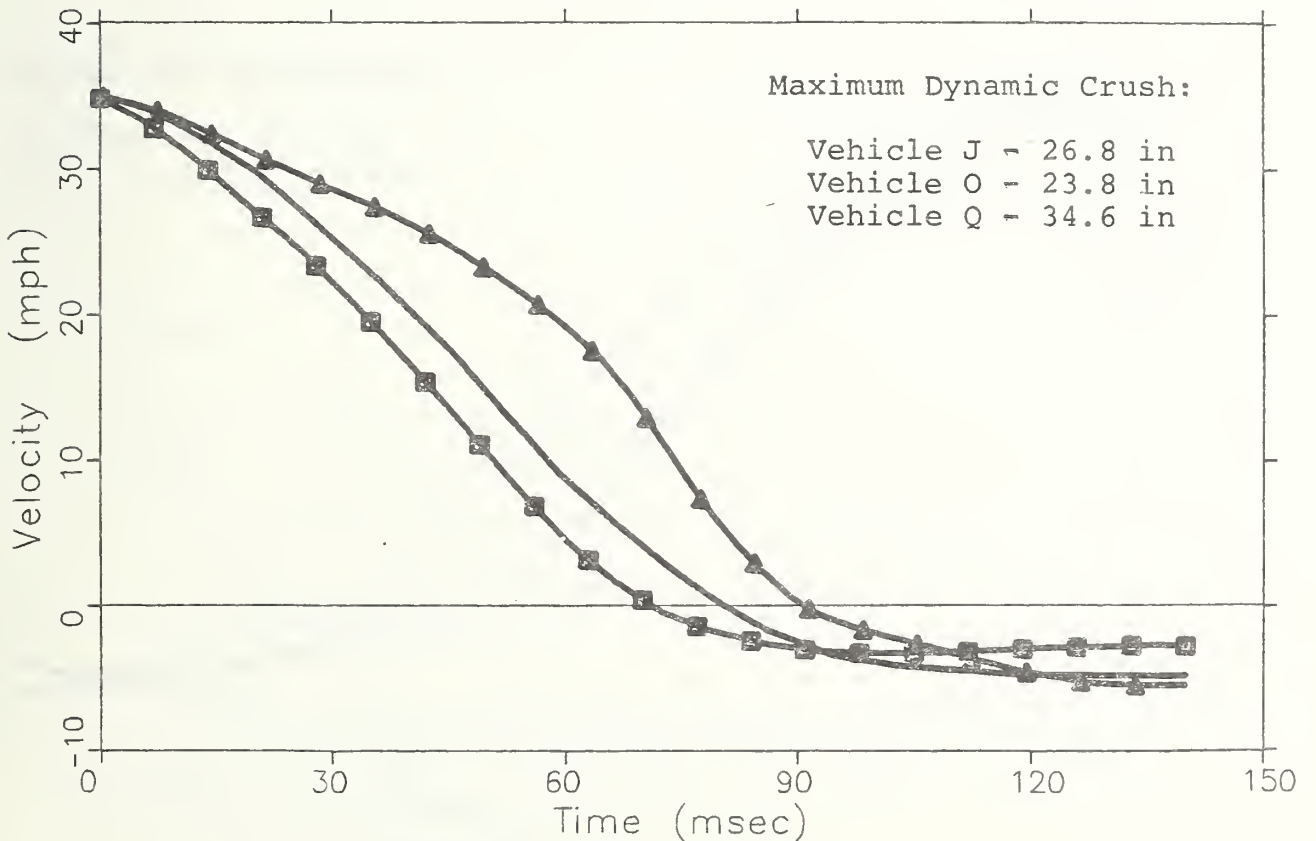


b) Velocity Response

FIGURE 21. Minicompact and Subcompact Vehicle Responses (ABAG Modeling Criterion)

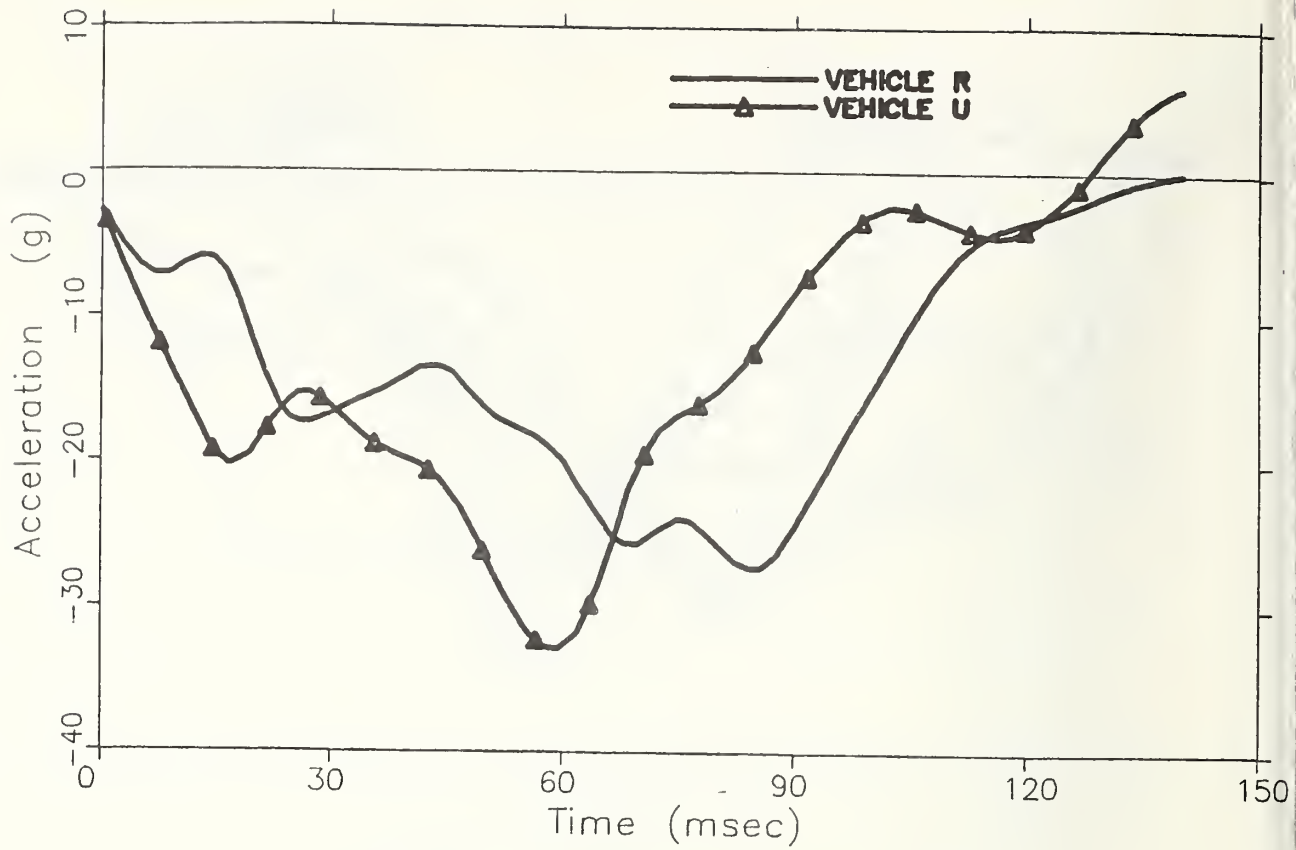


a) Acceleration Response

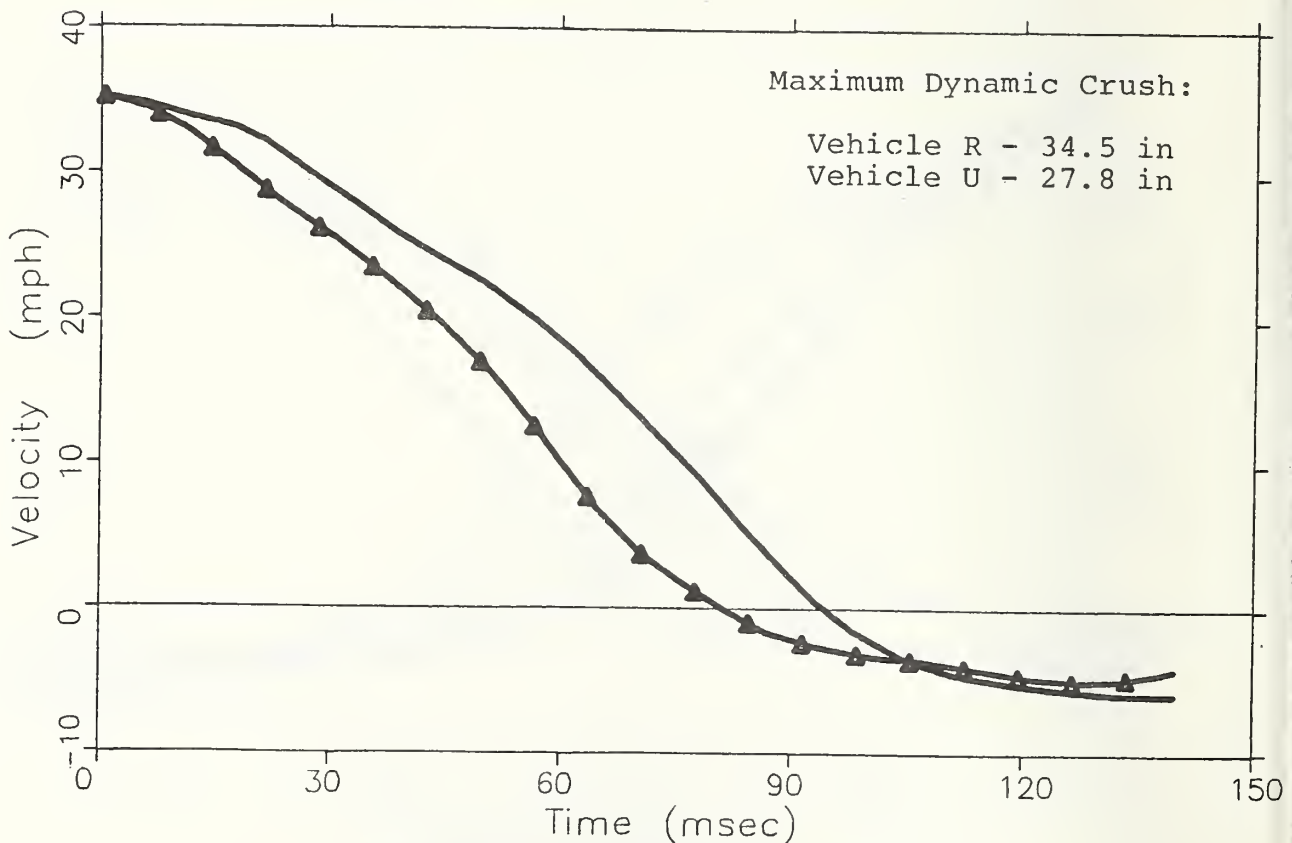


b) Velocity Response

FIGURE 22. Intermediate Vehicle Responses (ABAG Modeling Criterion)



a) Acceleration Response



b) Velocity Response

FIGURE 23. Standard Vehicle Responses (ABAG Modeling Criterion)

and both vehicles in the Sub-Compact category (H and I) were among the "best four"; therefore, these two categories were combined in Figure 21. Observations are as follows:

Mini-Compact and Sub-Compact:

Vehicle A -- "poor" occupant protection.

Vehicle H -- "good" occupant protection.

Vehicle I -- "good" occupant protection.

Acceleration pulse shapes were very similar for Vehicles H and I. Vehicle A's, however, was very different, having higher acceleration levels early in the event and a much shorter pulse duration. The dynamic crush of Vehicle A was also much less.

Intermediate:

Vehicle J -- "poor" occupant protection.

Vehicle O -- "poor" occupant protection.

Vehicle Q -- "good" occupant protection.

Acceleration responses were similar for Vehicles J and O, having early peaks and short durations. Although the peak acceleration for Vehicle Q was higher, it occurred very late, and the pulse shape was characterized by low values early in the event. Maximum crush was much greater for Vehicle Q.

Standard:

Vehicle R -- "good" occupant protection.

Vehicle U -- "poor" occupant protection.

The acceleration of Vehicle U rose to a higher peak earlier in the crash event than that of Vehicle R. Vehicle R had a substantially longer pulse duration and greater maximum crush.

In summary, vehicles offering "good" occupant protection had low accelerations early in the crash event, late peak accelerations, long pulse durations and large maximum dynamic crush values.

2.1.5 CONCLUSIONS

2.1.5.1 General Observations

A distinct and consistent trend of increased potential occupant survivability with increasing vehicle weight was seen. On average, including three indicators of occupant survivability (dummy measurements, RID calculations and ABAG modeling results), the analysis showed a 32% increase in occupant protection potential over the weight range from 1700 pounds to 4800 pounds (curb weight).

A strong correlation between maximum vehicle crush and occupant survivability (greater survival potential for higher crush values) was observed. Using dummy measurements as the occupant protection criteria, the difference between "best" and "worst" vehicles was found to be slight (less than two inches). Using the other criteria, however, very significant differences (nearly ten inches) were seen between "best" and "worst" vehicles. This suggests that when variabilities in restraint systems and dummy measurements are eliminated (as they are in the RID and ABAG determinations), the relationship between crush and protection potential for restrained occupants is shown clearly to be significant.

2.1.5.2 Reasons for Enhanced Crashsurvivability

A very large amount of variability among vehicles was observed in the dummy measurements. In the occupant modeling and stroking distance calculations, even though variability inherent with dummies and due to different restraints and compartment geometries was eliminated, significant variability was still evident. The required internal occupant stroking distances ranged from 2 to 9 inches, and chest accelerations from the ABAG modeling generally varied by a factor of two. This indicated that potential protection of restrained occupants is very dependent upon the structural response of the vehicle.

In general, vehicles showing potential for superior crashsurvivability experienced large dynamic crush values, and had occupant compartment responses which were characterized by long pulse durations, low accelerations early in the crash event, and late peak accelerations.

2.1.5.3 Selection of Vehicles for Future Modification

Only one vehicle was identified in the "best" crash survivability category according to all three criteria (dummy measurements, stroking distance calculation and ABAG modeling results). This was Vehicle H, a sub-compact. One other vehicle, (Vehicle Q, an intermediate), appeared among the "best" according to two criteria, stroking distance and ABAG modeling. However, recommending either of these specific vehicles for future modification to achieve and demonstrate further enhancement of frontal crash survivability is not justified on the basis of this analysis alone. Also needed would be a more thorough examination of other aspects of the vehicle and its crash response (such as interior geometry, steering column behavior, firewall intrusion, etc.). It can be concluded from this study that any vehicle having an occupant compartment crash response similar to those of these two vehicles (i.e., low accelerations early in the event and late peak accelerations) has a frontal structure which potentially offers superior protection for its occupants.

2.2 Characteristics of Non-Aggressive Vehicles

2.2.1 Introduction

Previous research has been conducted at the VRTC to determine vehicle characteristics which affect frontal structural aggressiveness (3,4). Parameters associated with increased aggressiveness (in addition to increased vehicle weight) are:

1. Increased stiffness of the frame forward of the front wheel suspension.
2. Increased frontal sheet metal stiffness.
3. Reduced bumper-to-engine clearance.

Parameters having little or no influence on aggressiveness are:

1. Stiffness of the frame between front wheel suspension and occupant compartment.
2. Weight of engine plus transmission.
3. Weight of bumper.

Thus, it appears that those parameters closest to the front of the vehicle, which are involved very early in the crash event, are the most significant in determining level of aggressiveness (with the exception of the weight of the bumper, which is evidently light enough to be insignificant).

In addition, preliminary evaluation of potential devices to measure vehicle aggressiveness indicated the possibility that the degree of structural aggressiveness exhibited by a vehicle in a frontal collision with a small car may be determined in a fixed rigid barrier (FRB) crash test by measuring only the maximum vehicle crush (and knowing the vehicle's weight). Measurement of vehicle aggressiveness is addressed further in Section 3.2.

In this project, additional crash tests were conducted and analyzed for purposes of further identifying aggressiveness characteristics (reported in this section of the report) and for more thoroughly evaluating the ability of different barriers for measuring aggressiveness (reported in Section 3.2).

2.2.2 Experimental Approach

The general approach was to select two fullsize passenger cars, one of which was hypothesized to be aggressive, and one, non-aggressive, on the basis of fixed rigid barrier test results. Each fullsize car would then be crashed into a crashworthy subcompact car in both full frontal and offset frontal collision modes. Analysis of the crash test results was expected to confirm the initial hypothesis regarding degree of aggressiveness of the large cars, and would also provide added knowledge regarding vehicle characteristics associated with aggressive (or non-aggressive) behavior. In addition to car/car tests, large car to barrier tests were to be conducted to determine the capability of different types of barriers for measuring aggressiveness (to be described in Section 3.2).

2.2.3 Vehicle Selection

Vehicles were selected to represent as nearly as possible typical full size and sub-compact vehicles expected to be produced in 1990. Prime factors considered were weights and sales as projected by the Transportation Systems Center (5). The TSC projections indicated that a small vehicle curb weight under 2000 lbs., and a large

vehicle curb weight of approximately 3200 lbs. should be reasonable vehicle weights for the crash test selection. A further point of consideration was the projected engine and drive configurations. By 1990, seventy percent of all U.S. cars are estimated to feature front-wheel drive with engines mounted transversely in the front of the vehicle (6). Unfortunately, at the time the vehicles were selected, a limited number of large production vehicles had these features, so the large vehicles selected for the aggressiveness testing were limited to conventional rear wheel drive.

Full frontal rigid barrier crash test data, compiled by the Office of Market Incentives under the New Car Assessment Program, were analyzed in order to select the aggressive and non-aggressive large vehicles and the crashworthy small vehicle. The vehicles were classified by weight as was shown in Table 2.

The large vehicle test data are summarized in Table 11. As shown in Figure 24, the AMC Concord and the Oldsmobile Cutlass were the two vehicles of comparable (and desirable) test weights having the largest difference in crush. From this it was expected that the AMC Concord would be a much more aggressive car than the Oldsmobile Cutlass. The compartment responses (Figure 25) also supported this conclusion. The Cutlass was much softer than the Concord in the early part of the pulse, and was expected to allow a much better cushion for the occupant of a struck vehicle. The 1980 AMC Concord and the 1979 Oldsmobile Cutlass initially were selected, then, to represent the aggressive and non-aggressive large cars, respectively. The specifications for these two cars are shown in Table 12.

TABLE 12

Large Car Specifications for Testing of Potential Aggressiveness Test Devices

Manufacturer	GMC	AMC	FORD
Make/Model	Oldsmobile Cutlass Supreme	Concord DL	Mercury Marquis
Body Style	2-door Sedan	2-door Sedan	2-door Sedan
Engine Cylinders*	V6	6	8
Engine Displacement*	3.8 L(232 in ³)	4.2L (258 in ³)	4.9L (302 in ³)
Transmission	Automatic 3-speed	Automatic 3-speed	Automatic 3-speed

*In the car-to-car test [described in a subsequent section], the Cutlass Supreme engine was a 260 cu.in. V8. The effect this has on the Cutlass Supreme level of aggressiveness is unknown. However, previous studies (3,4) have indicated that a reduced engine-to-bumper clearance slightly increases vehicle aggressiveness.

TABLE 11

Large Vehicle FRB Crash Test Summary

Class	Vehicle Test Data						
	Vehicle	Curb Weight	Test Weight	Impact Velocity	Static Crush	Dynamic Crush	
C O M P A C T / I N T E R M E D I A T E / S T A N D A R D / F U L L S I Z E / S T A T I C / D Y N A M I C	80 Chevrolet Citation	2750	3260	35.0	21.4	30.7	
	79 Ford Fairmont	2820	3300	35.4	25.0	28.3	
	79 Chevrolet Monza	2730	3240	35.1	25.5	28.6	
	79 Mercury Bobcat	2607	2998	35.1	20.0	26.6	
	80 AMC Concord	3130	3700	34.7	20.8	23.2	
	79 Plymouth Volare	3260	3820	35.0	23.9	26.6	
	79 Oldsmobile Cutlass	3298	3799	34.8	30.2	34.1	
	79 Ford Granada	3490	3950	34.6	27.8	31.2	
	79 Pontiac Firebird	3390	3908	35.2	27.8	33.6	
	79 Ford LTD	3790	4370	35.4	28.1	36.1	
79 Mercury Marquis	3695	4224	35.4	28.5	35.1		
79 Chevrolet Impala	3659	4179	35.2	24.1	29.2		
79 Chrysler LeBaron	3600	4160	35.0	24.6	27.4		

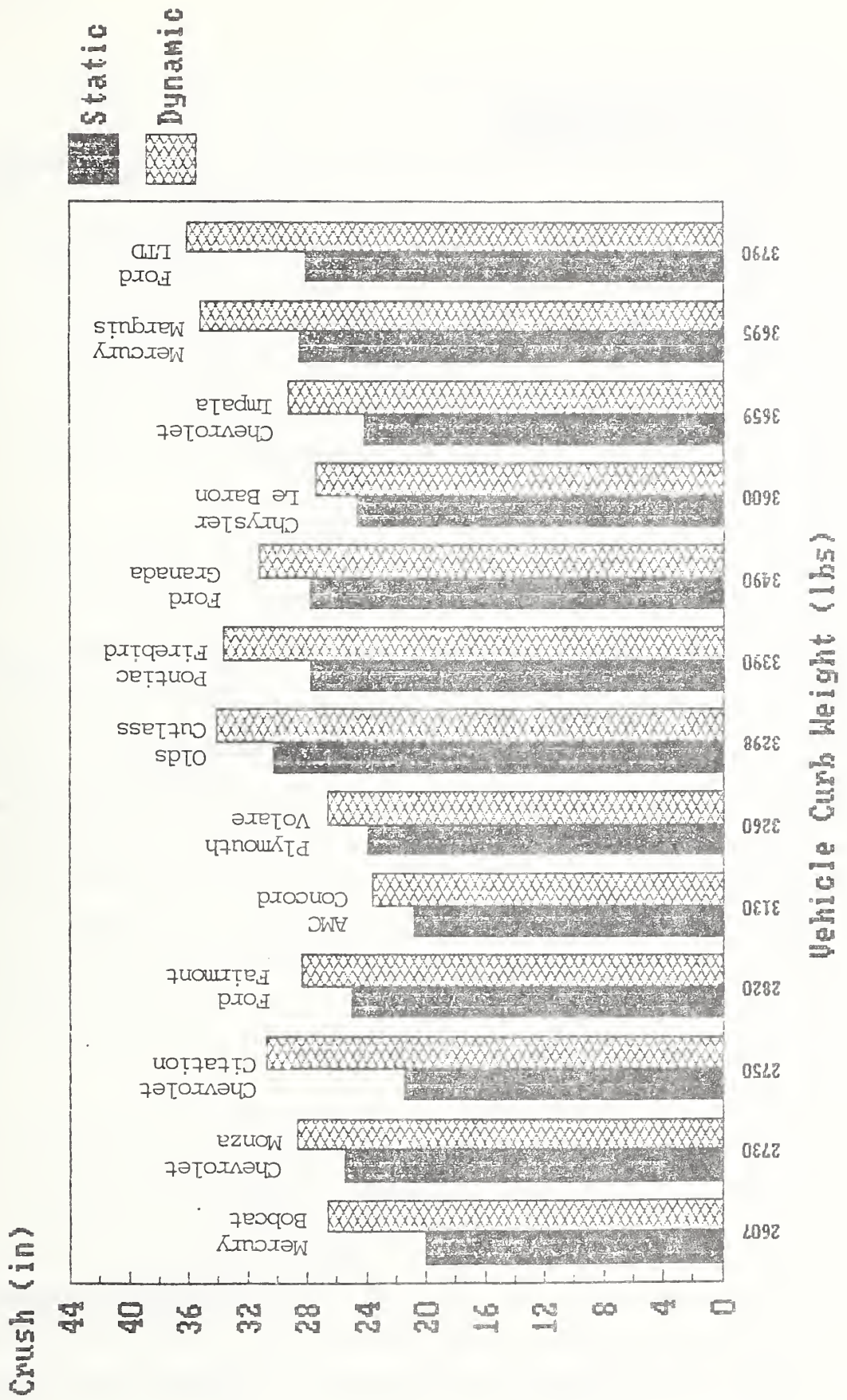
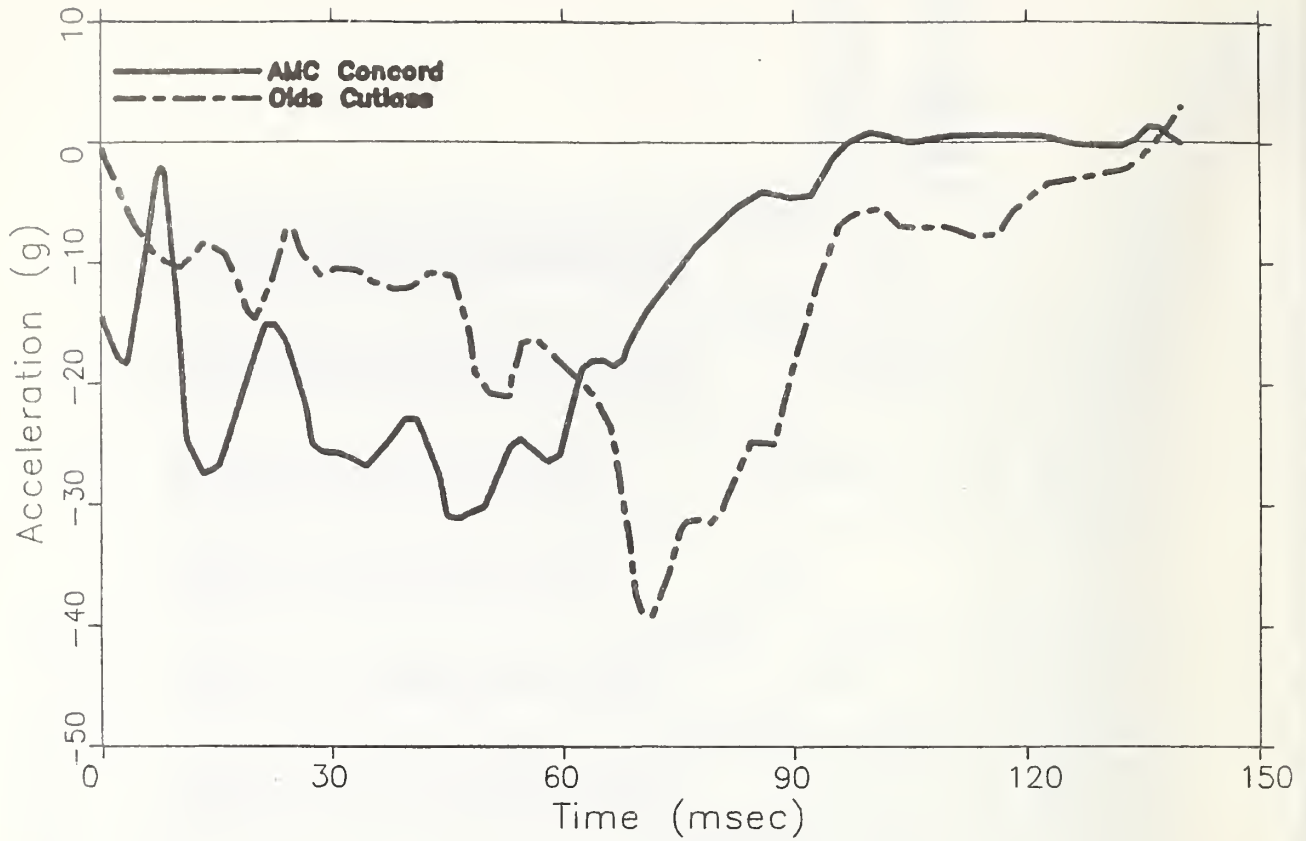
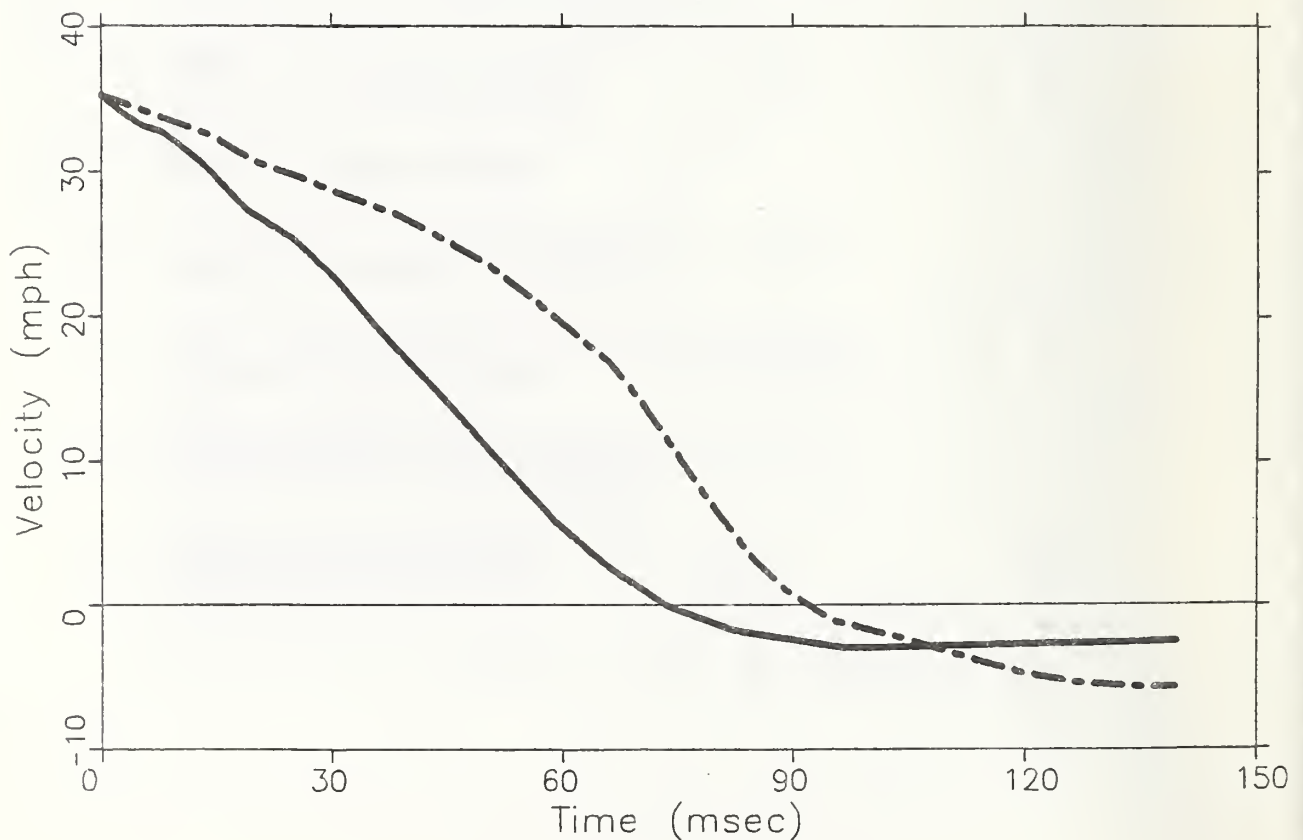


FIGURE 24. Crush Comparison From 35 mph Fixed Rigid Barrier Impact



a) Acceleration Response



b) Velocity Response

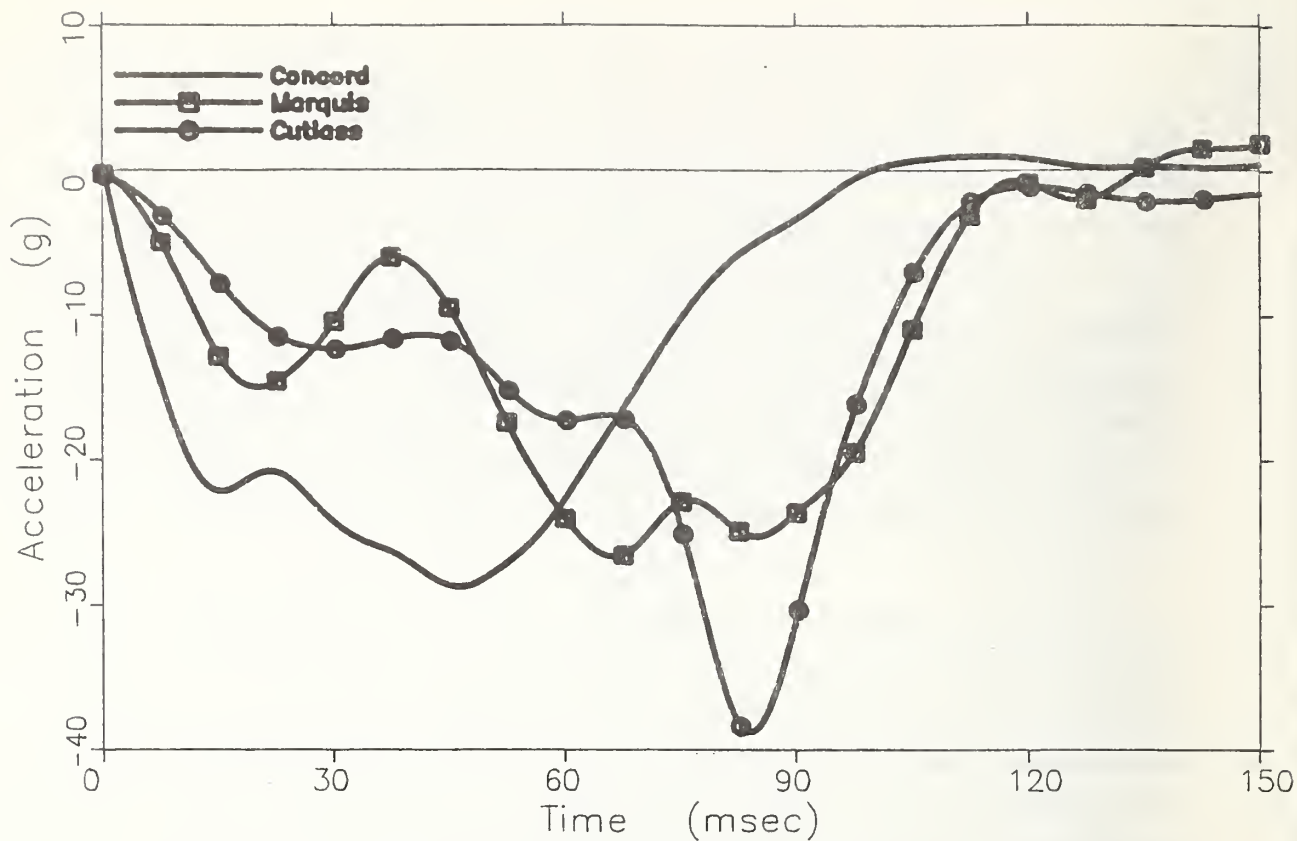
FIGURE 25. Compartment Responses of 1980 AMC Concord and 1979 Olds Cutlass Supreme in 35 mph Fixed Rigid Barrier Impact

It was learned in subsequent crash testing that the Cutlass had a tendency to structurally override the main structural elements of its crash partner. This phenomenon was observed in both car/car and car/moving deformable barrier tests, and was judged to have been caused by a design peculiarity in the Cutlass' frame geometry. It is generally accepted that there are three sources of vehicle aggressiveness: structural, geometric and mass effects. The occurrence of override (a geometric aggressiveness effect) had the effect of confounding the test results, so that it was not possible to separate structural from geometric influences on aggressiveness. It was originally intended that only structural aggressiveness be addressed in this program; therefore, another large non-aggressive vehicle was selected to replace the Cutlass.

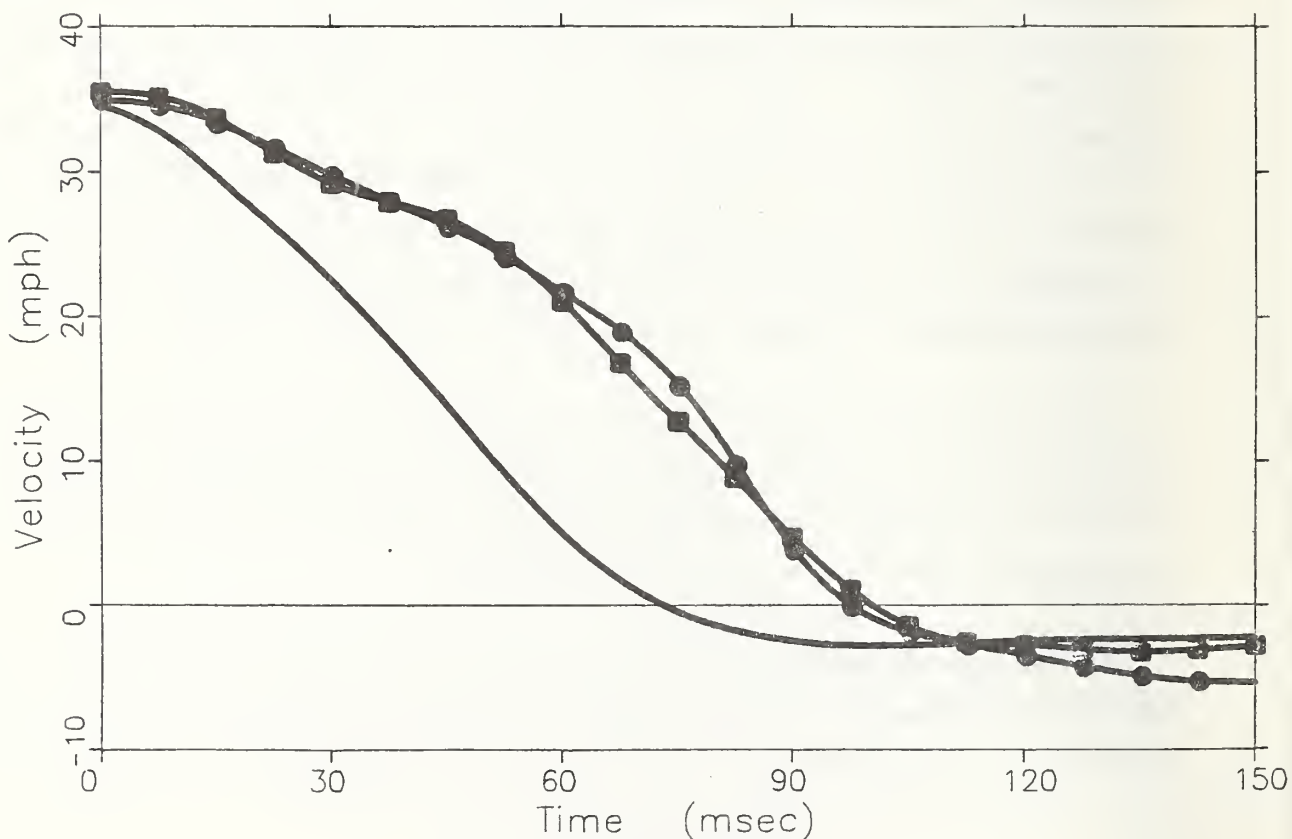
Referring to Figure 24, it is seen that the Mercury Marquis exhibited crush values which were approximately the same as the Cutlass. Figure 26 shows the compartment response of the Marquis compared with the Cutlass and Concord. Responses of the Marquis and Cutlass were very similar, and the relationship between Marquis and Concord responses were similar to that between Cutlass and Concord. A difficulty with the Marquis was that its curb weight was considerably greater than those of the Cutlass and Concord. However, the 1981 Mercury Marquis was downsized from the 1979 model year, and it was concluded that the test weight of the Marquis could be controlled to be approximately equal to that of the Concord, and possible mass effects on the aggressiveness difference between the two vehicles could be eliminated. A subsequent test of the Marquis into the load cell barrier, where the Marquis' weight was reduced from that of the FRB test, resulted in a response which was very similar to the FRB test response. Therefore, the Mercury Marquis was selected to replace the Cutlass in the aggressiveness test program. Its specifications are shown in Table 12.

It was clear that the tendency of the Cutlass to override was not an experimental anomaly, but was an occurrence which is typical in real world accidents. Consequently, both the full and offset frontal crash tests were conducted with the Cutlass and were analyzed along with the Concord and Marquis tests.

To select a crashworthy small vehicle, the vehicle crash pulses (7,8,9), dummy measurements, Restraint Survival Distance (RSD) calculations and ABAG computer simulations were examined. The use of dummy measurements to judge levels of



a) Acceleration Response



b) Velocity Response

FIGURE 26. Occupant Compartment Responses --
35 mph Fixed Rigid Barrier Impacts

crashworthiness were supplemented with RSD and ABAG in order to better assess the potential for crash survival in the vehicles. Primary attention was given to vehicles in the mini-compact classification.

One note should be made regarding the VW Rabbit and the Chevrolet Chevette restraint systems when comparing the dummy measurements. The front seat occupants of these two cars were restrained by production passive systems. The Rabbit employed an automatic diagonal torso belt with lower instrument panel knee bolster, while the Chevette had a manual lap belt with the automatic diagonal torso belt. The front seat occupants in the other cars were restrained with active three point systems.

The dummy measurements (summarized in Table 13) are compared in Figures 27 and 28. Of the four cars within the desired weight range (under 2000 lbs.), the VW Rabbit had the lowest dummy measurements.

The Restraint Survival Distances are summarized in Table 14 and Figure 29. The available internal distances (AID's) used for the RSD computations are based on a measured distance between the dummy's nose and the windshield. While it is not felt that this is the best determination of AID for computing RSD, it is the only common dimension included in each of the crash test reports. This analysis shows that the VW Rabbit has a better RSD than other vehicles under 2000 pounds in weight.

The ABAG computer simulations (Table 15 and Figure 30) show the Plymouth Champ, VW Rabbit, Datsun Sedan and Plymouth Horizon to be nearly equal and better than the other four vehicles.

The crash survivability predictions were more consistent and indicated better potential crashworthiness for the VW Rabbit than for the other vehicles. Because of this and the fact that the Rabbit is one of the lighter vehicles and has a transverse engine with front wheel drive, it was selected as the small, crashworthy car for the crash test matrix. The specifications for the VW Rabbit are shown in Table 16.

Table 16
Small, Crashworthy Car Specifications for the Crash Test Matrix

Manufacturer	VW of America, Inc.
Make/Model	VW Rabbit
Body	2-door Hatchback
Engine Cylinders	4
Engine Displacement	89 cu. in.
Transmission	4-speed, manual

TABLE 13
Crash Test and Dummy Measurement Summary from 35 mph Barrier Impacts

CLASS	Vehicle	TEST DATA					DUMMY MEASUREMENTS															
		Curb Wt.	Test Wt.	Crash Vel.	Static Crush L/R	Dynamic Crush	Driver					R.F. Passenger										
						Meas. Head Peak g's	Meas. HIC	Meas. Chest Peak g's	Meas. Femur Load	Meas. Head Peak g's	Meas. HIC	Meas. Chest Peak g's	Meas. Femur Load									
M C	VW Rabbit 2-D	1860	2600	34.8	22.7	24.3	90	1023.9	67	1170/630	47	428.8	33	937/1460								
I O																						
N M	79 Datsun 210-Sedan	1960	2425	35.1	24.9	30.1	122.4	1358	68.9	-/536	183.7	1745	59.4	781/218								
I P																						
A C	79 Honda Civic	1690	2180	34.8	20.9	23.9	116	2029.6	92.6	1080/838	142	2093.3	46	1520/1460								
T	79 Plymouth Champ	1830	2313	35.3	22.3	29.9	127.1	1270.2	72.1	892/435	206.9	1918.4	66.3	686/560								
S C	79 Chevy Chevette	2240	2720	34.8	21.9	26.0	118	871.4	47	1280/1600	88	858.6	45	990/1480								
U O																						
B M	79 Toyota Celica	2510	3025	34.8	24.2	28.1	94	848.8	61	2920/435	158	1861.7	59	400/520								
P																						
A	79 Plymouth Horizon	2206	2661	34.9	22.0	28.7	91.9	652.7	51.6	973/707	69.9	780.4	38.2	580/656								
C																						
T	79 Toyota Corolla	2239	2651	35.0	20.3	25.4	-----	-----	-----	4000/640	-----	-----	-----	1400/4401								

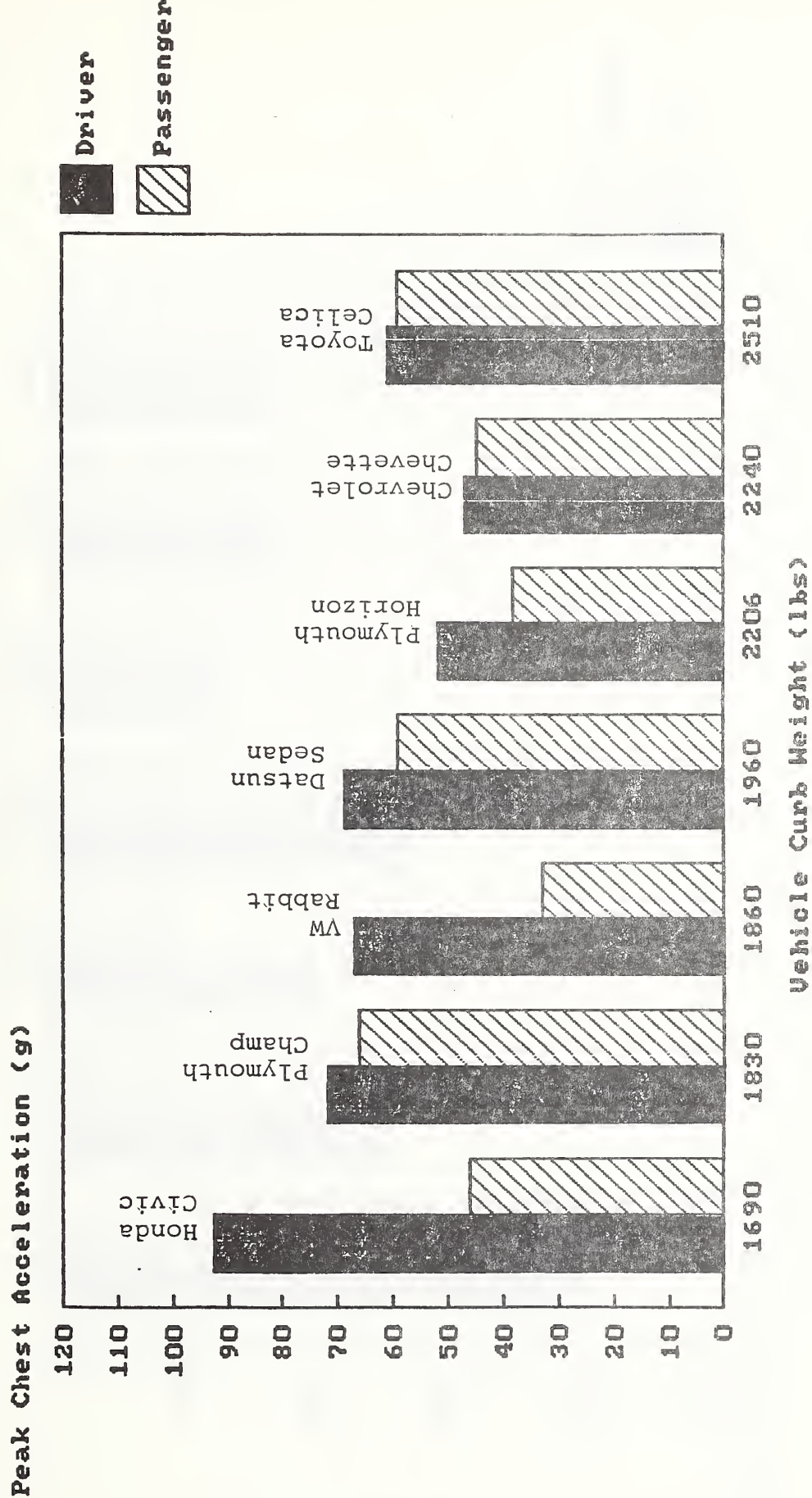


FIGURE 27. Dummy Peak Chest Acceleration Measurement Comparison -- 35 mph Fixed Rigid Barrier Impacts

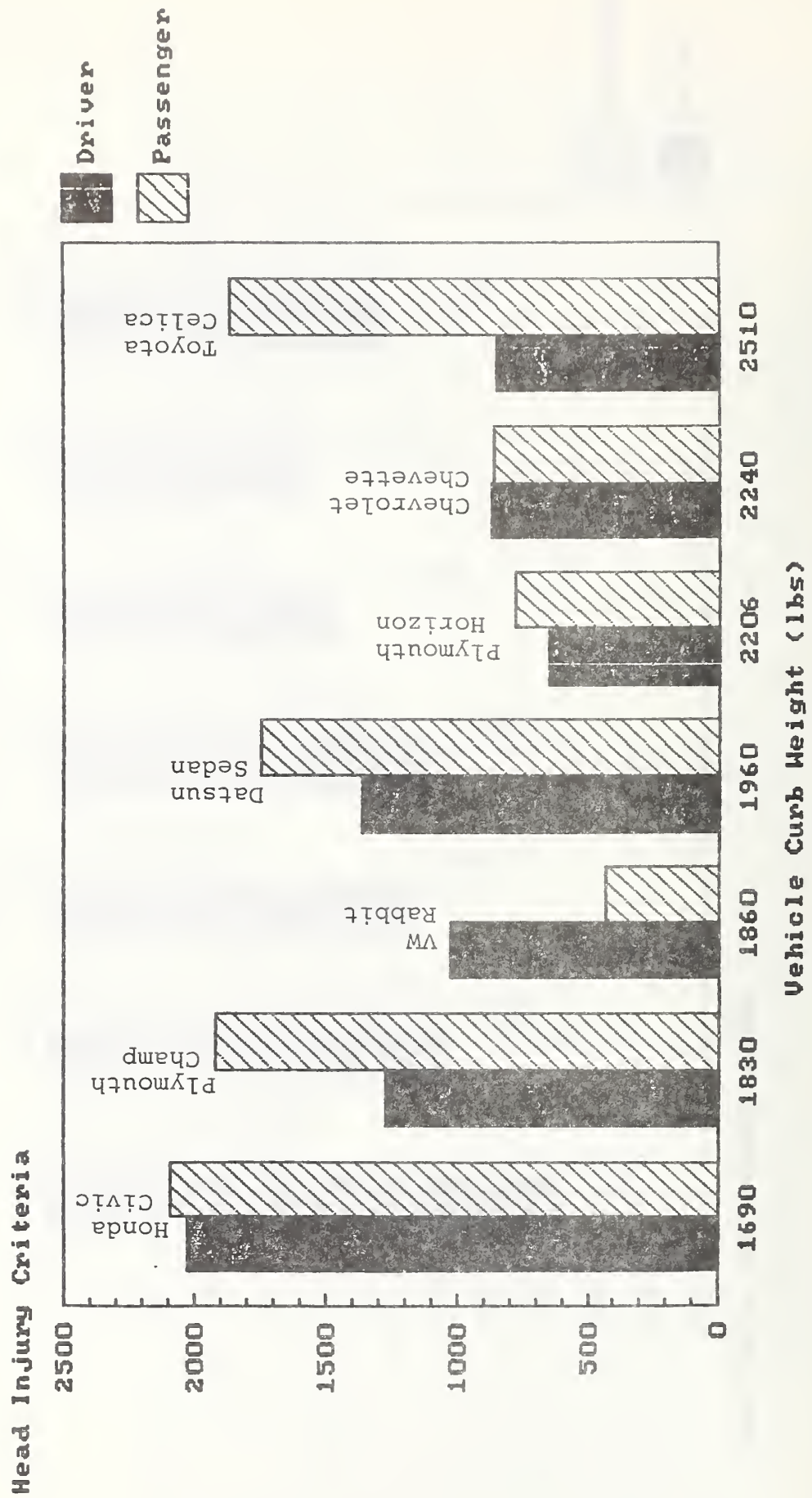


FIGURE 28. Dummy Measurement HIC Comparison -- 35 mph Fixed Rigid Barrier Impacts

TABLE 14
 Restraint Survival Distance Calculation Summary
 From 35 mph Barrier Impacts

Class	YEAR	VEHICLE	VO	T*	DC	AID	DP	RSD
C O M P A C T	1979	Volkswagon Rabbit	34.8	.057	25.62	23.5	31.17	17.94
	1979	Datsun Sedan	35.1	.0575	27.15	19.0	31.58	14.56
	1979	Honda Civic	34.8	.063	23.5	20.5	32.06	11.93
	1979	Plymouth Champ	35.3	.054	25.65	17.2	30.89	11.95
S U B C O M P A C T	1979	Chevrolet Chevette	34.8	.062	24.21	13.1	31.97	5.33
	1979	Toyota Celica	34.8	.058	25.6	16.5	31.38	10.71
	1979	Plymouth Horizon	34.9	.059	26.37	13.9	31.67	8.60
	1979	Toyota Corolla	35.0	.063	24.97	23.38	32.28	16.05

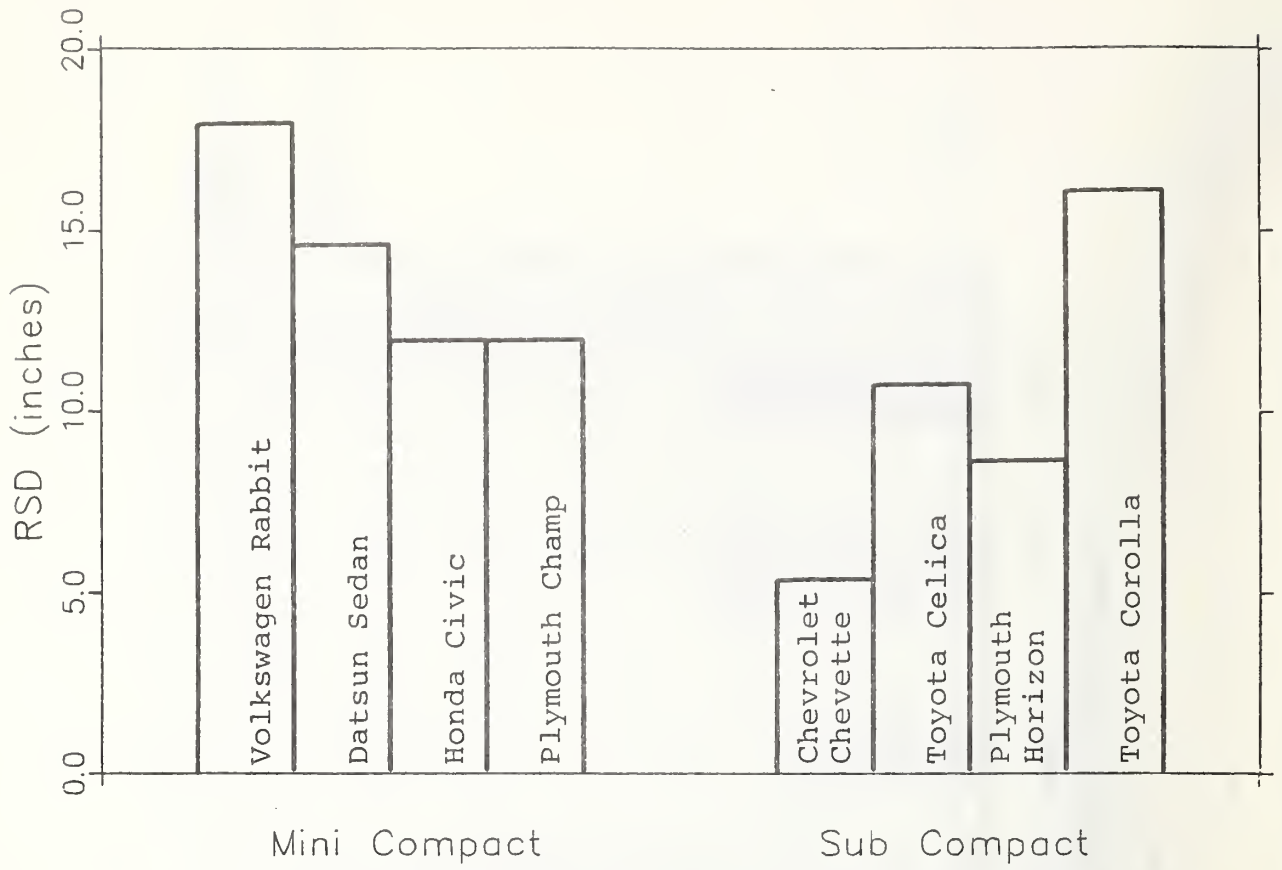


FIGURE 29. Restraint Survival Distances --
35 mph Fixed Rigid Barrier Impacts

TABLE 15
 ABAG Computer Simulation Summary from 35 mph Barrier Impacts

CLASS	Vehicle	ABAG SIMULATION			
		Drivers (50th % Male)		Passengers (50th % Male)	
		Max. Chest Acc. (G's)	Max. Col. Disp (in)	Max. Chest Acc. (G's)	Max. Chest Acc. (G's)
MINI	79 Plymouth Champ	35.1	Bottom	37.9	
	79 Datsun 210	38.8	Bottom	44.4	
	79 VW Rabbit	38.6	Bottom	42.9	
	79 Honda Civic	61.2	Bottom	48.7	
SUBARU	79 Toyota Corolla	83.7	Bottom	53.7	
	79 Plymouth Horizon	38.7	Bottom	42.4	
	79 Chevrolet Chevette	49.8	Bottom	47.1	
	79 Toyota Celica	46.2	Bottom	42.9	

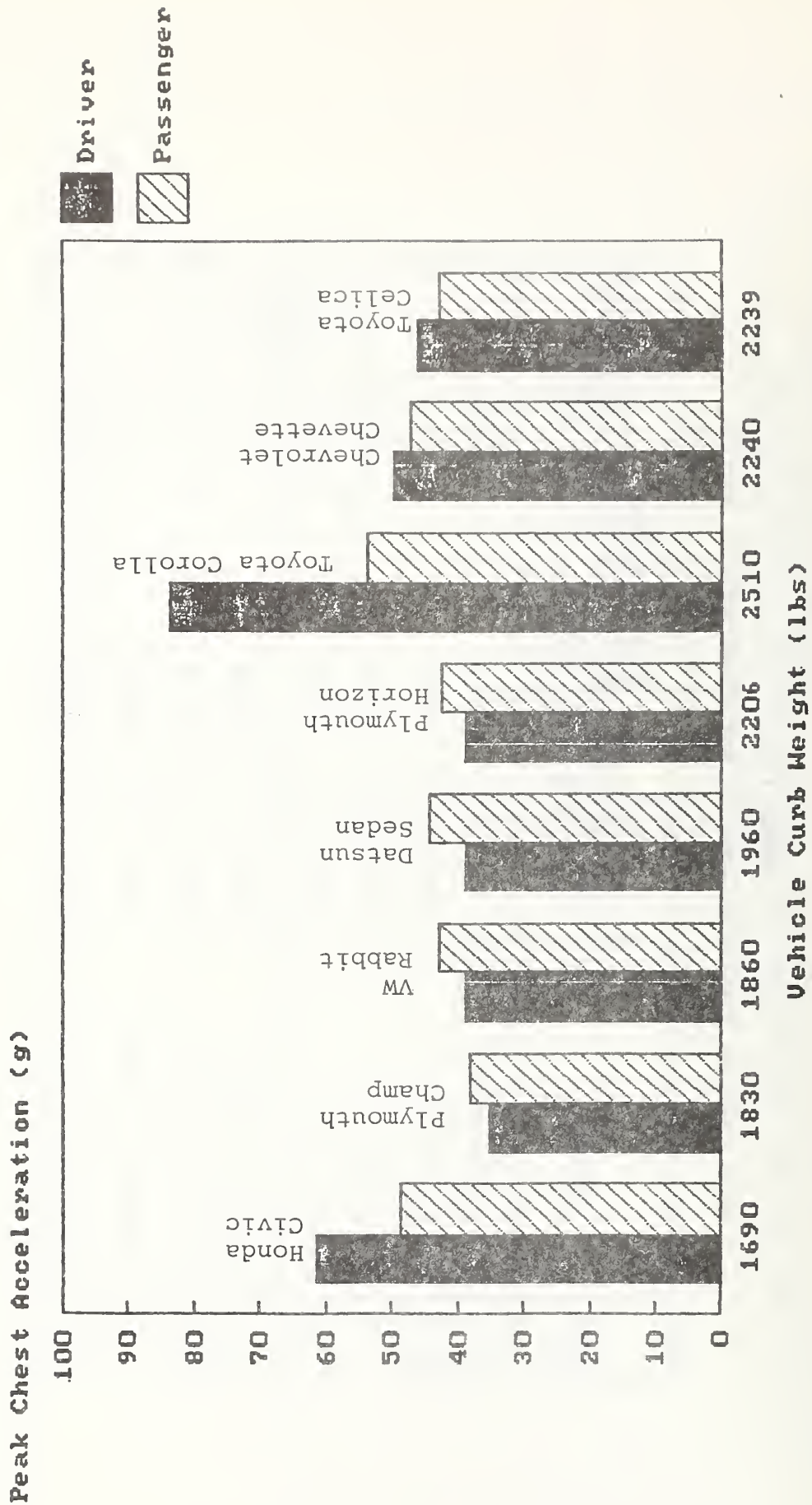


FIGURE 30. ABAG Computer Simulation Comparison for 50th Percentile Male -- 35 mph Fixed Rigid Barrier Impacts

2.2.4 Car/Car Crash Test Results

Five car/car frontal crash tests were conducted, each at a nominal closing velocity of 64 mph. The AMC Concord, Mercury Marquis and Oldsmobile Cutlass each were to be crashed into the VW Rabbit in full frontal and offset frontal collision modes. However, the offset collision between the Marquis and the Rabbit was not performed. A summary of vehicle data and test conditions is presented in Table 17.

2.4.4.1 Full Frontal Collisions

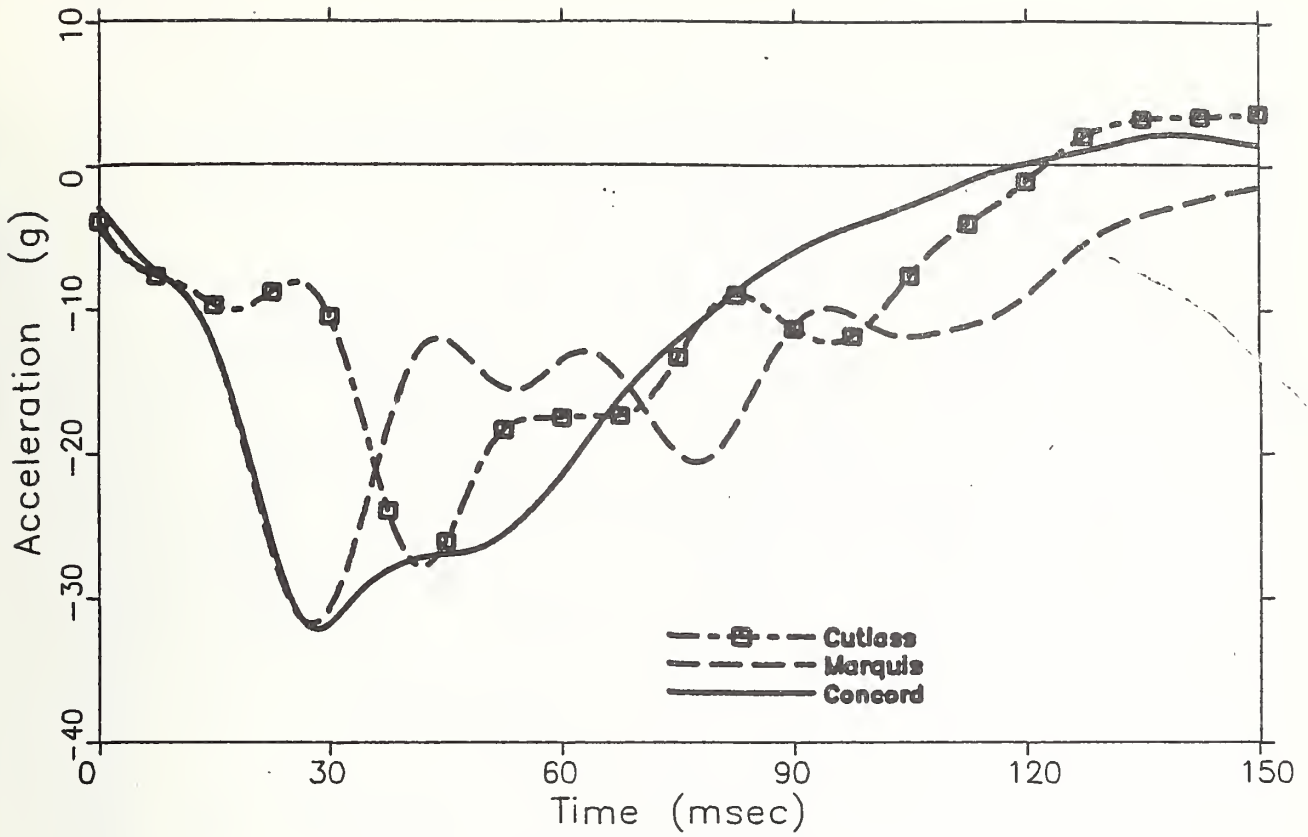
No significant differences in maximum crush occurred among the Rabbits in the three full frontal tests. However, maximum intrusion in the Rabbit struck by the Concord was nearly twice that in the other two Rabbits (see Table 17).

Figure 31 shows the Rabbits' occupant compartment responses resulting from the three tests. The Rabbit struck by the Concord, although very similar to the Marquis collision during the first 30 milliseconds, experienced a higher level of acceleration through the first 70 milliseconds of the event than in either the Marquis or Cutlass collisions. Consequently, the Rabbit collision with the Concord resulted in a more rapid velocity change between 30 and 70 milliseconds.

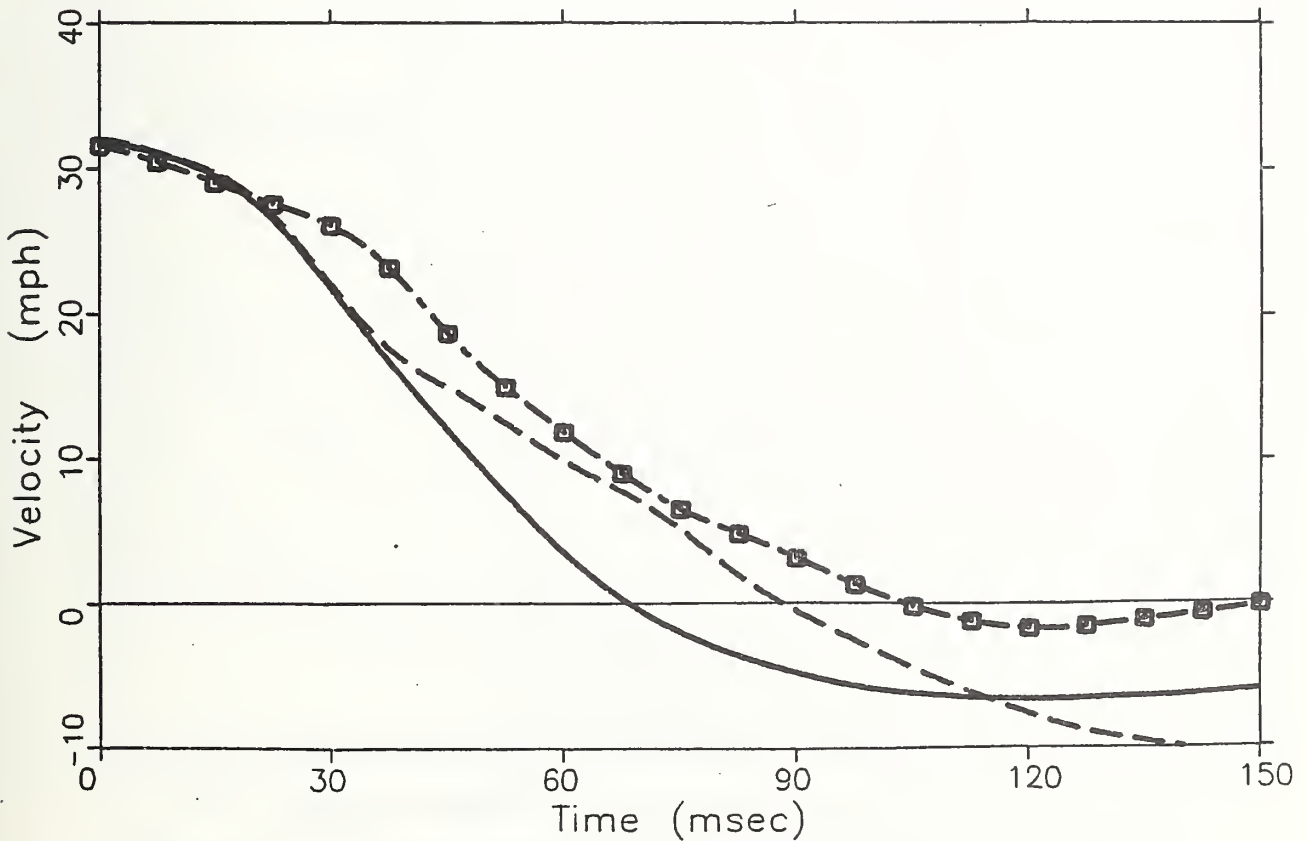
The dummy measurements for the Rabbits are shown in Table 18. HIC and peak chest accelerations were, in general, considerably higher for the Rabbit struck by the Concord, indicating the Concord to be more aggressive than either the Marquis or Cutlass. However, observation of the high speed films revealed that the shoulder belt slid partially off the driver's shoulder in each test, allowing excessive forward motion of the dummy. Consequently, the validity of comparing driver dummy measurements is questionable. Figures 32-34 show the driver positions before the collisions and at initial steering column contact for all three tests. A similar observation was made for the Rabbit passengers in the Concord/Rabbit and Cutlass/Rabbit tests. The belt slid from the shoulder, but not to the extent observed for the driver. In contrast, the Rabbit passenger in the Marquis/Rabbit test appeared to have been well restrained by the shoulder belt. Therefore, comparisons of passenger dummy measurements are also of questionable validity.

TABLE 17
 Vehicle Data and Test Condition Summary -- Car/Car Collisions

Crash Mode	Vehicle	Model Year	Body Style	Engine Displ (in ³)	Engine No. Cyl's	Transmission		Impact Velocity (mph)	Test Wt (lbs)	Max Crush (in)	Max Intrusion (in)
						Fwd Ratios	Actua- tion				
	AMC Concord	1980	2 Dr Sed	258	6	3	Auto	31.8	3930	20.6	2.8
	VW Rabbit	1980	2 Dr Hatch	89	4	4	Man	31.8	2580	31.8	10.1
	Merc Marquis	1981	2 Dr Sed	302	8	3	Auto	32.1	3960	23.1	1.7
	VW Rabbit	1982	2 Dr Hatch	105	4	4	Man	32.1	2570	31.1	6.1
Full Frontal	Olds Cutlass	1980	2 Dr Sed	260	8	3	Auto	31.5	3950	18.7	4.8
	VW Rabbit	1980	2 Dr Hatch	89	4	4	Man	31.5	2580	30.4	5.3
	AMC Concord	1980	2 Dr Sed	258	6	3	Auto	31.8	3930	20.8	3.7
	VW Rabbit	1980	2 Dr. Hatch	97	4	4	Man	31.8	2580	40.3	12.6
Offset Frontal	Merc Marquis	-----Test not conducted-----									
	VW Rabbit	-----Test not conducted-----									
	Olds Cutlass	1980	2 Dr Sed	260	8	3	Auto	30.9	3950	28.8	2.7
	VW Rabbit	1980	2 Dr Hatch	97	4	4	Man	30.9	2580	27.9	5.7



a) Acceleration Response

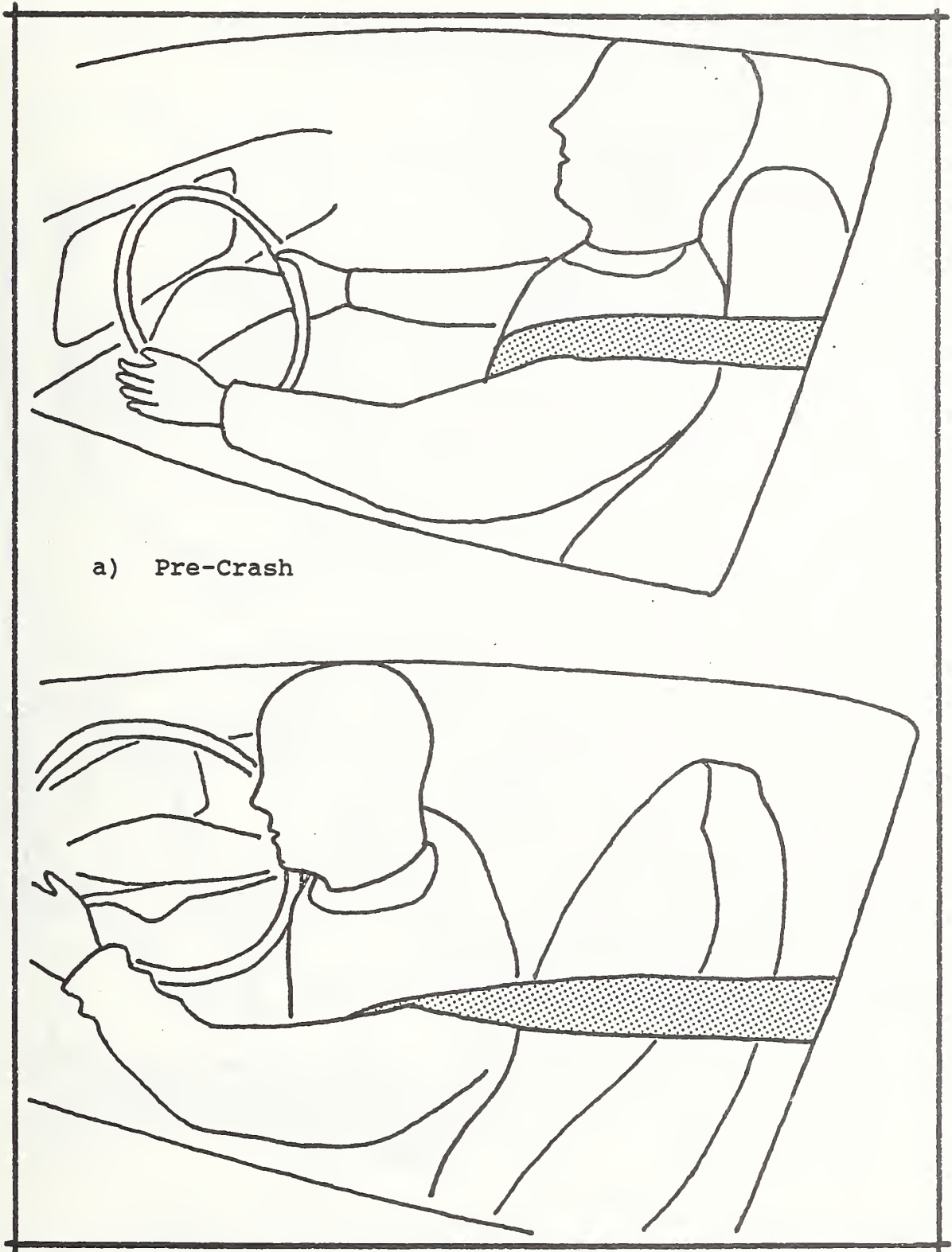


b) Velocity Response

FIGURE 31. Rabbit Occupant Compartment Responses -- Full Frontal Car/Car Collisions

TABLE 18
Rabbit Dummy Measurements -- Full Frontal Crash Tests

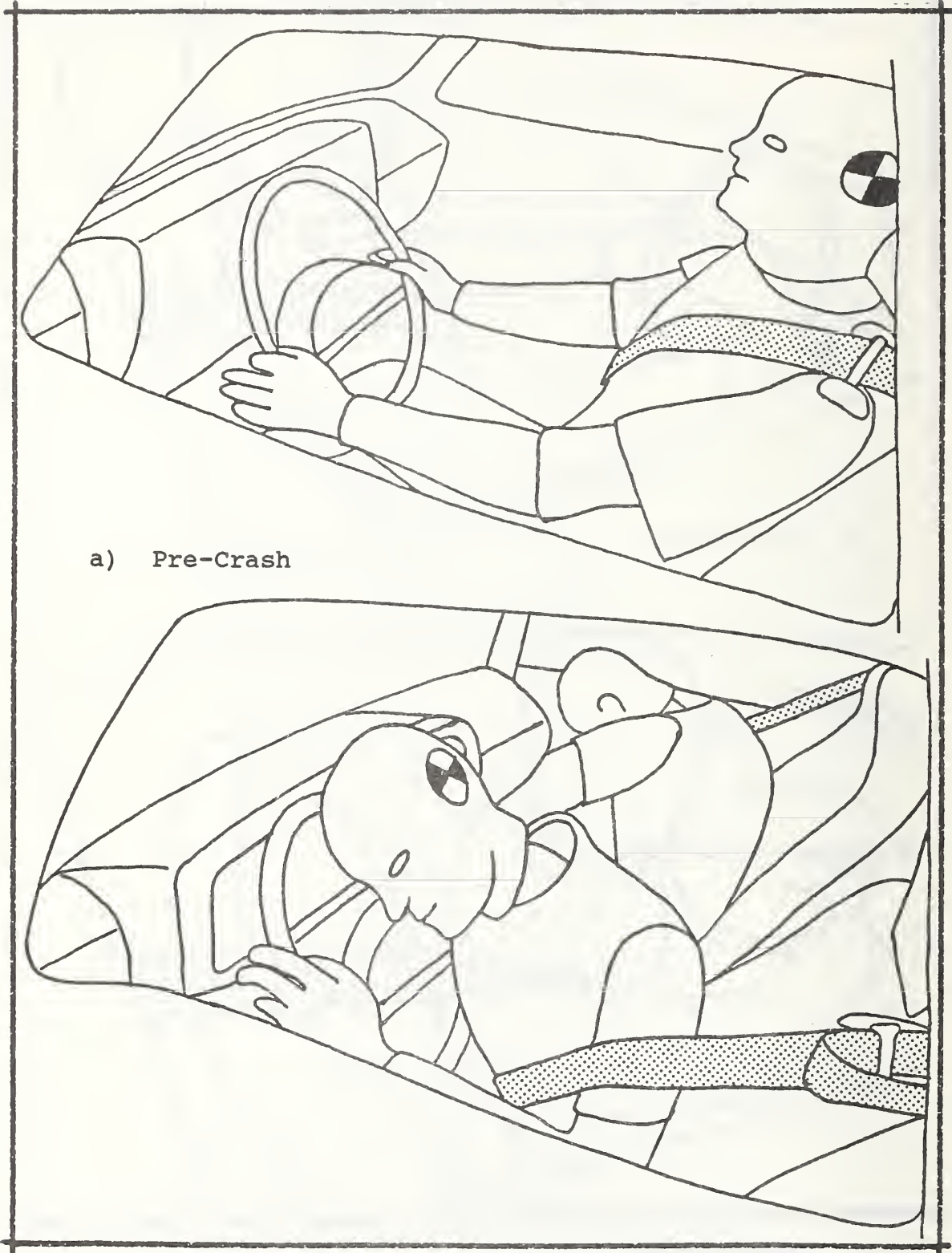
Test	DRIVER				PASSENGER			
	HIC	Peak Chest Accel's (g's)	Femur Loads (lbs) Left	Femur Loads (lbs) Right	HIC	Peak Chest Accel's (g's)	Femur Loads (lbs) Left	Femur Loads (lbs) Right
Concord/Rabbit	1099	63	740	440	975	46	220	840
Marquis/Rabbit	341	36	1575	175	473	50	625	475
Cutlass/Rabbit	986	38	375	337	531	30	338	360



a) Pre-Crash

b) During Crash

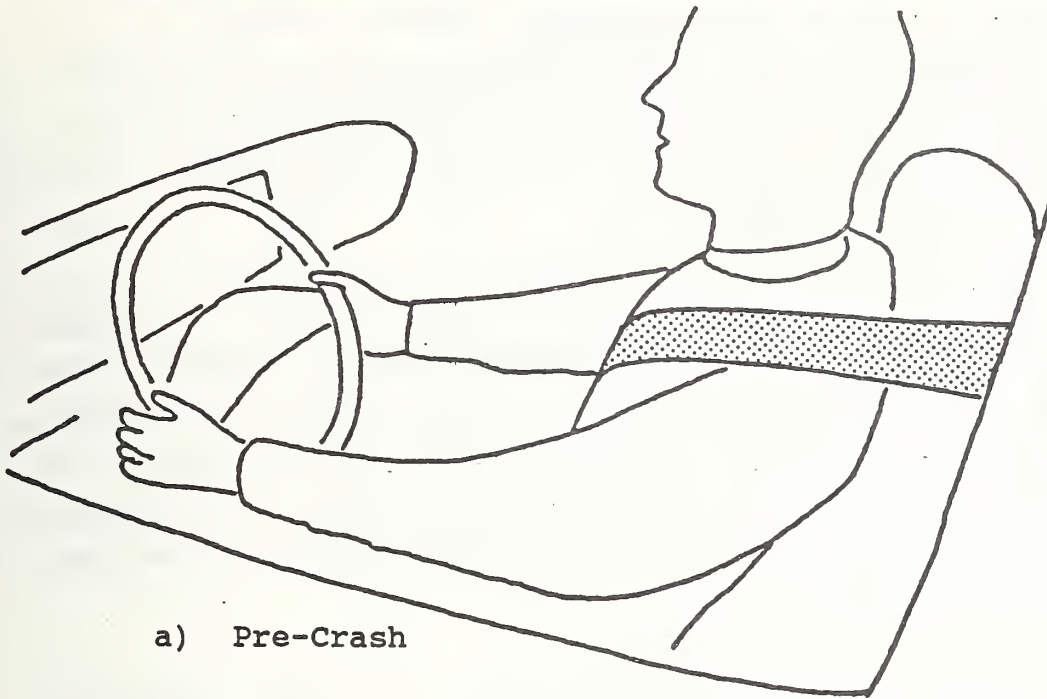
FIGURE 32. Rabbit Shoulder Belt and Steering Column Behavior -- Concord Collision



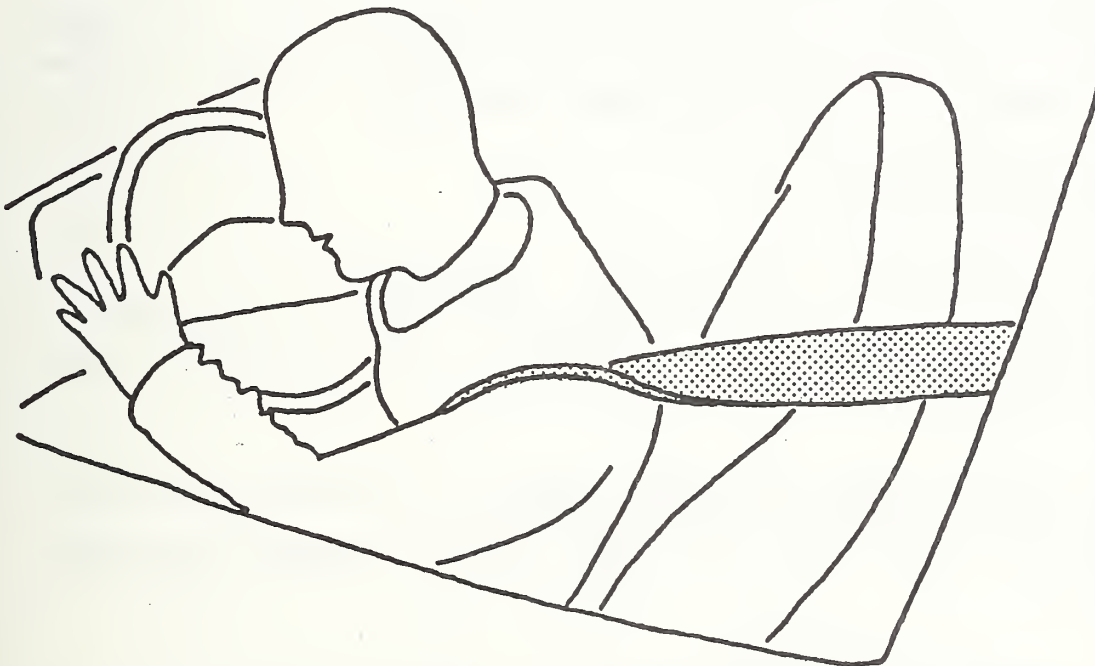
a) Pre-Crash

b) During Crash

FIGURE 33. Rabbit Shoulder Belt and Steering Column Behavior -- Marquis Collision



a) Pre-Crash



b) During Crash

FIGURE 34. Rabbit Shoulder Belt and Steering Column Behavior -- Cutlass Collision

Steering column behavior can also be observed in Figures 32-34. In the Marquis/Rabbit test, although the entire instrument panel of the Rabbit appeared to displace rearward, the column did not experience significant rearward or upward displacement. Similarly, the column in the Cutlass/Rabbit test did not displace significantly. However, in the Concord/Rabbit test, significant vertical displacement of the column occurred, probably resulting in a more severe head impact than would have occurred with no vertical displacement.

Restraint Survival Distances (RSD's) are shown in Table 19. Pre-test Available Internal Distances (AIDS's), measured from the occupant chest to the instrument panel, were used in the RSD calculations. Intrusion was not taken into account, since it occurred at the firewall and would not have reduced available stroking distance in the area of the thorax, where an airbag system would be deployed. The Concord is indicated as being only slightly more aggressive than the Marquis, but considerably more aggressive than the Cutlass.

Finally, the results of applying the ABAG model to the Rabbit occupants are presented in Table 20. Occupants of the Rabbit struck by the Concord would have experienced significantly greater peak chest accelerations, and column stroke would have been significantly greater in the Rabbit/Concord collision, indicating that the Concord is more aggressive than either the Marquis or the Cutlass.

2.2.4.2 Offset Frontal Collisions

As previously stated, the Marquis/Rabbit offset frontal collision was not conducted. Comparisons, therefore, are limited to the Concord/Rabbit and Cutlass/Rabbit offset tests.

Maximum crush and intrusion were much greater in the Rabbit struck by the Concord than in the Rabbit struck by the Cutlass (Table 17), indicating more severe structural loading.

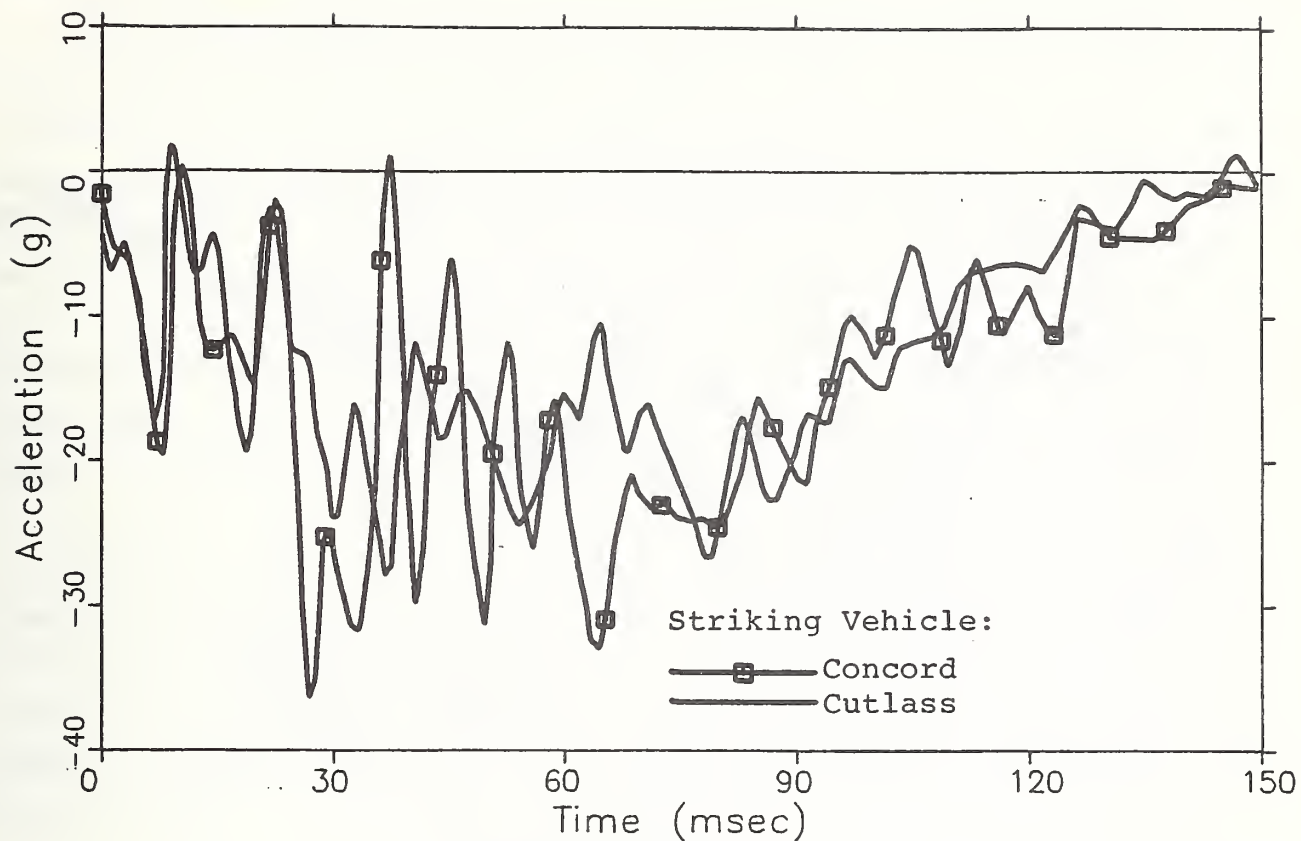
Occupant compartment responses in the Rabbits are shown in Figures 35 (driver side) and 36 (passenger side). Slightly higher driver side accelerations occurred in the Rabbit struck by the Concord between 25 and 75 milliseconds, resulting in a more rapid velocity change. On the passenger side, acceleration-time histories were very similar.

TABLE 19
 Restraint Survival Distance Calculations -- Full Frontal Crash Tests

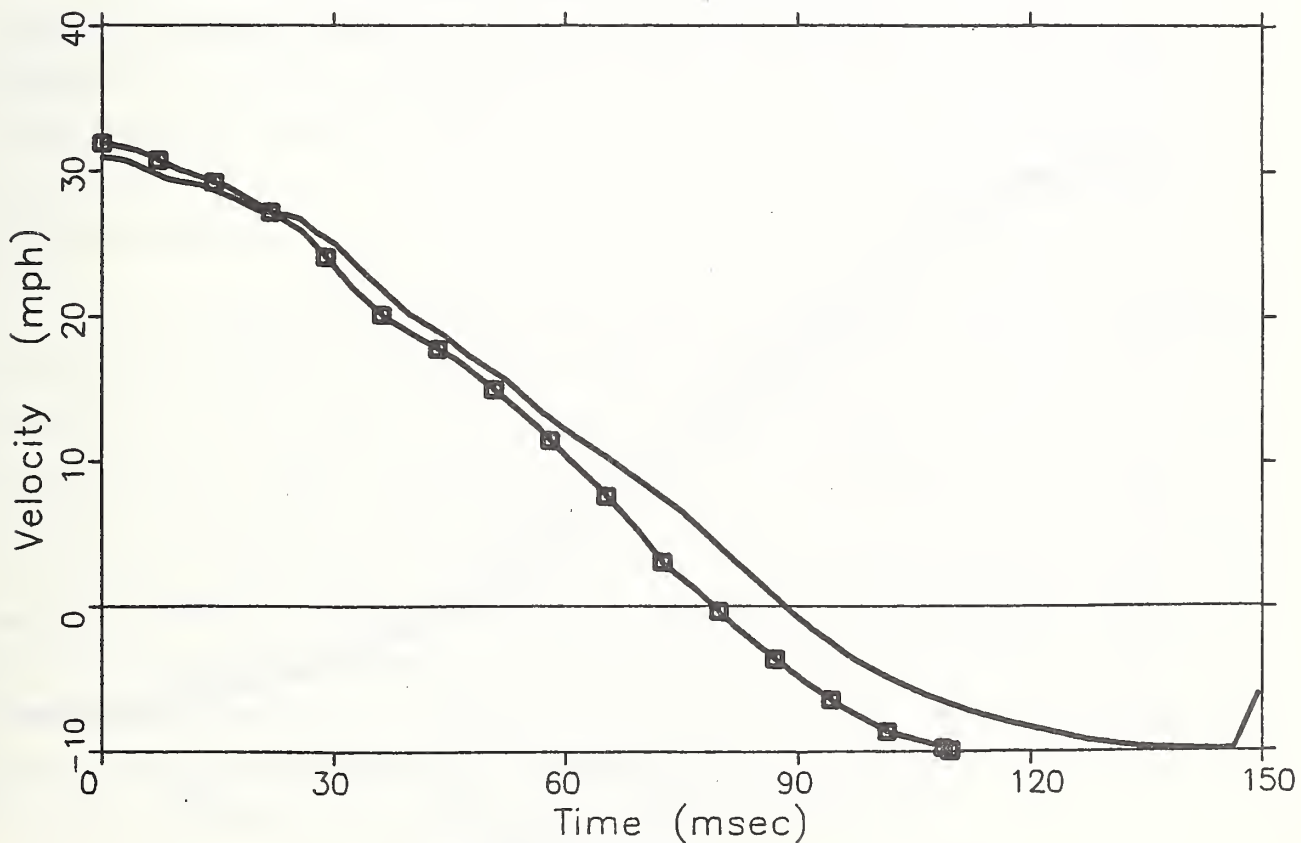
TEST	V_0 (mph)	T^* (sec)	D_c (in)	AID (in)	D_p (in)	RSD (in)
Concord/Rabbit	31.8	0.0625	21.13	26.0	28.73	18.41
Marquis/Rabbit	32.1	0.0566	21.80	26.0	28.40	19.40
Cutlass/Rabbit	31.7	0.0558	22.76	26.0	27.85	20.91

TABLE 20
 ABAG Simulation Results -- Rabbit Occupants
 -- Cut-lass/Rabbit, Marquis/Rabbit and Concord/Rabbit Full Frontal Crash Tests

Position	Occupant	PEAK CHEST ACCELERATION (g's)			COLUMN STROKE (in)		
		Cut-lass/ Rabbit	Marquis/ Rabbit	Concord/ Rabbit	Cut-lass/ Rabbit	Marquis/ Rabbit	Concord/ Rabbit
Driver	5th % F	45.5	47.8	59.4	1.82	1.93	2.39
	50th % M	44.5	43.9	58.1	2.86	2.85	3.76
	95th % M	44.8	42.3	56.9	3.81	3.65	4.93
Passenger	5th % F	65.3	66.4	72.3	N/A	N/A	N/A
	50th % M	46.6	49.3	58.4			
	95th % M	44.1	46.2	60.7			

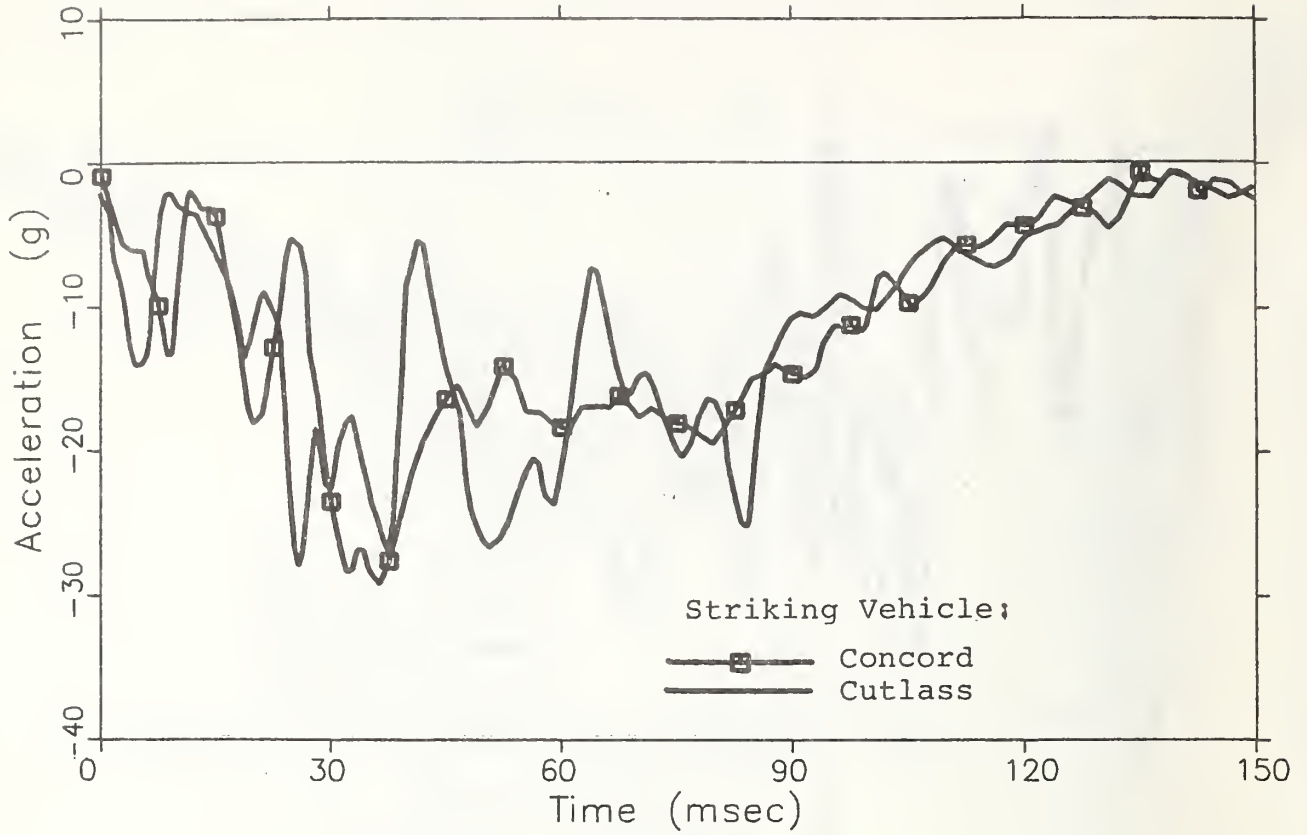


a) Acceleration Response

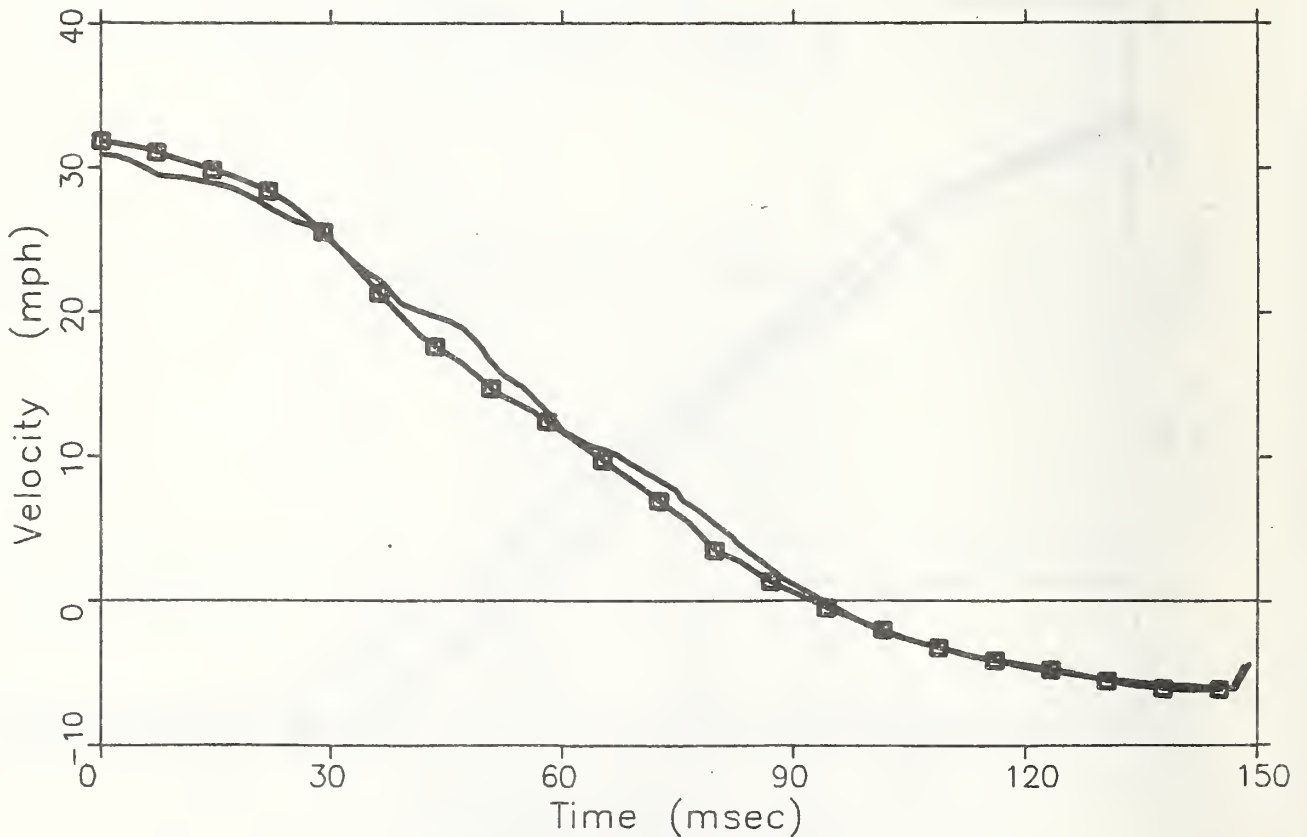


b) Velocity Response

FIGURE 35. Left Compartment Responses in Rabbits -- Offset Frontal Car/Car Collisions



a) Acceleration Response



b) Velocity Response

FIGURE 36. Right Compartment Responses in Rabbits -- Offset Frontal Car/Car Collisions

Table 21 contains dummy measurements for the Rabbits. In general, values were lower than in the full frontal collisions (Table 18). Also, there appear to be less differences in HIC and peak chest acceleration measurements resulting from the two striking vehicles than was observed in the full frontal tests. Viewing of the high speed films showed that the driver's shoulder belt stayed well in place, offering optimum restraint, in each collision. This contrasted markedly with the situation for the drivers in the full frontal tests (discussed in Section 2.4.4.1). For each of the passengers, some movement of the belt off the shoulder occurred, but not until reasonable restraint had been achieved. In view of the variances in shoulder belt behavior, comparisons of dummy measurements between full and offset collisions are of questionable validity.

Restraint Survival Distances are shown in Table 22. Significant A-pillar displacements occurred on the driver side in both collisions. Deformation in this region was especially severe in the Rabbit struck by the Concord. These displacements were subtracted from the pre-test AID's to obtain final AID's which were used to calculate RSD's. For the driver, the Concord was found to be significantly more aggressive than the Cutlass.

The ABAG modeling results are presented in Table 23. They indicate that the Concord is more aggressive than the Cutlass, especially to the driver. The aggressiveness difference is much less, however, than it was in the full frontal collision mode. (Compare Tables 20 and 23.)

2.2.5 Conclusions

It was concluded that a significant difference in aggressiveness exists between the Concord and either the Marquis or the Cutlass when impacted full frontally into a VW Rabbit, the Concord being more aggressive. It is noteworthy that, in spite of the Cutlass/Rabbit override, the responses of (and in) the Rabbits struck by the two relatively non-aggressive cars were remarkably similar. In the case of the Marquis, it is clear that the aggressiveness difference from the Concord was due exclusively to front structural stiffness differences. For the Cutlass, structural and geometric (override) effects are confounded; however, because the barrier responses of the Marquis and Cutlass were so similar, as well as occupant responses in the Rabbits struck by these cars, it is suspected that the front structural stiffness difference from that of the Concord was primarily the cause of the aggressiveness difference.

TABLE 21
 Rabbit Dummy Measurements -- Offset Frontal Crash Tests

Test	DRIVER			PASSENGER		
	HIC	Peak Chest Accel's (g's)	Femur Loads (lbs) Left Right	HIC	Peak Chest Accel's (g's)	Femur Loads (lbs) Left Right
Concord/Rabbit	631	44	1800 1080	364	28	760 40
Cutless/Rabbit	*	38	340 168	236	28	120 136

*Lost data

TABLE 22
Restraint Survival Distance Calculations -- Offset Frontal Crash Tests

Test	V ₀ (mph)	t* (sec)	D _C (inch)	Pre-Test AID (inch)	A-Pillar Disp (inch)	AID (inch)	D _P (inch)	RSD (inch)	
D R I V E R	Cutlass/Rabbit	30.9	0.0514	22.41	26.0	6.40+	19.60	26.06	15.95
	Concord/Rabbit	31.8	0.0540	22.80	26.0	15.75+	10.25	27.57	10.75
P A S S E N G E R	Cutlass/Rabbit	30.9	0.0514	22.41	26.0	0++	26.0	26.06	22.35
	Concord/Rabbit	31.8	0.0540	22.80	26.0	0++	26.0	27.57	21.23

+Determined through film analysis

++Based on door leading edge displacement

TABLE 23
 ABAG Simulation Results -- Rabbit Occupants
 -- Cutlass/Rabbit, Marquis/Rabbit and Concord/Rabbit Offset Frontal Crash Tests

Position	PEAK CHEST ACCELERATION (g's)			COLUMN STROKE (in)	
	Occupant	Cutlass/Rabbit	Concord/Rabbit	Cutlass/Rabbit	Concord/Rabbit
Driver	5th % F	36.6	40.1	1.47	1.60
	50th % M	36.6	43.0	2.36	2.75
	95th % M	38.0	44.9	3.28	3.86
Passenger	5th % F	49.8	55.3	N/A	N/A
	50th % M	42.6	43.6		
	95th % M	35.9	37.8		

There was also a clear aggressiveness difference between the Concord and the Cutlass in the offset collisions with the VW Rabbit. Again, the Concord was more aggressive. The aggressiveness difference was considerably less than in the full frontal collisions. It resulted primarily on the driver side due to much greater collapse in the A-pillar region of the Rabbit struck by the Concord. It is suspected that the primary cause of the difference was the greater front structural stiffness of the Concord, as was the case in the full frontal collision mode.

Based upon the FRB vehicle responses and the Rabbit occupant responses from the car/car crash tests, the following general characteristics for aggressive and non-aggressive vehicles were noted. The aggressive AMC Concord experienced a small crush value, and had an occupant compartment response characterized by a short pulse duration with acceleration rising rapidly to an early peak value when striking the FRB. In contrast, the less aggressive Cutlass and Marquis had large crush values (approximately 45% greater than the Concord), and responses with long pulse durations (about 30% longer), low accelerations early in the crash event, and late peak accelerations (about 65% later).

2.3 Comparison of Crashsurvivable and Non-Aggressive Characteristics

From conclusions reached in Sections 2.1.5 and 2.2.5, it appears that the characteristics of crashsurvivable and non-aggressive vehicles are the same. In fixed rigid barrier crash testing, both exhibit large crush values and long-duration occupant compartment responses, with low accelerations early in the event and late (but not necessarily low) peak values.

3.0 FRONTAL PROTECTION -- TEST PROCEDURE DEVELOPMENT

3.1 Ability of Fixed Rigid Barrier for Measuring Crashworthiness

3.1.1 Introduction

The Fixed Rigid Barrier (FRB) is widely accepted as a standard tool for determining the potential for occupant survivability in real world vehicle crashes.

Although the barrier collision duplicates in an exact manner only a small subset of highway accidents, it differentiates among vehicles the ability to perform well or poorly in a variety of collision configurations. However, direct comparisons of the responses of vehicles in barrier collisions with those in specific car/car collisions have rarely appeared in the literature.

In this study, responses in three different subject vehicles resulting from fixed rigid barrier collisions were compared with responses measured in the same subject vehicles when struck full frontally by other (larger) vehicles. The objective was to determine how well the occupant responses in full frontal car/car collisions can be expected to be simulated in fixed rigid barrier collisions.

3.1.2 Measurement of Occupant Protection

Several methods were used to determine and compare the level of occupant protection (i.e., the degree of crashworthiness) in the barrier and car/car tests.

First, the occupant compartment acceleration responses (and velocity and displacement responses derived therefrom) were examined. In general, high peak accelerations, peak accelerations occurring early in the crash event, short pulse durations and small values of dynamic crush have been found to indicate a high probability of poor occupant protection. (See Section 2.1.)

Second, dummy measurements were compared for most of the crash tests. (In some of the tests, for reasons to be discussed later, dummy measurements were felt to be of questionable validity and were not used.)

Third, the behavior of the steering column was determined from examination of the crash test films.

Fourth, Restraint Survival Distances (RSD's) were calculated for each crash pulse. (See Section 2.1.3.) In determining available internal distances (AID's), occupant compartment intrusion was taken into account by including A-pillar displacements.

Finally, the ABAG computer model was employed. (See Section 2.1.3.)

3.1.3 Crash Test Data

Data from three groups of crash tests (shown in Table 24) were analyzed. Each group contains two high speed full frontal car/car collisions and one high speed car/FRB collision. Within each group, the response of the small car striking the barrier was compared to the responses that the small car experienced when struck by each of the two larger cars.

TABLE 24 - Groups of Vehicle Crash Tests Analyzed

<u>GROUP I</u>
1975 Honda Civic/Fixed Rigid Barrier 1975 Honda Civic/1975 Ford Torino 1975 Honda Civic/1975 Plymouth Fury
<u>GROUP II</u>
1979 VW Rabbit/Fixed Rigid Barrier 1980 VW Rabbit/1980 Oldsmobile Cutlass 1980 VW Rabbit/1980 AMC Concord
<u>GROUP III</u>
1979 Plymouth Horizon/Fixed Rigid Barrier 1980 Plymouth Horizon/1980 Chevrolet Citation 1980 Plymouth Horizon/1980 Ford Mustang

In two of the groups (Groups I and II), the two large cars, although similar in weight, had markedly different structural characteristics. The Ford Torino had a relatively soft frontal structure (and, therefore, tended to be structurally non-aggressive), whereas the Plymouth Fury had a relatively stiff frontal structure (was structurally aggressive) (3). Similarly, as described in Section 2.2.4, the Oldsmobile Cutlass was soft (non-aggressive), whereas the AMC Concord was stiff (aggressive). Therefore, in each of Groups I and II, if the fixed rigid barrier were found to produce responses in the small car which tended to fall halfway between the responses in the small cars when struck by the two larger cars, then the barrier could be said to be simulating a median or average large car, and thereby providing a reasonable measure of crash survivability occurring in large car/small car fully aligned high speed frontal collisions.

Referring to Group III, the relative frontal structural aggressiveness of the Chevrolet Citation, compared with the Ford Mustang, was unknown. Therefore, the

Plymouth Horizon's response from the fixed rigid barrier collision was not necessarily expected to fall between the Horizon responses from the two car/car collisions in order to indicate the barrier's ability to measure crash survivability in car/car collisions. If the responses from all three collisions were found to be similar, however, then the barrier would be indicated to be a reasonable simulator of the car/car collision.

3.1.4 Equivalent Impact Velocity Assumptions

If a car/barrier collision is to accurately simulate a car/car collision, a choice must be made of the proper "equivalent impact velocity" (i.e., the impact velocity for the car/barrier test which produces compartment and occupant responses which are equivalent to those produced in the car/car collision being simulated). Two approaches for determining equivalent impact velocity have been developed: equivalent momentum and equivalent energy.

The equivalent momentum approach is based on the assumption that if the changes in momentum for the small car from the small car/barrier and large car/small car collisions are the same, then those two collisions will be equally injurious to the small car occupants. The equivalent impact velocity according to this assumption is derived in Reference 10, for the case where both vehicles in the car/car collision have the same impact speed. The derivation results in the following expression:

$$V_b = V_1 \frac{2M_2}{M_1 + M_2} \quad (1)$$

where:

- V_b = Impact velocity of vehicle 1 in the car/fixed rigid barrier collision.
- V_1 = Impact velocity of vehicle 1 in the car/car collision (half the closing velocity).
- M_1, M_2 = Masses of vehicles 1 and 2.

In the equivalent energy approach, it is assumed that the vehicles in the car/car collision share the amount of energy dissipation equally. It is further assumed that if the energy dissipated by the small car in the barrier collision is equal to half the energy dissipated in the car/car collision, then the two collisions are equally injurious to the small car occupants. This approach yields the following expression when, as before, the vehicles in the car/car collision have equal impact speeds: (10)

$$V_b = V_1 \sqrt{\frac{2M_2}{M_1 + M_2}} \quad (2)$$

The crash test impact velocities and the equivalent impact velocities calculated by both approaches for the tests listed in Table 24 are presented in Table 25. It is seen that in the Honda test series, the test velocities agreed closely with velocities derived by the equivalent momentum approach; in the Rabbit series, the test velocities agreed closely with velocities derived by the equivalent energy approach; and in the Horizon series, although both approaches yielded similar velocities, the test velocities were closer to those derived by the energy approach.

TABLE 25 - Test and Equivalent Impact Velocities

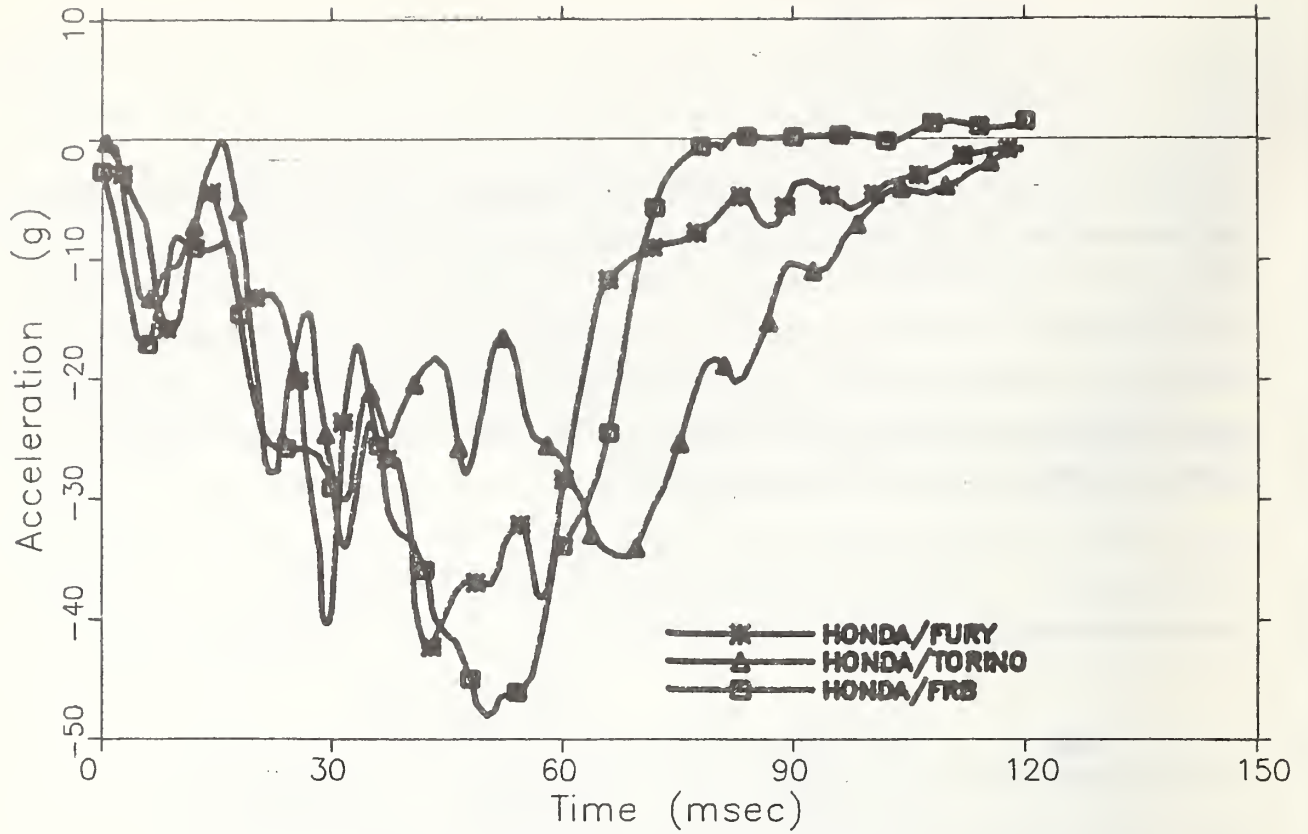
Test	Test Impact* Velocity (mph)	Equivalent Impact Velocity (mph)	
		Momentum Approach	Energy Approach
Honda/FRB	40.25	--	--
Honda/Torino	29.73	29.98	34.74
Honda/Fury	30.85	30.84	35.23
Rabbit/FRB	34.8	--	--
Rabbit/Cutlass	31.7	28.77	31.64
Rabbit/Concord	31.8	28.85	31.68
Horizon/FRB	34.86	--	--
Horizon/Citation	35.14	33.93	34.39
Horizon/Mustang	35.08	32.70	33.76

*For the car/car tests, the test impact velocity was half the closing velocity.

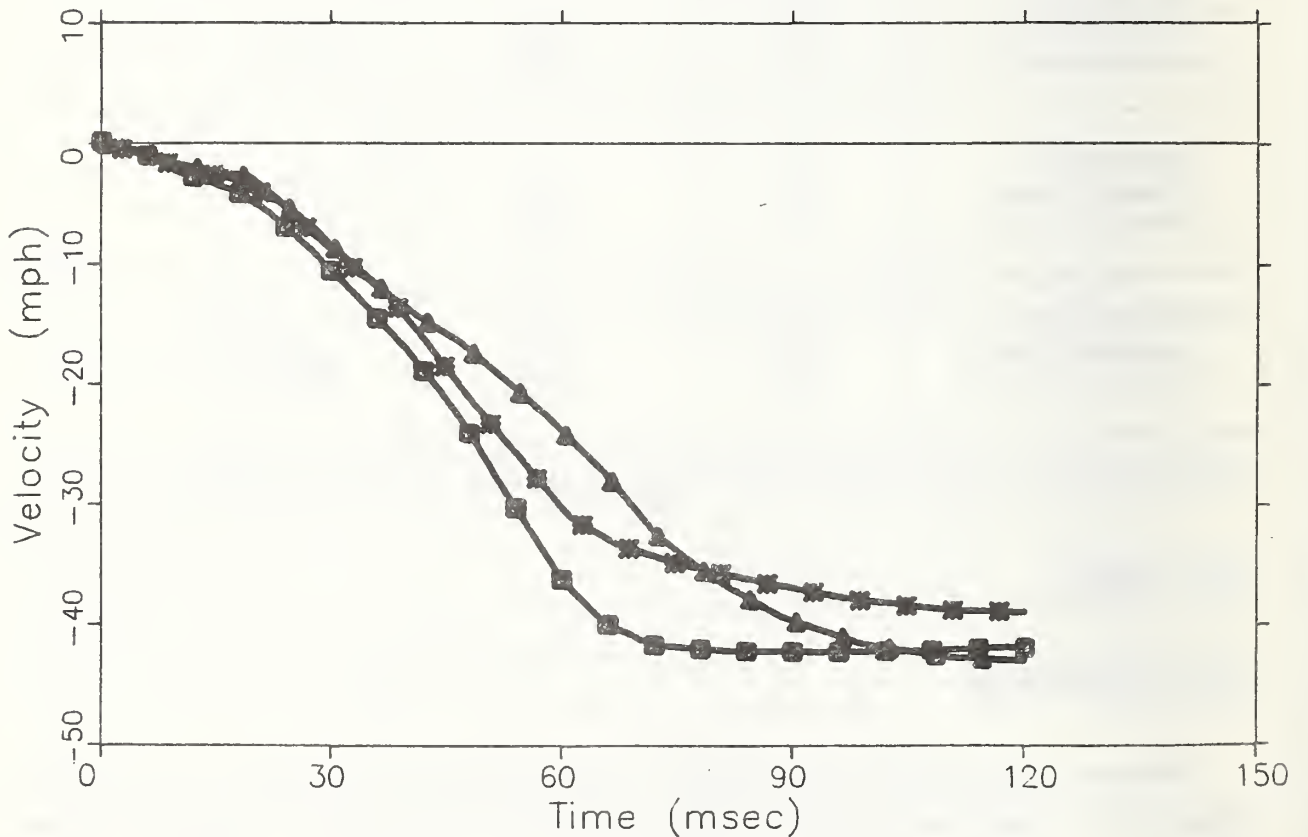
3.1.5 Results

3.1.5.1 Honda Series

Occupant compartment acceleration- and velocity-time histories for the three Honda crash tests are shown in Figure 37. The Honda/FRB response differed



a) Acceleration Response



b) Velocity Response

FIGURE 37. Honda Occupant Compartment Responses

substantially from those of the car/car collisions, exhibiting higher accelerations and a much shorter crash pulse, although maximum static crush values were similar. This would indicate the probability of a more severe environment for the occupants of the Honda in the barrier collision than in either of the car/car collisions.

Dummy measurements were not used in the Honda series. The Honda/Torino and Honda/Fury crash tests were conducted on a limited budget for the purpose of analyzing and comparing vehicle structural behavior. The dummies used were not standard Part 572 devices and were not calibrated or placed in the vehicles according to specified Part 572 procedures. Consequently, the accuracy of their responses, for the purposes of this study, was questionable.

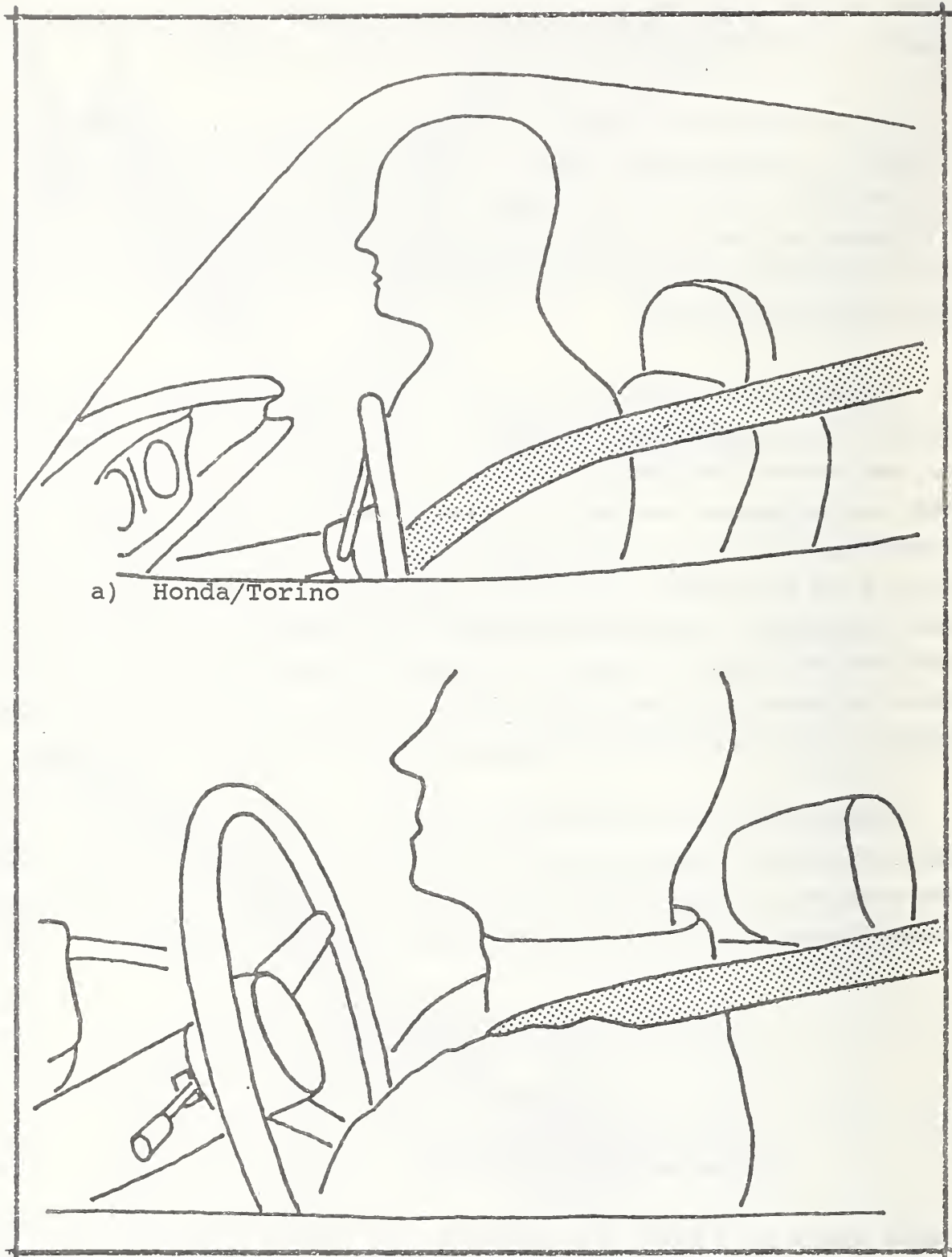
Steering column behavior in the car/car and car/FRB collisions is illustrated in Figures 38 and 39, which were traced from the high speed motion picture films. In each of these pictures, the driver had just contacted the steering column. Figure 38 shows that column behavior was quite different in the two car/car collisions. In the Torino/Honda crash, the column remained low, the steering wheel hub striking the driver in the lower thorax. In the Fury/Honda crash, the column displaced upward as well as rearward. In Figure 38B, the wheel had just contacted the driver's thorax. The hub continued upward and appeared to strike the driver's chin and neck. Figure 39 shows two views of the Honda/FRB collision. It is clear that the hub struck the upper thorax at a location between the contact points evident in the two car/car collisions.

Results of the RSD calculations are presented in Table 26.* RSD values in the two car/car tests were nearly the same. The RSD value resulting from the FRB collision was much less than those from the car/car tests, indicating that the barrier collision was significantly less crashsurvivable than either of the car/car collisions.

TABLE 26 - RSD Calculations -- Honda Series

TEST	RSD (in)
Honda/FRB	6.8
Honda/Torino	11.4
Honda/Fury	11.0

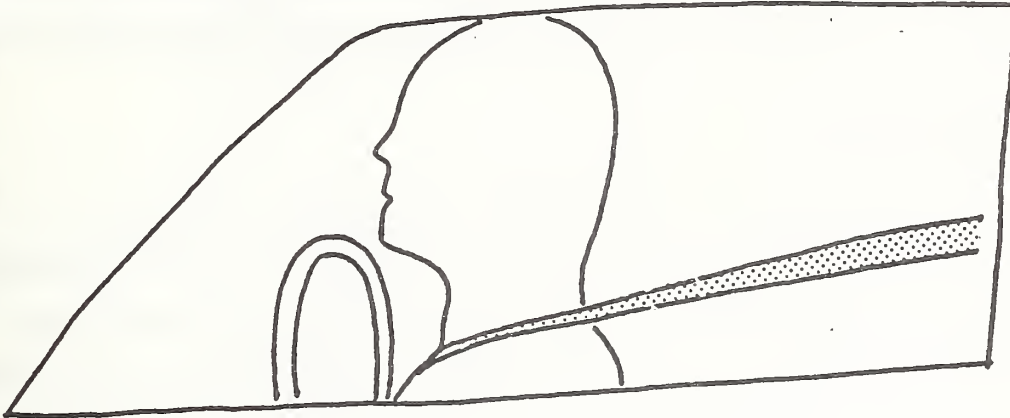
*Slight differences exist in RSD values for the car/car collisions from those in Reference 3. For Reference 3, computations were done by hand; for this study, a computerized procedure was used.



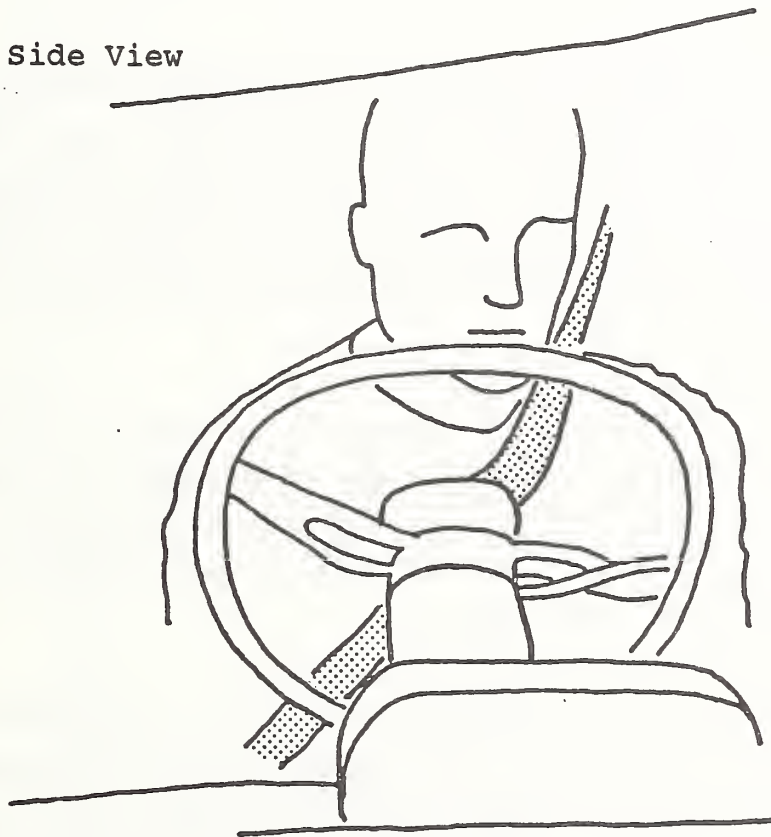
a) Honda/Torino

b) Honda/Fury

FIGURE 38. Honda Steering Column Behavior -- Car/Car Collision



a) Side View



b) Front View

FIGURE 39. Honda Steering Column Behavior -- FRB Collision

Results of the ABAG model simulations, presented in Table 27, indicate that the Fury was more aggressive than the Torino, and that the Honda/FRB collision was considerably more severe to the Honda's occupants than either of the car/car collisions.

3.1.5.2 Rabbit Series

Occupant compartment responses from the three Rabbit collisions are shown in Figure 40. (See Section 2.4.4.1 for further description of the Concord/Rabbit and Cutlass/Rabbit Collisions.) The velocity change of the Rabbit struck by the Concord was more rapid than that of the Rabbit struck by the Cutlass, indicating that the Concord is the more aggressive car. The barrier collision response was fairly well bracketed between the two car/car responses for nearly the full duration of the collision events.

The cause of the aggressiveness difference between the Concord and the Cutlass, as discussed in Section 2.2.3, is not clearly known. Two factors (front structural stiffness and frame geometry) may have contributed to the aggressiveness difference, and both are apt to influence the response of a small vehicle in a real world car/car collision. Therefore, it is felt that the difference observed between the two car/car responses of Figure 40 is realistic.

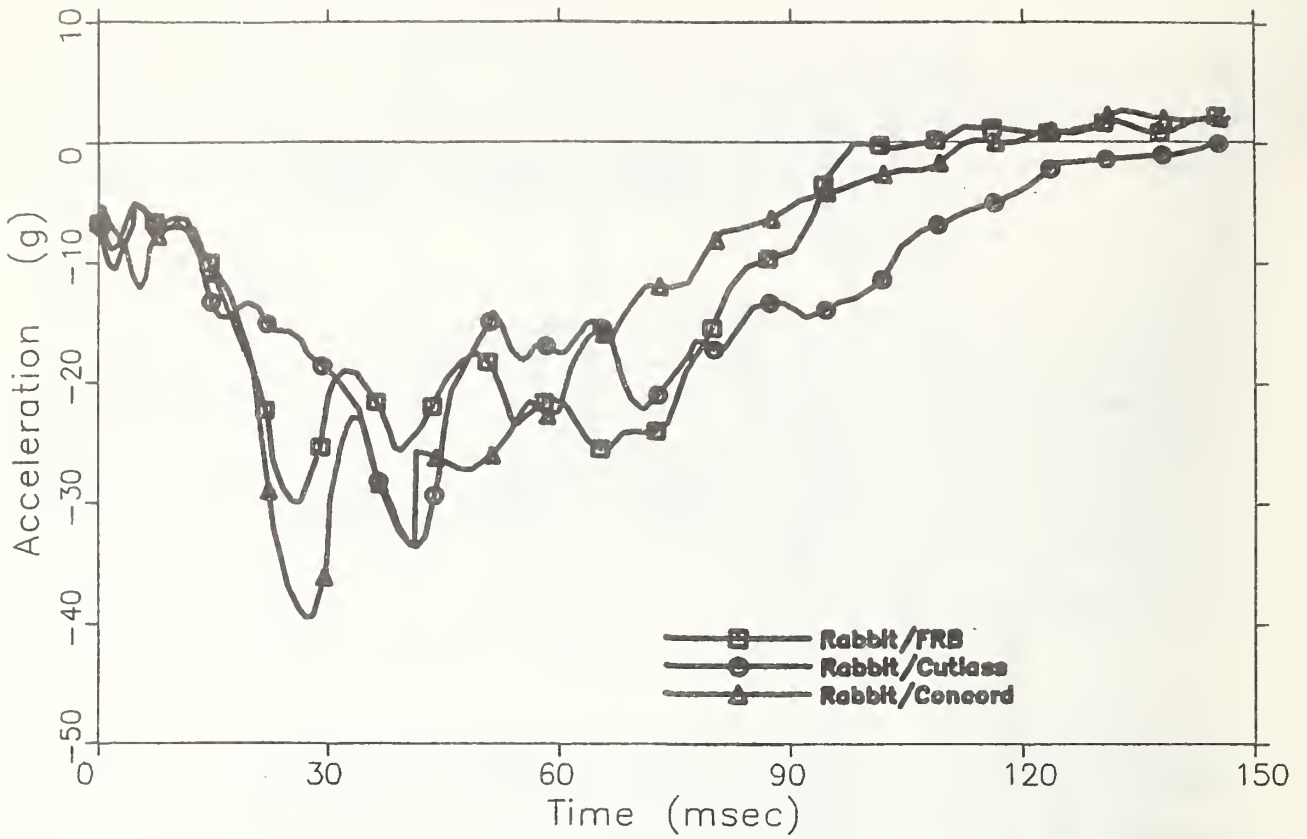
A summary of dummy measurements is presented in Table 28. These measurements indicate that the Concord was more aggressive to the Rabbit occupants than the Cutlass. The Rabbit/FRB collision resulted in head and chest measurements which were either between or very close to those of the two car/car collisions; and in femur and belt loads which were higher.

However, the validity of comparisons among dummy measurements from the three tests is questionable for two reasons. First, the Rabbit in the FRB collision had passive (automatic) belts, whereas the Rabbit used in the car/car tests had standard belts. Secondly, differences occurred in the Rabbit shoulder belt behavior for the two car/car tests (see Section 2.2.4.1.)

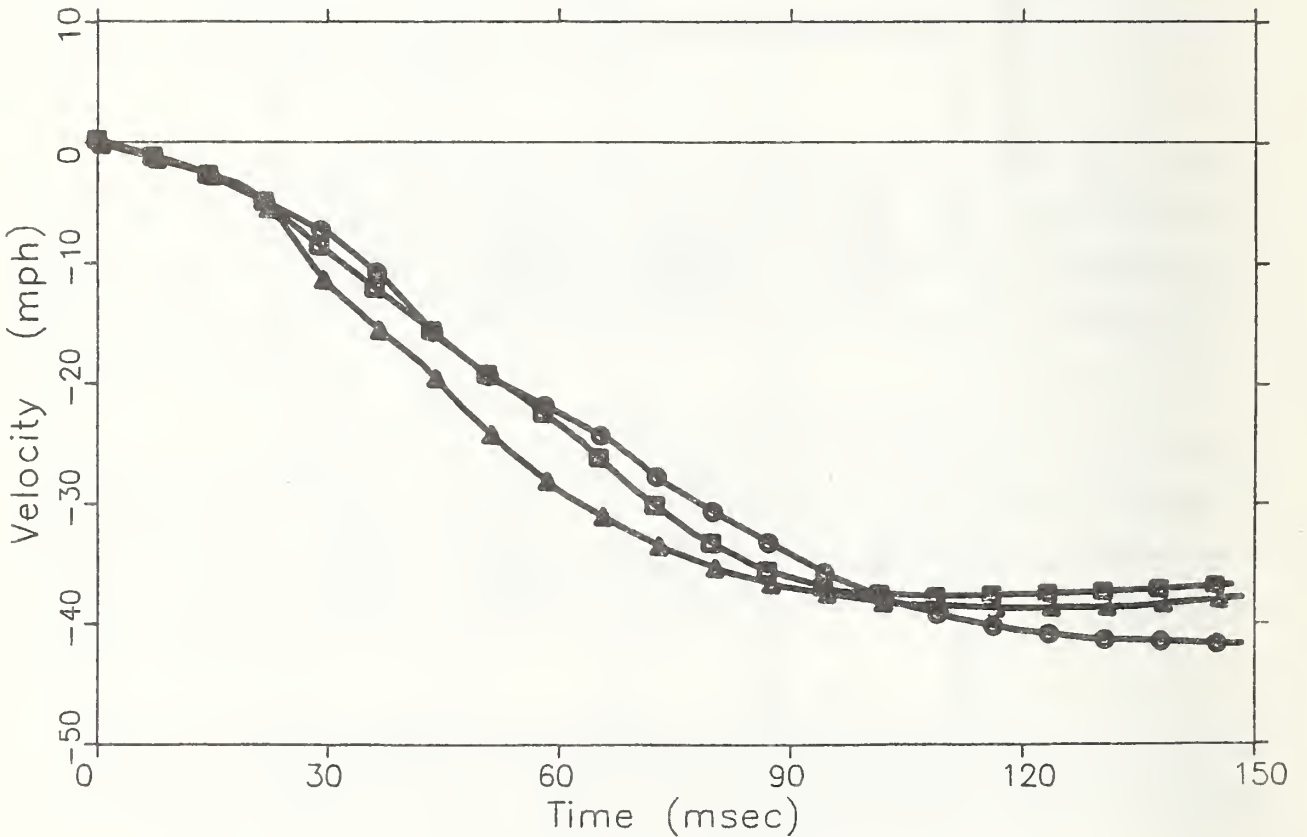
Steering column behavior is illustrated in Figures 32, 34 and 41. In the Concord/Rabbit crash, the column displaced upward considerably more than in the

TABLE 27
 ABAG Simulations -- Honda Series

Test	Occupant Size	DRIVER		PASSENGER
		Peak Chest Acc. (g's)	Column Displacement (in)	
Honda/FRB	5th % F	77.0	3.07	80.4
	50th % M	75.6	4.93	78.7
	95th % M	72.7	6.27	90.0
Honda/Torino	5th % F	48.8	1.96	66.6
	50th % M	52.9	3.42	52.2
	95th % M	54.6	4.72	52.2
Honda/Fury	5th % F	60.1	2.45	69.9
	50th % M	60.3	3.87	58.6
	95th % M	57.6	4.97	61.2



a) Acceleration Response

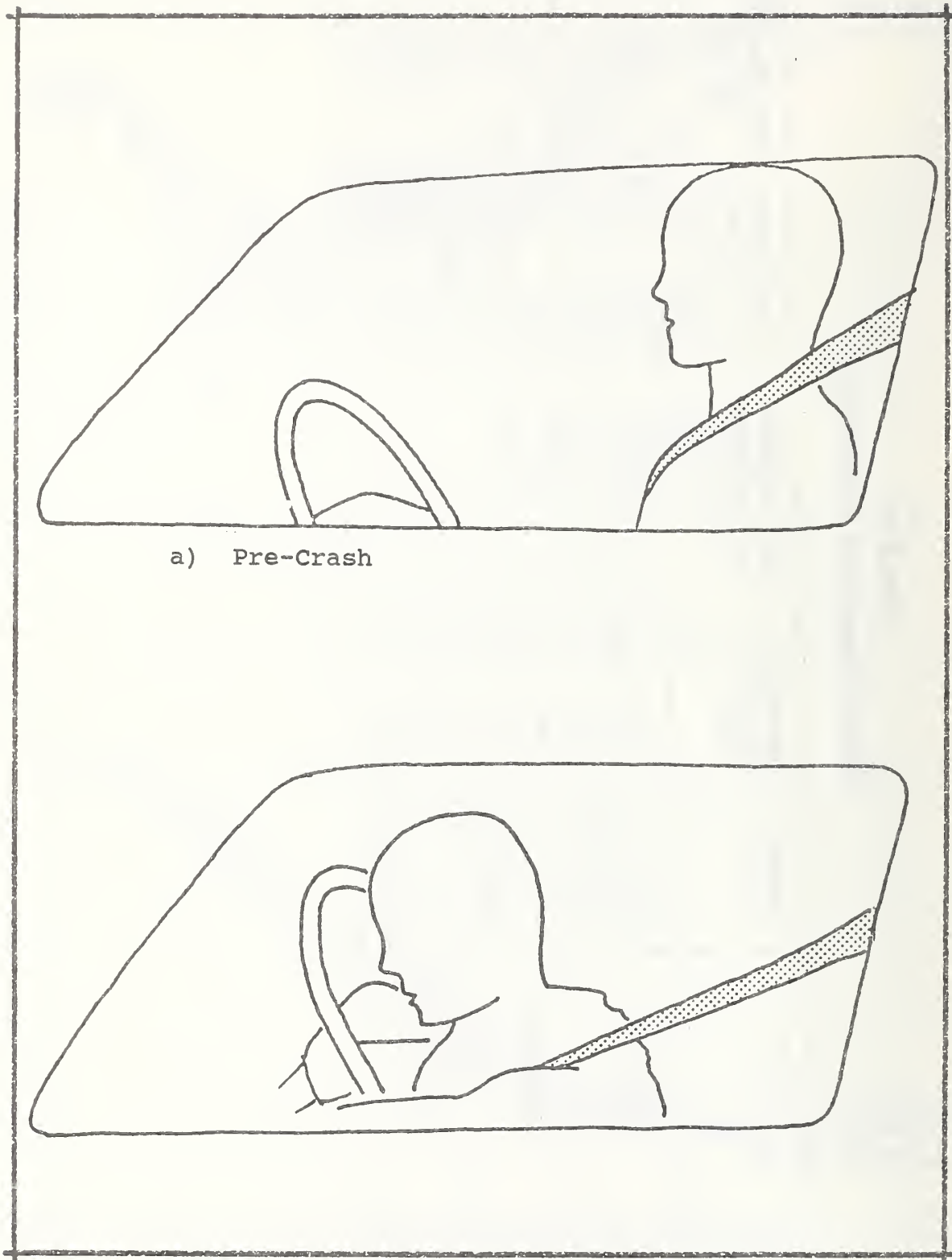


b) Velocity Response

FIGURE 40. Rabbit Occupant Compartment Responses

TABLE 28
 Dummy Measurements -- Rabbit Series

Test	Dummy Location	Head Injury Criterion (HIC)	Max. Resultant Chest Acceleration (3ms) (g's)	Max. Femur Load (lbs)		Max. Shoulder Belt Load (lbs)
				Right	Left	
Rabbit/FRB	Driver	1024	67	630	1170	1837
	Passenger	429	33	1460	937	1837
Rabbit/Cutlass	Driver	986	38	375	337	1325
	Passenger	531	29	338	360	1375
Rabbit/Concord	Driver	1099	63	740	440	1600
	Passenger	975	46	341	840	1600



a) Pre-Crash

b) During Crash

FIGURE 41. Rabbit Shoulder Belt and Steering Column Behavior -- FRB Collision

Cutlass/Rabbit crash. Because of the different camera angle, it is difficult to compare vertical motion of the column in the FRB test with that in either car/car test. It appears, however, to have displaced upward more than in the Cutlass collision, but somewhat less than in the Concord collision.

Results of the RSD calculations, presented in Table 29, indicate that the Concord was more aggressive than the Cutlass. The RSD value from the FRB collision fell between those from the two car/car collisions, but was much closer to the value from the Rabbit/Cutlass test.

TABLE 29 - RSD Calculations -- Rabbit Series

TEST	RSD (in)
Rabbit/FRB	20.6
Rabbit/Cutlass	20.9
Rabbit/Concord	18.4

The ABAG model simulation results appear in Table 30. They indicate, as did the RSD calculations, that the Concord was the more aggressive car. The Rabbit/FRB collision resulted in driver and passenger ABAG values which almost consistently fell between values from the two car/car collisions, but were closer to the Rabbit/Cutlass values.

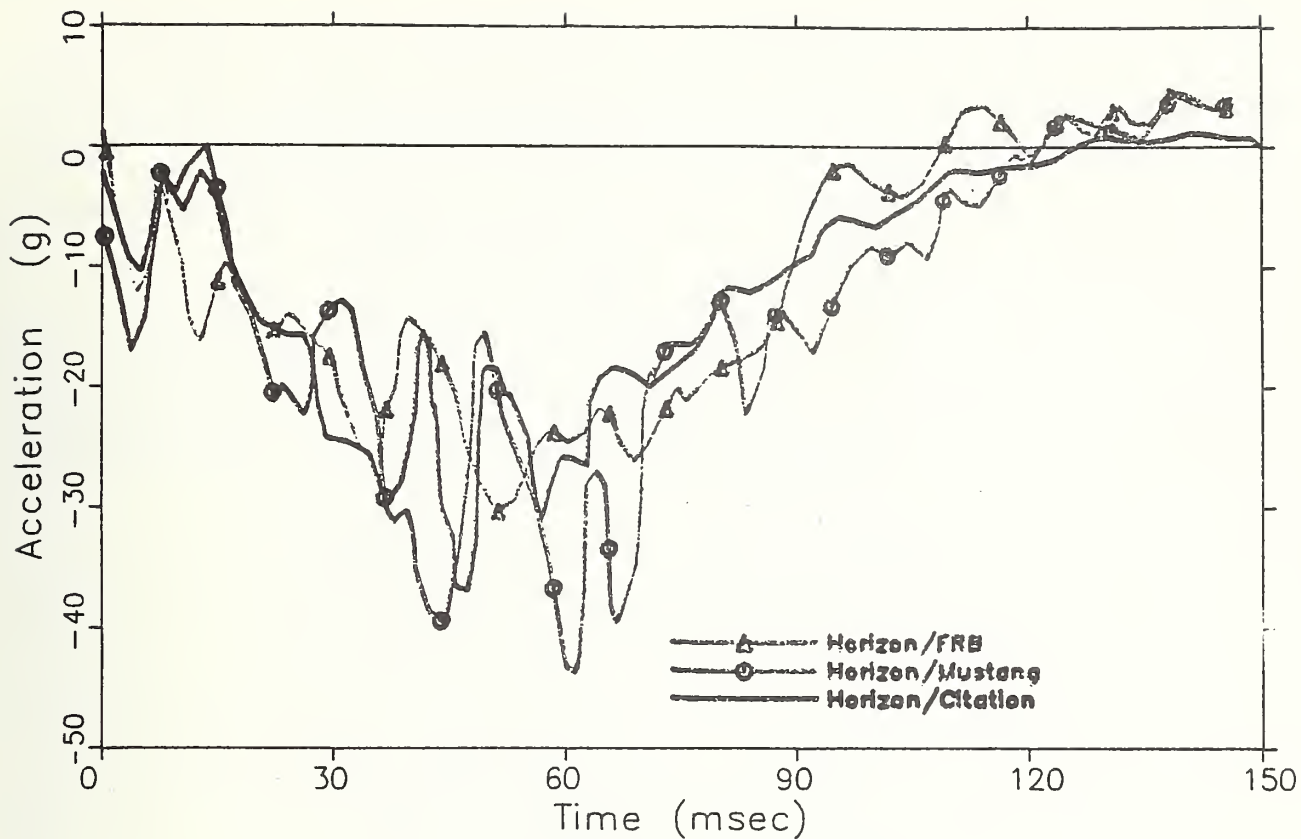
3.1.5.3 Horizon Series

The occupant compartment responses from the three Horizon tests, shown in Figure 42, were generally very similar. In particular, the Horizon/FRB and Horizon/Citation responses were essentially identical for the first 70 milliseconds of the event. The Horizon/Mustang collision resulted in a somewhat higher deceleration between 40 and 70 milliseconds. From the velocity curves, it is seen that the response from the FRB collision was well bracketed between the two car/car responses.

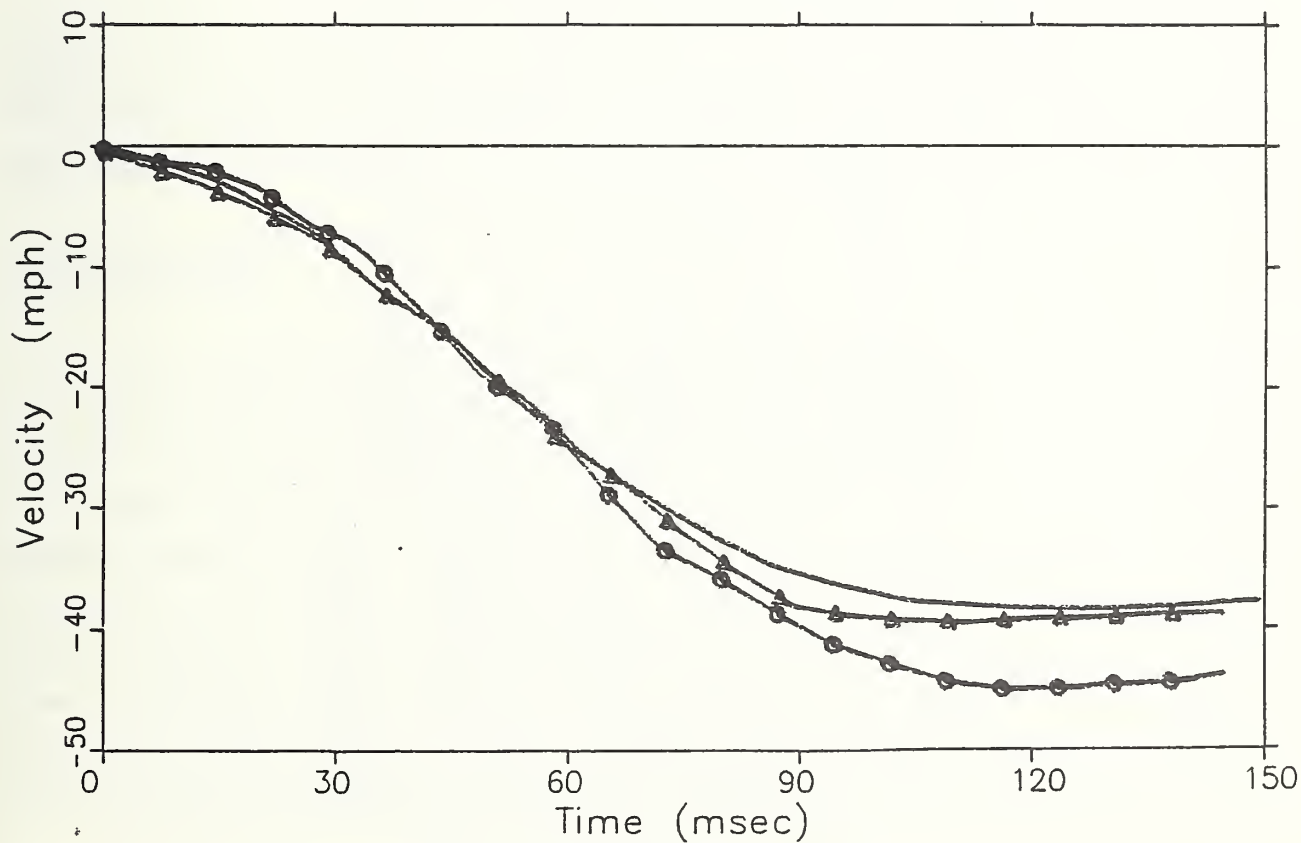
A summary of the dummy measurements is presented in Table 31. The Mustang was indicated as being somewhat more aggressive than the Citation. The barrier collision resulted in measurements which were comparable to those from the car/car collisions, except for values of HIC, which were lower. Observation of the films

TABLE 30
 ABAG Simulations -- Rabbit Series

Test	Occupant Size	DRIVER		PASSENGER
		Peak Chest Acc. (g's)	Column Displacement (in)	
Rabbit/FRB	5th % F	46.5	1.87	62.8
	50th % M	48.1	3.11	48.2
	95th % M	48.9	4.25	46.9
Rabbit/Cutlass	5th % F	45.5	1.82	65.3
	50th % M	44.5	2.86	46.6
	95th % M	44.8	3.81	44.1
Rabbit/Concord	5th % F	59.4	2.39	72.3
	50th % M	58.1	3.76	58.4
	95th % M	56.9	4.93	60.7



a) Acceleration Response



b) Velocity Response

FIGURE 42. Horizon Occupant Compartment Responses

TABLE 31

Dummy Measurements -- Horizon Series

Test	Dummy Location	Head Injury Criterion (HIC)	Max. Resultant Chest Acceleration (3ms) (g's)	Max. Femur Load (lbs)		Max. Shoulder Belt Load (lbs)
				Right	Left	
Horizon/FRB	Driver	653	52	708	974	*
	Passenger	780	40	657	581	*
Horizon/Citation	Driver	1774	44	590	1360	1560
	Passenger	1219	42	460	550	2120
Horizon/Mustang	Driver	1817	61	1375	1700	1400
	Passenger	2096	52	675	1300	1460

*Questionable data.

indicated that, in contrast to the Rabbit series, the shoulder belts stayed well in place during all three crashes for drivers and passengers. Figures 43-45 illustrate this for the drivers. Also apparent in these figures is the fact that steering column displacement was similar in all three tests.

Results of the RSD calculations appear in Table 32. The Citation appears to have been very slightly more aggressive than the Mustang; and the FRB, in turn, very slightly more aggressive than the Citation. However, since the maximum difference did not exceed one inch, it is not likely that the differences were significant.

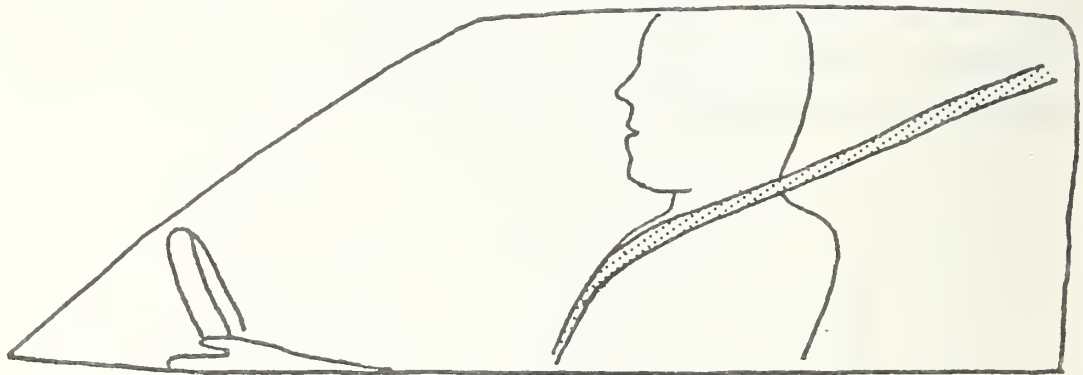
TABLE 32 - RSD Calculations -- Horizon Series

TEST	RSD (in)
Horizon/FRB	14.7
Horizon/Citation	15.2
Horizon/Mustang	15.6

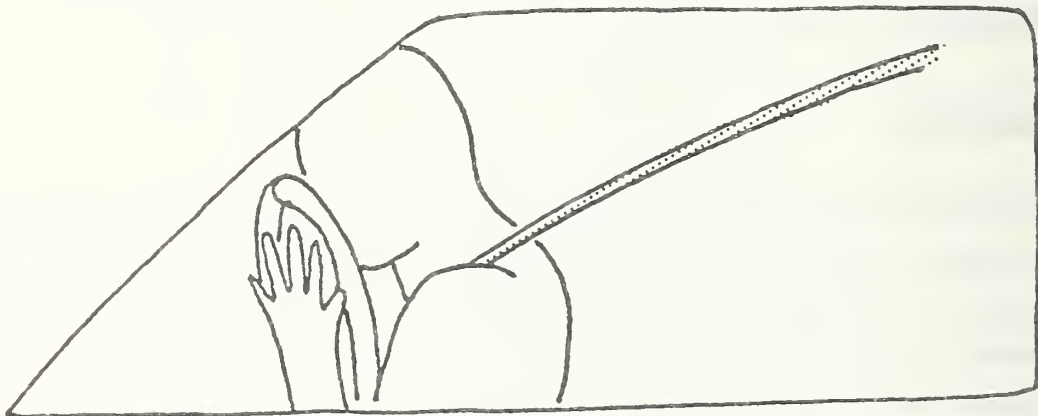
The ABAG model simulation results, Table 33, indicate the Mustang to have been slightly more aggressive than the Citation for the drivers (all sizes) and the 95th percentile passenger. For all occupants, the results of the FRB and Citation collisions were essentially the same.

3.1.6 Conclusions

In the Honda series, where the crash test velocities agreed closely with velocities derived by the equivalent momentum approach, all of the methods used to determine the potential for occupant protection indicated that the fixed rigid barrier was much more severe to the Honda occupants than were the two car/car collisions. In the Rabbit series, where test velocities agreed with velocities derived by the equivalent energy approach, the fixed rigid barrier caused vehicle and occupant simulation (RSD and ABAG) response levels which consistently fell between the response levels caused by the two striking cars. Since the two large cars in each of these two test series represented both ends of the large car structural aggressiveness spectrum, it appears that the fixed rigid barrier is an accurate crashworthiness-measuring device for high

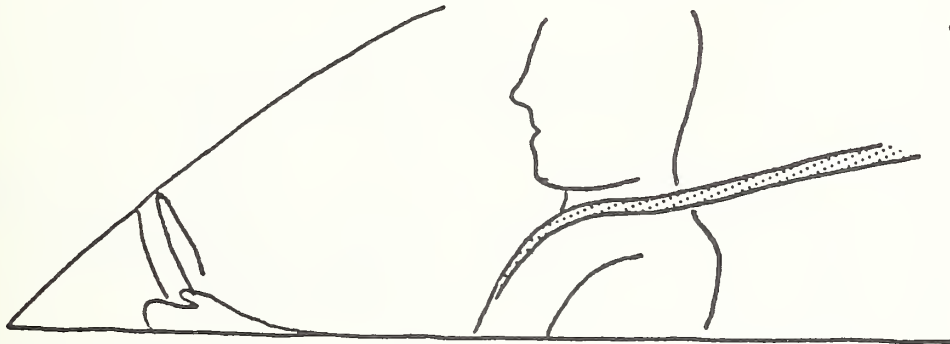


a) Pre-Crash

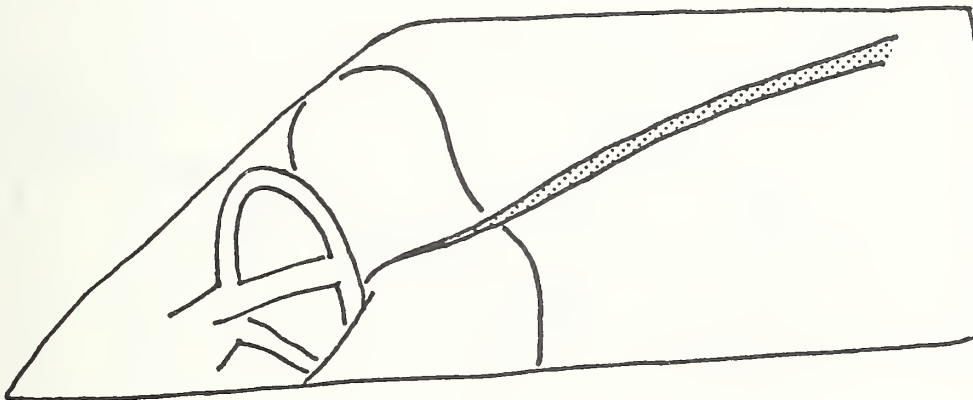


b) During Crash

FIGURE 43. Horizon Shoulder Belt and Steering Column Behavior -- Citation Collision

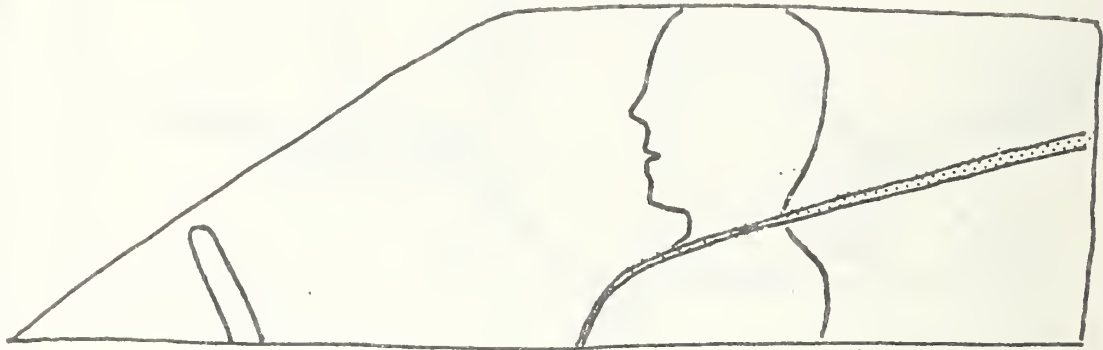


a) Pre-Crash

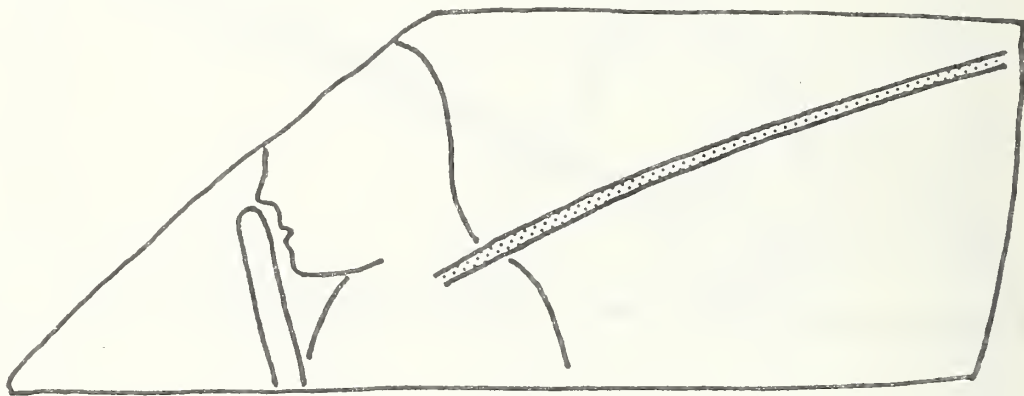


b) During Crash

FIGURE 44. Horizon Shoulder Belt and Steering Column Behavior -- Mustang Collision



a) Pre-Crash



b) During Crash

FIGURE 45. Horizon Shoulder Belt and Steering Column Behavior -- FRB Collision

TABLE 33
 ABAG Simulations -- Horizon Series

Test	Occupant Size	DRIVER		PASSENGER
		Peak Chest Acc. (g's)	Column Displacement (in)	
Horizon/FRB	5th % F	46.8	1.85	64.0
	50th % M	49.4	3.20	49.9
	95th % M	51.5	4.43	48.9
Horizon/Citation	5th % F	47.2	1.90	63.1
	50th % M	50.0	3.19	50.5
	95th % M	50.8	4.34	48.1
Horizon/Mustang	5th % F	55.1	2.21	63.3
	50th % M	60.0	3.83	52.2
	95th % M	57.7	5.02	56.2

speed full frontal car/car collisions, if test velocities are selected on the basis of equivalent energy between car/FRB and car/car collisions as opposed to equivalent momentum.

In the Horizon series, the distinction between equivalent energy and equivalent momentum approaches is much less, although test velocities were closer to those derived by the energy approach. This observation, together with the fact that most of the responses (compartment responses, RSD calculations and ABAG simulations) agreed so closely between fixed rigid barrier and car/car collisions, tend to confirm that the fixed rigid barrier is an accurate crashworthiness-measuring device for high speed full frontal collisions if equivalent velocities are computed by the energy approach.

3.2 Barriers for Measuring Aggressiveness

3.2.1 Introduction

Three crash barriers have been widely used by NHTSA in recent years in a variety of crashworthiness studies.

The fixed rigid barrier (FRB) is the most common and is used extensively throughout the safety community. (Section 3.1 provides an evaluation of its use as a crashworthiness-measuring device.)

The fixed load cell barrier (FLCB) consists of a load cell barrier unit which contains 36 independent loading surfaces, each of which transmits force through a single load cell (Figure 46). The unit attaches to a standard FRB. It does not deform under load, providing essentially identical loading to a vehicle as does the FRB, but allows load distribution over the vehicle's front surface to be measured with a high degree of resolution.

The moving deformable barrier (MDB) was developed primarily for side impact testing. It is illustrated in Figure 47 and described in Reference 11. The crushable front portion is constructed of aluminum honeycomb, and provides crush characteristics similar to a structurally stiff domestic automobile. It contains a bumper-height projection made from stiffer honeycomb than the rest of the surface, to allow simulation of the behavior of a striking car's bumper.

FRONT VIEW

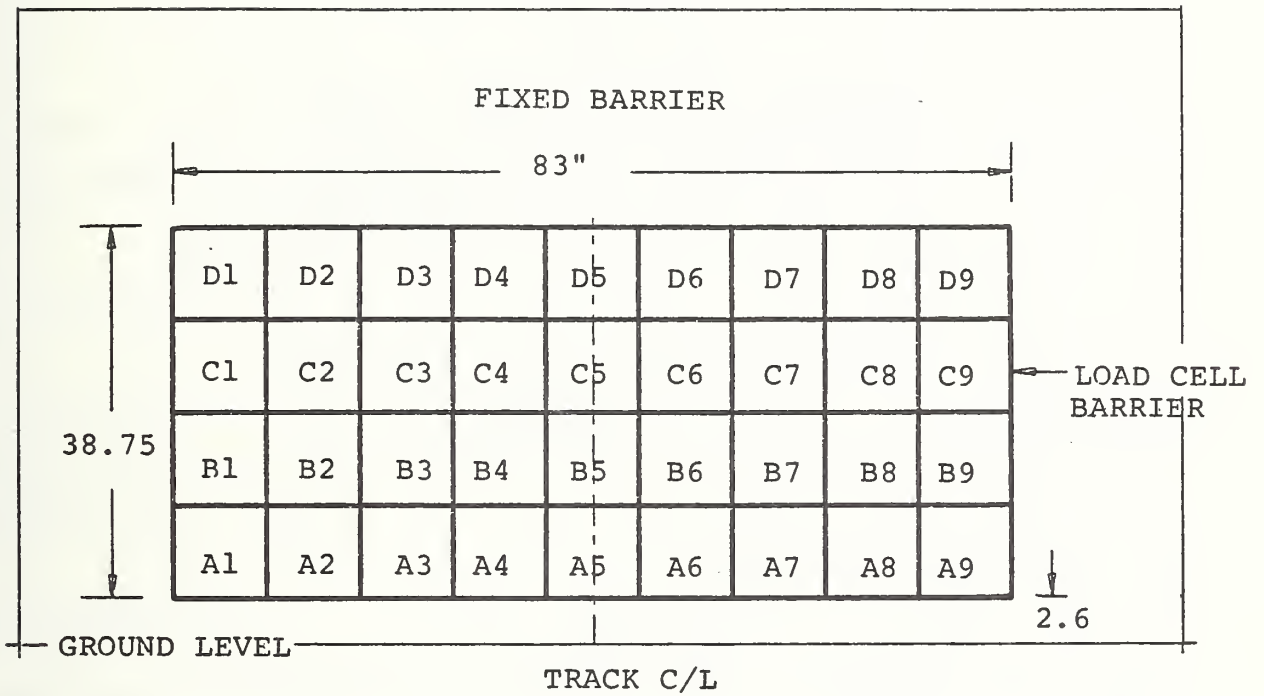
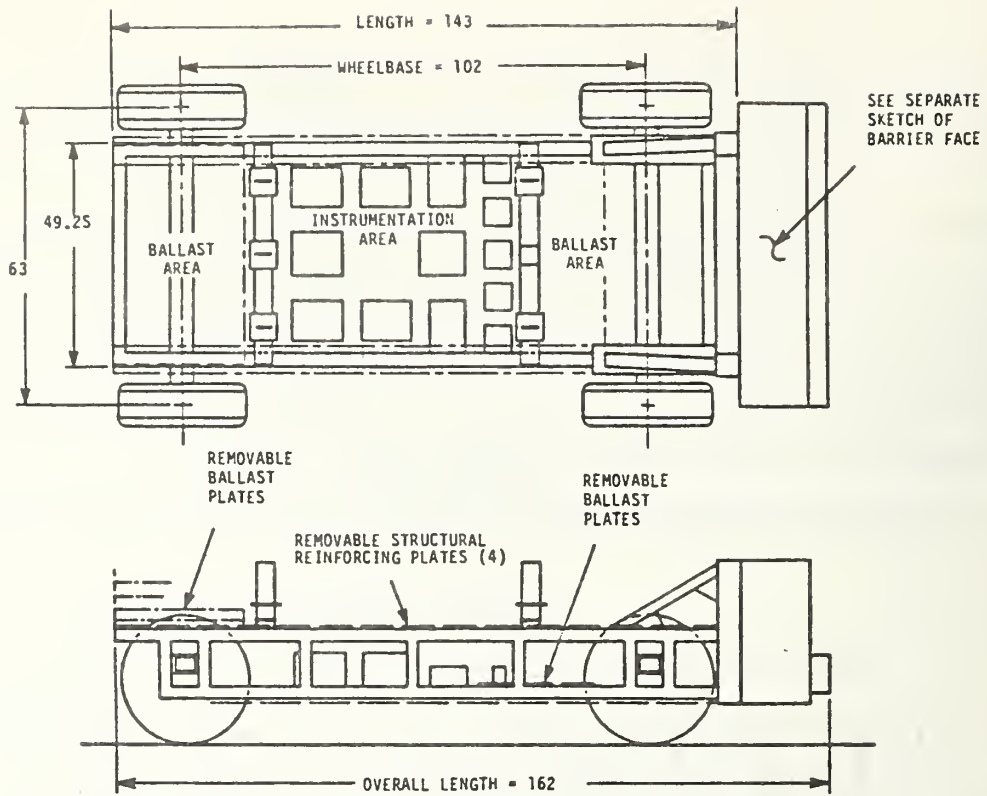


FIGURE 46. Fixed Load Cell Barrier



NHTSA VEHICLE CONFIGURATION - MOVING BARRIER SIDE IMPACTOR CONCEPT
(4-WHEELED VEHICLE SIMULATOR)

0.032 ALUM. BACK PLATE
26 ksi S052-H34

NHTSA BARRIER FACE

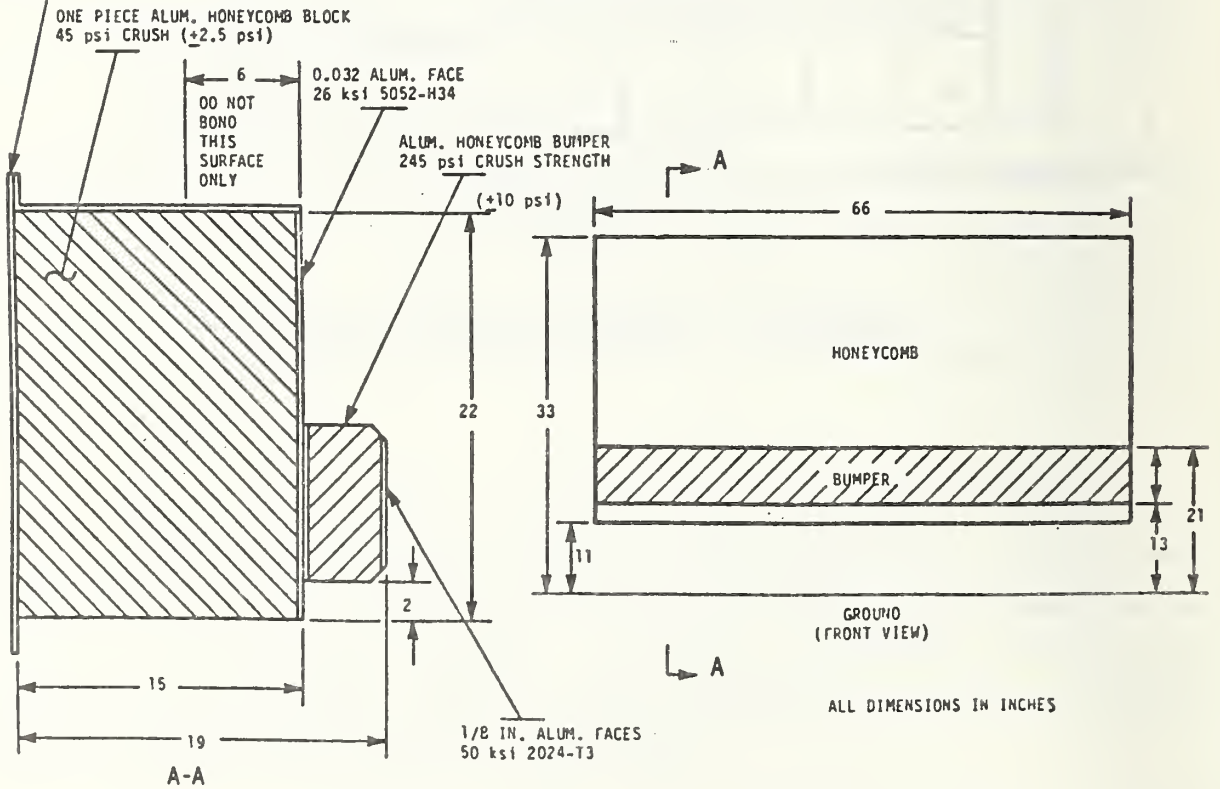


FIGURE 47. Moving Deformable Barrier

Sections 2.2.3 and 2.2.4 describe the selection of aggressive and non-aggressive large cars and the results of crash tests (full and offset frontal) between the large cars and a reasonably crashsurvivable small car. It was determined that a significant aggressiveness difference existed between the AMC Concord (aggressive) and the Mercury Marquis (non-aggressive). In this section, the results and analysis of crash tests of these two vehicles into three different types of barriers are presented. The objectives were:

1. To determine which measurements from which of the three barrier crash tests correlated best with the degree of aggressiveness of the large cars, and thereby provided the best measure of aggressiveness; and
2. To make preliminary compliance test procedure recommendations and develop a more extensive crash test program to support the test procedure (recommending test device or procedure modifications if necessary).

3.2.2 Test Results

Six car/barrier tests were conducted. The AMC Concord and the Mercury Marquis each were crashed into a FRB, a FLCB and a MDB. A summary of vehicle data and test conditions appears in Table 34.

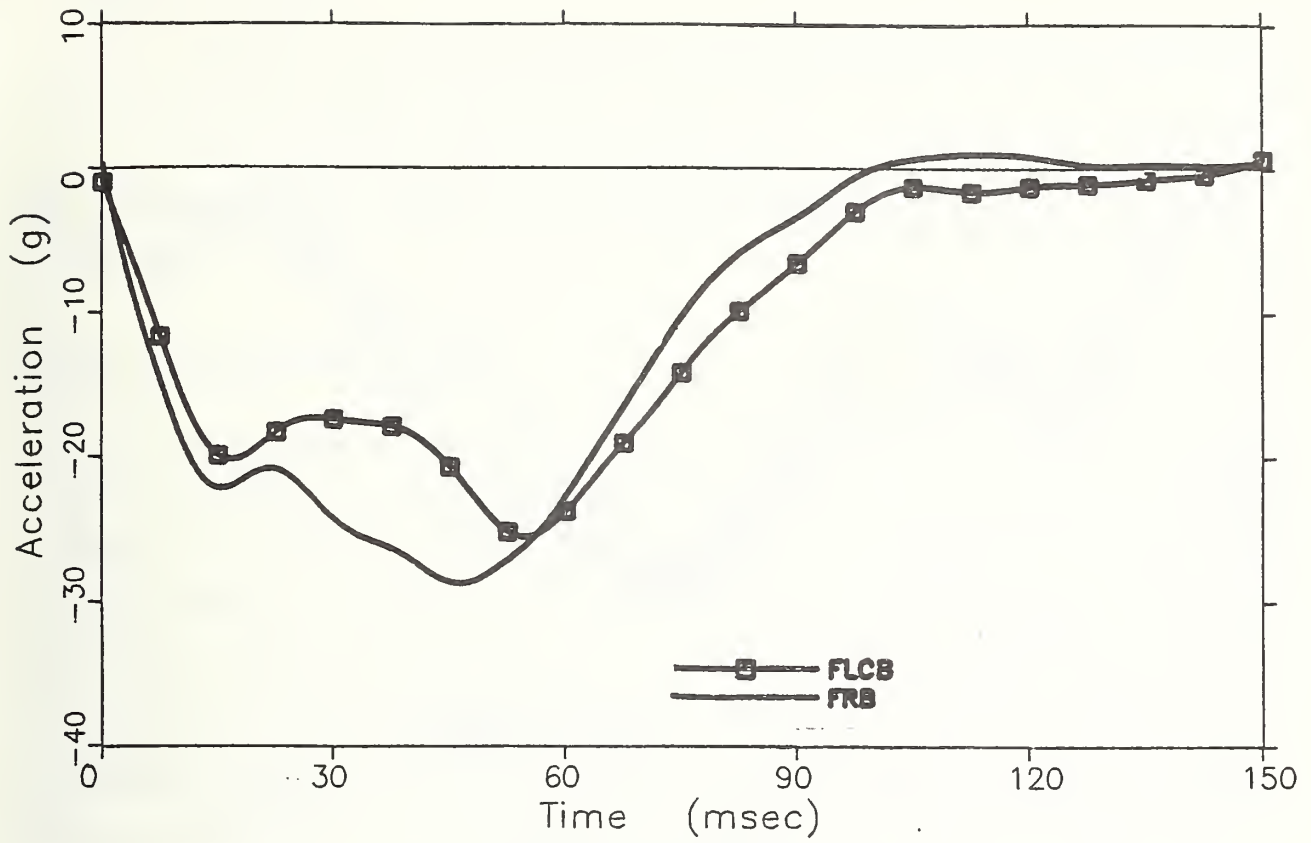
3.2.2.1 Repeatability

Since the FRB and the FLCB should provide identical loading to an impacting vehicle, the Concord and Marquis responses against these barriers were examined to provide an indication of the vehicle response repeatability. It should be noted in Table 34, however, that some substantial differences in test conditions existed between the two Concorde and the two Marquis'. First, vehicles tested were of different model years. Secondly, test weights were different. The Concord went into the FLCB with 5% greater kinetic energy than in the Concord/FRB collision; the energy difference in the two Marquis collisions was approximately 6%.

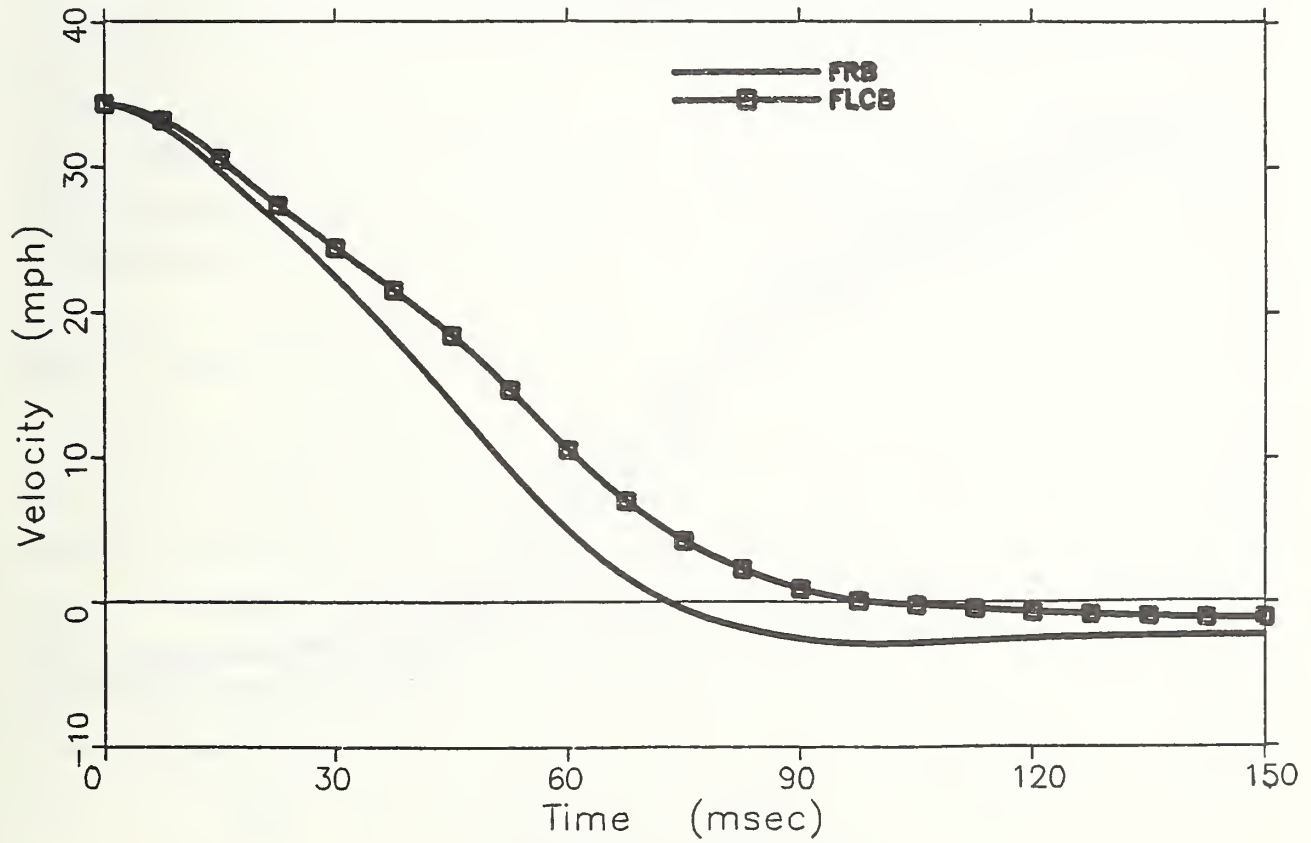
Occupant compartment responses are presented in Figures 48 and 49. For the Concord (Figure 48), the FRB produced higher accelerations and a shorter pulse

TABLE 34
 Vehicle Data and Crash Test Summary -- Car/Barrier Collisions

Barrier	Vehicle	Model Year	Body Style	Engine Displ (in ³)	Engine No. Cyl's	Transmission		Impact Velocity (mph)	Test Wt (lbs)	Max. Crush (in) Static Dynamic
						Fwd Ratios	Actua- tion			
FRB	AMC Concord	1979	2 Dr Sed	258	6	3	Auto	34.7	3700	20.8 23.2
	Merc Marquis	1979	2 Dr Sed	302	8	3	Auto	35.4	4224	28.5 35.1
FLCB	AMC Concord	1980	2 Dr Sed	258	6	3	Auto	34.5	3930	24.0 27.3
	Merc Marquis	1981	2 Dr Sed	302	8	4	Auto	35.5	3965	29.3 37.4
MDB	AMC Concord	1980	2 Dr Sed	258	6	3	Auto	32.7	3920	31.6 --
	Barrier	--	--	--	--	--	--	32.7	3450	16.0 --
	Merc Marquis	1981	2 Dr Sed	302	8	4	Auto	32.1	3960	28.9 --
	Barrier	--	--	--	--	--	--	32.1	3450	15.2 --

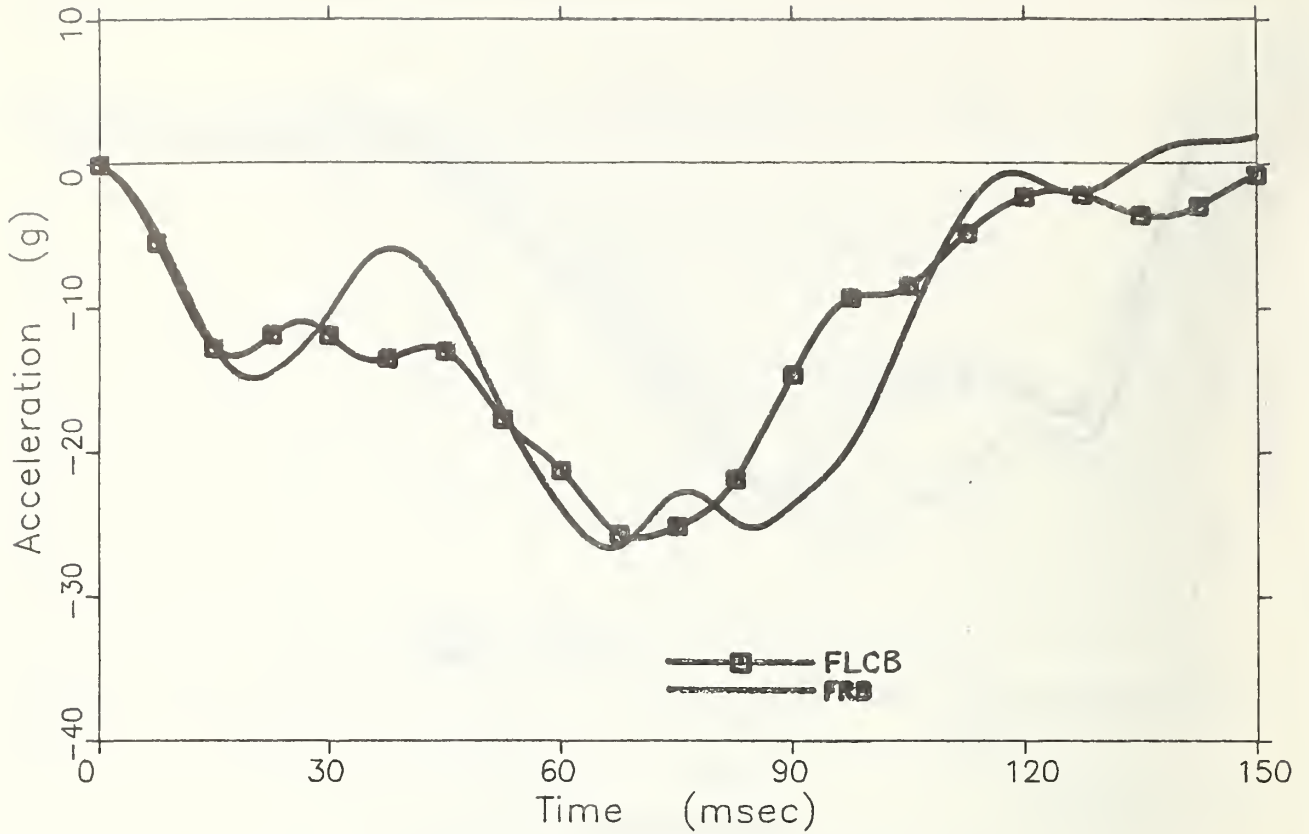


a) Acceleration Response

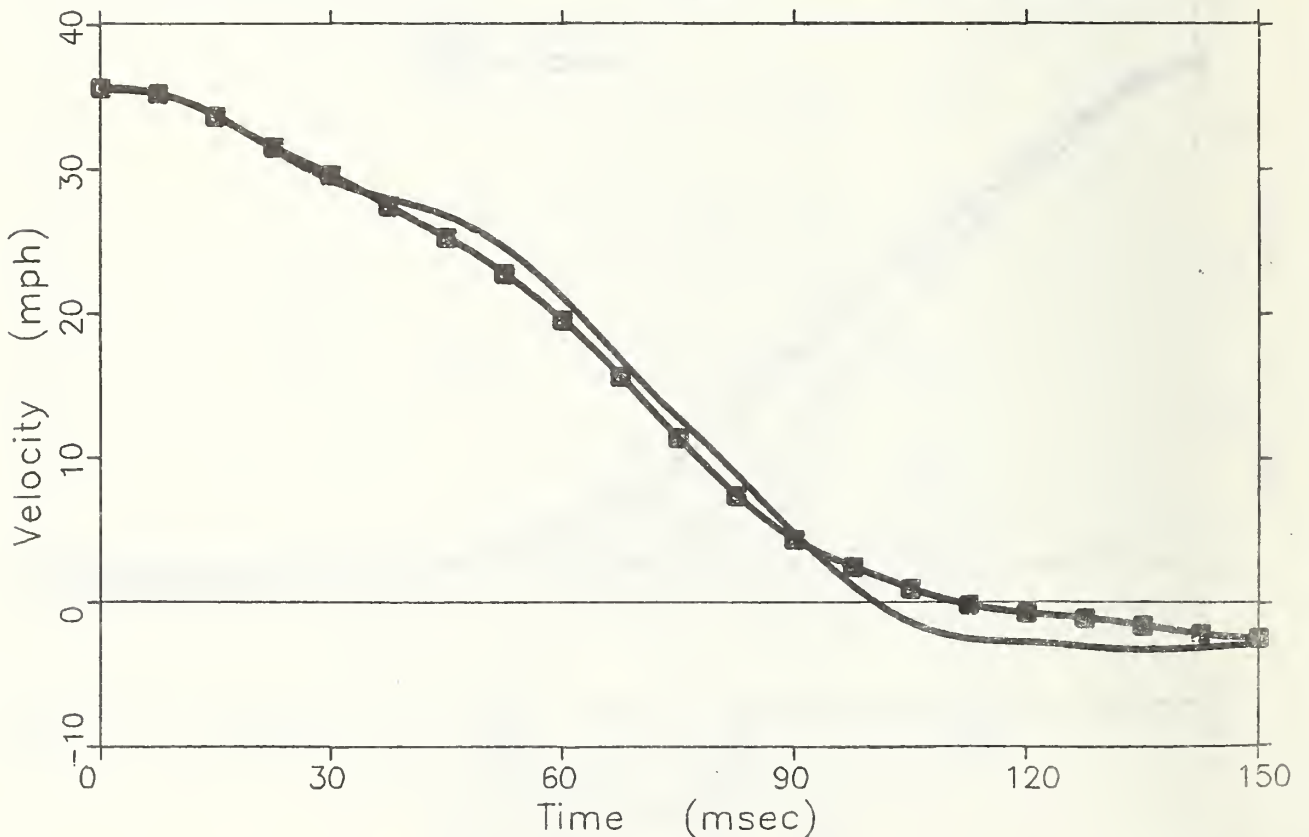


b) Velocity Response

FIGURE 48. Occupant Compartment Responses of Concords -- FRB and FLCB Collisions



a) Acceleration Response



b) Velocity Response

FIGURE 49. Occupant Compartment Responses of Marquis -- FRB and FLCB Collisions

duration. Consistent with these differences is the fact that the Concord's crush against the FLCB was considerably greater (15% to 18%) than that of the Concord in the FRB crash. (See Table 34.) No reasons, other than those mentioned above, have been found for these differences. Responses of the two Marquis' were very similar (Figure 49, Table 34).

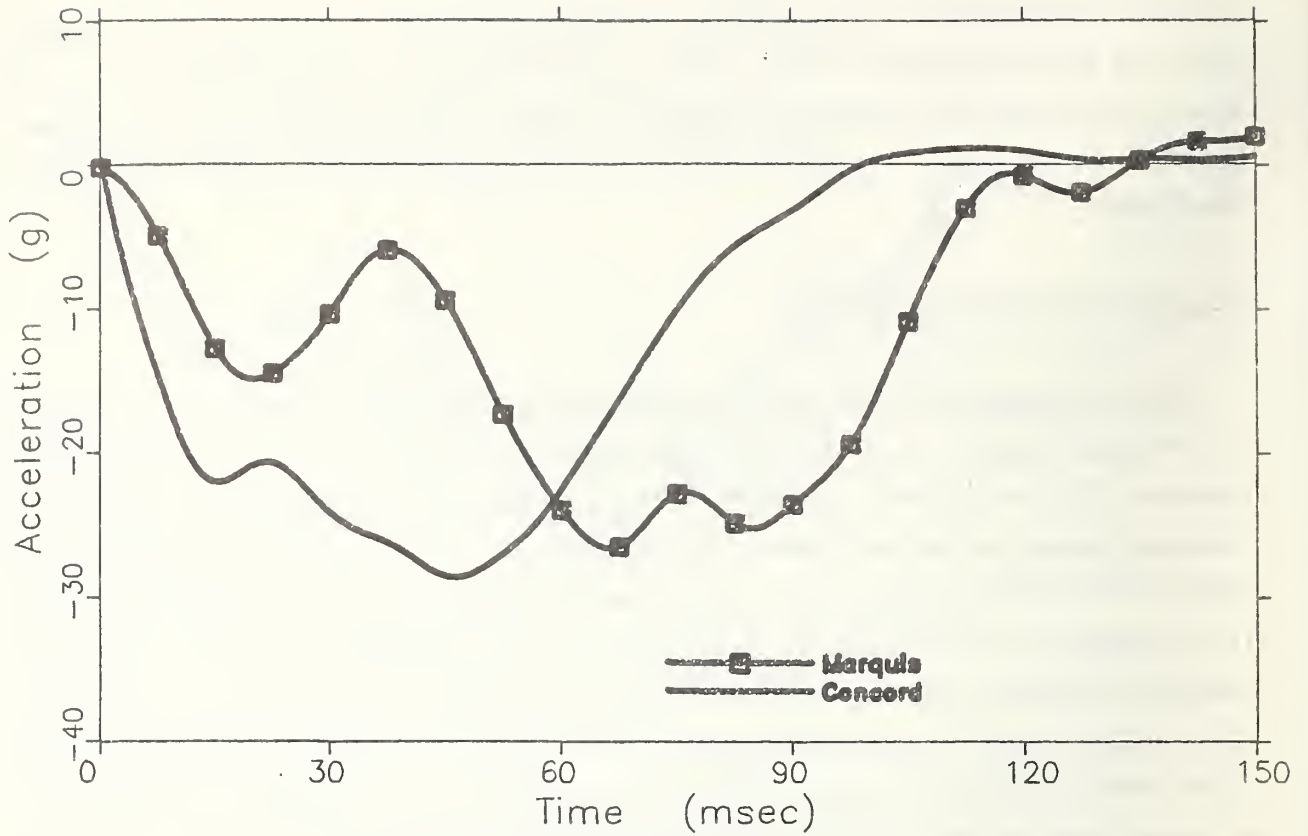
3.2.2.2 Fixed Rigid Barrier (FRB)

Since the aggressive Concord and nonaggressive Marquis were selected on the basis of FRB test results, it is obvious that substantial differences in their responses occurred. Figure 50 shows that the Concord's occupant compartment acceleration increased rapidly to its peak value. The Marquis experienced considerably more crush early in the event at relatively low force levels. Although peak accelerations from the two crashes were about the same, the time at which the peak occurred for the Marquis was 40% later than for the Concord. Total pulse duration was about 20% greater for the Marquis. From the velocity-time histories, it can be seen that it took nearly 40% longer for the Marquis to achieve 90% of its total velocity change than for the Concord to do so. Data in Table 34 show that the Marquis experienced much greater crush than the Concord: 37% and 51% greater, for static and dynamic crush values, respectively.

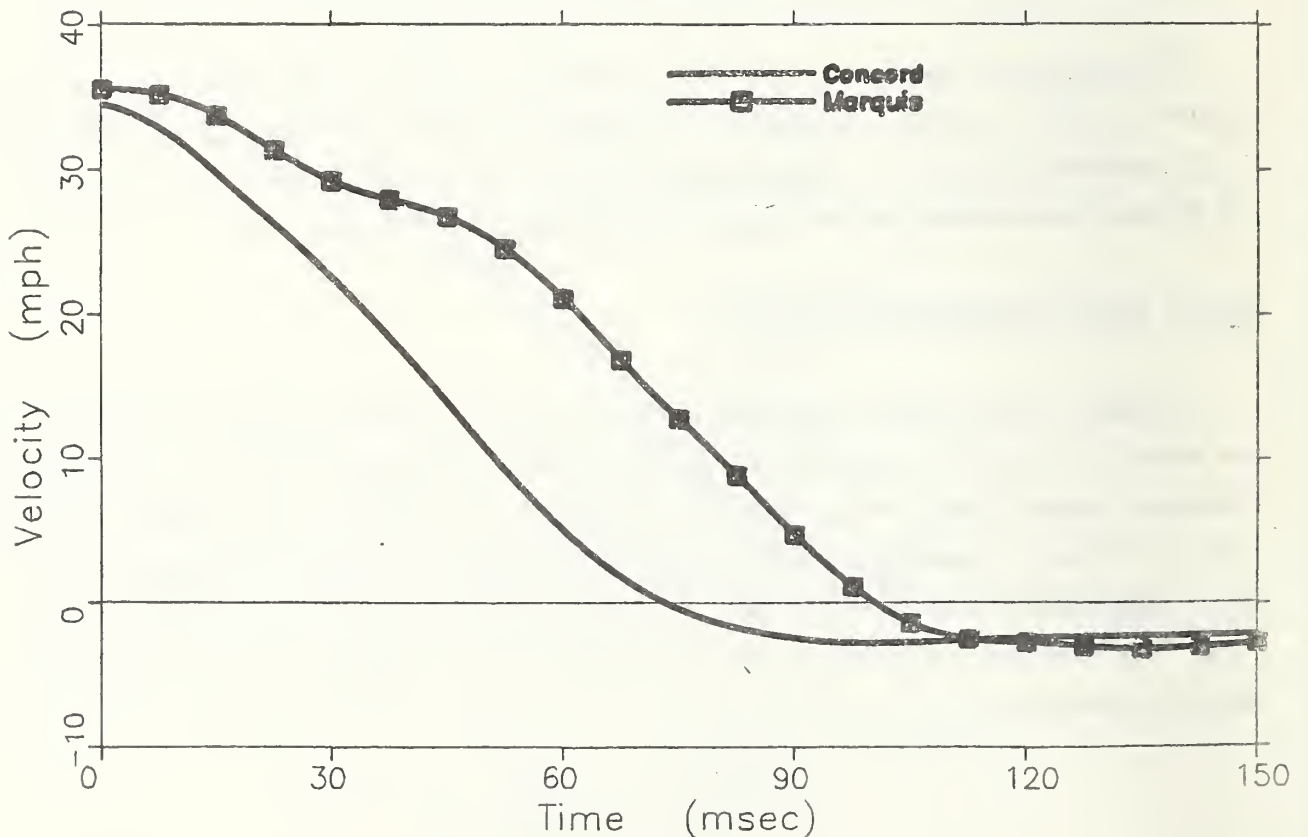
The differences seen between the Concord and Marquis FRB collisions are far greater than the differences described in Section 3.2.2.1 between the Concord FRB and FLCB collisions. Therefore, although some repeatability concern exists, it is clear that the differences between the two large car FRB responses are indisputable.

3.2.2.3 Fixed Load Cell Barrier (FLCB)

Occupant compartment responses of the Concord and Marquis impacting the FLCB are shown in Figure 51. Although differences were less pronounced than for the FRB collisions, observations were similar. The Concord acceleration pulse peaked earlier and was of shorter duration. The Marquis crushed early in the event, at relatively low force levels. Table 34 indicates very substantial crush differences between the two cars. The Marquis' maximum static and dynamic crush values were 22% and 37% greater, respectively.

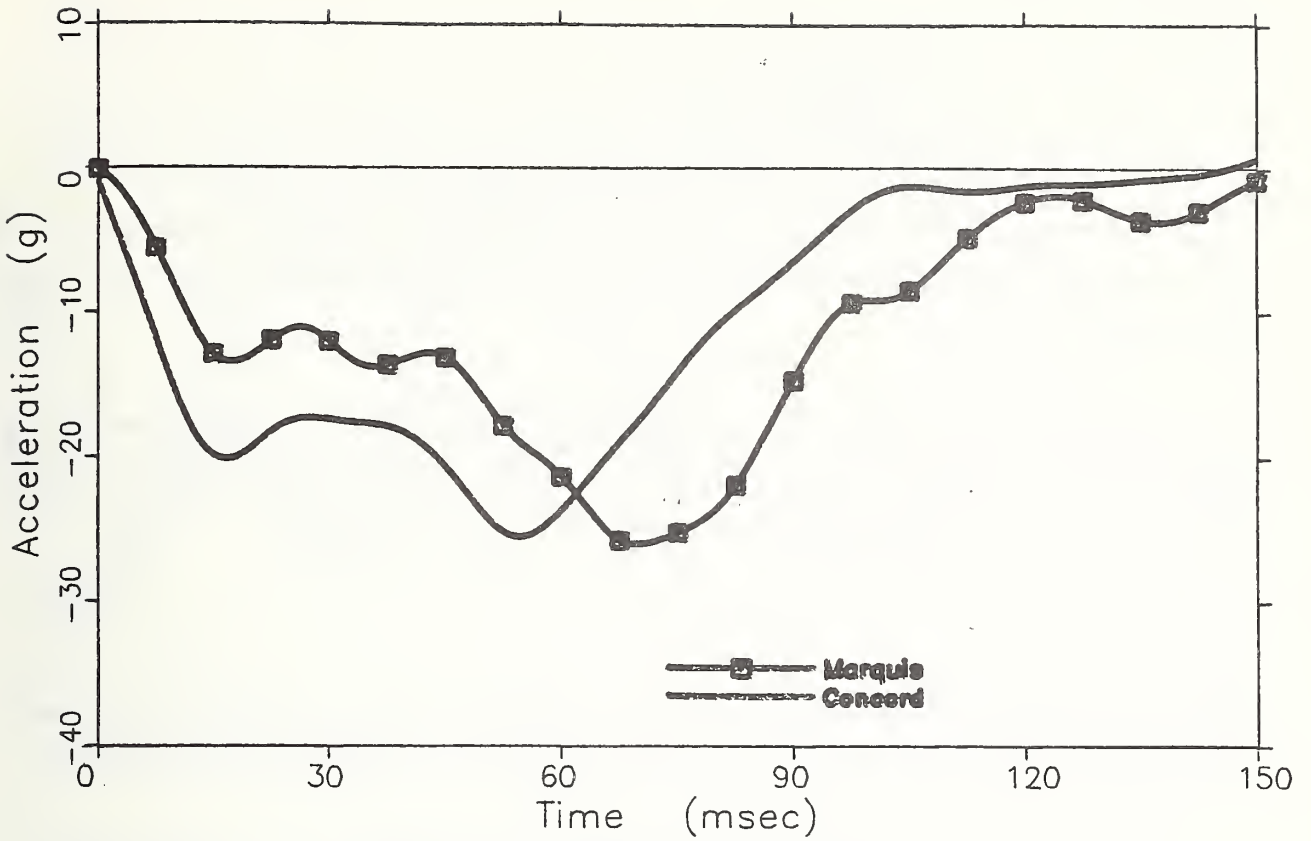


a) Acceleration Response

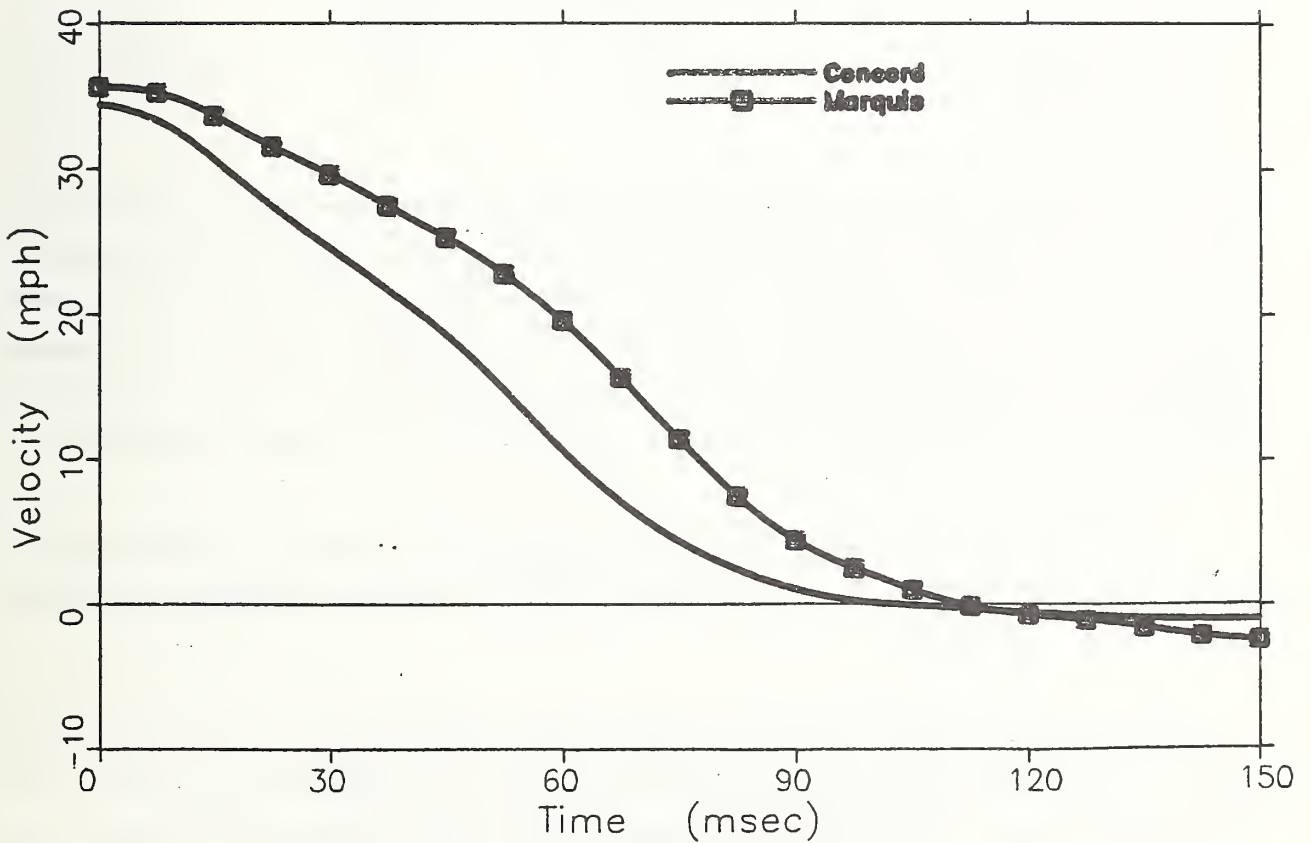


b) Velocity Response

FIGURE 50. Occupant Compartment Responses of Concord and Marquis -- FRB Collisions



a) Acceleration Response



b) Velocity Response

FIGURE 51. Occupant Compartment Responses of Concord and Marquis -- FLCB Collisions

The total forces recorded by the barrier load cells are presented in Figure 52. (Force-time data were processed through a phaseless, low pass Butterworth filter with a 100 Hz cutoff frequency and -40 db attenuation at a stop band frequency of 317 Hz.) Similarity with the cars' occupant compartment acceleration responses is apparent; the force from the Concord crash peaked earlier and was of shorter duration than that from the Marquis.

Accuracy of the total force measurement was checked for each vehicle by integrating the force-time curve to obtain total impulse and comparing that with vehicle momentum change, using the impulse-momentum relationship:

$$\int F dt = m\Delta V \quad (1)$$

To obtain values for ΔV , vehicle rebound velocities were estimated from both acceleration and photographic target displacement data. The results were as follows:

	<u>Concord</u>	<u>Marquis</u>	<u>% Difference</u>
$m\Delta V$ (lbs-sec)	6534	6953	+ 6.4
$\int F dt$ (lbs-sec)	6021	7560	+ 25.6
% Difference	-7.9	+8.7	

Agreement between the impulse obtained by integration of the force-time curve and through use of equation (1) was within 10% for each vehicle. Also, momentum changes of the two vehicles agreed to within 6.5%. However, the difference between integration-obtained impulses for the two cars was greater than 25%. Although substantial, this difference did not prevent the obtaining of useful information regarding impact force differences between the two cars, as will be seen subsequently.

For purposes of comparing force distributions, the load cells were grouped as shown in Figure 53. Forces from the individual load cells in each group were summed, and are presented in Figures 54-59.

Also shown in Figure 53 are the heights above ground level of each row of load cells and of the hood edges and the bottoms and tops of the bumpers of the Concord and Marquis (pre-test). Although initial contact between the vehicles and the barrier face

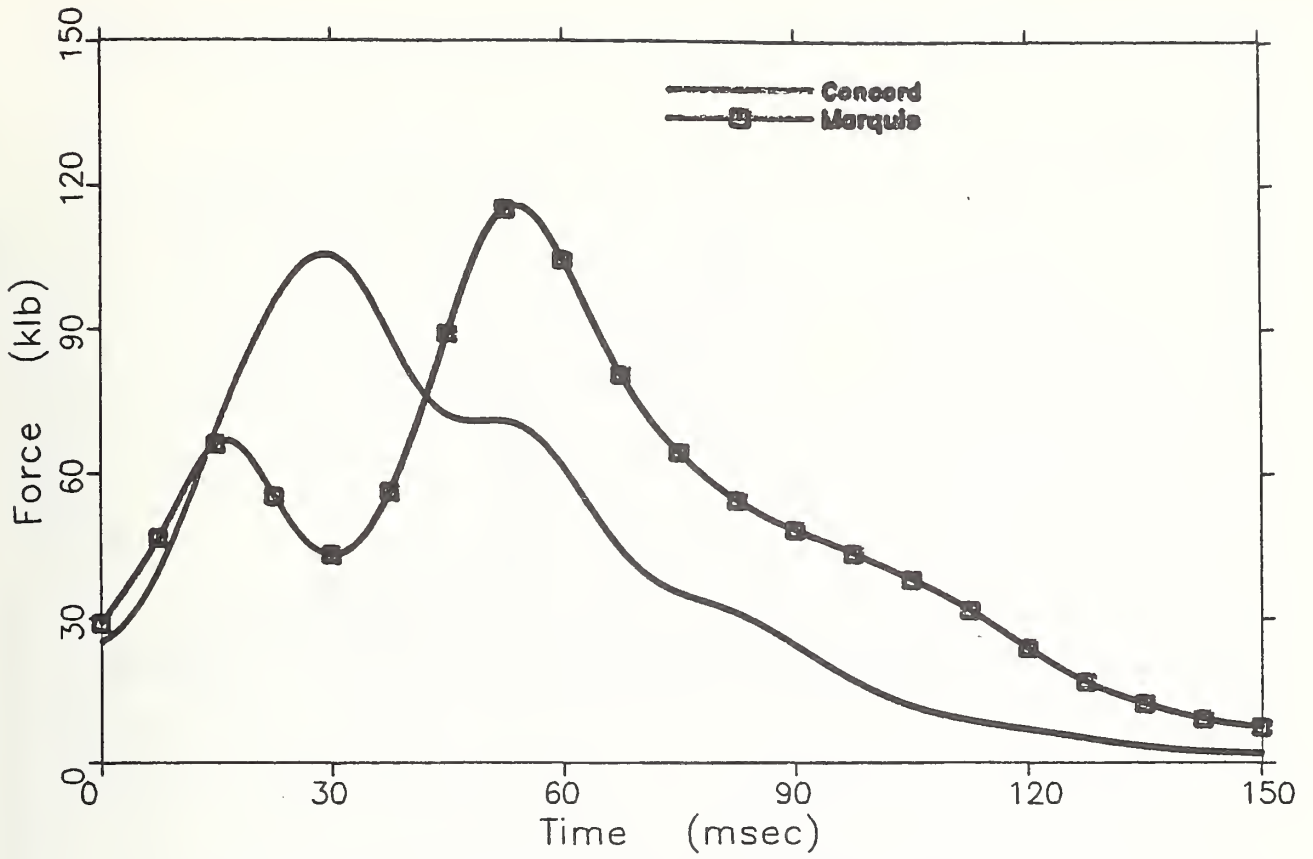


FIGURE 52. Total Force -- Concord and Marquis Collisions with FLCB

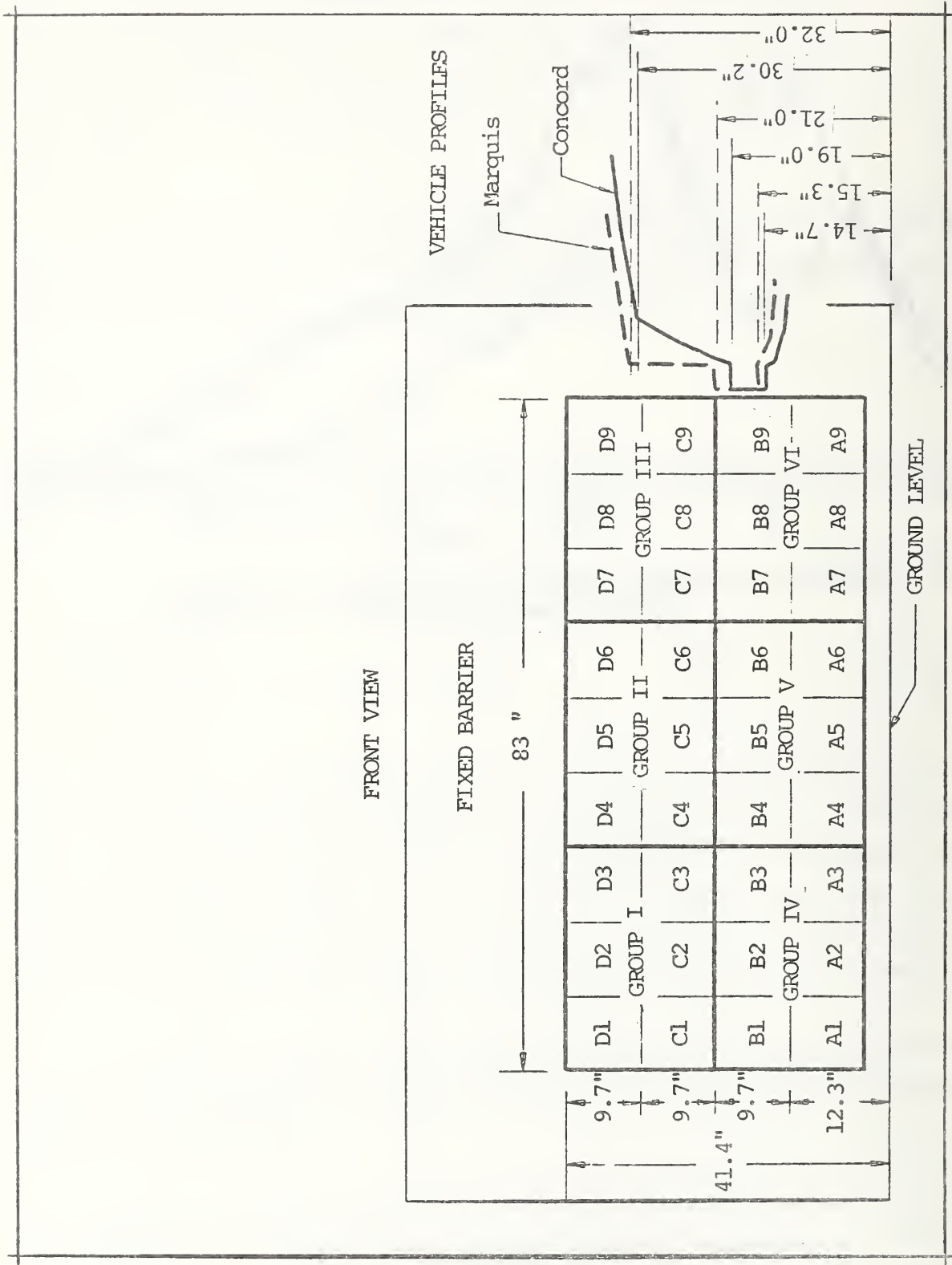


FIGURE 53. Load Cell Groups and Vehicle Profile Heights

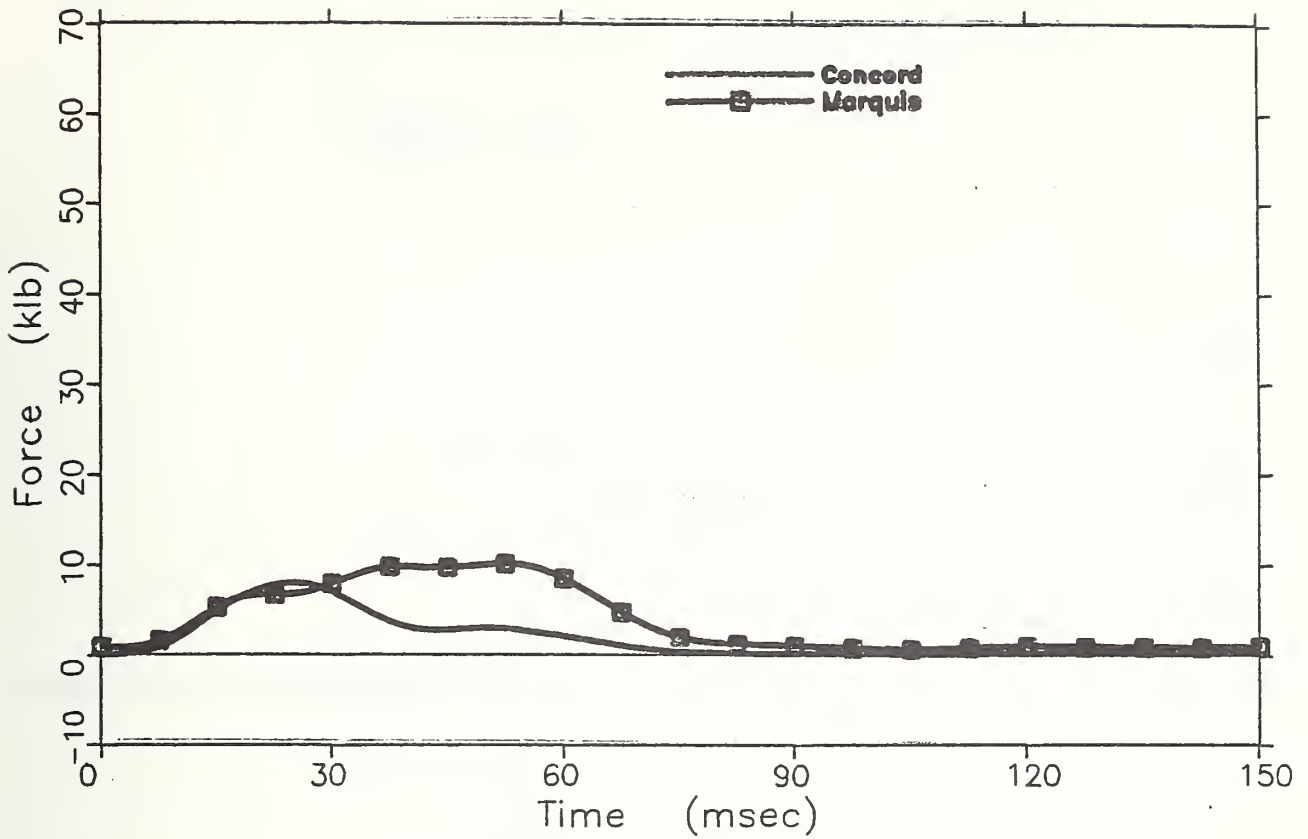


FIGURE 54. FLCB Group I Forces --
Concord and Marquis Collisions

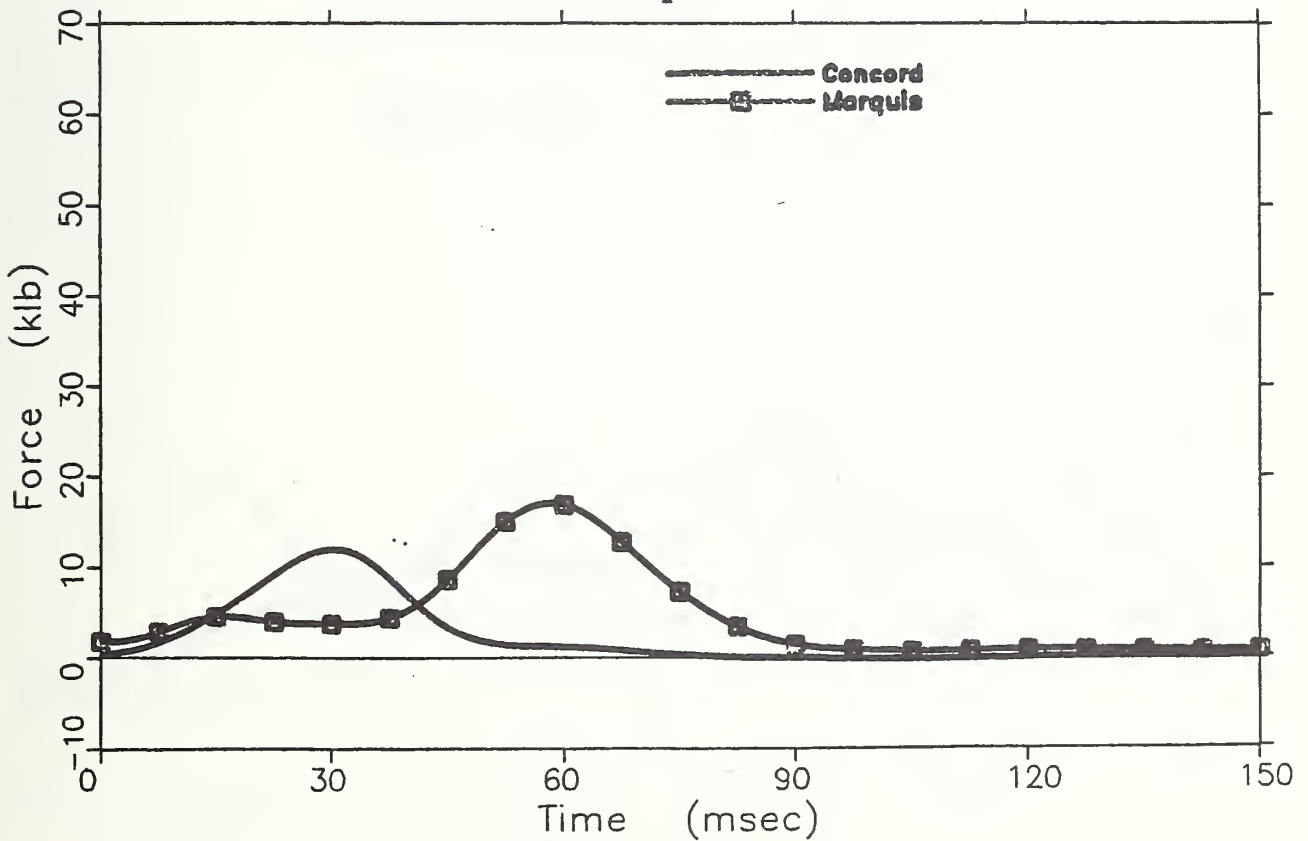


FIGURE 55. FLCB Group II Forces --
Concord and Marquis Collisions

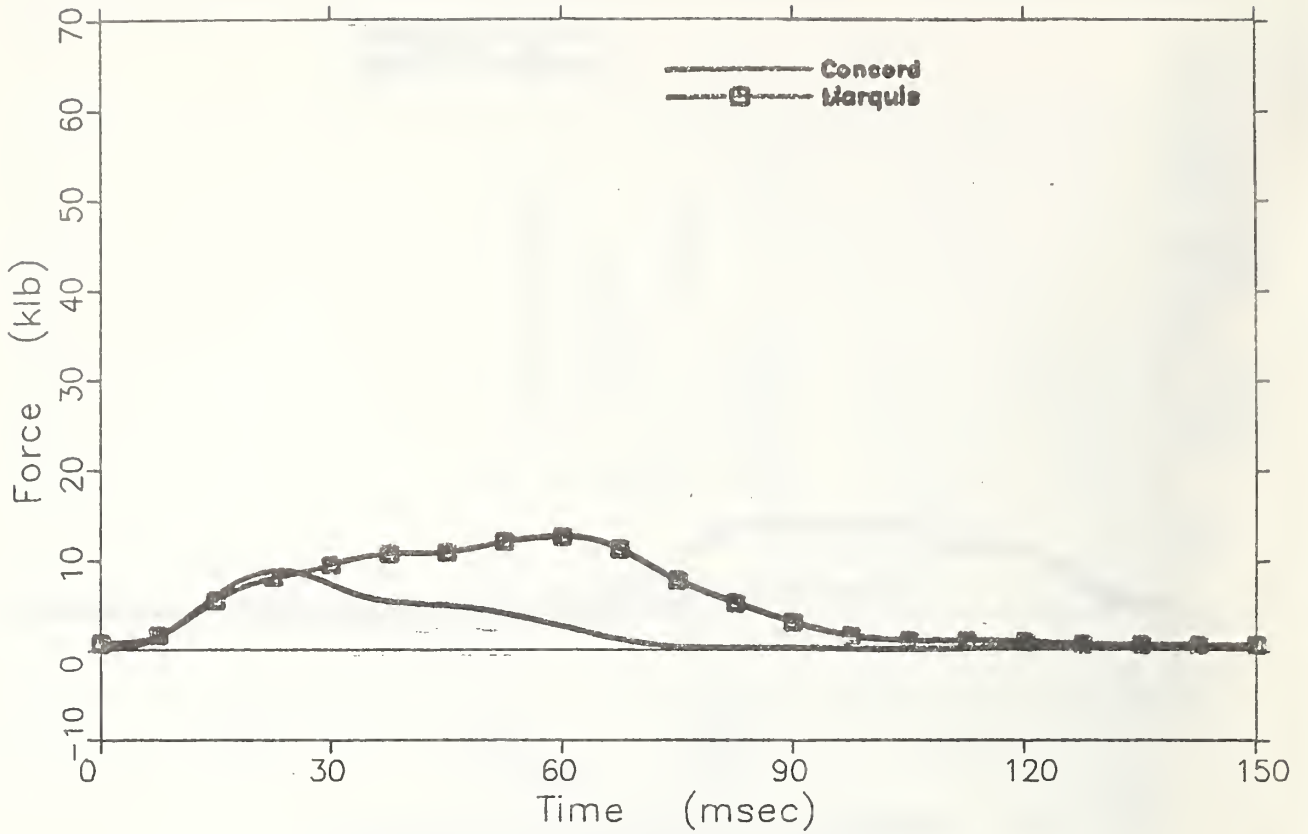


FIGURE 56. FLCB Group III Forces -- Concord and Marquis Collisions

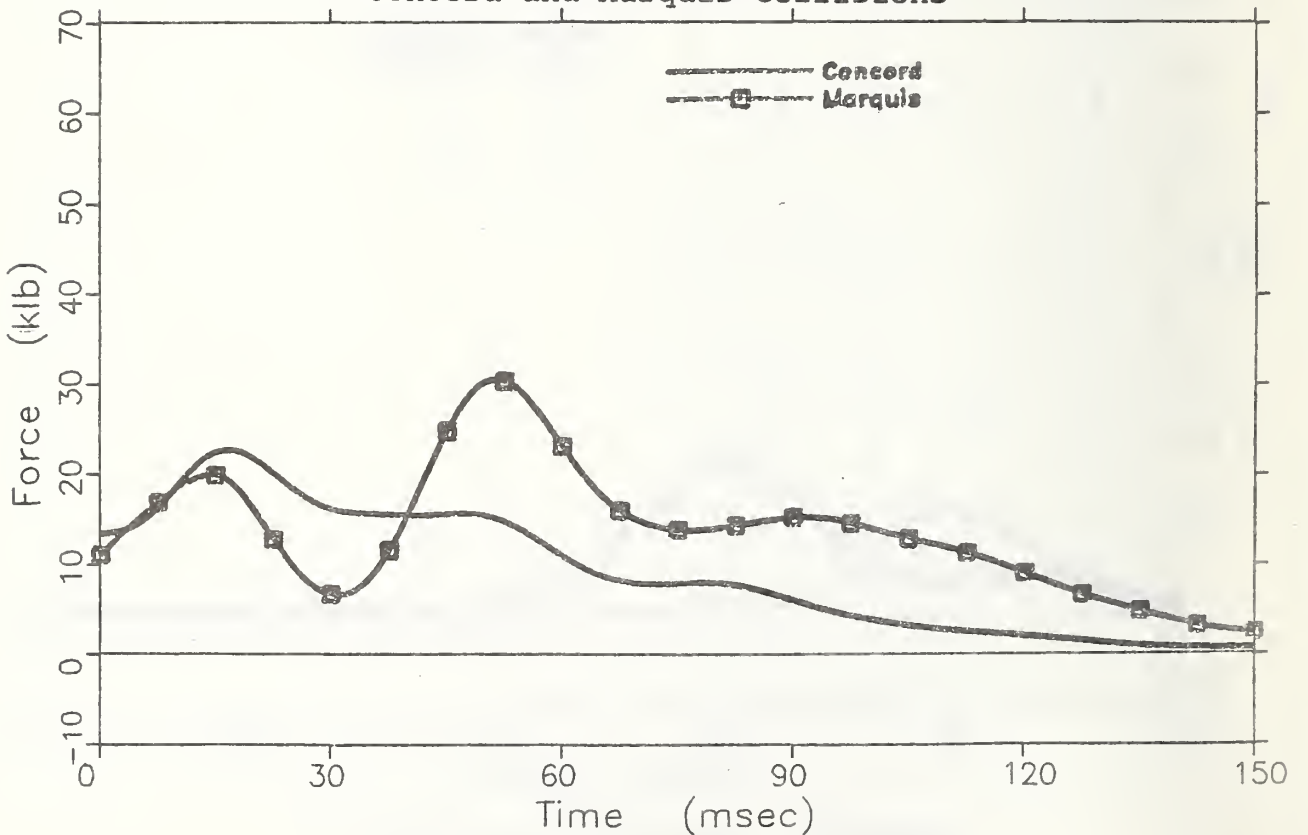


FIGURE 57. FLCB Group IV Forces -- Concord and Marquis Collisions

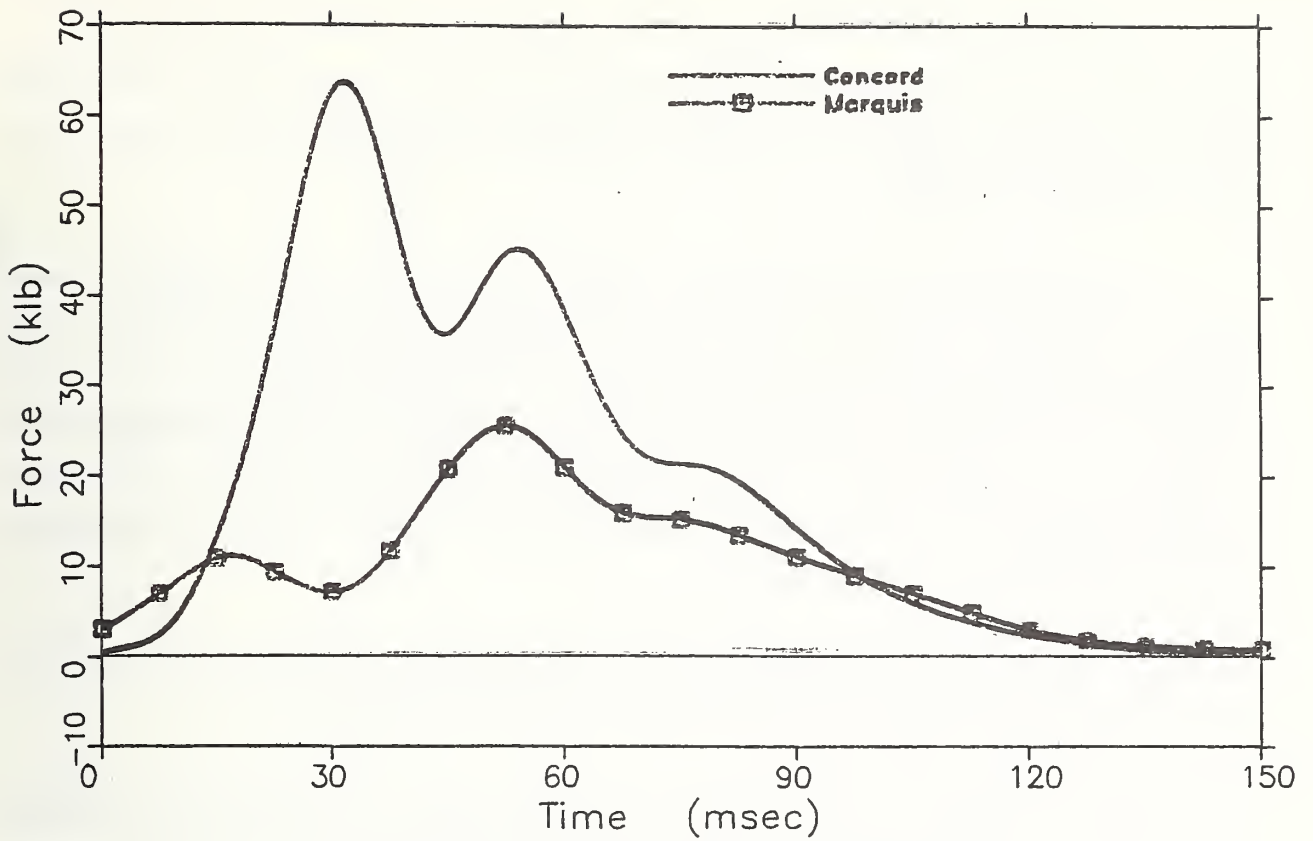


FIGURE 58. FLCB Group V Forces --
Concord and Marquis Collisions

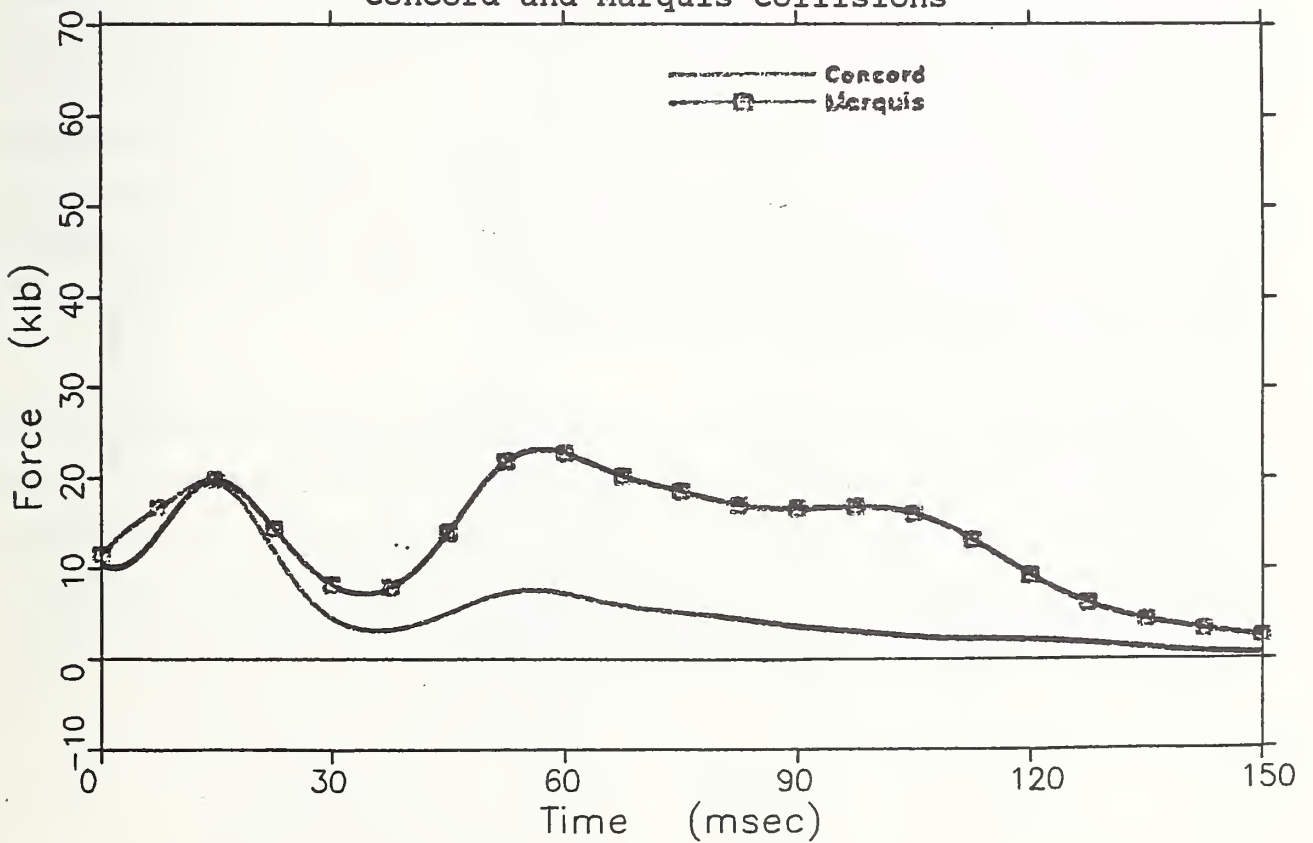


FIGURE 59. FLCB Group VI Forces --
Concord and Marquis Collisions

obviously occurred along rows B and C, several of the load cells in rows A and D also carried significant forces as the result of vertical deformation of the cars' front structures during crushing.

Two observations were made from Figures 54-59. First, the Marquis collision resulted in greater impulses in five out of the six load cell groups. In the sixth group (Group V), however, the Concord impulse was much greater than in any other group for either vehicle. This indicates that a very different stiffness distribution exists in these two cars. Specifically, much of the total Concord frontal structure stiffness appears to be concentrated in the center bumper area, while the Marquis' stiffness is reasonably well distributed over its frontal area.

The second observation was that in each load cell group, maximum force (and most of the impulse) occurred later for the Marquis than for the Concord.

In order to quantify the force distribution differences, the impulse from each load cell group was calculated and was normalized with respect to the total impulse on the barrier. This was done for each vehicle. The results appear on the left side of Figure 60. For the Marquis, about 75% of the total impulse was carried fairly uniformly over the lower three load cell groups (the bumper contact region). Impulse distribution was markedly different for the Concord. About 85% was carried by the lower three groups, with nearly 50% occurring on the center group. It is interesting that the Marquis, a vehicle which demonstrated less aggressiveness structurally in a full frontal collision than did the Concord, appears to be stiffer on the corners and may exhibit more aggressiveness in offset collisions than the Concord.

Quantification of the difference in the time phasing of the force application was accomplished by calculating the centroid of the force-time pulse in each load cell group (i.e., the time at which the impulse reached half its total magnitude). These results are shown on the right side of Figure 60. For five load cell groups, the centroids (times to achieve half the impulses) from the Concord collision were one-half to two-thirds of what they were from the Marquis. For the sixth load cell group (notably, the one

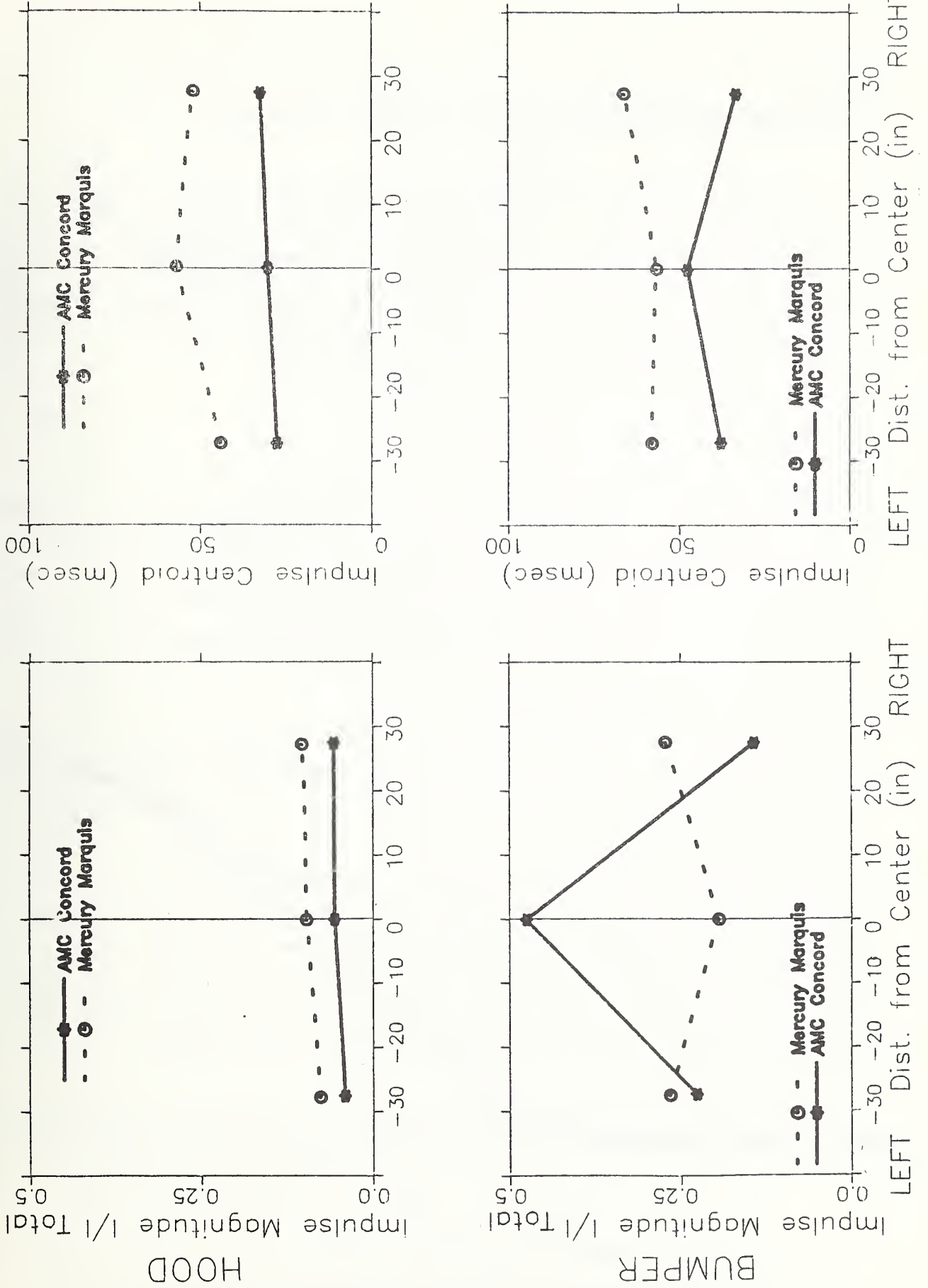


FIGURE 60. Magnitude and Centroid of Impulse on Load Cell Barrier From Collisions With AMC Concord and Mercury Marquis

heavily loaded from the Concord collision), centroids were nearly the same. Thus, loads increased much more rapidly in the Concord test except in the area where load was greatest, where force build-up occurred only slightly more rapidly.

It is interesting that force consistently increased more rapidly on the corners of the Concord, where impulse magnitudes were lower than for the Marquis. It would be highly desirable to conduct the Marquis/Rabbit offset frontal collision, as originally planned, in order to study the relative importance of corner stiffness (which appears greatest for the Marquis) and time of force build-up (shortest for the Concord) with respect to aggressiveness.

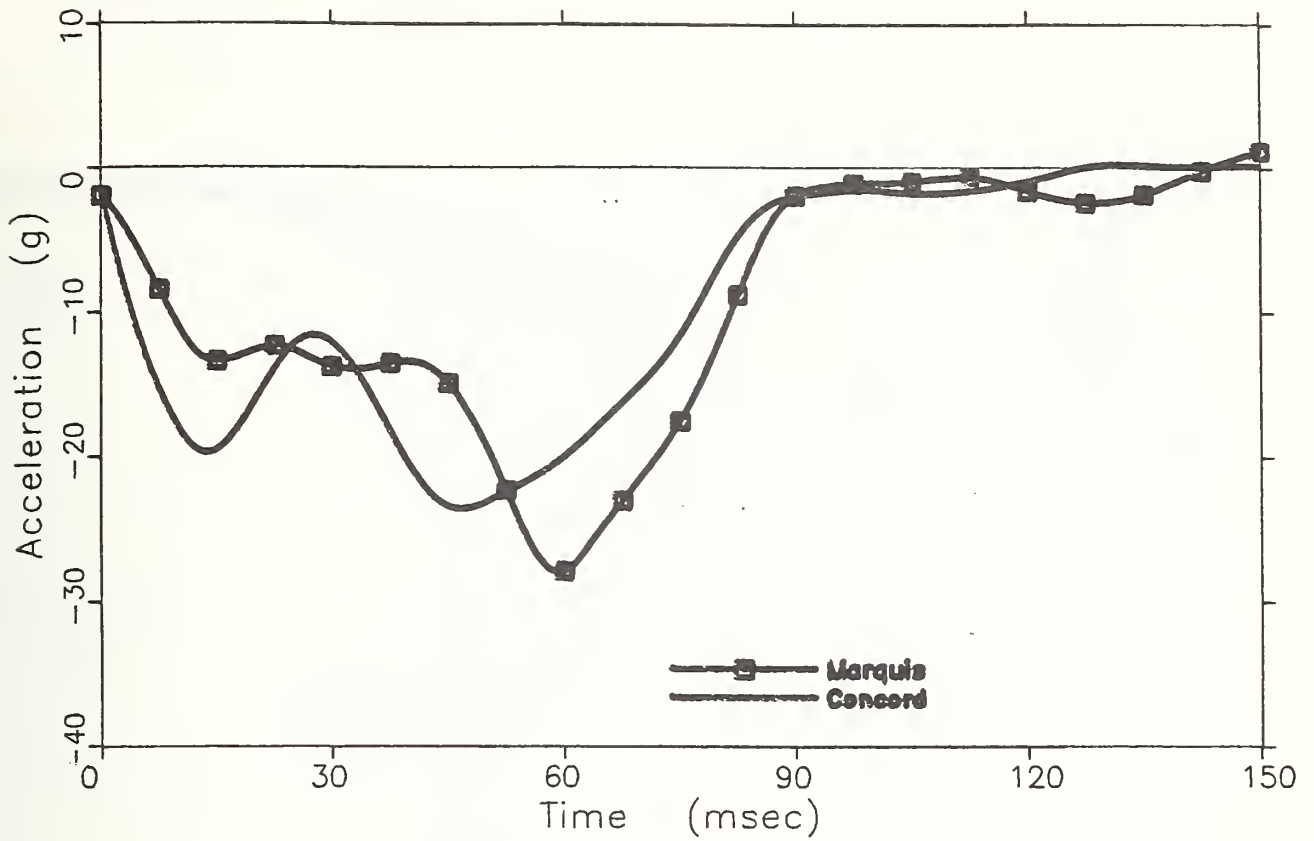
3.2.2.4 Moving Deformable Barrier (MDB)

Occupant compartment responses of the Concord and Marquis striking the MDB are presented in Figure 61. Responses were similar to those resulting from the FLCB, in that the Concord's acceleration level was higher early in the event. Differences were less pronounced, however. The velocity-time curves were considerably closer to each other than in the FLCB collisions, and the pulse durations were essentially the same for the two vehicles.

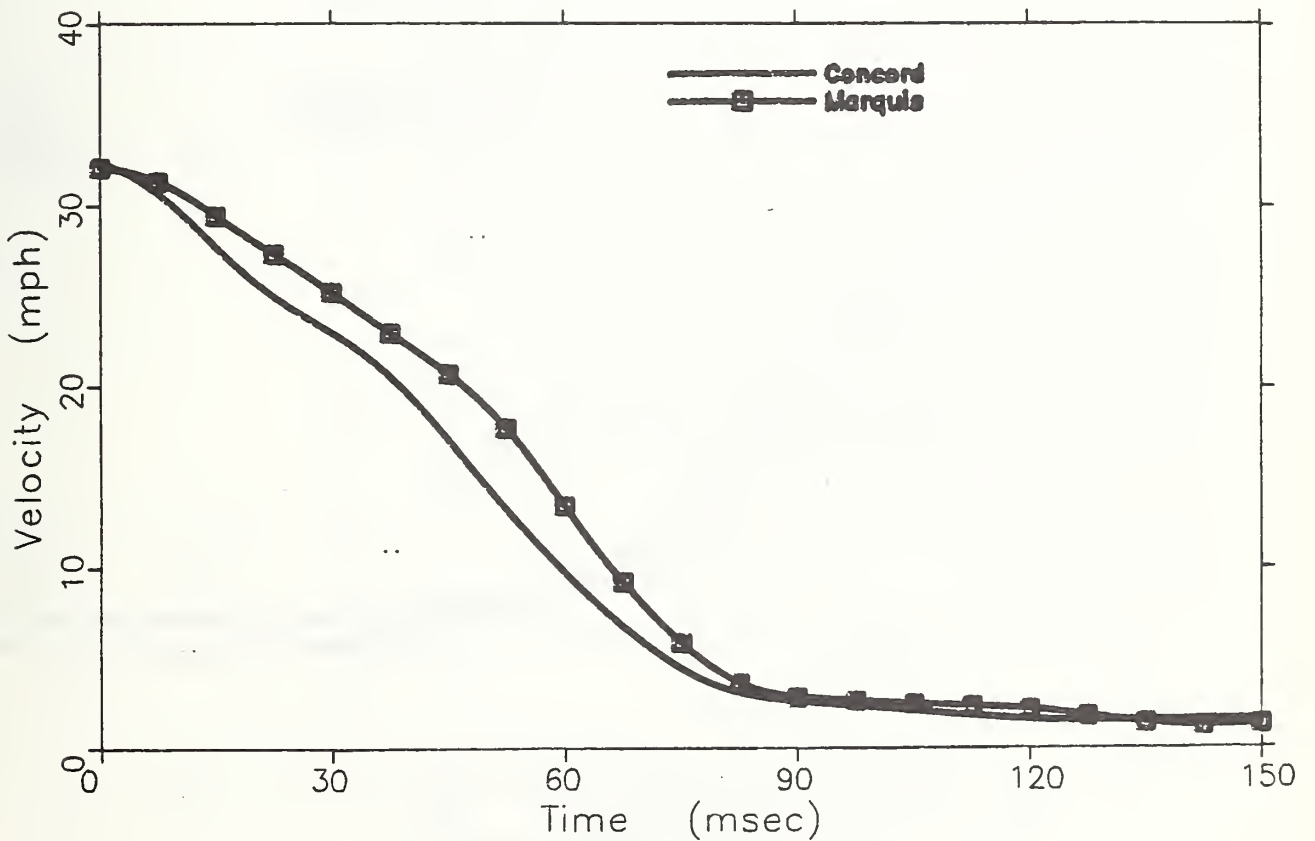
Figure 62 shows responses of the barrier from the two tests. As with the cars' occupant compartment responses, differences were small. The barrier striking the Concord had a slightly earlier acceleration peak and a slightly shorter pulse duration.

The magnitude and distribution of crush over the surface of the MDB are shown in Figure 63. Each of the four graphs is a plan view, depicting crush at a given elevation. The four elevations at which measurements were made were the heights of the car's lower bumper, upper bumper, half-way point between bumper and hood, and hood. The original honeycomb thickness was 15 inches for the upper two elevations, and 19 inches for the lower two (accounting for the "bumper" projection of four inches).

Figure 63 indicates that the Marquis' penetration of the barrier was reasonably uniform at all four elevations. The Concord's penetration, at the top three elevations,

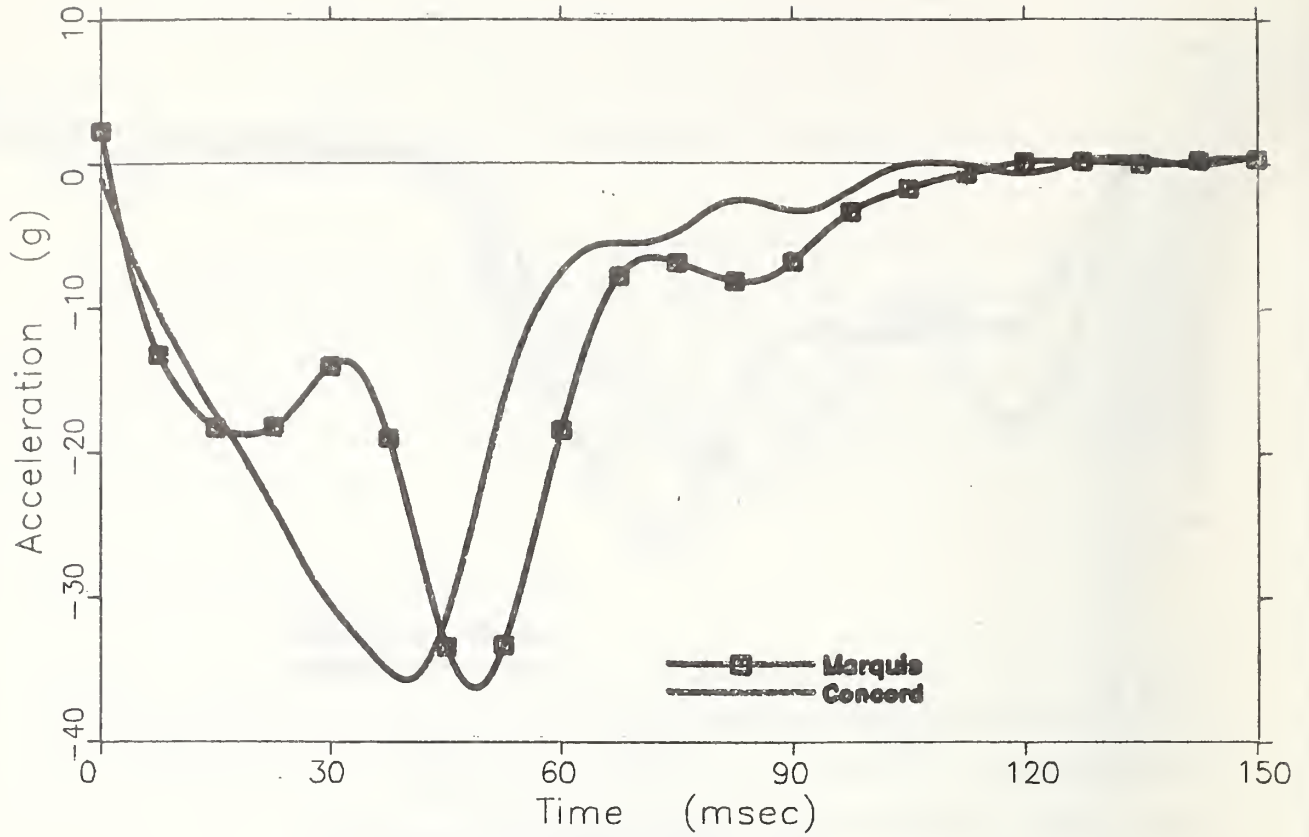


a) Acceleration Response

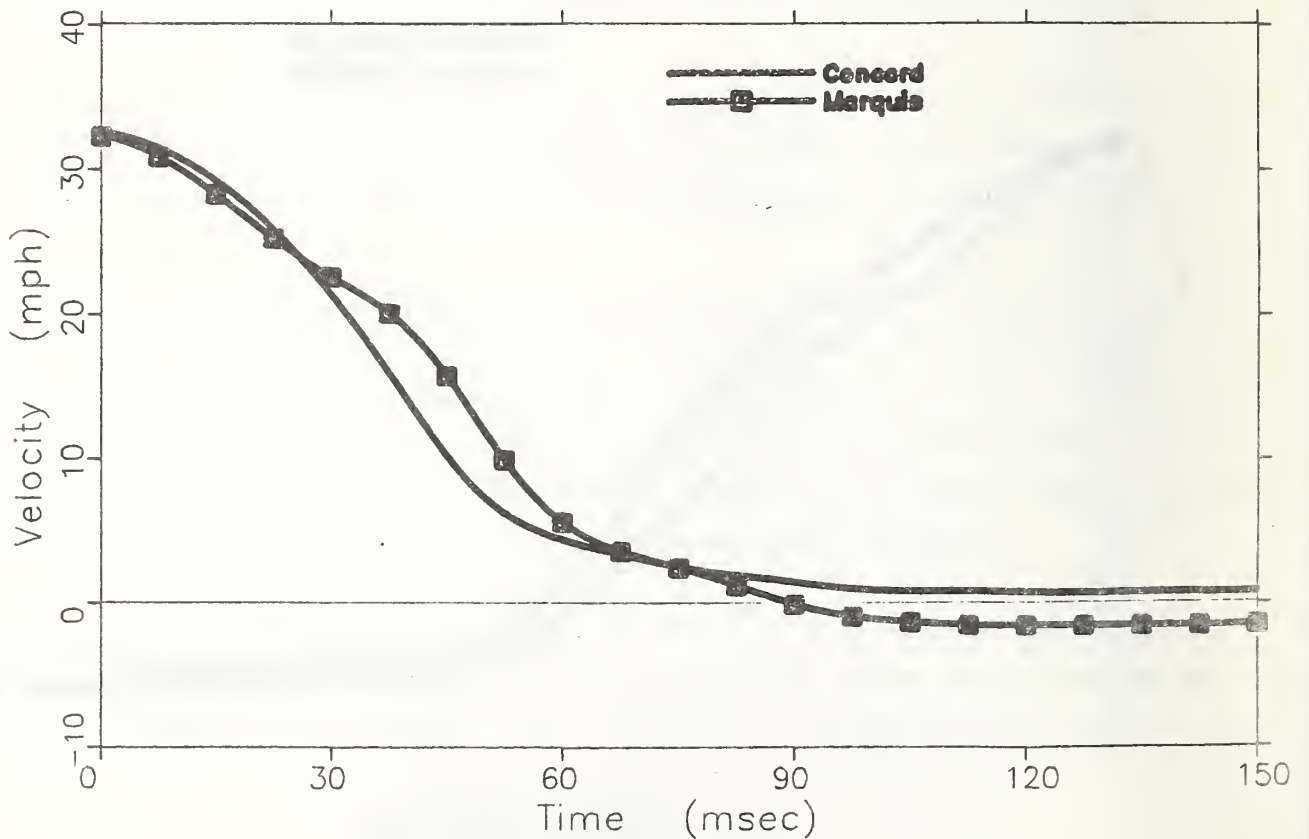


b) Velocity Response

FIGURE 61. Occupant Compartment Responses of Concord and Marquis -- MDB Collisions



a) Acceleration Response



b) Velocity Response

FIGURE 62. MDB Responses -- Collisions with Concord and Marquis.

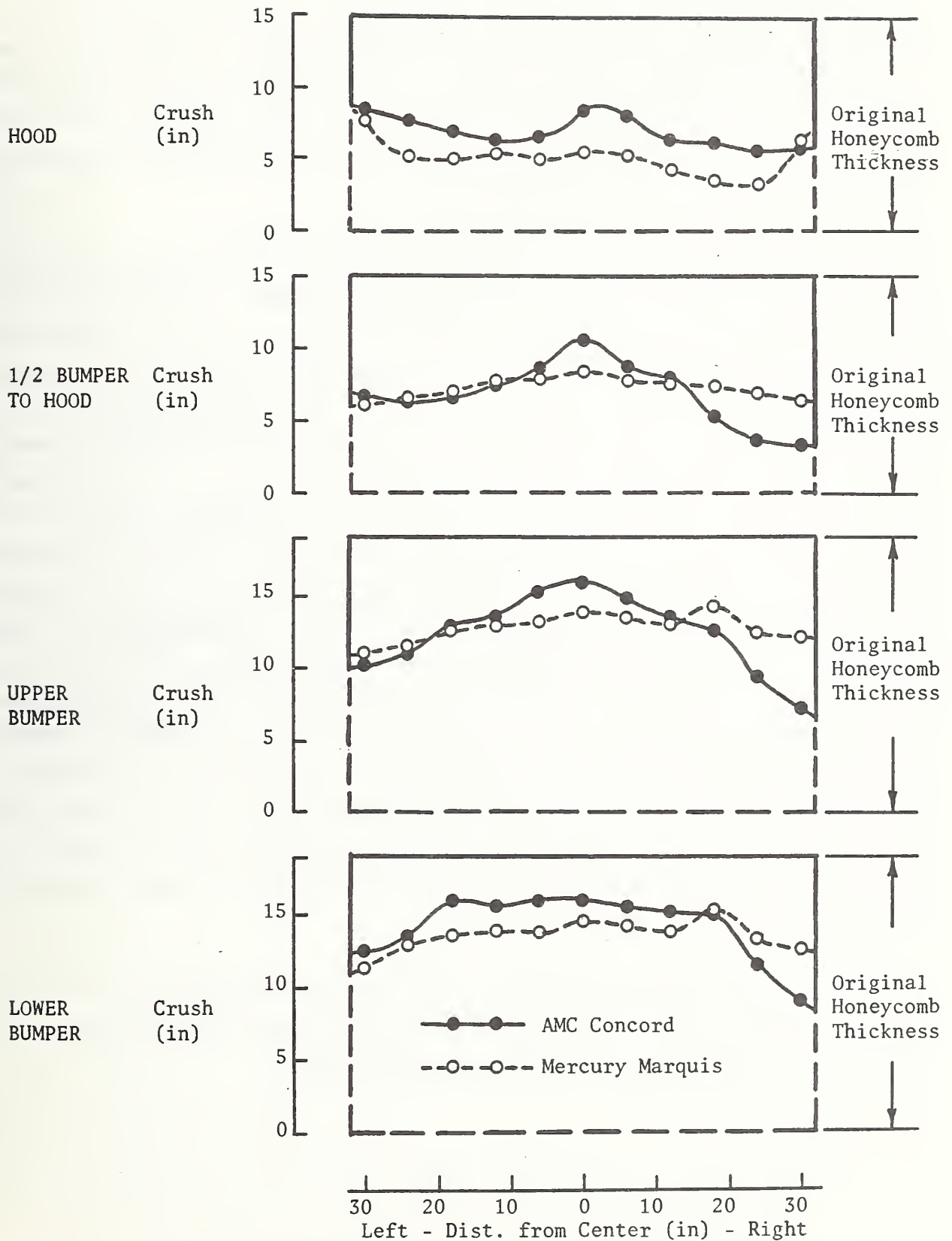


FIGURE 63. Crush of Moving Deformable Barrier from Collisions with AMC Concord and Mercury Marquis

was somewhat concentrated at the center. At the lower bumper elevation, it was more nearly uniform, but that was probably the result of bottoming the aluminum honeycomb. Note that penetration over the center 40 inches is within three to four inches of the back surface of the honeycomb. The fact that the Concord caused a more centrally concentrated deformation pattern is consistent with the results of the FLCB tests (Section 3.2.2.3), which indicated a higher, more concentrated force exerted by the center of the vehicle's front structure.

Maximum values of static crush of the cars and barrier faces are presented in Table 34. In contrast to the results of the other barrier tests, the maximum crush of the Concord was greater (by 9%) than that of the Marquis. To attempt to explain this apparent anomaly, estimates were made of the amount of kinetic energy dissipated through crush of the cars in the various barrier collisions. This calculation was very simple for each of the FRB and FLCB collisions, where all the vehicle's kinetic energy was dissipated in crushing the vehicle. For each MDB test, an approximation was made of the total crush of the barrier. It was important, but difficult, to estimate the amount of crush of the stiffer honeycomb which represented the bumper. By assuming that the bumper element was crushed 2 inches (half its depth), it was felt that an upper bound would be obtained for the amount of energy absorbed by the barrier face. Table 35 shows the results of the calculations (assuming purely plastic collisions). It is estimated that significantly more energy had to be dissipated by the cars in the MDB collisions than in the FRB or FLCB collisions. Figure 61 shows that the Marquis experienced higher accelerations late in the crash event than the Concord, indicating that the stiffness of the aft part of the Marquis' frontal structure (just forward of the occupant compartment) is greater than that of the Concord. These factors could account for the fact that total vehicle crush values did not follow the same trend as in the other barrier tests.

Maximum barrier face crush (again, refer to Table 34) was nearly the same in the two MDB collisions. This undoubtedly is due to the fact that the Concord essentially bottomed the honeycomb and the Marquis nearly did the same.

TABLE 35
Energy Dissipation Estimates -- Barrier Collisions

Test	Energy (ft-lbs) Dissipated by:	
	Car	Barrier
Concord/FRB	148,800	0
Marquis/FRB	176,800	0
Concord/FLCB	156,200	0
Marquis/FLCB	166,900	0
Concord/MDB	>194,000*	< 68,000**
Marquis/MDB	>190,000*	< 64,000**

*Lower bound values
**Upper bound values

3.2.2.5 Summary of Results

Differences in responses of the two cars (acceleration pulse shape and duration, and maximum crush) were somewhat greater in the FRB and FLCB tests than in the MDB tests (the more aggressive Concord having substantially less crush, a shorter duration pulse and an earlier peak acceleration than the less aggressive Marquis). Barrier load cell data from the FLCB collisions revealed substantial differences in load distribution and time-phasing between the two cars. The Concord's stiffness was more centrally concentrated and forces peaked much earlier. Energy levels in the MDB collisions were probably too high. Bottoming of the honeycomb occurred over a large area of the barrier face in the Concord collision and it appeared that the Marquis nearly caused bottoming. Thus, maximum barrier crush values were nearly the same in the two tests. Evidence of the Concord's more centrally located stiffness and the Marquis' more uniform stiffness distribution was seen, confirming results of the FLCB tests.

3.2.3 Conclusions and Recommendations

The three barriers were found to be approximately equal in their ability to discriminate structural aggressiveness differences between the AMC Concord and the Mercury Marquis. The FRB and the FLCB produced a somewhat greater response difference between the two cars than did the MDB. Both the FLCB and the MDB demonstrated their potential for measuring stiffness distribution over the front area of the vehicles. It could not be determined how significant the observed stiffness distribution differences were with respect to aggressiveness, however, since one of the planned car/car offset crash tests was not conducted.

It is recommended that the Marquis/Rabbit offset frontal crash test be performed. If the aggressiveness difference between Concord and Marquis in the offset mode were found to be considerably less than it was in the full frontal mode, the indication would be that stiffness distribution has a significant effect on aggressiveness. It could then be concluded that measuring the distribution of a car's frontal stiffness, by using either the FLCB or the MDB, is important in determining its aggressiveness. If the aggressiveness difference between Concord and Marquis in the offset mode were found to be the same as it was full frontally, this would indicate that stiffness distribution differences (to the

extent they exist for these two cars) are not important in relationship to aggressiveness. If this were true, the importance of measuring stiffness distribution would be greatly diminished, and use of the simple FRB test for measuring aggressiveness may be sufficient.

It is recommended that, in further car/MDB testing, vehicle impact velocities be reduced from what they were in the Concord and Marquis MDB collisions. This will prevent bottoming of the barrier's honeycomb face and will reduce the amount of energy being dissipated by the car to a more reasonable value.

If, upon conducting the Marquis/Rabbit offset test, it were determined that stiffness distribution is important, then consideration should be given to repeating the Concord and Marquis MDB tests at lower impact velocities. This would enable a better evaluation to be made of this barrier's ability to measure aggressiveness relative to that of the FLCB barrier.

In this study, test results from only two vehicles (Concord and Marquis) were evaluated to indicate how structural aggressiveness might best be measured. It is recognized that additional testing with later model year vehicles will be necessary to firmly establish a reliable aggressiveness-measuring test methodology.

4.0 SIDE PROTECTION -- VEHICLE STRUCTURAL CHARACTERISTICS

4.1 Introduction

It has been postulated that occupant injury severity in car-to-car side collisions may be a function of the frontal stiffness distribution of the striking car. A series of crash tests were analyzed in order to determine how much difference exists in the frontal stiffness distributions of similar weight cars.

4.2 Crash Test Data

The analyzed tests were moving load cell barrier (MLCB)-to-car frontal crash tests conducted by Dynamic Science, Inc. (12). The test data are summarized in Table 36. With the exception of test number 2.4, all tests were conducted with the test vehicle

TABLE 36
MLCB Car Crash Test Data Summary

Vehicle	Impact Angle (°)	Test Number	Test Vehicle Weights (lbs)	Test Barrier	Closing Speed (mph)	Vehicle Film	Velocity Change (mph) Load Cells	V% Difference (Load Cells - Accel) Accel
1980 Chevrolet Citation	0	3.1	3179	3991	40.22	24.7	23.08	-6.9
1980 Ford Fairmont	0	3.3	3349	3995	39.32	23.4	23.95	1.9
1979 Oldsmobile Cutlass	0	2.4	3803	3987	39.0	22.2	18.5	-17.8
1979 Chevrolet Impala	0	3.5	4241	3995	40.58	22.4	19.07	-15.3
1980 Chevrolet Citation	30	3.2	3214	3991	29.77	17.4	17.31	-2.4
1980 Ford Fairmont	30	3.4	3343	3995	29.79	17.3	14.79	-2.2
1979 Oldsmobile Cutlass	30	2.3	3794	3987	29.44	15.0	18.68	2.4
1979 Chevrolet Impala	30	2.1	4232	4013	30.00	16.60	15.91	-4.1

initially at rest being struck by the moving barrier. The barrier face was an earlier version of the one described in Section 3.2.2.3. It contained 40 load cells, each covered with a 1-1/2" thick plywood striking surface, arranged in four horizontal rows. (In test number 2.1, 6" thick pieces of energy-absorbing honeycomb were used in place of the plywood.)

4.3 Analysis Results

As a check on the load cell recordings for each test, the total force-time history was integrated and used in the Impulse-Momentum Equation to calculate the car's velocity change. (The total force-time histories are shown in Figures 64 -- 67.) The calculated velocity change was then compared with the velocity change obtained by integrating the measured accelerometer data. As shown in Table 36, large percentage differences existed between the velocity changes obtained from load cell and accelerometer data for the Citation, Cutlass, and Impala in the full frontal crash tests. Therefore, the value of comparison of frontal stiffness distribution was questionable. The cause of the low velocity changes as derived from the load cells is not known. However, it is possible that the load cells bottomed out as in other tests with this barrier configuration (13) (especially since they were conducted at 40 mph impact velocities).

Although the full frontal data were questionable, the 30° frontal crash tests (conducted at 30 mph impact velocities) did provide a good comparison of frontal stiffness distribution. The Car/MLCB load cell interface and load cell grouping (six groups) are shown in Figure 68 for the 30° frontal tests. Figures 69 -- 71 show the load cell data for the Citation and Fairmont divided into three groups and sequenced by contact time with the car. Although the total force-time histories for the Citation and Fairmont were comparable (Figure 66), Figures 69 and 70 indicate that significant differences existed in the frontal stiffness distribution. The Citation was much stiffer than the Fairmont on the front left corner (Figure 69), while it was much softer in the center as indicated by contact with the load cells in groups 5 and 6 (Figure 70). Forces sustained by the load cells in groups 1 and 2 (Figure 71) were most likely caused by rotation of the vehicle late in the crash event, and were not significant in terms of the stiffness distributions. Finally, the load cell data for all six groups are shown in Figures

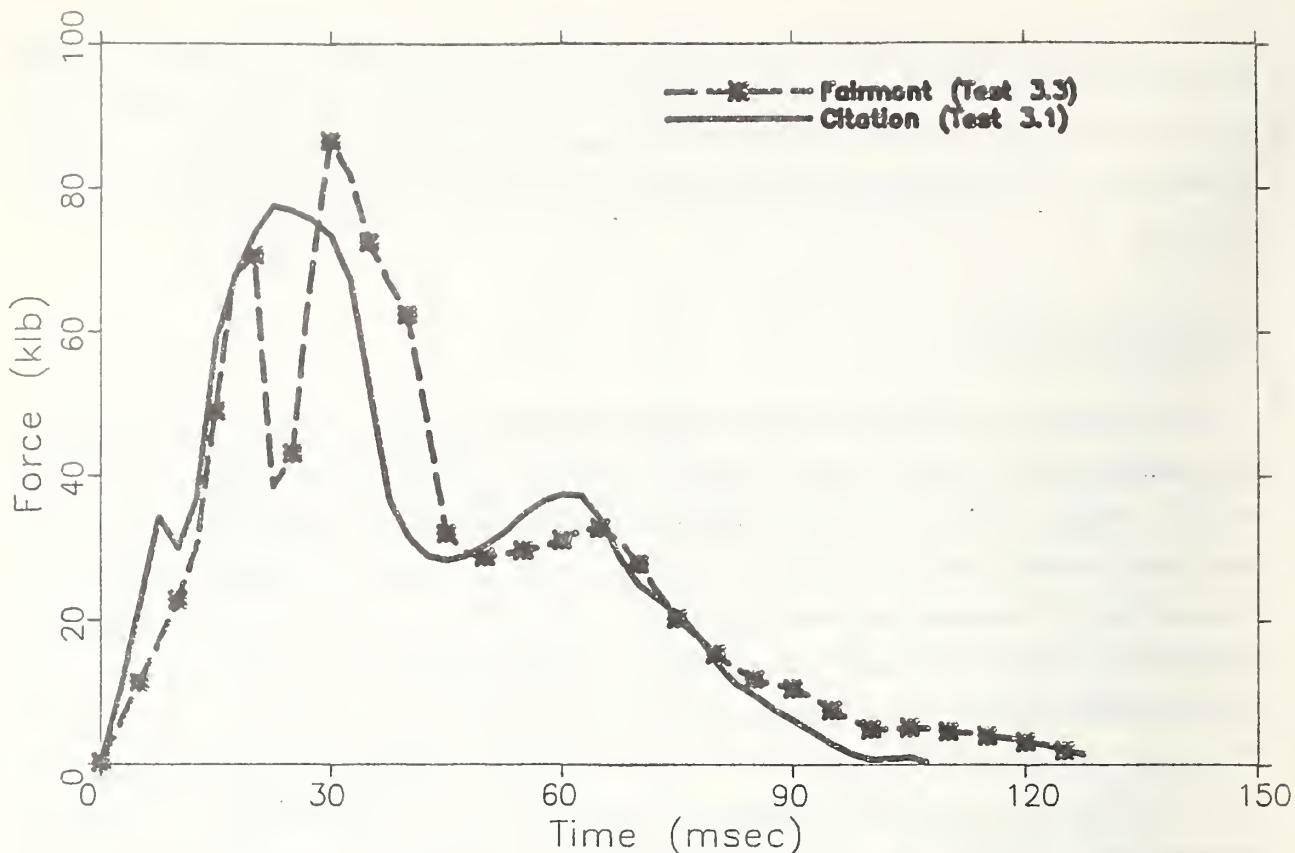


FIGURE 64. Citation and Fairmont Total FLCB Force -- Full Frontal

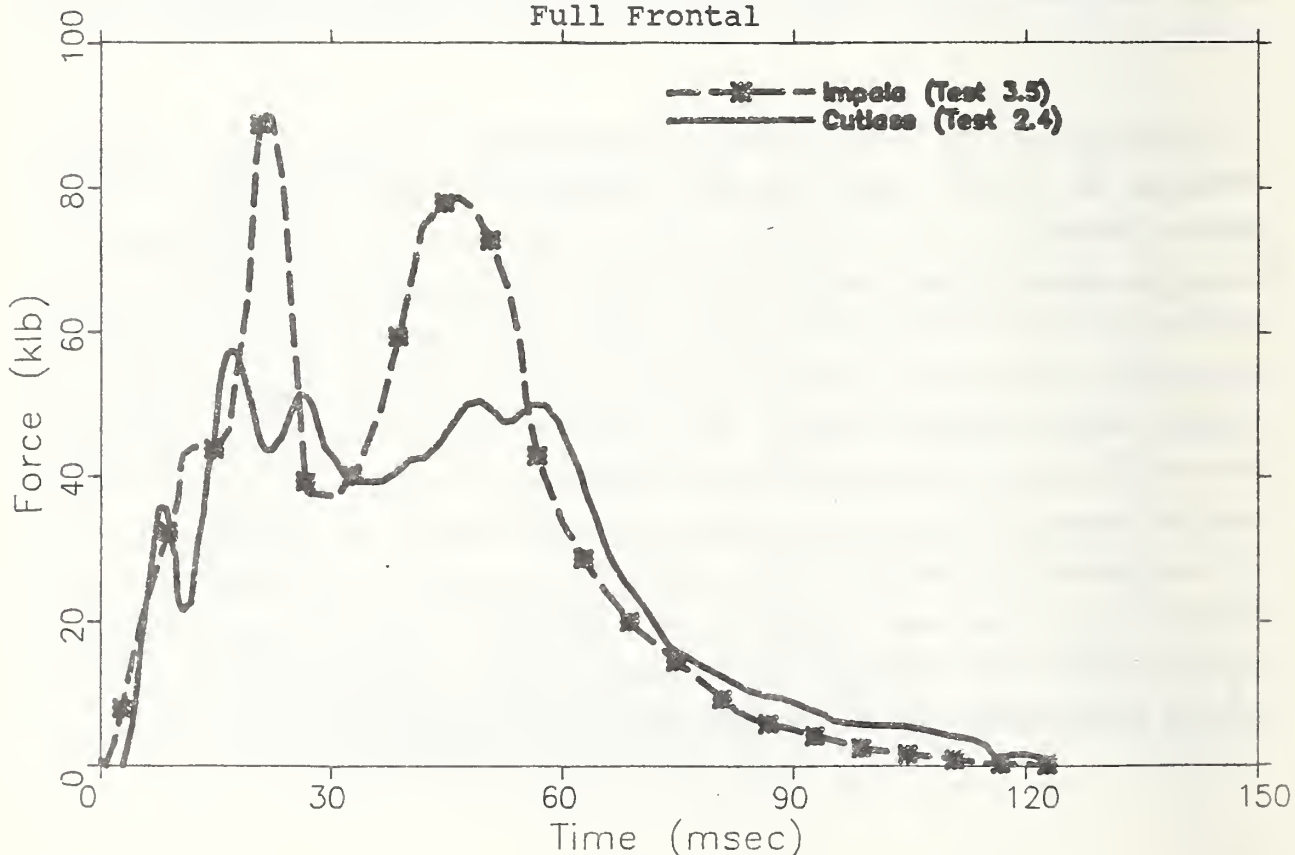


FIGURE 65. Cutlass and Impala Total FLCB Force -- Full Frontal.

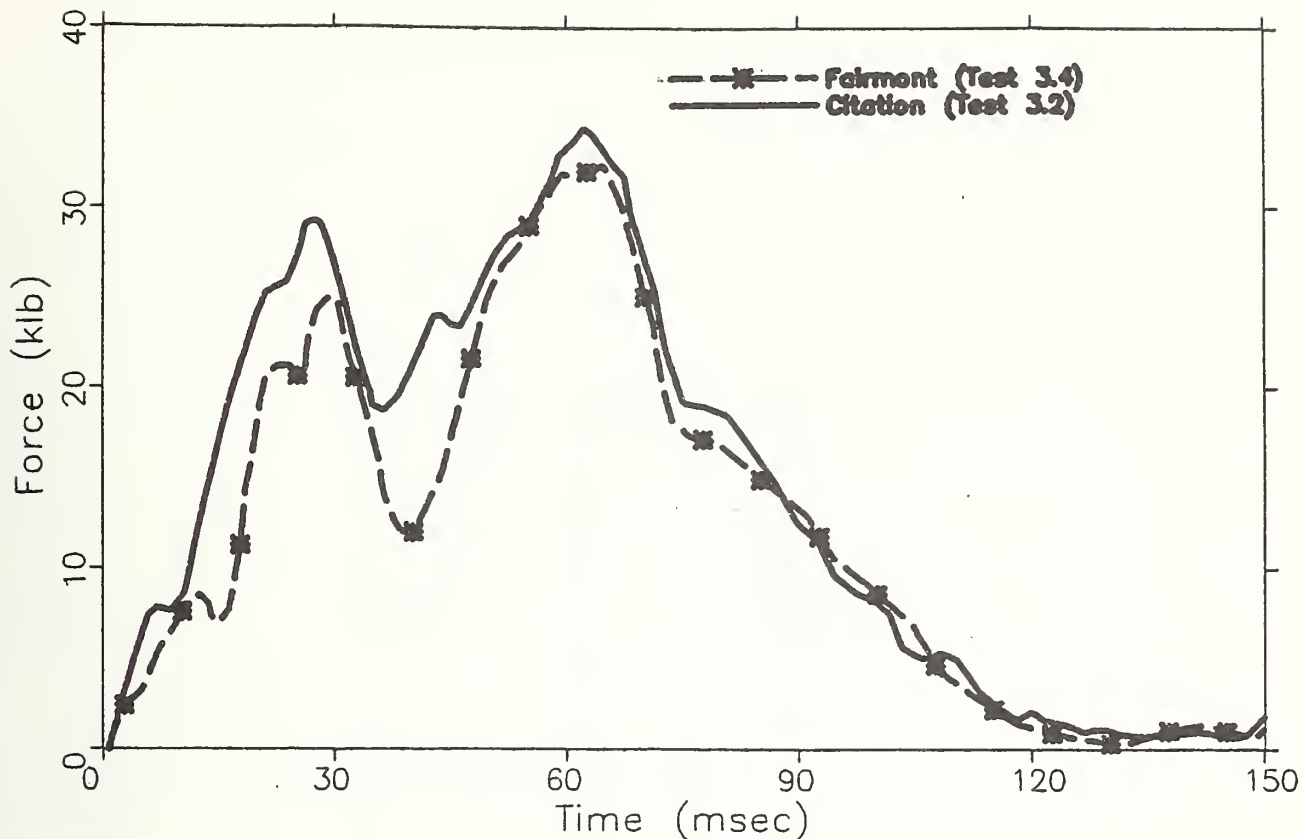


FIGURE 66. Citation and Fairmont Total FLCB Force -- 30° Frontal

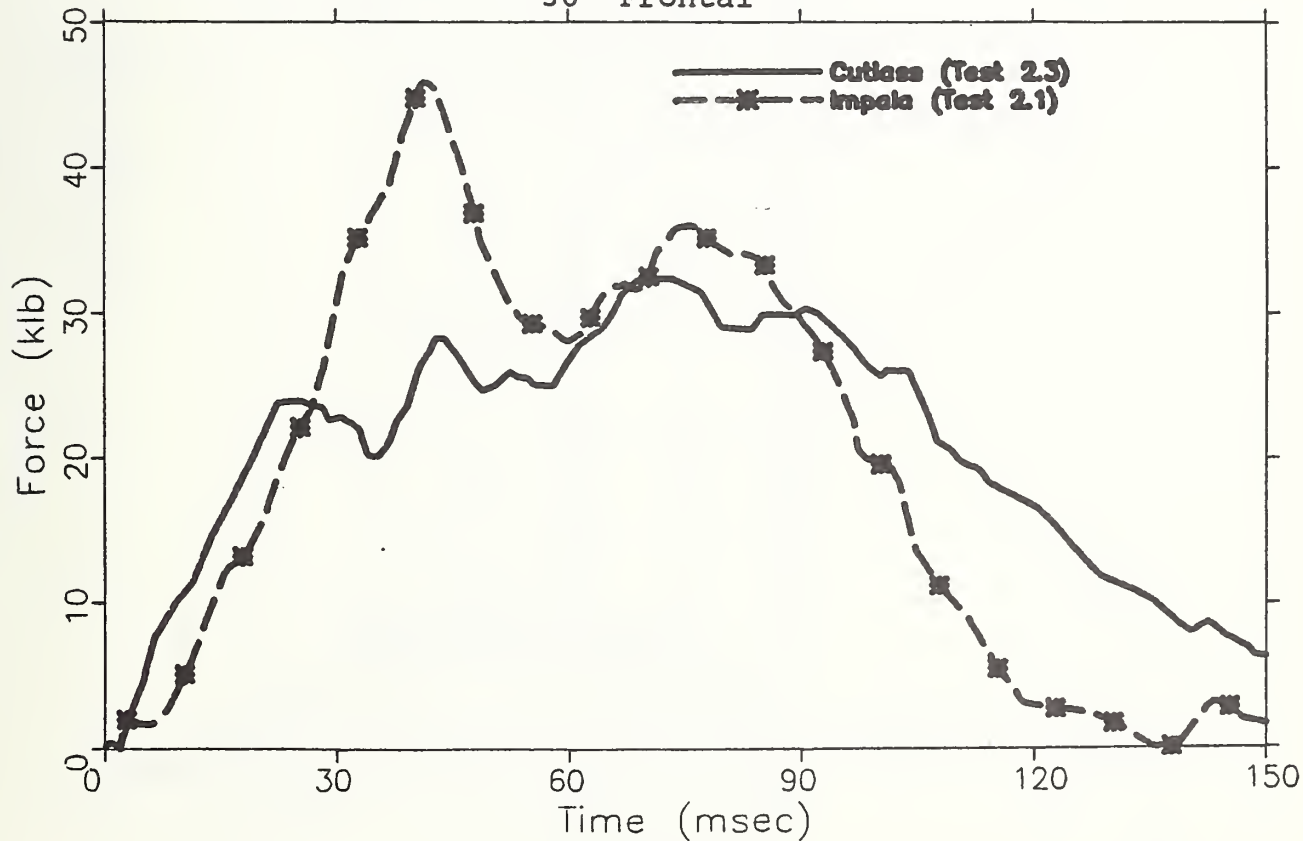


FIGURE 67. Cutlass and Impala Total FLCB Force -- 30° Frontal

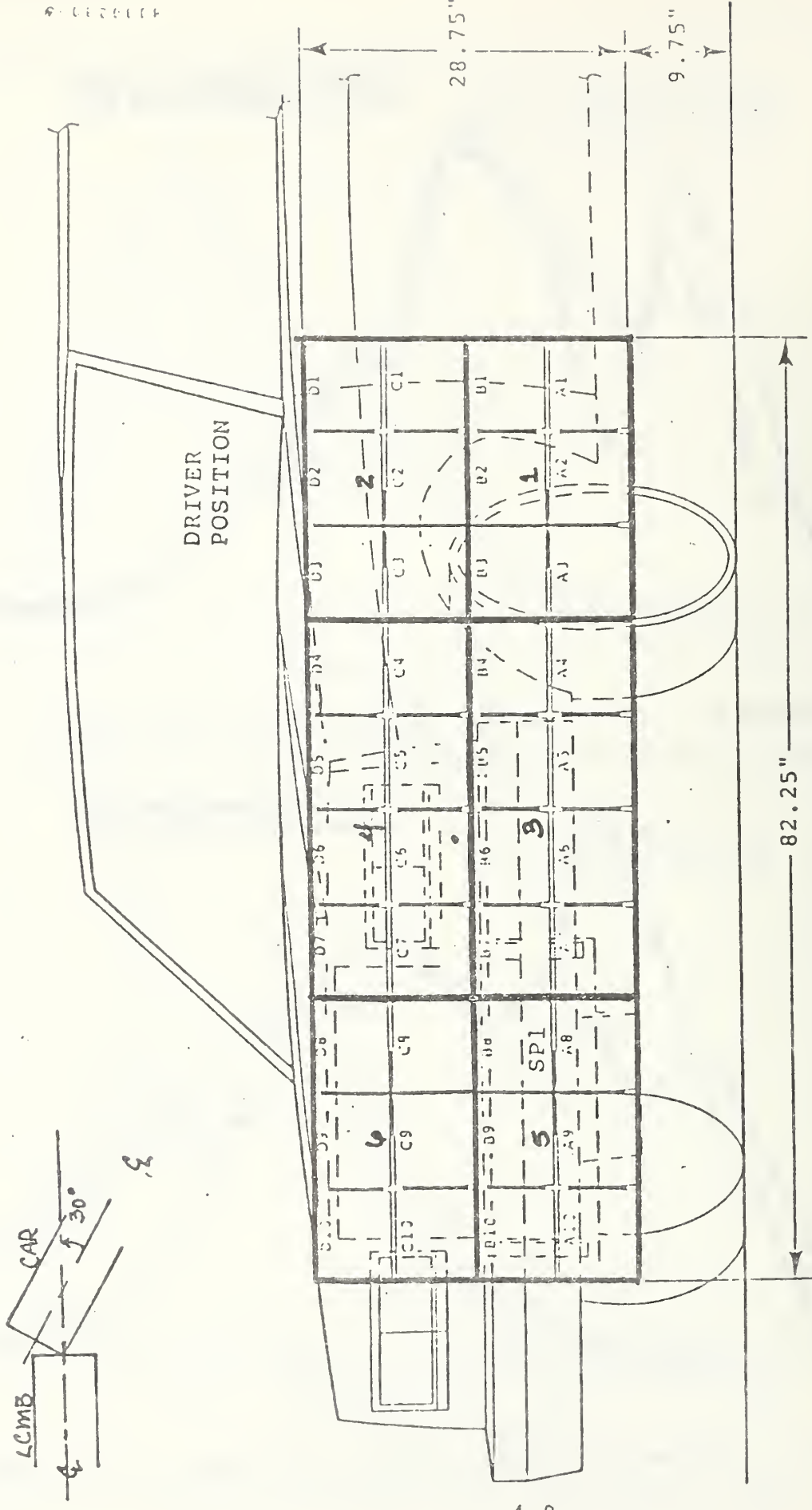


FIGURE 68. Car/MLCB Load Cell Interface and Load Cell Grouping -- 30° Frontal Impacts

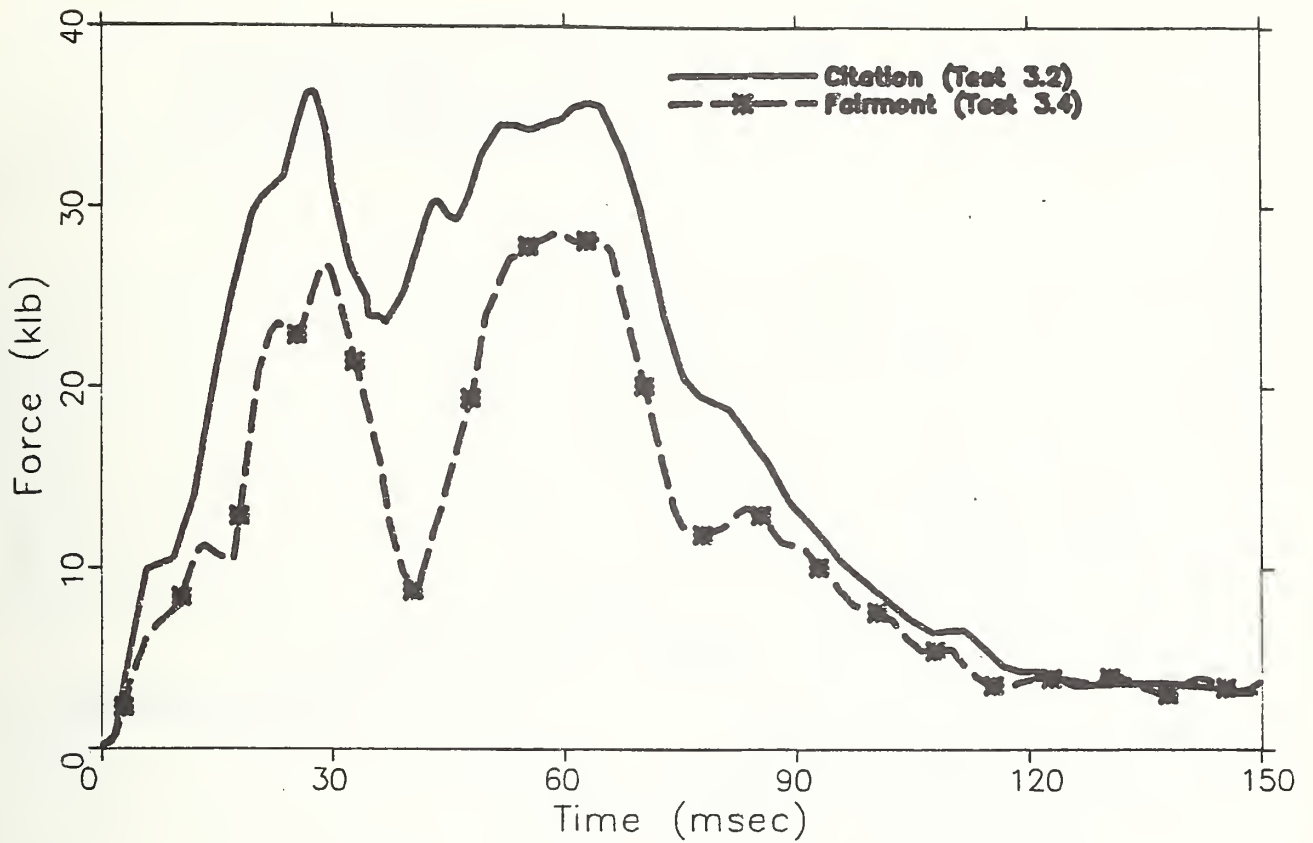


FIGURE 69. MLCB Group 3 and 4 Forces --
Citation and Fairmont 30° Frontal

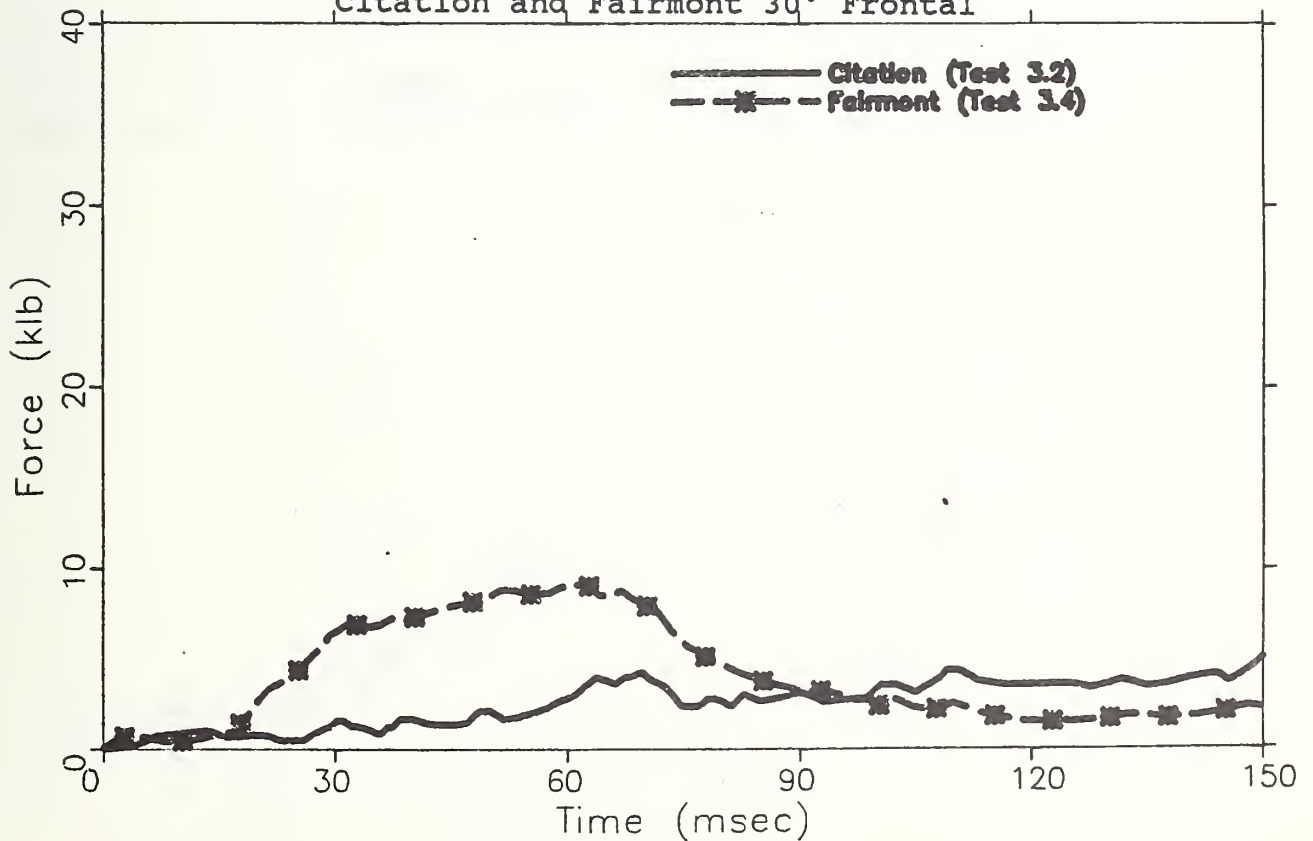


FIGURE 70. MLCB Group 5 and 6 Forces --
Citation and Fairmont 30° Frontal.

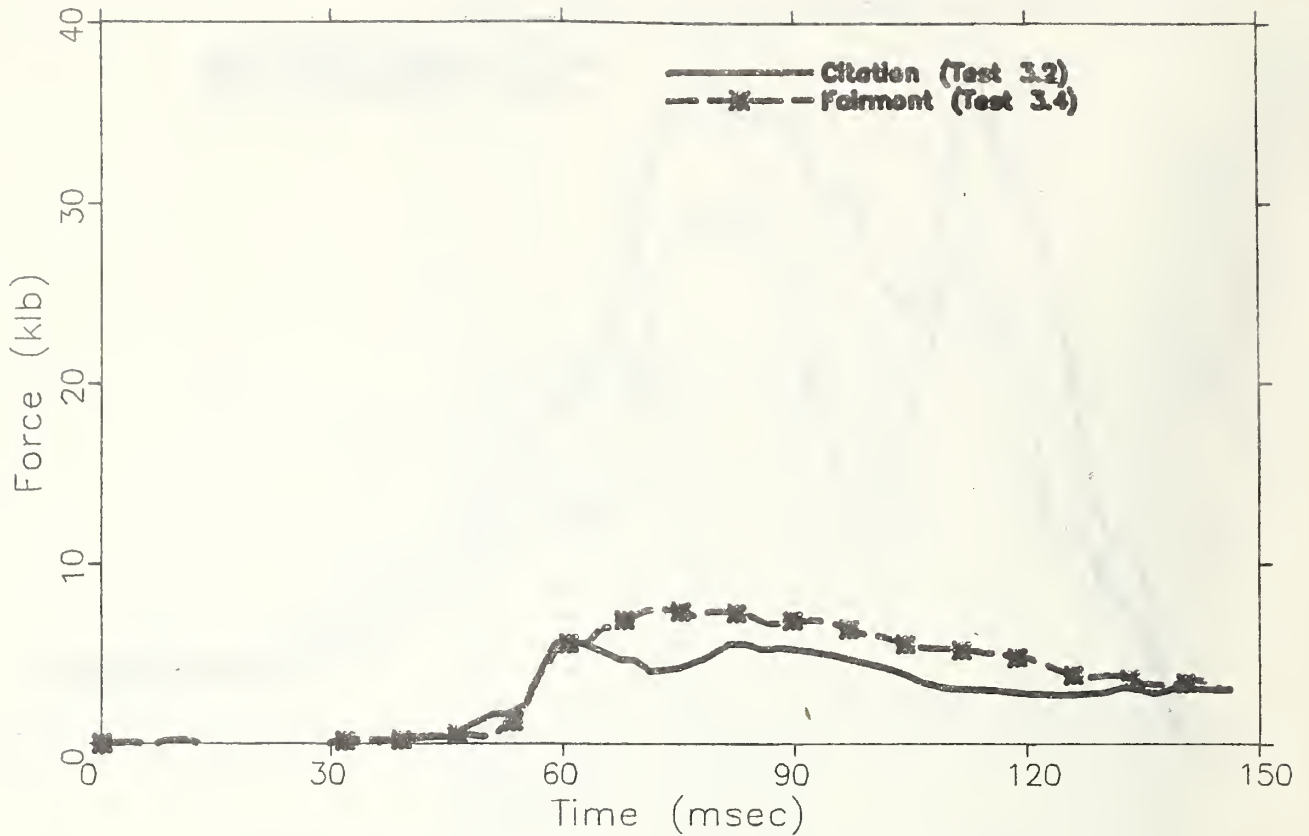


FIGURE 71. MLCB Group 1 and 2 Forces -- Citation and Fairmont 30° Frontal

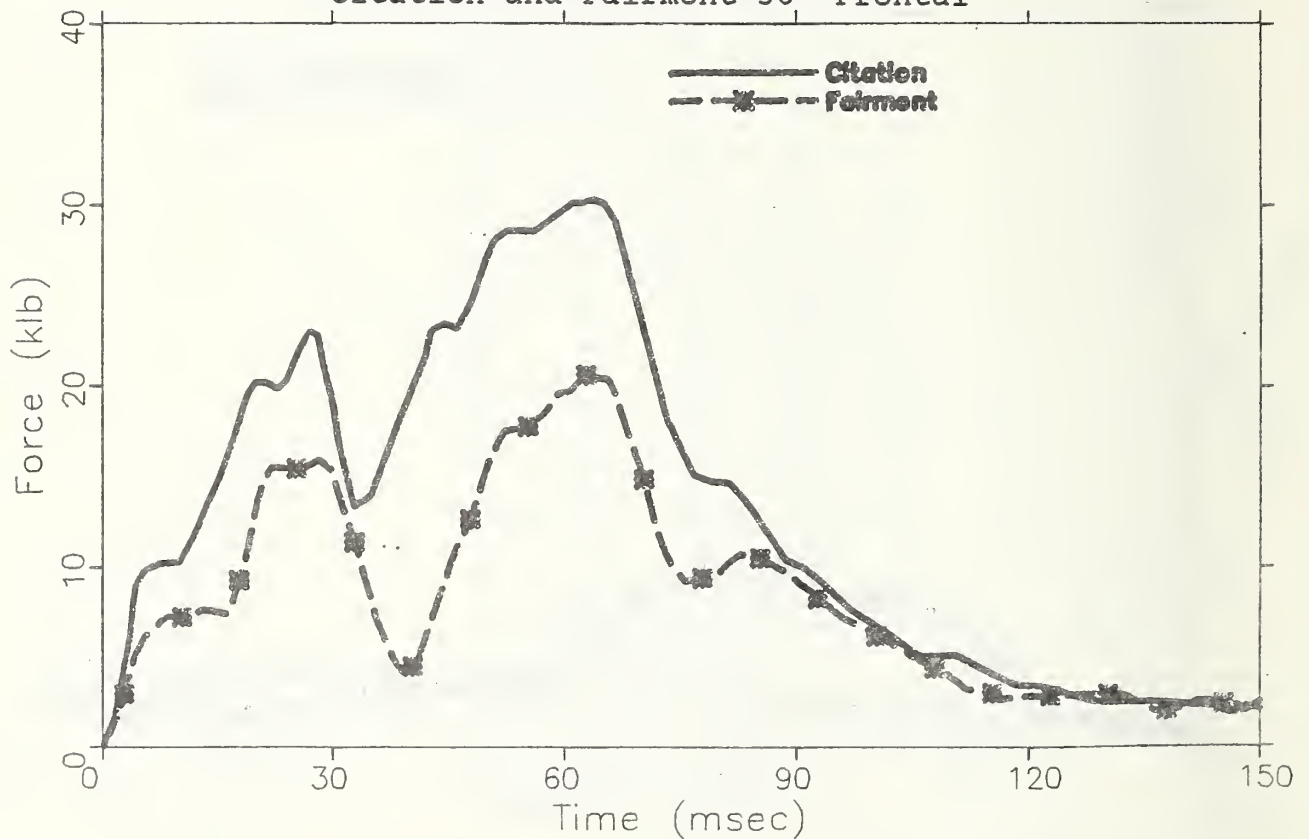


FIGURE 72. MLCB Group 3 Forces -- Citation and Fairmont 30° Frontal.

72 -- 77. These figures show that the significant differences in frontal stiffness distribution exhibited in Figures 69 and 70 were due primarily to stiffness differences at the bumper level.

Force-time history comparisons for the Cutlass and Impala 30° frontal crash tests are shown in Figures 78 -- 80. Conclusions regarding possible differences in the frontal stiffness distribution for the Cutlass and Impala are not possible. The Impala sustained higher force levels both on the corners and in the center (Figures 78 and 79). This effect was probably due to the weight differences of the two cars. In addition, the duration of force for the Cutlass was somewhat different than for the Impala. On the corner, the Impala force duration was shorter than the Cutlass, while in the center it was longer. This was possibly caused by the difference in velocity change.

4.4 Conclusions and Recommendations

Significant differences were found in the frontal force distributions between the Citation and the Fairmont in 30° frontal collisions. It is recommended that frontal stiffness distribution differences among vehicles be further explored, and that the effects of these differences on struck car occupant injury severity be investigated. This could be done by component testing, sled testing, and/or crash testing with either car/car or MDB/car impacts.

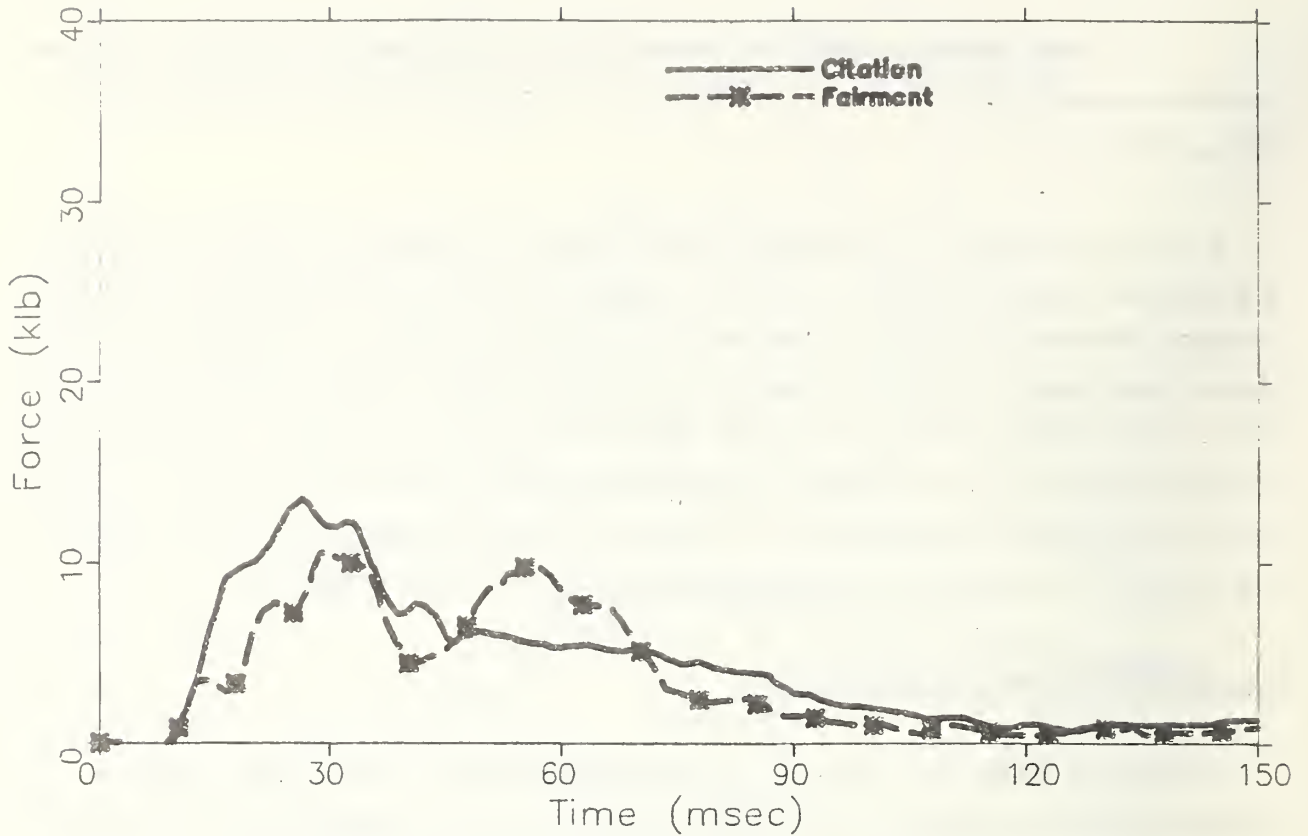


FIGURE 73. MLCB Group 4 Forces -- Citation and Fairmont 30° Frontal

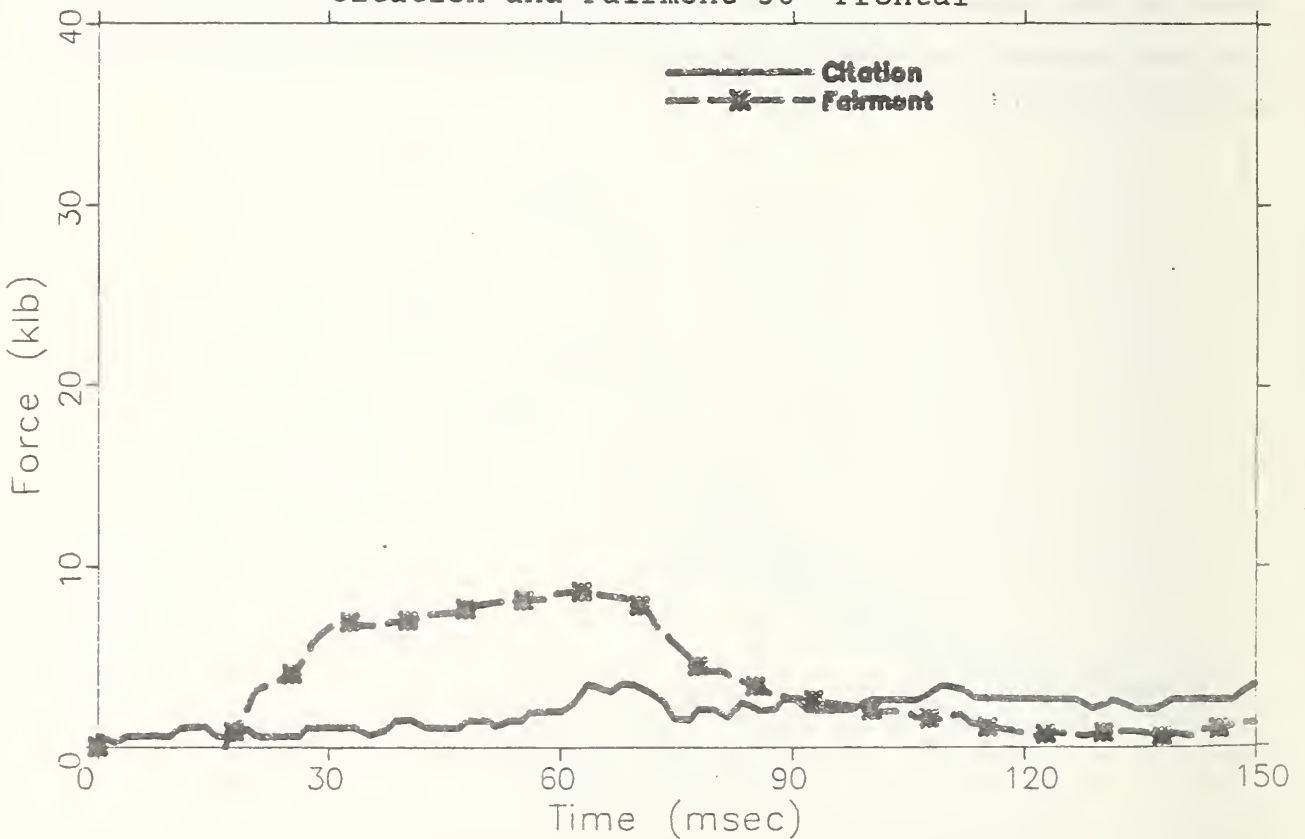


FIGURE 74. MLCB Group 5 Forces -- Citation and Fairmont 30° Frontal.

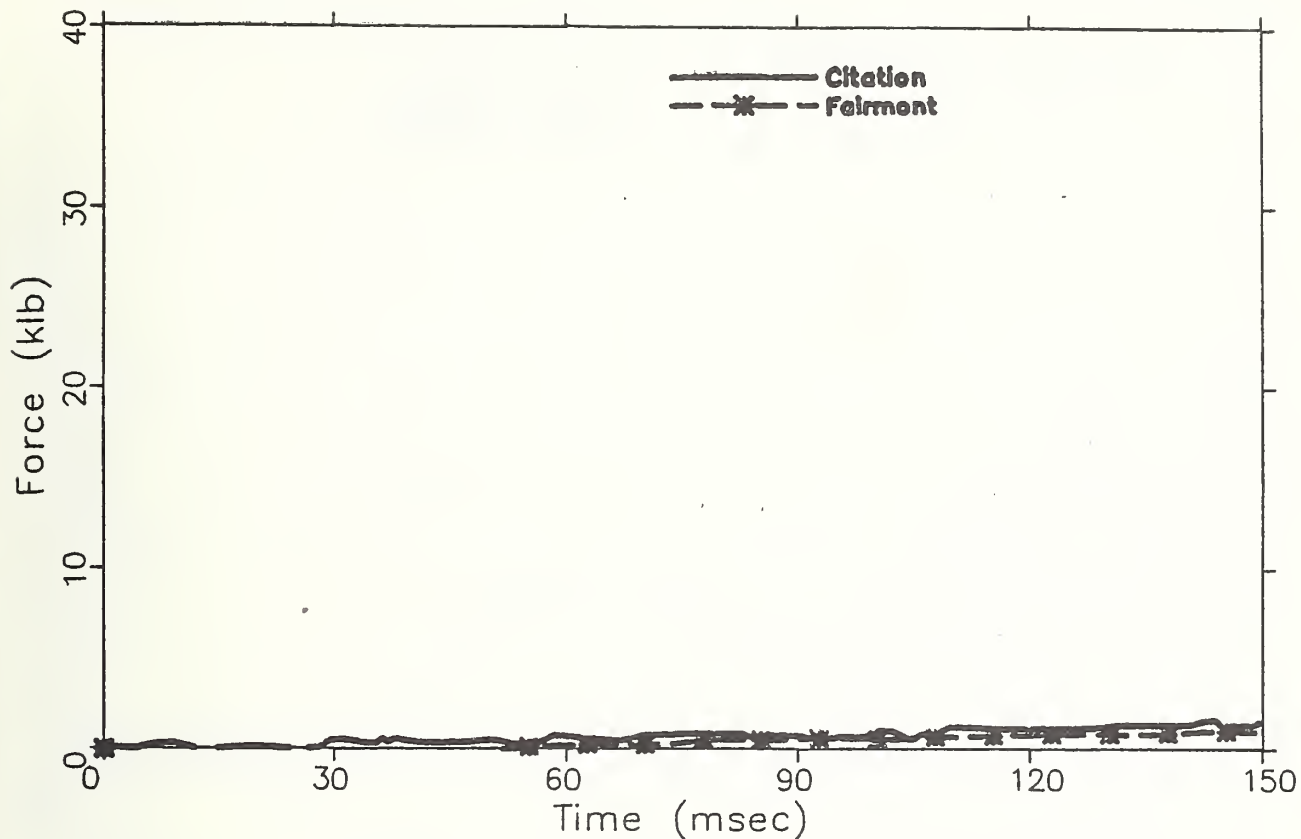


FIGURE 75. MLCB Group 6 Forces -- Citation and Fairmont 30° Frontal

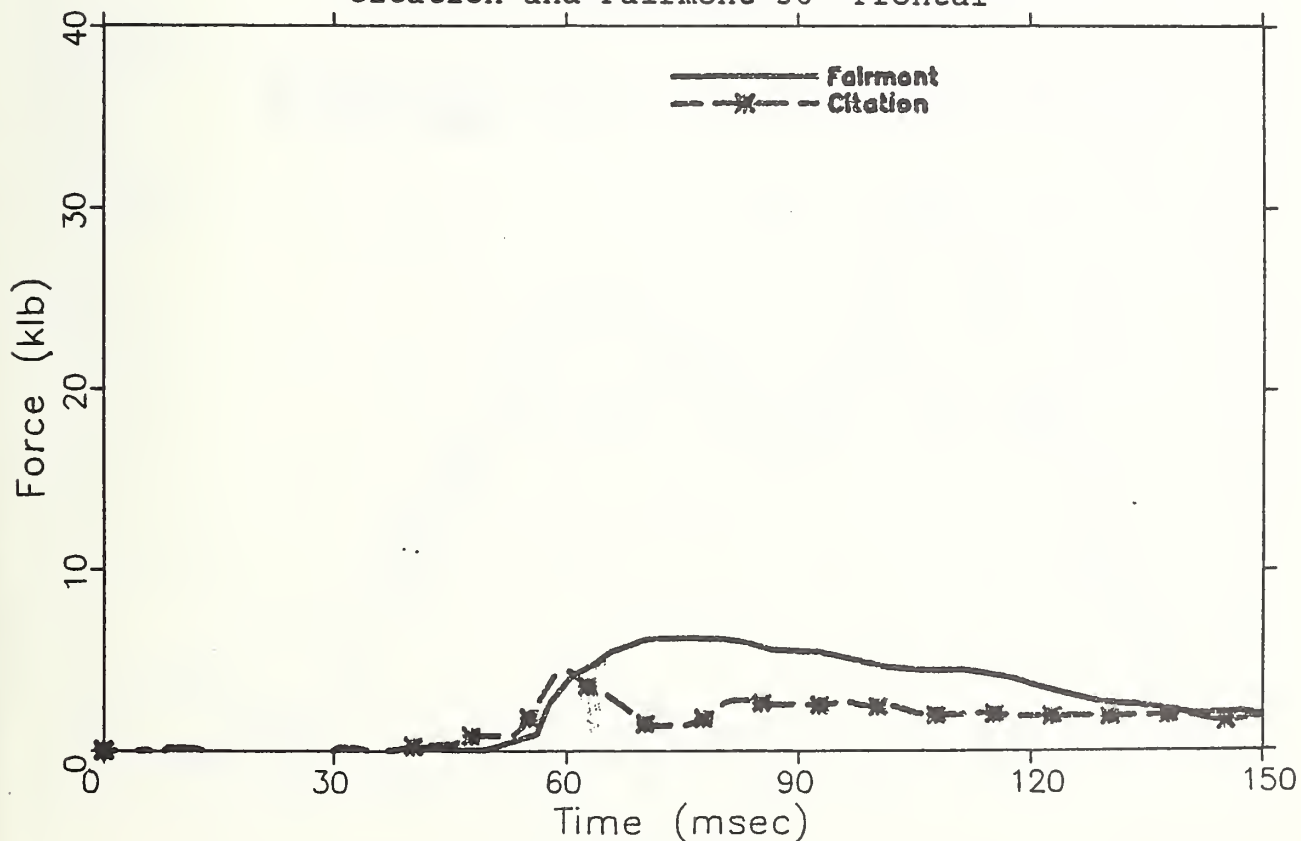


FIGURE 76. MLCB Group 1 Forces -- Citation and Fairmont 30° Frontal.

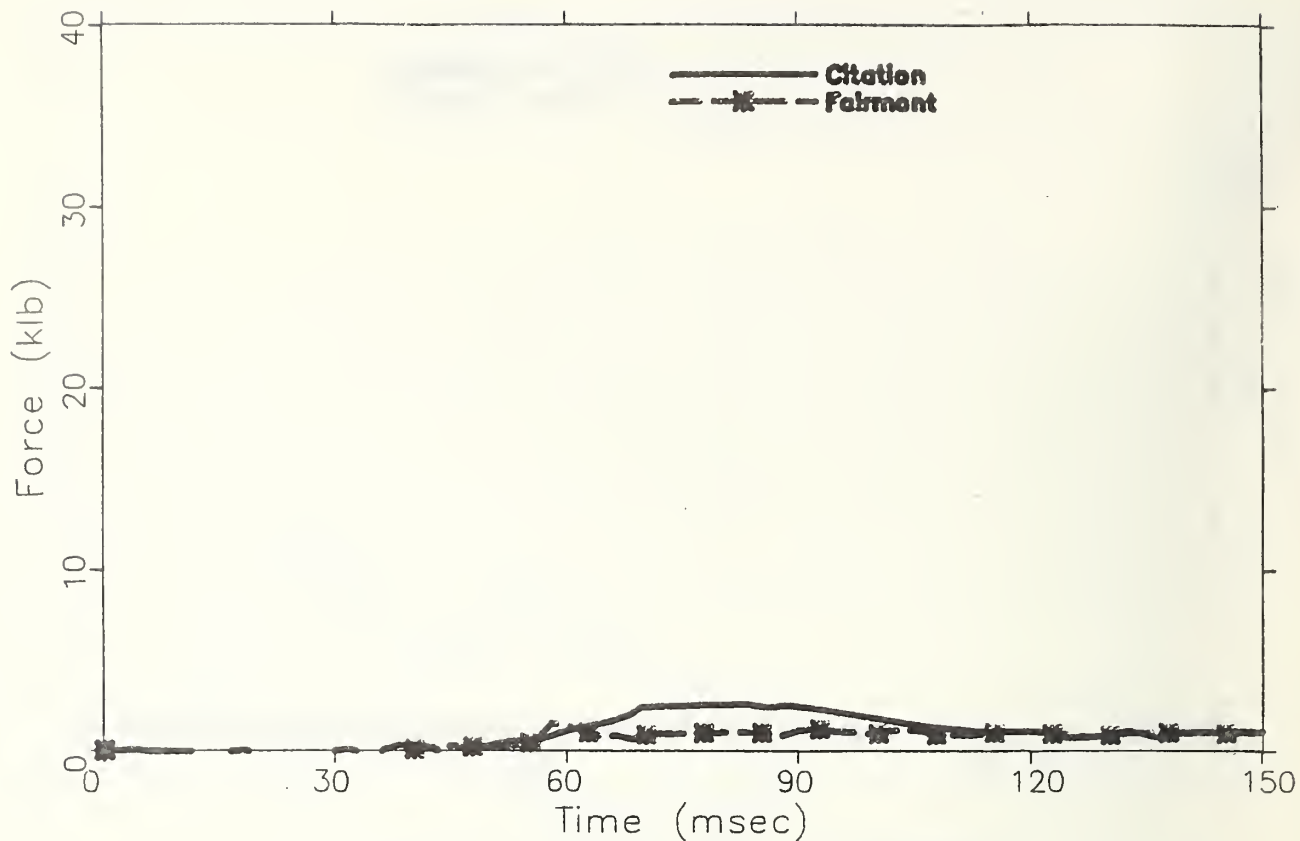


FIGURE 77. MLCB Group 2 Forces -- Citation and Fairmont 30 Frontal

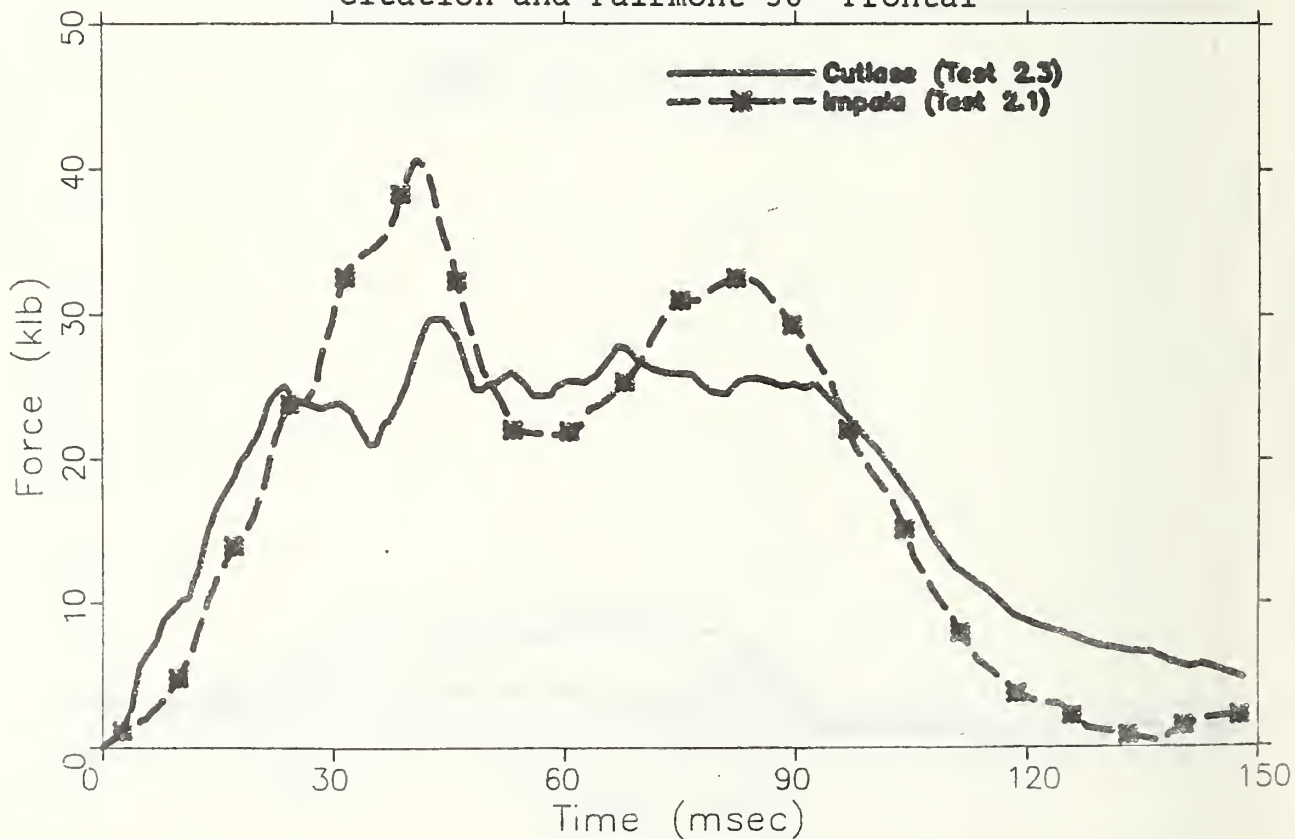


FIGURE 78. MLCB Group 3 and 4 Forces -- Cutlass and Impala 30 Frontal.

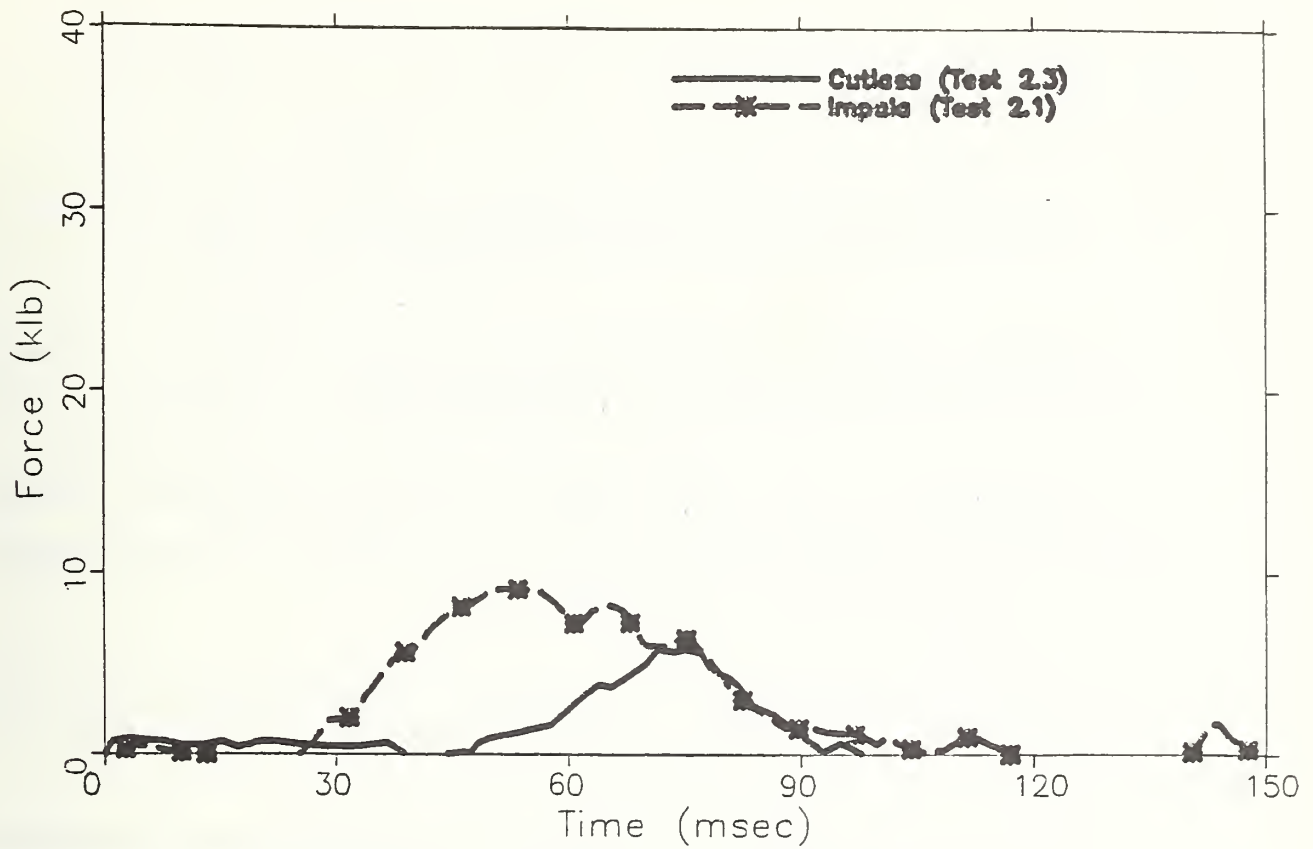


FIGURE 79. MLCB Group 5 and 6 Forces --
Cutlass and Impala 30° Frontal

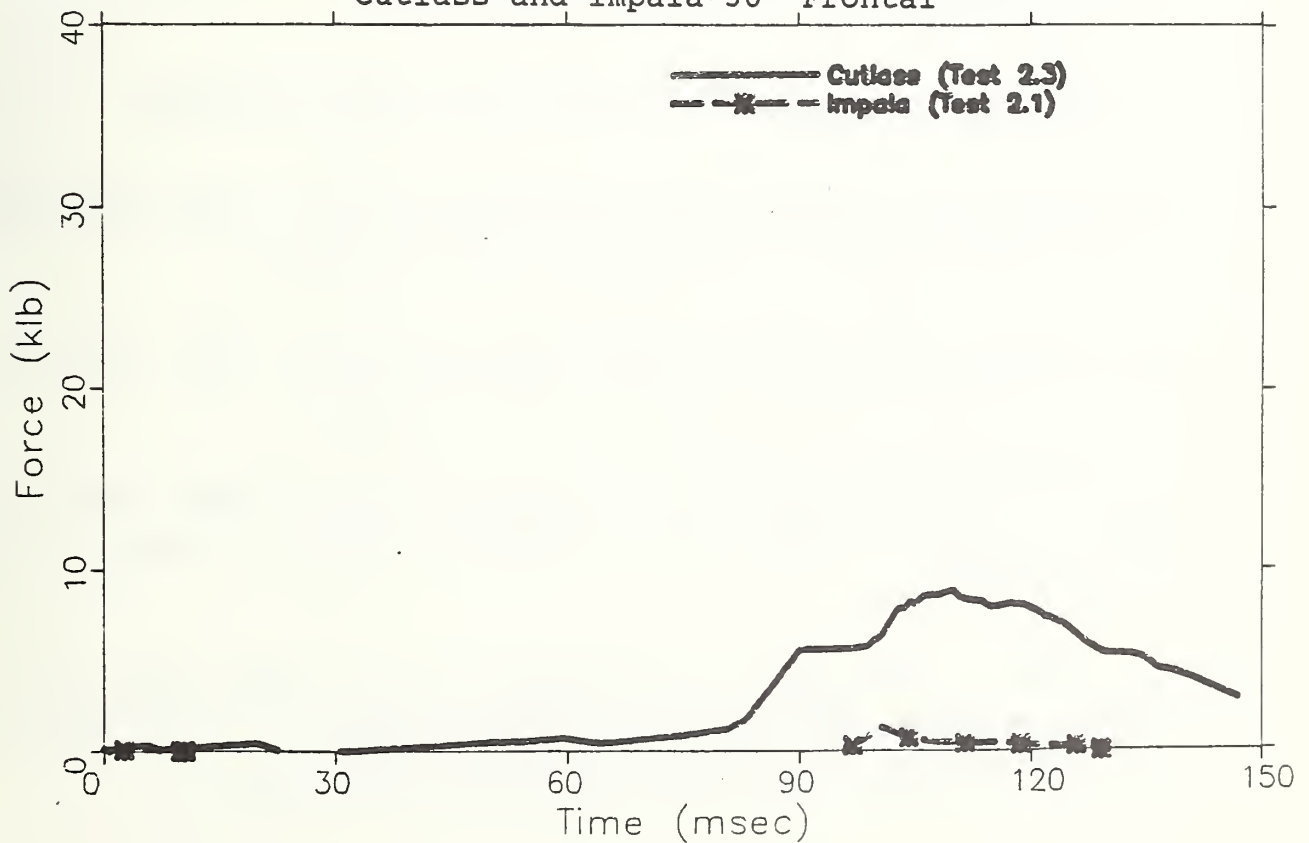


FIGURE 80. MLCB Group 1 and 2 Forces --
Cutlass and Impala 30° Frontal.

REFERENCES

1. T.F. MacLaughlin, "Derivation and Application of Restraint Survival Distance in Motor Vehicle Collisions," SAE Technical Paper 810092, February 1981.
2. S.W. Enouen, "Comparison of Models Simulating Occupant Response in Airbags," Master of Science Degree Thesis, The Ohio State University, January 1982.
3. T.F. MacLaughlin, R.A. Saul, and S. Daniel, "Causes and Measurement of Vehicle Aggressiveness in Frontal Collisions," Twenty-Fourth Stapp Car Crash Conference, SAE Technical Paper 801316, October 1980.
4. T.F. MacLaughlin, R.A. Saul, and R.M. Morgan, "Vehicle Crashworthiness and Aggressiveness," NHTSA Technical Report # DOT-HS-805-712, January 1981.
5. J.K. Pollard and K.H. Schaeffer, "Passenger Car Fleet Projection Parameters," Department of Transportation, Transportation Systems Center, Memorandum, February 14, 1980.
6. "Auto Revolution of the 80's," p.55, Mechanical Engineering, March 1980.
7. "New Vehicle Assessment and Standards Enforcement Indicant Testing," Crash Test Reports, Dynamic Science, Inc., Contract No. DOT-HS-6-01478.
8. "New Vehicle Assessment and Standards Enforcement Indicant Testing," Crash Test Reports, Calspan Corporation, Contract No. DOT-HS-8-01938.
9. "New Vehicle Assessment and Standards Enforcement Indicant Testing," Crash Test Reports, Mobility Systems and Equipment Company, Contract No. DOT-HS-9-02136.
10. R.A. Saul, T.F. MacLaughlin, C.A. Ragland, Jr., and D. Cohen, "Experimental Investigation of Crash Barriers for Measuring Vehicle Aggressiveness -- Fixed Rigid Barrier Initial Results," SAE Technical Paper 810093, February 1981.

11. T.F. MacLaughlin, R.J. Wasko, and NHTSA/MVMA Task Group, "Evaluation of Full Vehicle and Component Test Procedures for Improving Side Impact Crash-Survivability," SAE Technical Paper 830463, February 1983.
12. "Test Device and Test Procedure to Assess Side Structures," Dynamic Science, Inc., Contract No. DOT-HS-8-01933.
13. "Development of a Test Methodology for Evaluating Crash Compatibility and Aggressiveness," Final Report, Contract No. DOT-HS-7-01758.

APPENDIX A

Difficulties in Obtaining Static Crush Values

Uncertainties in extracting static crush values from the test reports were encountered. In general, static crushes are reported in at least three locations in the test reports, depending on the contractor. Dynamic Science, Inc. (DSI), and Calspan Corporation use a similar procedure to obtain pre- and post-crash measurements. In addition, DSI publishes a Vehicle Profile Data Sheet, showing crush values at several locations across the front of the vehicle. In Table A-1, crush values X1, X19, X20 and the maximum crush value appearing in DSI's Vehicle Profile Data Sheet are presented. The word "center" indicates that the maximum value in the Vehicle Profile Data Sheet is at the centerline of the vehicle.

It is clear from Table A-1 that discrepancies exist in the static crush values. For this reason, only dynamic crush values were used in the analysis.

TABLE A-1
Comparison of Static Crush Values

VEHICLE		STATIC CRUSH -- INCHES			MAX. VALUES FROM "VEHICLE PROFILE DATA SHEET, "DSI REPORTS"		
CLASS	YEAR	SYMBOL	TEST CONTRACTOR	VALUES FROM FIG., "PRE-TEST & POST-TEST MEASUREMENT POINTS"			
				LEFT X20	CENTER X1	RIGHT X19	
Mini-Compact	1979	A	Calspan	18.6	20.9	19.2	--
	1979	B	Dynamic Science	22.2	20.9	22.3	24.7 (center)
	1979	C	Calspan	21.7	22.7	22.1	--
	1979	D	Dynamic Science	25.3	25.0	24.9	25.8
Sub-Compact	1979	E	Dynamic Science	23.1	23.1	22.0	22.1 (center)
	1979	F	Calspan	21.9	23.4	21.5	--
	1979	G	Calspan	21.6	24.2	23.1	--
	1979	H	Dynamic Science	16.5	21.1	16.5	23.4
	1979	I	Dynamic Science	16.8	21.4	18.1	29.9 (center)
Intermediate	1979	J	Dynamic Science	20.1	20.2	20.0	25.1
	1979	K	Calspan	21.1	25.5	23.3	--
	1980	L	Calspan	21.4	22.8	21.3	--
	1979	M	Calspan	22.7	25.0	22.2	--
	1979	N	MSE	27.3	NA	28.3	--
	1980	O	Calspan	20.8	19.5	19.7	--
	1979	P	Calspan	21.0	23.9	22.6	--
	1979	Q	Dynamic Science	30.2	30.9	29.5	30.9 (center)
	Standard	1979	R	Dynamic Science	26.8	23.0	27.3
1979		S	Calspan	24.8	24.1	27.8	--
1979		T	Calspan	22.3	24.6	22.7	--
1979		U	Dynamic Science	22.2	25.0	24.1	25.0 (center)
1979		V	Dynamic Science	26.2	30.3	28.5	30.1 (center)
1979		W	Calspan	24.1	27.8	28.1	--
1979		X	Calspan	23.1	27.4	25.1	--
1979		Y	Dynamic Science	*	27.5	*	29.7
1979		Z	Dynamic Science	28.8	29.2	28.0	26.3 (center)
1979		2	Dynamic Science	26.8	27.0	30.6	30.6
1979		3	Dynamic Science	32.8	34.0	32.8	34.2
1979		4	Dynamic Science	30.8	26.9	28.6	30.8

*NA -- Obscured

APPENDIX B

Summary of Occupant/Airbag Modeling Improvements

The objective of this task was to define a revised ("standard") set of input parameters for each of two models, ABAG and HSRI-3D, which would be aimed at providing a model which could predict occupant survivability in many different vehicles. The "original" sets of parameters for the models were derived from 30 mph barrier crash test data, and are described in the SRL-8/9 final report (for ABAG) and in documentation from G.E. and HSRI (for HSRI-3D). Since the development of the "original" parameters, 35 mph barrier crash data have become available, enabling validation of parameters for higher speed simulation. Of all the crash tests, the Citation (Minicars Test No. 1853) is the one best suited for assessing a model's capability to determine crashsurvivability potential. (Most other tests experienced some performance complication, such as steering column uploads, bagslap, etc.) Therefore, results of Test No. 1853 were used in deriving the revised ("standard") model parameters; then the models with "standard" parameters were used to determine how well other test results were simulated.

It was concluded that:

1. Using revised ("standard") parameters, the degree of simulation of Citation Test No. 1853 was about equal for both models, and was reasonably good. Furthermore, simulation of the other vehicle tests, using parameters derived from Test No. 1853, was felt to be reasonably good, considering the fact that some steering column behavior problems occurred in the tests. HSRI-3D driver simulations for some of the vehicles experienced abrupt and premature terminations due to a lack of convergence in an integration subroutine. The program error appears to have been caused by very high contact forces which would have to be changed for each vehicle in order to alleviate the problem.

2. The "standard" set of parameters for the ABAG model gave results which appeared reasonable for 5th percentile female and 95th percentile male occupants.
3. The ABAG model, due to its relative simplicity, ease of use and improved documentation compared with the HSRI-3D model, was felt to be more suitable for use in comparing general overall crashsurvivability levels in different vehicles. The HSRI-3D model indicated a strong potential for use in specific modeling of detail for design purposes in a particular vehicle.
4. Both models required the use of dynamic, rather than static, steering column force-deflection characteristics.

TL 242 .M

- MacLaughlin

- Crashworth
- aggressi

Form DOT F 1720
FORMERLY FORM DO

DOT LIBRARY



00092385